Potentiating oncolytic virus therapy for the treatment of Acute Myeloid Leukaemia

Basem Ahmed Askar

Submitted in accordance with the requirements for the degree of Doctor of Philosophy

The University of Leeds

School of Medicine

Leeds Institute of Medical Research

February 2023

Intellectual Property Rights Statement

I confirm that the work submitted is my own and that appropriate credit has been given where reference has been made to the work of others.

Acknowledgements

First and foremost, I would like to thank my supervisor Dr Fiona Errington-Mais for her unwavering support, insightful guidance, and endless encouragement throughout my PhD journey. Her expertise and dedication have been invaluable in shaping my research and helping me achieve my goals. I would also like to extend my thanks to my second supervisor, Dr Peter Laslo, for his invaluable contribution during the various stages of my research.

I am thankful to Dr Victoria Jennings, Dr Tyler Barr, Samuel Heaton, Noura Alzamel and all FEM group for their friendship, support, and collaboration. Your friendship has made this journey much more enjoyable. I would also like to acknowledge Dr Milene Volpato for expert assistance with the *in vivo* experiments, and Karen Scott and Emma West for help with the Luminex experiment, and Stewart McConnell for collecting patient samples. I am also thankful for all the patients and healthy donors who have given their time, support, and clinical samples which have been involved in this work.

I would like to express my gratitude to my family, especially my dad and mum, for their unwavering love and support throughout the years. Your encouragement and belief in me have meant the world to me.

Finally, I would like to acknowledge the financial support provided by the Libyan Ministry of Education. Their generosity has been essential in enabling me to complete this research.

Abstract

Acute myeloid leukaemia (AML) is a cancer of the blood and bone marrow and is characterised by the overproduction of immature myeloid cells. AML is most common in older adults, 65 being the median age of diagnosis, and is associated with a poor overall survival. Therefore, novel therapies are urgently required. Oncolytic viruses (OV) replicate preferentially within cancerous cells causing cell death and induce innate and adaptive anti-tumour immune responses. However, whilst OV have demonstrated promising results in solid malignancies, their potential for the treatment of AML remains poorly understood. Therefore, herein, we have investigated the efficacy of OVs against AML and developed a combination approach to boost OV efficacy.

Using a panel of OV; reovirus, Maraba (MG1), coxsackievirus (CVA21) and herps simplex virus 1716 (HSV-1) we evaluated whether OV-induced pro-inflammatory cytokines or OV-direct oncolysis can kill AML cells, and examined whether apoptotic modulators (SMAC/ BH3 mimetics) could be used to increase OV efficacy.

Our data has demonstrated that cytokines secreted from peripheral blood mononuclear cells (PBMCs) can kill AML cell lines. Moreover, OV-induce bystander cytokine killing was significantly enhanced when combined with either Smac or BH3 mimetics, depending on the AML cell line used. Interestingly, direct infection of AML cell lines with live or UV-inactivated reovirus can stimulate an inflammatory milieu that, when combined with SMAC or BH3 mimetic, can also induce death of AML cells. Furthermore, we have shown that reovirus can activate NK cells from healthy donors and primary patient samples, and that reovirus-activated NK cells induced significant AML cell death. Overall,

the work presented in this thesis demonstrates that apoptotic modulators could be used in combination with OV to enhance OV-induced cytokine killing, thus, suggesting a novel treatment approach for AML.

Table of Contents

List of Figures

List of Tables

List of abbreviations

allo-HSCT:	allogeneic hematopoietic stem cell transplant
ALP:	Alkaline phosphatase
AML:	Acute myeloid leukemia
APC:	Antigen-presenting cells
BCL-2:	B-cell leukemia/lymphoma-2
bFGF:	basic fibroblast growth factor
BM:	Bone marrow
BSA:	Bovine serum albumin
CIN:	Chromosomal instability
CLL:	Chronic lymphocytic leukemia
CM:	Conditioned medium
CMC:	Carboxymethylcellulose
Cpm:	Counts per minute
Cr:	Chromium
CR:	Complete remission
CTCL:	Cutaneous T-cell lymphoma
CTLA-4:	Cytotoxic T-lymphocyte-associated protein 4
CVA21:	Coxsackievirus A21
DAF:	Decay Accelerating Factor
DAMPs:	Damage-associated molecular pattern signals
DCs:	Dendritic cells
DISC:	Death inducing signalling complex
DMEM:	Dulbecco’s modified eagle medium
DMSO:	Dimethyl sulphoxide
E:T:	Effector:target
EGF:	Epidermal growth factor
ER:	Endoplasmic reticulum
FAB:	French American-British
FADD:	FAS-associated death domain
Fas:	First apoptosis signal
FCS:	Foetal calf serum
FDA:	Food and Drug Administration
HBSS:	Hanks' balanced salt solution
HCC:	Hepatocellular carcinoma

HHT:	Homoharringtonine
HMA:	Hypomethylating agent
HSV:	Herpes simplex virus
HVEM:	Herpesvirus entry mediator
IAPs:	Inhibitors of Apoptosis Proteins
i.p:	intraperitoneal
i.t:	intertumoral
i.v:	intravenous
IAP:	Inhibitors of apoptosis proteins
ICAM-1:	Intercellular adhesion molecule 1
IDO1:	Indoleamine 2,3-dioxygenase-1
IL-12:	Interleukin-12
IRF3:	IFN-related factor 3
JAM-A:	Junctional adhesion molecule-A
LDAC:	Low-dose cytarabine
LDLR:	Low-density lipoprotein receptor
LFA:	Lymphocyte function-associated antigen
LSCs:	Leukemic stem cells
MACS:	Magnetic cell sorting
MDA5:	Melanoma differentiation-associated protein 5
MDSC:	Myeloid-derived suppressor cells
MG1:	Maraba virus
MM:	Multiple myeloma
MMV:	Measles and mumps viruses
MV:	Measles virus
MYXV:	Myxoma virus
NDV:	Newcastle disease virus
NHL :	Non-Hodgkin lymphoma
NK :	Natural killer
NSCLC:	Non–small cell lung cancer
OS:	Overall survival
OVs:	Oncolytic viruses
OVT:	Oncolytic virotherapy
OVV:	Oncolytic vaccinia virus
PAMPs:	Pathogen-associated molecular patterns
PBMC:	Peripheral blood mononuclear cells

PBS:	Phosphate buffered saline
PD-1:	Programmed cell death protein 1
PDGF:	Platelet-derived growth factor
PFA:	Paraformaldehyde
PGE2:	Prostaglandin E2
PKR:	Protein kinase receptor
Reovirus:	Respiratory enteric orphan virus
RIG-I:	Retinoic acid-inducible gene I
RIP1:	Receptor-interacting protein 1
ROS:	Reactive oxygen species
RPMI:	Roswell Park Memorial Institute
RSV:	Respiratory syncytial virus
RT:	Room temperature
s.c:	subcutaneous
SCF:	Stem cell factor
SCLC:	Small-cell lung carcinoma
TAA:	Tumour associated antigen
TAM:	Tumour associated macrophages
TGF-β:	Transforming growth factor-beta
TLRs:	Toll-like receptors
TME:	Tumour microenvironment
TNFR:	TNF receptor
TNFSF:	Tumour Necrosis Factor superfamily
TRAF3:	TNF receptor-associated factor 3
TRAIL :	Tumour necrosis factor-related apoptosis inducing ligand
UV:	Ultraviolet
VEGF:	Vascular endothelial growth factor
VSV:	Vesicular stomatitis virus
VV:	Vaccinia virus
WHO:	World Health Organization
XAF1:	XIAP-associated factor 1

Chapter 1 : Introduction

1.1 Acute myeloid leukaemia

Acute myeloid leukaemia (AML) is a malignancy characterised by uncontrolled proliferation and differentiation of clonal myeloid stem cells that have acquired genetic abnormalities [1]. Myeloblasts are poorly differentiated cells that accumulate in the blood and bone marrow following uncontrolled proliferation. Infiltration of immature blasts into the blood can cause anaemia, intravascular coagulation, infection, bleeding and bone marrow failure [2]. AML is the most common form of acute leukaemia seen in adults and accounts for around 80% of all leukaemia diagnoses [3]. The most significant risk factor for AML is a patient's age, with over 74% of AML patients being above the age of 55. There are around 3090 new cases each year in the UK [4]. Unfortunately, the median survival duration is only 8.5 months with current treatments, and the overall 5-year survival (OS) rate is just 24%. Moreover, the 5-year survival rate declines to 5-10% in patients over 65 because of increasing disease heterogeneity, or treatment-related toxicities [5, 6].

AML can occur in people who already have an underlying haematological malignancy, such as Fanconi anaemia or myelodysplastic syndrome, both of which are illnesses that lead to failure of the bone marrow. However, there is no one reason that can be attributed to the formation of AML [7]. Environmental risk factors, such as radiation, smoking and exposure to benzenes or chemotherapeutics, are additional contributors to an increased likelihood of developing AML [8, 9]. Therapy-related AML can also develop after an individual has received treatment for a solid tumour, and this subtype of AML accounts for 10–15% of all diagnoses [10].

1.1.1 Classification of AML

Prior to the year 2008, the French American-British (FAB) classification was used to categorise AML subtypes on the basis of their morphological characteristics (Table 1-1) [11, 12]. Since that time, the World Health Organization (WHO) has developed (and amended in 2016) a classification system that is based on cytogenetic and molecular studies [13, 14]. AML is now defined as having >20% blasts in the peripheral blood or bone marrow; with the exception of certain genetic abnormalities, such as t(8;21)(q22;q22),inv(16)(p13.1q22), or t(16;16)(p13.1;q22) and t(15;17)(q22;q12), whose existence is enough for an AML diagnosis, independent of blast proportion [13]. In addition to morphological analysis, cytogenetic analysis of a bone marrow sample is now routinely performed throughout the diagnostic process. The WHO classification considers the various genomic changes observed in AML patients (Table 1-2) including chromosomal aneuploidies (31%), gene mutations (46%) and fusion genes (20%). However, in 3% of cases, no visible genetic mutations are observed [15].

Table 1-1: AML Subtypes in the FAB system

Type	Cells where cancer starts	Name
M0	Immature white blood cells	Undifferentiated acute myeloblastic leukemia
M1	Immature white blood cells	Acute myeloblastic leukaemia with minimal maturation
M2	Immature white blood cells	Acute myeloblastic leukaemia with maturation
M3	Immature white blood cells	Acute promyelocytic leukaemia
M4	Immature white blood cells	Acute myelomonocytic leukaemia
M4 eos	Immature white blood cells	Acute myelomonocytic leukaemia with eosinophilia
M5	Immature white blood cells	Acute monocytic leukaemia
M6	Very immature red blood cells	Acute erythroid leukaemia
M7	Immature platelets	Acute megakaryoblastic leukaemia

Table 1-2: WHO classification of AML

Subtype	AML and related neoplasms
AML with recurrent genetic abnormalities	AML with t(8;21)(q22;q22.1);RUNX1-RUNX1T1
	AML with inv(16)(p13.1q22) or t(16;16)(p13.1;q22);CBFB-MYH11
	APL with PML-RARA
	AML with t(9;11)(p21.3;q23.3);MLLT3-KMT2A
	AML with t(6;9)(p23;q34.1);DEK-NUP214
	AML with inv(3)(q21.3q26.2) or t(3;3)(q21.3;q26.2); GATA2, MECOM
	AML (megakaryoblastic) with t(1;22)(p13.3;q13.3);RBM15-MKL1
	Provisional entity: AML with BCR-ABL1
	AML with mutated NPM1
	AML with biallelic mutations of CEBPA
	Provisional entity: AML with mutated RUNX1
AML with myelodysplasia-related changes	
Therapy-related myeloid neoplasms	
AML, Not Otherwise Specified	AML with minimal differentiation (FAB M0)
	AML without maturation (FAB M1)
	AML with maturation (FAB M2)
	Acute myelomonocytic leukaemia (FAB M4)
	Acute monoblastic/monocytic leukaemia (FAB M5)
	Pure erythroid leukaemia (FAB M6)
	Acute megakaryoblastic leukaemia (FAB M7)
	Acute panmyelosis with myelofibrosis
	Acute basophilic leukaemia

t: translocation, inv: inversion, APL: Acute promyelocytic leukaemia, PML-RARA: promyelocytic leukaemia/retinoic acid receptor-a fusion, GATA2: GATA-binding factor-2, MECOM: MDS1 and EVI1 complex locus protein EVI1. Adapted from Arber *et.al* [12, 13].

1.1.2 Hallmarks of AML

After a quarter-century of dramatic changes in cancer research, scientists now know that cancer is a disease caused by dynamic changes in the genome. Characterization of mutations observed in human and animal cancer cells, and the phenotypes they elicited in experimental models, identified a class of cancer genes with recessive loss of function, known as tumour suppressor genes [16]. The hallmarks of cancer are a set of functional capabilities acquired by human cells as they transition from a normal growth state to a neoplastic growth state. More specifically, these hallmarks are essential for the formation of malignant tumours. To date, ten hallmarks have been identified: evading growth suppressors, replicative immortality, tumour-promoting inflammation, sustained proliferative signalling, resistance to cell death, increased vasculature, genome instability and mutation, invasion and metastasis, reprogrammed cellular metabolism and immune evasion (Figure 1-1) [16].

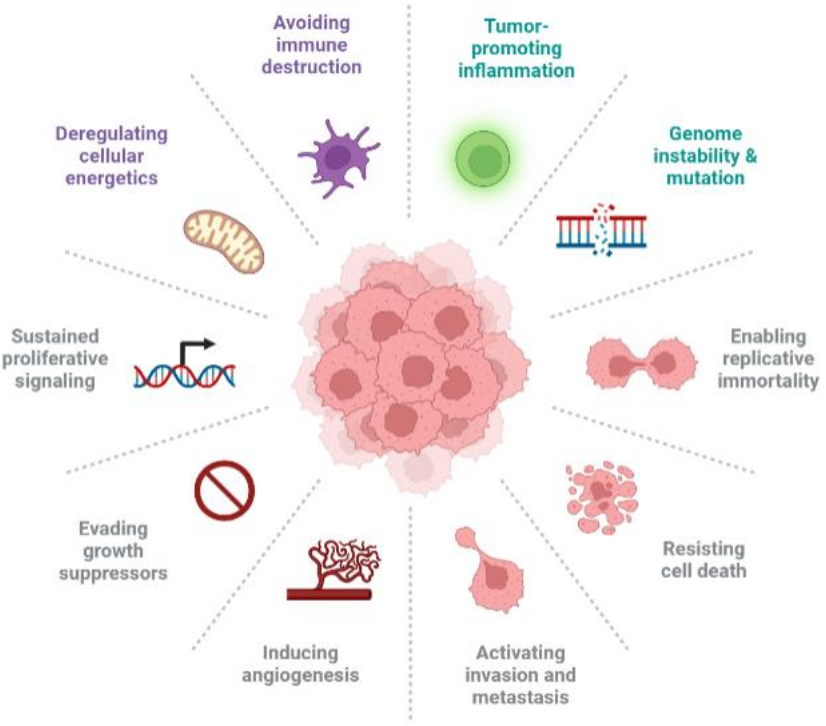

Figure 1-1: The hallmarks of cancer. This figure illustrates the10 known hallmarks of cancer as identified by Hanahan [16]. Figure created by Biorender.

1.1.2.1 Chromosomal instability (CIN)

CIN is one of the hallmarks of a variety of cancers, including AML. This instability presents as an increase in the rate at which cells acquire new chromosomal abnormalities. CIN has been recognised as a crucial mechanism in the development, progression, and relapse of AML [17]. Additionally, CIN pathways have been described in AML, with CIN signatures - chromosome rearrangements, telomere dysfunction, defects in the spindle assembly checkpoint, centrosome dysfunction and assembly of multipolar mitotic spindles, defective DNA damage response - identified in three of the most common forms of AML (*de novo* AML, secondary-AML, and therapy-related-AML) [17]. The risk of developing CIN rises with age because of a deficient DNA damage response

and an accumulation of genetic defects, which reflects the heterogeneity and complexity of the disease [17].

1.1.2.2 Tumour promoting inflammation

It is becoming apparent that inflammation is a defining characteristic of clonal myeloid diseases [18]. For example, myeloid malignancies produce an inflammatory environment containing factors such as interleukin IL-1β, basic fibroblast growth factor (bFGF) and Vascular endothelial growth factor (VEGF-)C [18], which can promote AML blast survival and growth [18]. Moreover, there is a correlation between high plasma levels of VEGF-A and VEGF-C and a poor prognosis in myeloid cancers [19].

1.1.2.3 Tumour immune evasion

Tumours escape the immune system through a variety of methods, including loss of immunogenicity, increased resistance to cell death, or induction of immune tolerance. In AML patients, blasts can escape the immune system through various mechanisms including; (i) impaired T-cell and NK-cell activities by overexpression of inhibitory ligands, such as PD-L1, galectin-9 (Gal-9), cluster of differentiation 155, 112 and 86 (CD155, CD112, CD86); (ii) release of soluble proteins which bind to NKG2D, namely ULBP2, ULBP1, ULBP3 and MICA; (iii) depletion and apoptosis of T cells; (iv) recruitment of regulatory T cells (T_{regs}), Myeloid-derived suppressor cells (MDSCs) and tumour-associated macrophages (TAMs); and (v) modulation of the cytokine microenvironment (e.g. IL-10, IL-35 and transforming growth factor-beta (TGF-β)) within the bone marrow (BM) niche, or other soluble molecules, including reactive oxygen species (ROS) and indoleamine 2,3-dioxygenase-1 (IDO1) [20]. Furthermore, AML blasts can decrease the expression of antigen presentation molecules (human leukocyte

antigen; HLA-I and HLA-II), making them invisible to some immune cells including CD8 and CD4 T cells (Figure 1-2) [20].

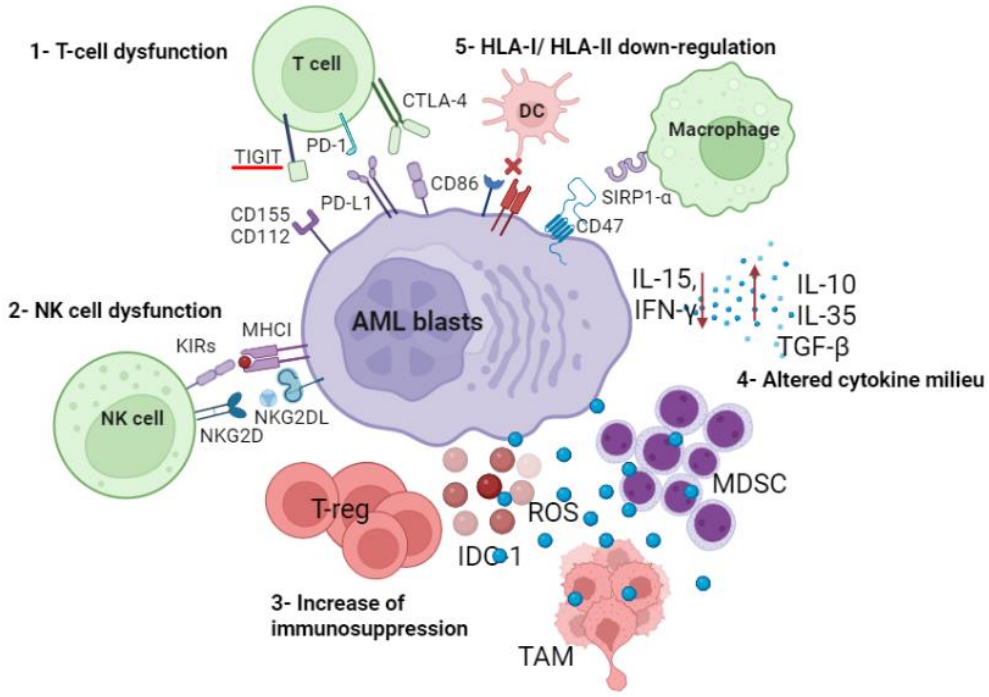

Figure 1-2: AML cell immune evasion. A summary of the most common immune evasion strategies used by AML blasts to escape detection by the immune system. This include (1) T cell dysfunction by overexpressing T cell ligands (i.e. PD-L1, Gal-9, CD86, CD122 and CD155), (2) natural killer (NK) cell dysfunction by releasing NKG2DL via extracellular vesicles, (3) increased immunosuppression through the presence of inhibitory immune cells (Treg, MDSC and TAM), (4) an altered cytokine milieu and the releasing of other factors such as ROS and IDO1, and (5) defective antigen presentation molecules and upregulation of immune checkpoints (CD47), hence escaping recognition from macrophages and T-cells . Figure derived from Tettamanti *et al*. and created using Biorender.

1.1.2.3.1 Loss of immunogenicity

Tumour-associated antigens (TAA) and/or neoantigens specific to tumour cells can be displayed on MHC Class I molecules to promote an adaptive T cell-mediated immune response against the tumour. In tumours that have avoided immune recognition, a decrease in MHC Class I molecules (HLA-A/B/C) has been observed [21]. In addition, changes in antigen presenting mechanisms (for example, antigen transporters, proteasome or mutations in β-2-Microglobumine) leads to reduced HLA expression [22]. Down-regulation of HLA class I and II molecules in various donor transplant situations, prevents the detection of AML blasts by CD8 and CD4 T cells, respectively [20]. However, while evading adaptive immunity, abnormal cells that lack MHC class I expression become targets for NK cell cytotoxicity [23]. However, to avoid NK cell killing, many tumour cells such as melanomas, carcinomas (e.g. colorectal, ovarian, breast, lung and renal) and leukaemia express non-classical MHC Class I molecules (e.g. HLA-E and HLA-G) which inhibit NK cell activity [24].

1.1.2.3.2 Increased resistance to immune cell death

Immune effector cells kill target cells by binding to their death receptors First apoptosis signal (Fas) ligand (FasL) or Tumour necrosis factor-related apoptosis-inducing ligand (TRAIL) or by releasing perforin and granzymes from pre-formed granules [25]. However, tumour cells develop resistance to immune cell killing by (i) releasing exosomes which contain inhibitory proteins such as PD-L1 [22], (ii) increased expression of the anti-phagocytosis protein, CD47, (iii) modulation of immune checkpoints proteins (e.g. Cytotoxic T-lymphocyte-associated protein 4 (CTLA-4) and Programmed cell death protein 1 (PD-1)), and (iv) altered apoptotic

signalling pathways (e.g. increased expression of B-cell leukemia/lymphoma-2 (BCL-2) family members and/or inhibitors of apoptosis proteins (IAP)) [26].

Fas receptor is a death receptor that expressed on a variety of cell types. The binding of Fas to its respective cell surface receptor (FasL) on target cells, stimulates the death of the target cells. FasL can be expressed on various tumour types, including AML [27], allowing them to trigger apoptosis of immune cells [28]. Furthermore, tumour cells can also express the Fas receptor and become susceptible to FasL-mediated apoptosis, therefore, many tumour cells down-regulate Fas from their cell surface [29].

TRAIL expression on immune cells (e.g. T-cells) can also be suppressed in a variety of malignancies, leading to a more aggressive phenotype [30]. Moreover, it has been found that AML patient samples express high levels of decoy receptors e.g.,TRAIL-R3 (DcR1) [31, 32]. Binding of TRAIL to its receptor, TRAIL-R1 (DR4) or TRAIL-R2 (DR5), results in the formation of death inducing signalling complex (DISC), which activates caspase 8 and 3 and promotes apoptosis [33]. DcR1 prevents the formation of DISC, leading to TRAIL-mediated apoptosis resistance [31]. Furthermore, cancer cells also alter the intrinsic apoptosis pathway to avoid immune-mediated killing. For example, in AML overexpression of anti-apoptotic proteins, such as BCL-2 [34], prevents the activation of caspase signalling resulting in resistance to apoptosis [35]. Additionally, high levels of IAPs inhibit both intrinsic and extrinsic apoptosis pathway in a variety of malignancies, including AML [36, 37]. More details relating to apoptosis pathways are outlined in section 1.2.

1.1.2.3.3 Soluble suppressive factors

Many immunosuppressive soluble factors, such as TGF-β, VEGF, IL-10, prostaglandin E_2 (PGE_2) and IDO1, can be secreted by cancerous cells, including AML cells, into the tumour microenvironment (TME). Although TGF-β is a strong growth inhibitor in normal cells, cancer cells have evolved mutations that allow them to avoid its anti-proliferative effects [20, 38]. However, since immune cells continue to be receptive to TGF-β signalling, its release within the TME can inhibit anti-cancer immunological responses [39]. In addition, TGF-β can transform naive T cells into T_{regs}, which suppress effective T cell responses [40]. The secretion of both IL-10 and PGE_2 inhibits the cytolytic effector function of NK cells and the secretion of IFN-γ [41], PGE_2 also interferes with the early phases of DC maturation, resulting in DC dysfunction [42]. Moreover, in addition to its angiogenic capabilities, VEGF is involved in the migration of immature myeloid cells to the TME [43]. Here, VEGF, IL-10, and TGF-β inhibit DC development and function which results in poor activation of a T cell-mediated anti-tumour immune response [44]. Importantly, the ability of AML blasts to secrete immunoinhibitory substances including IL-10, IL35, TGF-β and IDO1 has been linked to the accumulation of T_{regs} in the AML niche [20].

1.1.2.3.4 Induction of suppressive cells

The cellular suppression of cancer immunosurveillance was established decades ago [45]. Since then, various cell types that are capable of preventing effective anti-tumour immunity have been discovered. The proportion of T_{regs} that are present in the TME correlates with a worse prognosis in a variety of malignancies, including AML [20], Hepatocellular carcinoma (HCC) [46], ovarian [47], and breast cancers [48]. T_{regs} block the immune response through a number

of mechanisms, including; perforin-mediated direct cytotoxicity of $CD4^+$ and $CD8^+$ T cells, monocytes, and DC; secretion of immunosuppressive cytokines (IL-10 and TGF-β); and the induction of IDO1 by antigen-presenting cells (APC) [49], which directly suppresses T and NK cell activity [50, 51]. Moreover, T_{regs} can induce the expression of the inhibitory receptor B7-H4 on APC (e.g. monocytes, macrophages, and myeloid DC) making them immunosuppressive [52].

TAMs play a number of functions in the development of cancer, including promoting the invasion and migration of cancer cells, supporting angiogenesis, and suppressing anti-tumour immune responses. It is thought that TAMs account for up to 50% of some tumours [53] and can be classified as either M1 or M2 macrophages. The major TAM population found in the TME has an M2 phenotype and produces IL-10, TGF-β, and PGE_2, which are all factors that lead to immunosuppression [54]. The presence of high numbers of TAMs in the bone marrow of AML patients is associated with poor prognosis [55].

MDSCs are a heterogeneous group of cells that are composed of myeloid progenitor cells and immature myeloid cells. MDSCs, in addition to their immunosuppressive effects, also promote tumour angiogenesis and growth through the production of cytokines and growth factors including, GM-CSF, M-CSF, G-CSF, IL-6, and VEGF [56]. Additionally, MDSCs inhibit immune responses by depleting arginine from the TME; arginine is necessary for T cell proliferation, ζ-chain peptide and TCR complex expression, and the formation of T cell memory [57, 58]. Furthermore, MDSC limit the activity of NK cells and recruit T_{regs} to the TME via both released and membrane-bound forms of TGF-β [56]. MDSCs are increased in the blood and BM of AML patients and have been

associated with poor prognosis, more aggressive disease and drug resistance [59].

1.1.2.4 The bone marrow microenvironment in AML

The microenvironment of the BM has significant influence on the progression of AML and on resistance to treatment. The persistence of leukemic stem cells (LSCs) in the BM after treatment causes disease recurrence. Moreover, interaction of leukemic blasts with the milieu within the BM is a factor in AML treatment resistance [60]. For example, it is well known that the BM microenvironment protects leukaemia cells from treatment through a variety of cytokines and growth factors, including CXCR2, IL6R, Lymphocyte function-associated antigen (LFA), RANK, Platelet-derived growth factor (PDGF), Epidermal growth factor (EGF), VEGF, stem cell factor (SCF), or through cell-cell interactions (e.g. stromal cell-derived factor-1/ C-X-C chemokine receptor type 4, expressed on AML cells, (SDF1/CXCR4), very late antigen-4/ vascular cell adhesion molecule-1 (LA4/VCAM1) and/or CD44/E-selectin interactions) [61-66]. Moreover, interactions within the BM cause resistance to FMS-like tyrosine kinase 3 (FLT3) tyrosine kinase inhibitor [67].

1.1.3 AML prognosis

Prognosis in AML is classified by risk, which may be either favourable, moderate, or adverse. Patients with fusion genes have a better prognosis than those with chromosomal aneuploidies, which may range from moderate to unfavourable risk, depending on the number of aneuploidies present [68]. Genetic changes result in different outcomes, with individuals who present with NRAS and/or RAD21 mutations exhibiting favourable results [69]. By contrast, individuals with mutations in Nucleophosmin (NPM1), isocitrate dehydrogenase 1/2 (IDH1 or

IDH2), DNA Methyltransferase 3 Alpha (DNMT3A), or fms-like tyrosine kinase 3 internal tandem duplication (FLT3-ITD) are considered “adverse risk” and have a larger probability of relapse than patients without these mutations [15, 70, 71]. With this updated categorization and risk stratification in place, prognosis can be predicted more accurately, and therapies can be stratified according to risk.

The symptoms of AML are non-specific, although the majority are linked to the cytopenia that results from the leukemic invasion of the bone marrow. Patients often experience exhaustion, infections, fever and bleeding because the function of leukocytes and platelets is impeded [72]. Death from infection or haemorrhage often occurs within a few months after diagnosis if no treatment is given. AML can cause mortality via multi-organ dysfunction. Additionally, infections may also be fatal [73].

1.1.4 AML treatment

1.1.4.1 Standard therapy

In the last 50 years, intensive chemotherapy and/or palliative care have been the standard treatment for AML. Standard treatment consists of two parts, induction and consolidation therapy. Patients aged < 60 years old, induction treatment is administered to induce complete remission (CR), which is defined as less than 5% blasts in the bone marrow and the recovery of platelets and neutrophils [1]. For most AML patients in the favourable-to-moderate risk group, the 7+3 regimen has been the standard treatment since 1973 (Table 1-3) [72, 74]. This therapy consists of a continuous infusion of the nucleoside analogue, cytarabine (ara-c), for 7days alongside an infusion of daunorubicin, for 3 days [75]. Of individuals *with de novo* AML who receive induction treatment, 60-80% of patients aged <60 will achieve a CR but this is reduced to 40-60% in patients

>60 [75]. A small population of leukaemia cells persist after induction; hence, consolidation treatment is used to avoid relapse and enhance OS [2].

Consolidation treatment often consists of high doses of ara-c, with around 40% of young patients achieving CR for about 5 years [76]. This therapy is administered every 4 weeks for a total of 3 to 4 cycles. Also, an allogeneic hematopoietic stem cell transplant (allo-HSCT) can be used in the consolidation phase and is the most effective treatment to obtain a CR. Nevertheless, it is associated with a high risk of treatment-related toxicity (e.g. graft-versus-host disease (GVHD)) and death [77]. Therefore, allo-HSCT is only used for younger patients who have a compatible donor and without comorbidities present [75, 78]. Unfortunately, around 50% of younger patients, and 80-90% of older patients treated with standard therapy will relapse despite intensive induction and consolidation treatment, at which point patients typically succumb to the illness [79] [80].

Table 1-3: Treatment system according to cytogenetic and molecular prognosis

Risk status	Induction	Post-remission
Better-risk cytogenetics	Standard dose cytarabine (100-200 mg/m^2) intravenously for 7 days in combination with idarubicin (12 mg/m^2) or daunorubicin (90 mg/m^2) for 3 days.	High-dose cytarabine 3 g/m^2 every 12 hrs on days 1, 3, 5 (x 3-4 cycles). 1 to 2 cycles of high-dose cytarabine - based consolidation followed by autologous HSCT.
Intermediate-risk cytogenetics	Low-intensity therapy (azacytidine, decitabine). Intermediate-intensity therapy (clofarabine).	Standard dose cytarabine (100-200 mg/m^2) infusion for 7 days accompanied with idarubicin (12 mg/m^2 for 3 days) or daunorubicin (90 mg/m^2) for 3 days.
Treatment-related disease or poor-risk cytogenetics	Standard-dose cytarabine (100-200 mg/m^2) for 7 days with idarubicin (12mg/m^2) or daunorubicin (45-60 mg/m^2) for 3 days.	Combination 5-azacytidine, decitabine Clofarabine. Best supportive care (hydroxyurea, transfusion support).

1.1.4.2 Emerging Therapies for AML

1.1.4.2.1 Targeted therapies

During the last decade, several developments including targeted treatments, immunotherapy, and antibody-drug conjugates, have provided alternative therapeutic options for AML [81]. These innovative treatments are most suited for patients who fall into the intermediate-to-high risk category and who would not be eligible for standard chemotherapeutics [82].

A worse prognosis is related with FLT3 gene mutations, which are found in 30% of all *de novo* AML cases. Midostaurin, a FLT3 inhibitor that was approved in 2017, is one of several drugs tested in clinical trials. Midostaurin was proven to boost CR rates and OS, and reduced the risk of death to 22% when combined

with 7+3 induction treatment, in comparison to 7+3 therapy used in isolation [83, 84].

IDH1 and 2 mutations are also an effective genetic target in AML, and they are present in ~20% of AML patients [85]. Ivosidenib and enasidenib are small-molecule inhibitors of mutated IDH1 and IDH2, respectively, and they have been approved for the treatment of refractory AML with mutated IDH1/2 [86]. In this patient group, enasidenib improved CR by ~20% and increased the OS rate in ~40% of patients [87].

BCL-2 is an anti-apoptotic protein that is overexpressed in AML cells and LSCs and it enhances the viability of AML cells and LSCs [88, 89]. Venetoclax targets BCL-2 and enhances apoptosis (see section 1.2.4 for more details). Whilst venetoclax has only a modest effect as a single agent compound [90], when administered in combination with cytotoxic hypomethylating drugs, such as decitabine or azacitidine, 67% of elderly AML patients achieved a CR [91].

1.1.4.2.2 Immunotherapy

In addition to targeted treatments, immunotherapies also show potential for the treatment of AML; yet, their clinical development is still under investigation. One promising immunotherapy is IFN-α, which was investigated in the early era of immunotherapy because of its cytotoxic impact on cancer cells including myeloid leukaemia [92]. IFN-α has been evaluated for use in three distinct therapeutic contexts: (1) induction of AML remission; (2) as a rescue therapy for patients who relapsed after HSCT; and (3) as a post-remission treatment to prevent disease relapse [93]. Aside from direct cytotoxicity, IFN-α also limits the release of growth cytokines, suppresses cell proliferation, enhances the immunogenicity

of AML cells [94], and has the potential to promote an anti-tumour immune response, particularly the formation of adaptive anti-tumour immunity [92].

Using a different immunotherapy strategy, PD-1 and CTLA-4, are the most two studied immune checkpoints for the treatment of cancer. Monoclonal antibodies that target immune checkpoints can be used to re-activate immune cells (e.g. anti-tumour T cells) and induce an anti-tumour immune response [95]. Using anti-PD-1, great success has been obtained against a variety of lymphomas, most notably Hodgkin's lymphoma where up to 17% of patients had CR in clinical studies, with 70% displaying a partial response and 13% having stable disease [96].

Nivolumab is a monoclonal antibody that binds to PD-1 and it is currently being tested in a phase-II clinical study in AML. Promising results have been observed for individuals who have relapsed or are resistant to standard treatment options, with 71% of patients obtaining a CR for 6 months [97]. Another study by Albring *et al*. showed that when nivolumab was administered to three AML patients who had relapsed after receiving allo-HSCT, a CR was achieved in the first patient, disease was stable in the second patient, and the treatment was ineffective in the third patient [98, 99].

Other monoclonal antibodies are now being developed for therapeutic use and these include magrolimab, which binds to the anti-phagocytic protein, CD47. CD47 is recognised as the primary macrophage checkpoint, and macrophages are essential for innate immune responses. CD47 is overexpressed in many malignancies including AML allowing tumours to avoid phagocytosis by macrophages. Blocking CD47 results in the eradication of the disease and pre-

clinical studies have demonstrated a strong anti-cancer action in a variety of hematologic cancers, including AML [100].

1.2 Targeting apoptosis for cancer treatment

1.2.1 Apoptotic pathway

The apoptotic process in cells is evolutionally conserved and is necessary to develop and maintain tissue homeostasis. Programmed apoptosis can prevent tissues from being transformed through oncogenesis; however, cancer tissues can develop resistance to apoptosis and chemotherapy treatment [101]. Cancerous cells frequently show alterations in pathways which regulate apoptotic activity [102] and anti-apoptotic proteins are often over-expressed [103]. Cell apoptosis can occur through two different pathways; intrinsic or extrinsic (Figure 1-3) [104]. Promotion of intrinsic apoptosis occurs through intracellular signalling of stress, such as growth factor starvation, oxidative stress or damaged DNA, causing the mitochondrial external membrane to become permeable. In comparison, the extrinsic pathway occurs when extrinsic ligands bind to receptors which induce death, these can include TRAIL and Fas receptors, as well as the TNF receptor (TNFR). The extrinsic pathway leads to the production of a DISC and caspases -3, -8 and -10 are activated. Promotion of the intrinsic pathway takes place when cytochrome c is released from the mitochondria and the apoptosome complex is produced, thus activating caspase -3, -9, -6 and -7; the intrinsic pathway is strongly regulated by both anti- and pro-apoptotic Bcl-2 protein family members [105]. A number of apoptosis-suppression processes can be harnessed in cancerous cells, including: (i) inhibiting the expression of death receptors FAS and DR5 at the surface of the cell [106], (ii) the balance of anti- and pro-apoptotic Bcl-2 family members can be dysregulated so anti-apoptotic

proteins are overexpressed while pro-apoptotic proteins are downregulated [107], and (iii) cancer cells can also enhance the expression and function of IAPs [108]. Based on the above, attention has turned to modulating apoptotic pathways within the cancerous cell to facilitate the induction of apoptosis as a potential therapeutic strategy. This is approached through targeting BCL-2 family members and IAPs [109, 110].

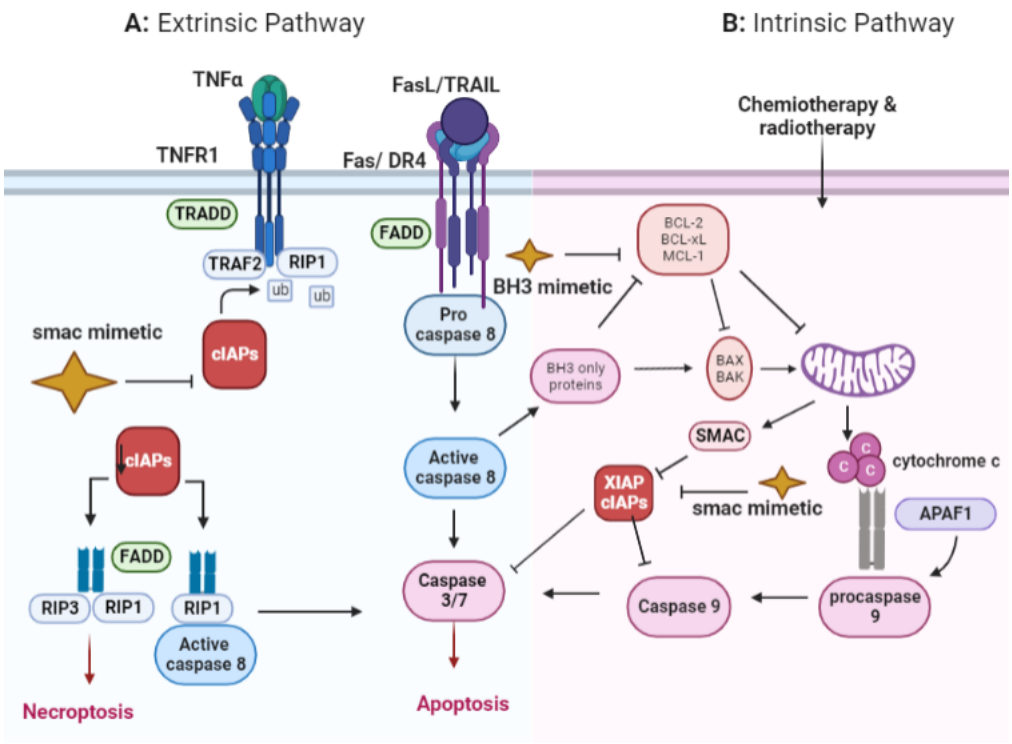

Figure 1-3: The intrinsic and extrinsic apoptotic pathway. **A**: The extrinsic apoptotic pathway is activated when death receptors DR4, TNFR1 or Fas are activated by their respective ligands. This causes the recruitment of the adaptor protein FAS-associated death domain (FADD), activation of caspases-8, -3 and -7 and apoptosis. Activation of TNFR1 receptor blocks ubiquitination of receptor-interacting protein 1 (RIP1), thus causing RIP1 to form a pro-apoptotic cytoplasmic complex with FADD and caspase-8. Additionally, non-ubiquitinated RIP1 interferes with FADD and receptor-interacting protein 3 (RIP3) to cause necroptosis through a caspase independent pathway. cIAP ubiquitylation of RIP1 prevents the development of death-inducing complexes, Smac mimetics and BH3 mimetics can antagonize IAPs and anti-apoptotic proteins, respectively, and sensitize cancer cells to apoptosis inducing factors. **B**: Stimuli such as irradiation, treatment with chemotherapy or elimination of the growth factor activates the intrinsic cell death pathway. Activation of pro-apoptotic BH3-only members (e.g. Bad, Bmf, PUMA, Bim, Bid, Bik, Hrk, and Noxa) neutralises the anti-apoptotic proteins (e.g. BCL-2, Bcl-xL, Bcl-w, A1 and MCL-1) and release BAX and BAK (pro-apoptotic Bcl2 family members). Release of BAX and BAK causes the release of cytochrome *c* and second mitochondrial-activator of caspases (Smac) from the mitochondrial membrane. These events result in Apaf-1–mediated caspase-9 activation, caspase-3 and caspase-7 activation and apoptosis. XIAP/cIAPs can inhibit caspases 3, 7 and 9 activation and regulate cell death. Figure derived from Vucic & Fairbrother [110] and created using Biorender.

1.2.2 Inhibitors of Apoptosis Proteins (IAPs)

IAPs proteins are an alternative class of anti-apoptotic protein which inhibit programmed apoptosis, as they bind, and inhibit the action of a number of proteins involved in the apoptotic signalling cascade (e.g. caspase 3, 7 and 9) (Figure 1-3) [111]. Eight different IAPs have been detected in mammals [112] (Figure 1-4) which are; cellular IAP1 (cIAP1), cellular IAP2 (cIAP2), X-chromosome-linked IAP (XIAP), testis-specific IAP (Ts-IAP), neuronal apoptosis inhibitory protein (NAIP), BRUCE, SURVIVIN and LIVIN. The most frequently researched in the context of cancer research are cIAP-1, cIAP-2 and XIAP [113]. IAPs are predominant in an estimated 3% of cancers [114], where some are capable of presenting as proto-oncogenes which originate from genetic modifications in numerous types of cancers [115] including cervical cancer [116], liver cancer [117], prostate cancer [118] and AML [119]. XIAP interacts with caspases -3, -7, -9 and Smac [120], and cIAP1/2 interacts with Smac and TRAF2 proteins [121]. The ability of IAPs to support the survival of cells following chemotherapy and Tumour Necrosis Factor superfamily (TNFSF) ligands, is associated with poor prognosis and unsuccessful therapeutic measures in various forms of cancers [122]. For instance, the expression of XIAP is connected with resistance to cisplatin in ovarian cancer [123], associated with disease severity in AML [124], and is also a predictive biomarker in renal cell carcinoma [125].

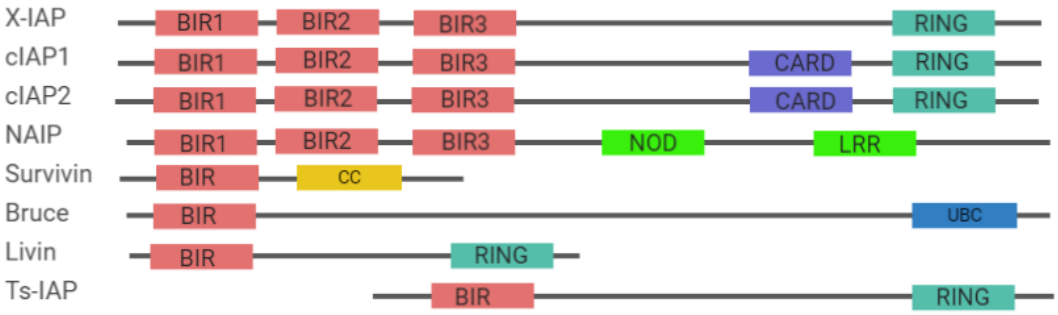

Figure 1-4: Domain structure of the mammalian IAPs members. The domain group for the eight mammalian IAPs is shown. The presence of at least one baculovirus IAP repeat (BIR) domain is a defining feature of IAP members. IAPs have either one (survivin, BRUCE, livin and Ts-IAP) or three tandem amino-terminal BIR domains (XIAP, cIAP1, cIAP2 and NAIP). Several IAPs contain an E3 ubiquitin ligase zinc-finger (RING) domain at the carboxy terminal. cIAP1 and cIAP2 have a caspase-recruitment (CARD) domain in the linking region between the BIR and RING domains. NAIP has a nucleotide-binding and oligomerization (NOD) domain as well as a leucine-rich repeat (LRR) domain. BRUCE contains a ubiquitin-conjugate (UBC) domain, and no RING domain whilst survivin contains a coiled-coil (CC) domain. Figure adapted from LaCasse *et al*. and created using Biorender [126].

1.2.3 Smac mimetics

Smac mimetics are designed on a rational basis, using the characteristics of the Smac protein, which is an endogenous pro-apoptotic protein. When Smac is released from the mitochondria, it binds to a number of IAPs and acts as an antagonist (Figure 1-3). Thus, targeting Smac:IAPs interactions has been investigated as an anti-cancer strategy due to their regulation of apoptosis [115]. Clinical assessment of a number of Smac mimetics for the treatment of a range of cancers, including multiple solid tumours, lymphomas, multiple myeloma (MM) and AML [127] is in progress in either early or mid-stage clinical trials. The benefits of Smac mimetics includes reduced drug resistance and the potential for increased efficacy when used in combination with established (and/or future) therapies which rely on activation of pro-apoptotic pathways [127].

1.2.3.1 Mechanism of action of Smac mimetics

Smac mimetics, including BV-6 and LCL161, are capable of targeting cIAPs and XIAP and can be used therapeutically to abrogate the inhibitory mechanisms which prevent apoptosis [128]. When IAPs are modulated by Smac mimetics, significant impacts are observed, specifically Smac mimetics cause the cancerous cell to become sensitive to: (i) extrinsic apoptosis induced by death-inducing ligands, such as tumour necrosis factor alpha (TNF-α), TRAIL and FAS, causing cell death via necroptosis or apoptosis [128], and (ii) intrinsic apoptosis, induced by agents such as chemotherapy and/or radiotherapy, which lead to DNA damage and oxidative stress.

Smac mimetic therapy causes cell death mainly through pathways regulated by the death receptor family (e.g. TNFα, TRAIL and Fas) [129]. This is important since TNFα is a target gene of nuclear factor kappa B (NF-kB), whose signalling pathways are also influenced by Smac mimetics. For example, depletion of c-IAP can cause activation of the non-canonical NF-kB pathway due to NIK aggregation [130]. The recruitment of NF-kB by Smac mimetics results in autocrine release of TNFα, which engages TNFR1, and subsequently activates RIP1, FADD and caspase-8 mediated apoptosis [130, 131]. Furthermore, a study by Marschall and Fulda has demonstrated that BV-6 in combination with temozolomide (TMZ) stimulates the expression of IFN-β in an NFκB-dependent manner and causes cell death in glioblastoma cells [132]. Also, LCL161 demonstrated anti-tumour activity in individuals with refractory MM, which was mediated by increased IFN signalling and the promotion of a pro-inflammatory responses [114].

1.2.3.2 Types of Smac mimetics

In recent years, there have been formulations of several Smac mimetics with divergent chemical characteristic. Two types of Smac mimetics; monovalent (e.g.

LCL161) and bivalent (e.g. BV-6) have been reported. The bivalent compounds consist of two N-terminal amino acid residues Ala-Val-Pro-Ile (AVPI) binding motif mimetics bound together by a linker, whereas the monovalent substances mimic the binding of a single AVPI binding motif [133], and mimic the interaction of the N-terminus of Smac with the BIR3 domain of XIAP or cIAPs to enhance apoptosis [134]. Monovalent and bivalent Smac mimetics vary in their pharmacological activities, while intravenous (i.v) administration is required for bivalent compounds, monovalent compounds are orally administrated [135]. Nevertheless, the bivalent variation of Smac mimetics have elevated cytotoxic effects compared to their structurally associated monovalent IAP antagonists [134]. Li *et al*. designed the first bivalent Smac mimetic (named compound 2) with the potential for strong binding and blocking of cIAP-1, cIAP-2 and XIAP. Furthermore, when combined with TRAIL and TNF-α this led to synergistic activation of caspases and induced apoptosis in both *in vitro* and *in vivo* [127]. Comparing SM-164 (a bivalent Smac mimetic), with a corresponding monovalent compound (SM-122) determined that bivalent SM-164 induced greater apoptosis at lower concentrations in the HL-60 leukaemia cell line [136]. Comparable findings have also emerged for compound 3, a bivalent Smac mimetic targeting XIAP [137].

1.2.3.3 Pre-clinical efficacy of Smac mimetics

In solid malignancies several studies have shown that treatment of breast cancer cells with Smac mimetics as a single monotherapy [138, 139], or in combination with other cancer treatments [140, 141] can substantially decrease cell cycle progression and increase apoptosis. For example, treating cancer cell lines, including the breast cancer line MDA-MB-231, as well as the melanoma line A2058, with Smac mimetics (isostere 8) enhanced doxorubicin-induced

apoptosis [138]. In addition, the combination of SM-164 with TRAIL, as well as other death-inducing inflammatory cytokines, including TNFα, demonstrates synergistic cytotoxicity when tested *in vitro* on various cancer cell lines (breast, prostate, and colon cancer) [142]. Brands *et al*. also confirmed that combination of LCL161 with FasL leads to cIAP1 degradation and significantly induced cell death in five different Head and neck squamous cell carcinoma (HNSCC) cell lines [143]. Interestingly, the combination of LCL161 with immune checkpoint inhibitors (e.g. anti-PD-1) has also been reported to be effective in pre-clinical models, including multiforme glioblastoma [144]. Here, Beug *et al*. suggested multiple complimentary mechanisms of action between Smac mimetics and anti-PD-1, in particular, blockade of the PD-1/PD-L1 axis enhanced T cell activation, whilst, depletion of the IAPs antagonism of XIAP, resulted in enhanced Granzyme B (GrzB)-mediated death [144]. Moreover, decreased expression of cIAPs increased the production of TNF-α by T-cells, and TNF-α-induced cell death was potentiated by LCL161 [144].

In haematological malignancies, pre-clinical studies in different cancer types, including childhood acute leukaemia and chronic lymphoblastic leukaemia have shown that Smac mimetics can sensitise cancer cells for cell death in response to various cytotoxic stimuli, such as TRAIL and TNF-α, γ-irradiation or chemotherapies (e.g. alkylating agents dacarbazine and temozolomide) [145, 146]. Moreover, treating primary cancer cells sourced from relapsed refractory MM patients with the Smac mimetic, LBW242, significantly induced apoptosis in drug resistant cells and was association with caspase-8, -9, and -3 activation, as well as Poly (ADP-ribose) polymerase 1 (PARP-1) cleavage. In addition, in a MM xenograft mouse model, LBW242 alone, or combination with additional therapies

(e.g. TRAIL or proteasome inhibitors), induced additive anti-MM activity, caused tumours to regress and prolonged survival [147].

Importantly, the combination of BV-6 and ara-c synergistically enhanced cell death in AML cell lines, which was dependent on TNF-α/ TNFR1 signalling and the autocrine/ paracrine TNF-α loop; this combination induced caspase activation, DNA fragmentation and mitochondrial disruption [148]. Moreover, birinapant treatment activated the extrinsic cell death pathway in AML cells when used in combination with the demethylating agents (5-Aza or Decitabine (DAC)) and synergistically enhanced AML apoptosis [149]; birinapant as a monotherapy increased the survival of mice harbouring AML xenografts (Molm13/ NSG mice) and the survival benefit was improved by 5-Aza co-treatment [149]. In this study, birinapant decreased cIAP1 expression and activated the non-canonical NFκB pathway to produce TNF-α, while the demethylating agent increased pro-apoptotic caspase-8 and XIAP-associated factor 1 (XAF1), and further decreased anti-apoptotic IAPs [149]. Additional combination approaches tested in AML have shown that: (i) TNF-α-dependent apoptosis was enhanced by birinapant and this was further potentiated by p38 inhibitors, which enhanced TNF-α production [150], and (ii) necroptosis was potentiated by birinapant when used in combination with the caspase-8 inhibitor, emricasan/IDN-6556 [151]. Importantly, Smac mimetics have transitioned to clinical trials for the treatment of both solid and haematological malignancies, this progression is discussed further in section 1.2.3.4.

1.2.3.4 Clinical efficacy of Smac mimetics

Several researchers have reported the efficacy of Smac mimetics in clinical trials and a summary of clinical trial activity is shown in Table 1-4. A phase I study has shown that birinapant caused the inhibition of cIAP1 and induced apoptosis upon

activation of caspase 8 in patients with advanced solid tumours and lymphomas, including non–small cell lung cancer (NSCLC), colorectal cancer and liposarcoma [152]. In addition, birinapant was generally well tolerated at doses ranging from 0.18 to 47 mg/m^2 [152]. Following administration of GDC-0917 in patients with mucosa-associated lymphoma or ovarian carcinoma, two patients (4.8%) had full remissions and four patients (9.5%) had stable disease for ~3 months [153]. Confirmed tumour colon cancer regression was also reported following HGS1029 treatment in one patient (2.3%) and two patients (4.5%) with NSCLC had stable disease for six months [154, 155]. Moreover, one patient (3.2%) demonstrated a decrease in melanoma metastasis by 11% and five patients (17%) had stable disease upon Debio1143 treatment [135, 156].

Importantly, Infante *et al.* reported that LCL161 antagonised the action of IAPs in patients, was well tolerated up to the maximum dose of 1,800mg and induced cell death in patients with advanced solid tumours including rectum, colon, pancreas and lung [157]. Moreover, LCL161 also induced rapid release of cytokines with dose-dependent increases of MCP1, IL8, IL10 and TNFα [157]; however, some adverse effects were also reported such as nausea, vomiting, diarrhoea, fatigue, anorexia and cytokine release syndrome, when higher doses were administrated [157]. Notably, Lueck *et al*. demonstrated that the Smac mimetic, BV-6, could activate TNFR1 and NFκB signalling in AML patients and induce apoptosis [158]. Furthermore, in most patients, a combination of BV-6 with the standard chemotherapy drug ara-c exerted additive killing effects [158]. Similarly, another Smac mimetic, AEG35156, was also efficacious in decreasing XIAP levels in circulating myeloid leukaemia blasts at a dosage of 350 mg/ m^2, subsequent to apoptosis induction [159].

Table 1-4: Summary of Smac mimetics in clinical trials.

Smac mimetic	Phase of development	Combination treatment	Tumour type	Trial number and/ references	Outcome
LCL161	Phase I/II		Advanced-stage solid tumours, breast cancer, CRC	NCT01098838 [157, 160, 161]	Well tolerated
LCL161	Phase II		Polycythaemia vera, myelofibrosis	NCT02098161 [162]	Well tolerated
LCL161	Phase I	Everolimus (mTOR inhibitor), panobinostat (HDAC inhibitor)	CRC, NSCLC, triple negative breast cancer	NCT02890069	No results posted
Debio 1143	phase I	Avelumab	Advanced solid malignancies	NCT03270176 [163]	Mild toxicity
Debio 1143 (AT-406)	Phase I		Advanced solid tumours and lymphomas	NCT01078649 [156]	Safely administered
Debio 1143	Phase Ib/II	Anti-PD-1 (Nivolumab)	Solid tumours	NCT04122625 [164]	Well tolerated
Birinapant	Phase II	pembrolizumab	Advanced-stage solid tumours	NCT02587962 [165].	Safe and tolerable
Birinapant	Phase I		Head and neck, squamous cell carcinoma	NCT03803774 [166]	Well tolerated
Birinapant (TL32711)	Phase II		Relapsed Platinum Resistant or Refractory Epithelial	NCT01681368 [167]	Well tolerated
BI 891065	Phase II	Anti-PD1 (BI 754091)	Advanced/ metastatic malignancies	NCT03166631	No results posted
AEG35156	Phase I/II		AML	NCT00363974 [159]	desirable efficacy
HGS1029	Phase I		Solid tumour	NCT00708006 [155]	Well tolerated
GDC-0917	Phase I		Refractory solid tumours or lymphoma	NCT01226277 [153]	favourable safety

CRC, colorectal cancer cells; MM, multiple myeloma; NHL, non-Hodgkin lymphoma; NSCLC, non-small-cell lung carcinoma; SCLC, small-cell lung carcinoma.

1.2.4 BCL-2 family members

The BCL-2 protein family has at least seventeen members, each with specific homologous regions, called BCL-2 Homology (BH) domains. This group contains 3 functional sub-groups, which are (i) BH3-only, (ii) pro-apoptotic, and (iii) anti-apoptotic [168]. Four BH domains (BH1, BH2, BH3 and BH4) are conserved in the anti-apoptotic subgroup, whose members include A1, BCL-2, MCL-1 and Bcl-xL. The pro-apoptotic subgroup also encodes BH domains, e.g. BAK and BAX. The BH3-only group contains numerous pro-apoptotic proteins; Bid, Bad, Bim, Bik, Hrk, Bmf, PUMA and Noxa [169]. Importantly, these three protein groups interact together to regulate cell apoptosis. The interaction of BH3-only proteins with distinct BCL-2 family proteins is illustrated in Figure 1-5. When pro-survival mode is active, BAK/BAX interact with anti-apoptotic proteins and apoptosis is inhibited. By contrast, when apoptosis is activated by stress pathways, as well as upstream signals [170, 171], binding of BH3-only proteins to BCL-2 family proteins causes [172, 173] BAK/BAX to dissociate from anti-apoptotic proteins. This exposes BAK/BAX BH3 domains and causes the formation of oligomers, which can break through the mitochondrial lipid bilayer causing the mitochondria to herniate, the release of cytochrome *c* and activation of initiator caspases (Figure 1-3 and Figure 1-5) [174]. BH3 mimetics are small compound that mimic the interaction of BH3 only proteins, thus binding to anti-apoptotic BCL-2 family proteins and inducing apoptosis (Figure 1-3).

A

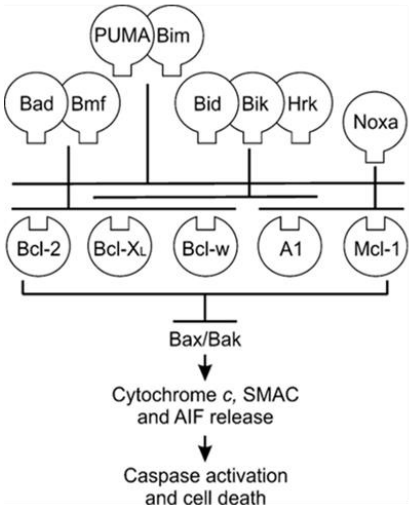

B

BH3 mimetic	Targets
ABT-199	BCL-2
ABT-263	BCL-2, Bcl-xL and Bcl-w
AZD5991	Bcl-xL
A-1155463	Bcl-xL
MIK665	Bcl-xL
ABBV-155	Bcl-xL
A-1210477	MCL1
S63845	MCL1
BI-97D6	MCL1
EM20-25	BCL-2
GX15-070	BCL-2
cpm-1285	BCL-2
S55746/BCL201	BCL-2
APG-1252	BCL-2/Bcl-xL
S44563	BCL-2/Bcl-xL
BCL2-32	BCL-2/Bcl-xL
BM1197	BCL-2/Bcl-xL
ABT-737	BCL-2, Bcl-xL and Bcl-w

Figure 1-5: BH3-only proteins have specific affinities for anti-apoptotic proteins. A: The anti-apoptotic proteins (BCL-2, BCL-xL, BCL-W, A1 and MCL-1) enhance cell survival by blocking the mitochondrial outer membrane from being permeabilized by the down-stream pro-apoptotic proteins, BAX and BAK. The permeabilization of the mitochondrial outer membrane leads to the release of cytochrome c and other proteins, which causes the activation of the caspase cascade and leads to cell death. The BH3-only pro-apoptotic proteins enhance death by selectively inhibiting the action of anti-apoptotic proteins and/or by directly activating the BAX/BAK pathway. **B**: A list of BH3 mimetics that are mentioned in this study and their molecular targets.

1.2.4.1 BH3 mimetics and clinical trials

In the last several years, BH3 mimetics have emerged as promising treatments for many malignancies including hematological cancers, both as monotherapy or combined with other treatments [175]. Loriot *et al*. confirmed the efficacy of BCL-2/ Bcl-xL inhibitor, S44563, in small-cell lung carcinoma (SCLC) cells. S44563 caused apoptosis and sensitised SCLC cells to radiation. Moreover, the combination of S44563 with cisplatin significantly suppressed tumour growth and increased survival in a xenograft mouse model of SCLC [176]. Another BCL-2/ Bcl-xL inhibitor, Bcl2-32, showed a potent efficacy against acute lymphocytic leukaemia as a monotherapy, and enhanced the efficacy of standard

chemotherapy against non-Hodgkin lymphoma (NHL) in xenograft mouse models [177]. Furthermore, Ye *et al*. demonstrated the effectiveness of BCL-2/Bcl-xL inhibitor, BM1197, in CRC cell lines. BM1197 treatment activated caspase-3 and induced mitochondria-dependent cell death [178]. In addition, the MCL1 inhibitor, S63845, showed a cytotoxic effect against MM, leukaemia and lymphoma cells dependent on BAX/BAK-mediated apoptosis [179]. Another MCL1 inhibitor, A-1210477, induced apoptosis of MM and NSCLC cells. Moreover, A-1210477 synergized with navitoclax (ABT-263; BCL-2, Bcl-xL, and BCL-w inhibitors) and caused cell death in a variety of cancer cell lines (e.g. Oesophageal carcinoma, head and neck carcinoma and triple-negative breast cancer) [180]. Another study by Tao *et al*. using a different BH3 mimetic showed that the administration of Bcl-xL inhibitor, A-1155463, into H146 small cell lung cancer bearing SCID mice significantly inhibited tumour growth [181].

One of the first BH3 mimetics to be developed was ABT-737, which had high binding affinity to BCL-2, BCL-w and Bcl-xL [182]. The fact that ABT-737 could not be taken orally was the most significant disadvantage of the drug, this resulted in the development of navitoclax [183]. Navitoclax also targeted BCL-2, Bcl-xL and BCL-w, and its efficacy was encouraging in clinical studies; however, chronic lymphoblastic leukaemia (CLL) and NHL patients treated with navitoclax experienced thrombocytopenia following Bcl-xL inhibition [184, 185]. To date, the most promising BH3 mimetic in clinical development is the BCL-2-specific inhibitor, venetoclax (ABT-199), which causes less thrombocytopenia. ABT-199 was successful in clinical trials and was rapidly approved for the treatment of CLL, with investigations now being translated to other malignancies, including AML [175, 186, 187]. An overview of BH3 mimetic clinical trial activity is shown in Table 1-5.

Table 1-5: Summary of BH3 mimetics in clinical trials

Agent		Phase of development	Tumour type	Trial number and/ refs	Outcome
BCL-2 And Bcl-xL inhibitors	ABT-263	Phase I/II	CLL, advanced-stage solid malignancies, melanoma, NSCLC	NCT02079740, NCT02520778, [188, 189]	Mild toxicity
	APG-1252	Phase I/II	advanced-stage solid tumours and SCLC	NCT03387332 [190]	Well tolerated
BCL-2 inhibitors	ABT-199	Phase I-II	AML,	[90, 191]	Acceptable tolerability
	ABT-199	Phase I	CLL	[192]	Well tolerated
	S55746/BCL201	Phase I	NHL, AML	NCT02920697, [193]	Partial response
	S55746/BCL201	Phase 1	Lymphoma	NCT02603445 [194]	No result posted
	APG-2575	Phase I	CLL, NHL	NCT03913949, NCT03537482 [195, 196]	Well tolerated
Bcl-xL inhibitors	ABBV-155	Phase I	Solid tumours	NCT03595059 [197]	Acceptable tolerability
	MIK665	Phase I	AML, NHL, MM	NCT02992483, NCT02979366, NCT03672695[198, 199]	No result posted
	AZD5991	Phase I	NHL, AML, ALL, MM	NCT03218683 [200]	Ongoing

ALL , acute lymphoblastic leukaemia; AML , acute myeloid leukaemia, CLL , chronic lymphocytic leukaemia; CRC, colorectal cancer cells; MM, multiple myeloma; NHL , non- Hodgkin lymphoma; NSCLC, non- small- cell lung carcinoma; SCLC, small- cell lung carcinoma.

Promising clinical studies have resulted in the approval of venetoclax to treat AML patients in an incredibly short timescale, beginning with its first description in 2013. Specifically, in 2020 venetoclax was approved by the Food and Drug Administration (FDA) for use in combination with hypomethylating agent (HMA) or low-dose ara-c (LDAC) in elderly AML patients [201].

Table 1-6: The progression of ABT-199 from the experimental stage to the clinical setting in AML identified by Parry *et al.*

1993	High BCL-2 expression associated with poor response to AML therapy	[202]
1995	BCL-2 present in 87% of new AML cases and 100% at relapse	[203]
1997	High BCL-2 expression correlates with CD34 positivity and CR rate in AML patients	[204]
1999	BCL-2 overexpressed in AML cells compared with healthy cells	[89]
2000	First description of BCL-2 binding peptides inducing apoptosis in AML	[205, 206]
2004	BCL-2 required for myeloid leukaemia cell maintenance in murine model	[207]
2005	First described of BCL-2 and Bcl-xL inhibitors (ABT-737)	[183]
2008	First described orally available BCL-2 and Bcl-xL inhibitors (ABT-263)	[184]
2012	Combination of ABT-737 with azacitidine synergistically induce apoptosis in AML cells.	[186]
2013	ABT-199 was first proven to be effective in AML cell lines and to be safe for platelets. Phase II research of ABT-199 as a monotherapy for AML	[208] [90, 209]
2014	Pre-clinical evaluation of ABT-199 as a monotherapy in AML, MLL-rearranged AML and APL. Phase 1b/2 clinical trials for ABT-199 with LDAC in AML patients .	[210, 211] [191]
2015	ABT-199 particularly effective in AML with IDH1/2 mutations.	[186]
2016	FDA approved ABT-199 in combination with HMA in older, treatment-naïve AML patients . Phase 3 clinical studies of the combination of ABT-199 and azacitidine in AML patients. Pre-clinical study show ABT-199 resistance in AML cells can be reversed by ara-c.	[186] [201] [212]
2017	Phase 3 clinical studies for ABT-199 and LDAC in AML patients	[213, 214]
2018	Accelerated FDA approval for ABT-199 in combination with HMA or LDAC when chemotherapy isn't practicable.	[186]
2020	Full FDA approval for ABT-199 in combination with HMA or LDAC when chemotherapy isn't practicable	[186]

1.2.4.2 Pre-clinical development of BH3 mimetics for AML

Recent years revealed the importance of BCL-2 family members in haematological malignancies and have prompted extensive and ongoing research to determine whether this pathway can be targeted to eradicate malignant cells. Several pre-clinical and clinical studies tested different classes of BH3 mimetics in a variety of cancers, including AML [175]. Moujalled *et al*. demonstrated the anti-leukemic activity of the BCL-2 inhibitor, S55746, was enhanced when used in combination with the MCL-1 inhibitor, S63845, against chemo-resistance primary AML cells. The efficacy of this combination approach was dependent on BAX/BAK, and co-targeting BCL-2 and MCL-1 was more effective against leukemic cells than normal cells. Moreover, the combination treatment extended survival in AML xenograft models and inhibited patient-derived leukaemia cell engraftment in the bone marrow of engrafted animals [215]. In addition, the BCL-2 inhibitor, cpm-1285, induced apoptosis in AML cell lines and caused low level cell death on healthy human peripheral blood cells and inhibited the growth of human myeloid leukaemia cells in immunodeficient mice [204]. Another study by Tron *et al.* also showed that the MCL-1 inhibitor, AZD5991, induced apoptosis in cancer cells most notably MM and AML in a BAK-dependent manner. Following AZD5991 treatment as a monotherapy, or in combination with bortezomib or venetoclax, AZD5991 displayed significant anti-cancer activity *in vivo*, resulting in the regression of both MM and AML [200]. Importantly, Pan *et al*. have also reported that AML cell lines, primary patient samples, and murine primary xenografts are sensitive to the BCL-2 inhibitor, ABT-199, and that cell death was dependent on the Bad-mitochondrial apoptotic pathway. In addition, therapy with ABT-199 significantly decreased leukemic burden in the bone marrow of mice engrafted with primary cells from

AML patients [210]. These promising pre-clinical data supported the inclusion of AML patients in clinical trials incorporating BH3 mimetics, as outlined in Table 1-5.

1.2.4.3 Clinical response to BH3 mimetics in AML patients

Many studies have demonstrated the success of BH3 mimetics in the clinical setting, and an overview of clinical trial activity, including AML, can be found in Table 1-5. The heterogeneous genetic landscape, along with various co-morbidities and age, makes AML treatment challenging, and more individualised treatment strategy is important [186]. In a phase 2 clinical study, patients with relapsed and/or refractory AML, ABT-199 treatment induced an overall response rate of 19%. However, 33.3% (4 out of 12) of patients with IDH1/2 mutations achieved a CR [90]. A phase 1b study included 145 patients that were ≥ 65 years old and ineligible for intensive chemotherapy; ABT-199 was given orally in combination with azacitidine. Common side effects (>30%) observed were appetite loss, nausea, constipation, diarrhoea, low white blood cell count, hypokalemia, and fatigue. Overall, the median time on the trial was 8.9 months and encouragingly, 67% of patients achieved CR [91]. Following this, a large phase 3 study enrolled 443 naïve AML patients (aged ≥75) and patients were treated with ABT-199 in combination with azacitidine or azacitidine alone. The OS and CR rate were improved in patients treated with the combination treatment (14.7 months; 66.4%) when compared with azacitidine alone (9.6 months; 28.3%) [201]. Several ongoing clinical trials using ABT-199 combined with; ponatinib (a Tyrosin-kinase inhibitor) (NCT04188405), MBG453 (a TIM-3 immune check inhibitor) (NCT04150029), or homoharringtonine (a targeting alkaloid) (NCT04824924) are still awaiting the final results. In addition, various BH3 mimetics targeting MCL-1 pro-survival protein are also being investigated in

clinical trials as a treatment for AML, these include S64315 (NCT02979366), AMG176 (NCT02675452), AMG397 (NCT03465540) and AZD5991 (NCT03218683) which are currently in phase 1 clinical testing.

1.3 Oncolytic virotherapy (OVT)

The therapeutic use of viruses in the fight against cancer is not a novel concept; in fact, the oncolytic potential of viruses has been recognised since the late 19th century [216]. However, this finding was not the outcome of any research-led hypothesis but a coincidence of clinical observations. At a time when the only treatment for cancer was surgery and chemotherapy, people noticed that cancer patients who suffered concurrent infection would sometimes enter into a short period of remission [217]. In 1904, George Dock reported his finding that spontaneous infection with the influenza virus can provide a short remission to leukaemia patients [217]. In the 1950s and 1960s, various viruses were explored clinically; however, due to a lack of effectiveness and concerns over safety, these studies were discontinued [216]. Despite this, there has been a recent renaissance in the field due to an improved knowledge of virology and molecular approaches to boost effectiveness and safety. Oncolytic viruses (OVs) selectively replicate and lyse cancer cells and can be natural, attenuated, or genetically engineered. The direct cytotoxic impact of oncolysis has been the primary focus of research involving oncolytic viruses; however, recent studies are increasingly focussed on their alternative mechanisms of action, including anti-tumour immunity [218, 219].

Several viruses have a natural tropism for cancer cells through specific receptors. These viruses are often asymptomatic in people or are linked with minor symptoms. These include vesicular stomatitis virus (VSV) [220], echovirus-1

[221], newcastle disease virus (NDV) [222], reovirus [223], parvovirus H1 [224], coxsackievirus A21 (CVA21) [225], and seneca valley virus [226]. Additionally, naturally attenuated viruses can also display cancer selectivity. One example of this is the Edmonston strain of measles virus (MV) [227]. In addition to this, viruses can also be genetically manipulated to preferentially infect neoplastic cells by taking advantage of defective anti-viral responses that are often present in tumour cells, examples of genetically engineered OVs include herpes simplex virus (HSV) [228], influenza virus [229], vaccinia virus (VV) [230], and adenovirus [231].

1.3.1 Mechanism of action

The most fundamental idea behind OVT is that many alterations detected in cancer cells that promote their survival and capability to escape the immune system, can also make them susceptible to OV infections. These include altered cell surface receptor expression, disruptions in the cellular signalling pathways, and dysfunctional antiviral responses. OVs have a number of different modes of action; the most well-described are direct oncolysis and stimulation of anti-tumour immunity. Also, OVs can cause disruption of tumour blood flow and modulate the TME [232, 233]. An overview of OV mechanisms of action is provided in Figure 1-6.

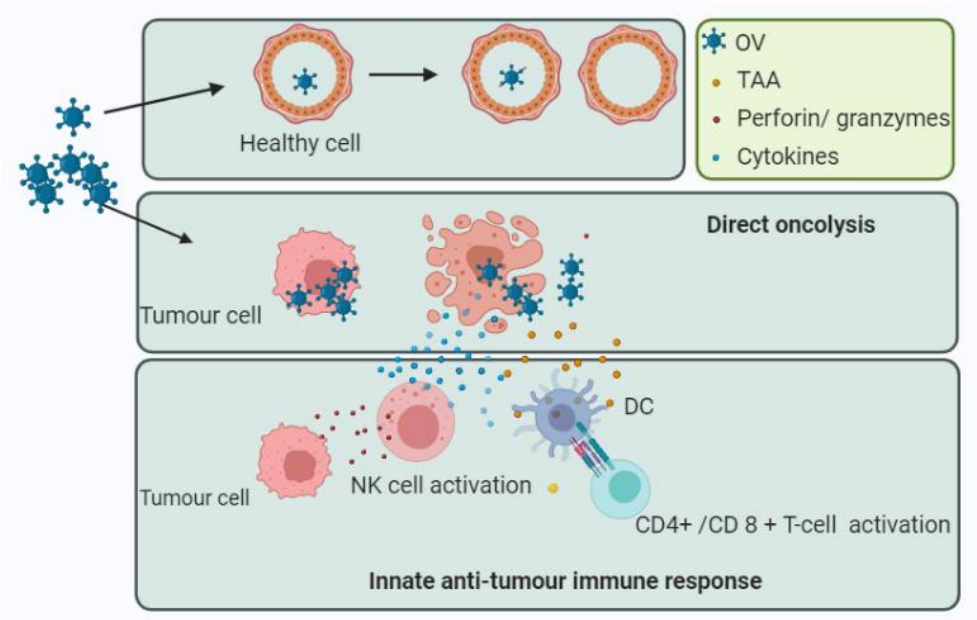

Figure 1-6: Principal mechanisms of action of oncolytic viruses. In the healthy cell, viral replication after infection is constrained by an anti-viral immune response, avoiding lysis. Conversely, in cancerous cells, the antiviral response is frequently compromised, leaving the cells vulnerable to OV infection and oncolysis. The OV is directly cytotoxic when cells are killed due to viral replication. Subsequently, OV spread to adjacent cancerous cells and cell lysis is enhanced. When cancerous cells are infected and lysed, this stimulates TAA and cytokine release resulting in anti-tumour immunity. Innate anti-tumour responses may comprise bystander killing mediated by cytokines, as well as cell mediated cytotoxicity by NK cells. Adaptive anti-tumour immune responses are stimulated when APCs phagocytose TAA which is presented on MHC molecules to CD8+ or $CD4^+$ T cells [234]. Figure derived from Kaufman *et al.* and created using Biorender.

1.3.1.1 Receptor-targeted viruses

Viruses can be either genetically modified or have a natural affinity for specific receptors overexpressed on malignant cells. For example, the selectivity of the Edmonston strain MV is related to high expression of its cellular receptor, CD46, on cancer cells [235]. Also, CVA21 naturally targets cancer cells that overexpress human intercellular adhesion molecule 1 (ICAM-1) and decay accelerating factor (DAF) [236]. On the other hand, as mentioned above, viruses can also be genetically modified, one of the first effective instances of this is modification adenovirus (Onyx-015) with deletion of its P53 inhibitory protein, E1B-55KD,

allowing preferential infection of cancer cells harbouring a P53 mutation [237]. Furthermore, adenovirus (serotype 5) has been genetically manipulated to re-direct its normal viral tropism for coxsackie and adenovirus receptor (CAR), which is often either low or non-existent on cancer cells, to cell surface adhesins or additional adenoviral receptors present on cancer cells to increase its selectivity [238]. For instance, the adenovirus 3 receptor (B7.1 and B7.2) is expressed on ovarian cancer cells; accordingly, an adenovirus 5/3 chimeric virus (Ad5/3luc1) showed highest virus replication of ovarian cancer cells in comparison to adenovirus 5 wild-type [239].

1.3.1.2 Defects in anti-viral response

1.3.1.2.1 Double-stranded RNA (dsRNA) dependent protein kinase receptor (PKR)

PKR is an intracellular stress sensor that can be triggered by viral infection. During viral infection, dsRNA can activate PKR and prevent protein synthesis by phosphorylating the alpha subunit of the translation initiation factor eIF2 in healthy cells [240]. By contrast, in tumour cells, defects in PKR signalling lead to a dysfunction anti-viral response. Therefore, viruses take advantage of faulty PKR signalling and replicate preferentially in tumour cells. Viruses that take advantage of defective PKR signalling include the naturally occurring OV, reovirus, and a genetically engineered HSV-1 strain that has deleted ICP34.5, a viral protein that acts to suppress PKR activity [241-243].

1.3.1.2.2 Interferon response

In healthy cells, a range of different signalling pathways are engaged to detect and destroy virus particles. These pathways can be induced either by the local production of IFN or by activation of intracellular Toll-like receptors (TLRs), in response to viral elements. TLRs can be found on both the surface and inside the cell, and are activated in response to pathogen-associated molecular patterns (PAMPs), which are typical of viral infection. PAMPs can be components of virus capsids, viral DNA or RNA, or viral associated proteins. Activation of host cell antiviral responses and systemic innate immunity is achieved by TLR signalling or engagement with other pattern recognition receptors (PRRs; e.g. melanoma differentiation-associated protein 5 (MDA5), retinoic acid-inducible gene I (RIG-I)) [244, 245]. Various host cell factors that are important in oncolytic viral clearance have been identified. These include RIG-I, TNF-associated factor 3 (TRAF3), IFN-related factor 3 (IRF3), and IRF7. These factors stimulate the Janus kinase–signal transducer and activator of transcription pathway (JAK–STAT), which is responsible for coordinating the anti-viral immune response in infected cells [234]. However, these processes are often impeded in tumour cells, for example, downregulation of critical signalling elements within the innate signalling pathway, including RIG-I, IRF3, and IRF7, have been reported in cancer cells [246-249].

The oncolytic action of naturally occurring OVs such as VSV [250] and NDV [251] is limited to cancer cells with faulty IFN responses. While genetic alteration of HSV (ICP0-null) [252], influenza virus (NS-1-deleted) [229], and VV (B18R-null) [253] was required to make these viruses replicate preferentially in tumour cells with a dysfunctional IFN response.

1.3.2 Oncolytic viruses and the immune system

The direct oncolytic action of OVs against cancer cells was the original aim of OVT. However, OVs can induce immediate (innate) or long-term (adaptive) anti-tumour immune responses. The release of TAA and pro-inflammatory cytokines after OV treatment can reverse the TME immunosuppressive properties, leading to the formation of an anti-tumour immune response. Initial research comparing OVT in immunodeficient and immunocompetent mouse models has shed light on the significance of the immune system for successful OVT. Initial investigations by Toda *et al*. indicated that OVT, involving HSV, was successful in an immunocompetent mouse. However, the anti-tumour response was eliminated in athymic mice, revealing the importance of T cells for efficient OVT [218]. In addition to this, it has been reported that VSV treatment was dependent on CD8+ T cells and NK cells [254]. Additional OVs have also been reported to induce anti-tumour immunity, including parvovirus [255], VV [219], NDV [256], reovirus [257], and CVA21 [258].

Tumour eradication using OVs can be dependent on the activation of innate and adaptive immune responses. Following infection with OV, an antiviral response is initiated which involves endoplasmic reticulum (ER) stress. As a consequence, ROS are upregulated and anti-viral cytokines (e.g. type I IFNs, TNF, and interleukin-12 (IL-12)) are produced. ROS and cytokines, particularly IFN I, can be secreted by cancer cells and/or immune cells to activate immune cells such as APCs, CD8+ T cells, and NK cells. In addition, OV-induced oncolysis results in the production of viral progeny, damage-associated molecular pattern signals (DAMPs; for example, heat shock proteins, high mobility group box 1 (HMGB1) protein, calreticulin, ATP, and uric acid), PAMPs, and TAAs. Both PAMPs (composed of viral particles) and DAMPs (composed of host cell material)

activate the immune system by triggering PRR such as TLRs [234], which enhance the maturation of macrophages and dendritic (DCs), resulting in the activation of both $CD4^+$ and $CD8^+$ T cell responses. Once activated, CD8+ T cells have the potential to differentiate into cytotoxic effector cells, where they are able to mediate anti-tumour immunity [234].

The process of recruiting and activating NK cells as part of OV treatment is essential for viruses to achieve their full destructive potential [254]. It has been reported that reovirus induces activation of NK cells by increasing NK degranulation and the release of IFN-α [259]. In addition, reovirus can activate NK cells via the maturation of DCs, which subsequently engage NK cells leading to their activation [260]. The primary NK cell recognition signal for cellular defects is the down-regulation of MHC Class I expression, which results in activation of NK cells [261]. OVs can reduce the expression of MHC-I on the surface of infected tumour cells, which in turn makes them more visible to NK cells [255]. Whilst tumour cells can produce an immunosuppressive environment that inhibits NK cell function, OVs can activate NK cells through the secretion of pro-inflammatory cytokines [259] (e.g. type I IFNs), enhancing cytotoxicity through increased perforin-dependent toxicity [262] and/or upregulation of TRAIL [263, 264]. The main mechanism of NK cell-mediated killing is by the release of cytotoxic granules within the immunological synapse. However, another method by which NK cells can kill target cells is by activating death receptors on cancer cells via the expression of FasL or TRAIL on the surface of NK cells. Death receptor ligation activates a caspase cascade, leading to apoptosis (Figure 1-3) [265].

1.3.3 Clinical experience of OVT

The majority of OVs that have been, or are currently undergoing testing in clinical trials are derived from genetically modified viruses, with the exception of a few naturally occurring RNA viruses (e.g. reovirus and CVA21). Reovirus is an unaltered dsRNA virus and is clinically the most advanced oncolytic RNA virus. Other OVs that have been investigated in clinical trials are mostly DNA viruses that are members of the herpesviridae, poxviridae, or adenoviridae virus families [266]. To date, only three OVs have been approved worldwide to use as a treatment of advanced cancers [267]. The first was in 2004, when the use of Rigvir, an ECHO-7-derived picornavirus RNA virus, was approved for the treatment of melanoma in Latvia [268]. After that, in 2005 in China, the genetically modified adenovirus, Oncorine® (H101) was approved to treat nasopharyngeal carcinoma in combination with chemotherapy [269]. Later, in 2015, FDA approved a HSV-1-based OV, known as Imlygic® (T-Vec), for the treatment of advanced melanoma [114].

Several OVs being studied in clinical trials, including reovirus, HSV, MV, VV, NDV, Seneca valley virus, and adenovirus are safe and well-tolerated [270]. In addition, studies have shown that it is possible to obtain therapeutic effectiveness despite the initiation of an anti-viral response. For instance, reovirus was effectively recovered from blood cells after i.v treatment and in the presence of anti-reovirus neutralising antibodies [271].

T-Vec, a second generation HSV-based OV, progressed to phase III studies in melanoma, after a promising phase II study in which 13 patients had clinical responses including regression of injected and distant non-injected lesions. The eradication of non-injected lesions was consistent with the development of an

antitumor immune response [272]. Furthermore, many studies have explored the combination of existing cancer treatments, such as chemotherapy and radiotherapy, in combination with OVs. For example, a genetically engineered adenovirus H101 (E1B-55 kDa- deleted) was tested in a phase III clinical study where intertumoral (i.t.) infusions of H101 were administered in combination with cisplatin. Response rates of 78.8% were obtained with the combination treatment, compared to just 39.6% with cisplatin alone. Since then, the combination of H101 and cisplatin was approved for the treatment of head and neck cancer in China [273]. Moreover, alternative studies have investigated the efficacy of combining OV with immune checkpoint antibodies, for example T-Vec has been tested in combination with anti-CTLA-4, and CVA21 has been tested in combination with anti-PD-1, both of which have reported encouraging outcomes [274].

1.3.4 OVT in AML

OVT has promise for treating a disorder like AML because of their ability to infect tumour cells, as well as eliminate minimal residual disease [275]. Encouragingly, it has been reported that MV can infect AML cell lines and primary AML cells, which reduces the viability of leukemic blasts by stimulating apoptosis [276]. Another study also reported that reovirus can replicate in primary AML samples and reduce cell viability [277]. In response to reovirus therapy, AML cells produced IFN-α as well as the chemokine, RANTES. Furthermore, reovirus activated NK cells to stimulate an anti-leukaemia response [277]. An alternative oncolytic virus that is utilised for the treatment of AML is myxoma virus (MYXV), a member of the Poxviridae family. MYXV was able to prevent the formation of myeloid sarcoma and bone marrow engraftment of two different human AML cell lines (KG-1 and THP-1) [278]. In addition to this, MYXV was also active against

xenografts AML tumours, and targeted leukaemia cells while leaving normal hematopoietic progenitor cells unharmed [279]. Moreover, a study by Muller *at al*. demonstrated that CVA21 induced a potent immune response against AML cells via different mechanisms including cytokine-induced bystander killing, enhanced NK-mediated killing, and the induction of tumour-specific T cells. This occurred despite the fact that AML cells were resistant to CVA21 direct oncolysis [258].

Wang *et al*. investigated the oncolytic adenovirus known as rAd5pz-zTRAIL-RFP-S24E1a (A4), which contains the viral capsid protein IX coupled to TRAIL. A4 was further developed to zA4, by coating A4 with soluble TRAIL. zA4 increased the virus interaction with leukaemia cells and significantly reduced the proliferation of AML cell lines and primary patient samples [280]. More recently, Lei *et al*. showed that a newly generated oncolytic vaccinia virus (OVV) expressing Beclin-1 (OVV-BECN1) infected leukaemia cells and exhibited potent anti-cancer efficacy, in an autophagic-dependent manner [281].

An alternative oncolytic adenovirus is SG235-TRAIL, with an Ad5/F35 chimeric fibre and modified to express TRAIL. SG235-TRAIL has been investigated in combination with homoharringtonine (HHT) in AML cell lines (Kasumi-1, HL-60 and KG-1); the combination increased apoptosis and enhanced caspase-3 and -9 activity. When compared to treatment with either HHT or SG235-TRAIL alone, the combined therapy significantly reduced BCL-2, MCL-1, and Bid levels, this suggests that HHT sensitises leukaemia cells to SG235-TRAIL virus via modulation of anti-apoptotic signalling [282].

Rhabdovirus has also been considered in AML treatment. VSV-IFNβ-NIS, a VSV coding IFN-β and the NIS reporter, was administered i.v in mice containing

syngeneic C1498 AML tumours. Virus infection was confirmed by imaging for NIS expression. Moreover, the addition of the anti-PD-L1 immune checkpoint inhibitor enhanced the anti-leukemic effect of VSV-mIFNβ-NIS and prolonged animal survival compared to either treatment alone. Interestingly, the anti-leukemic activity was lost when CD8 and NK cells were depleted [283].

Furthermore, using a xenograft mouse model of AML derived from the U937 cell line, measles and mumps viruses (MMV) showed improved tumour suppression and increased survival. Additionally, when co-administered with ara-c, MMV was able to eliminate blasts from 16 of 20 AML patients and had greater killing impact on 11 individuals [284]. Finally, UV-HSV-1 increased PBMC cytolysis of leukemic cells, in part through Toll-like receptor-2, protein kinase C and NF-kB signalling, which enhanced the CD69 expression, degranulation, migration, and cytokine release in NK cells [285].

The most appropriate virus to treat AML remains unknown. However, in this project, the therapeutic potential of four molecularly distinct OVs (reovirus, MG1, CVA21 and HSV-1) has been tested.

1.3.5 Reovirus

The respiratory enteric orphan virus (reovirus) is a common environmental virus that can cause mild enteric or respiratory illness in children but is usually harmless to adults. Reovirus is a member of the Reoviridae family and can be isolated from human gastrointestinal and respiratory systems [286]. Reovirus is an nonenveloped dsRNA virus [287] and uses junctional adhesion molecule-A (JAM-A) receptor to enter the host cells [288]. JAM-A is highly expressed on endothelial cells and haematological cells, particularly hematopoietic stem cells (HSC) [289]. There are three known strains of reovirus: Type 1 Lang, Type 2

Jones, and Type 3 Abney and Dearing [286]. Hashiro *et al.* were the first to notice that Reovirus Type 2 Jones replicated in malignant cell lines and not normal cells [223]. However, the wild-type (WT) reovirus Type 3 Dearing strain (T3D), clinically formulated as pelareorep (formally known a Reolysin®), has progressed to phase III clinical testing [290]. Importantly, reovirus can kill cancer cells by a variety of different methods, including apoptotic cell death, necroptotic cell death, oncolysis and activation of innate and adaptive anti-tumour immune response [291-293].

1.3.6 CVA21

Coxsackieviruses are members of the Picornaviridae family, which are non-enveloped, single strand, positive-sense RNA viruses [294]. Coxsackieviruses are members of the Enterovirus genus, which also includes paramyxoviruses. Coxsackieviruses have been divided into two categories; (CVA; 23 serotypes and CVB; 6 serotypes) according to their pathogenicity in mice [295]. Eleven of the CVA serotypes, including CVA21, are classified as species of human enterovirus. CVA infection can cause cold-like symptoms in humans [296]. *Coe* and *Kuykendall* strains of CVA21 were found to be prototypes; however, *Kuykendall* is the strain that has been developed into a therapeutic OV. CVA21 binds to host cells through DAF and internalises via human ICAM-1 [297]. ICAM-1 is generally expressed on a various types of cells, including haematopoietic cells, such as myeloid blasts, monocytic cells, B lymphocytes, and plasma cells as well as epithelial and endothelium cells [298]. Importantly, overexpression of ICAM-1 has been observed on a variety of tumour cells, including MM [299], CLL [300], malignant melanoma [301], colorectal cancer [302], renal carcinoma [303], and pancreatic cancer [304], which is crucial for the oncolytic impact of CVA21. CVA21 can generate anti-tumour responses through different mechanisms

including, pro-inflammatory cytokines-mediated killing, NK cell-mediated killing and priming of tumour specific T cells [258].

1.3.7 Maraba virus (MG1)

Maraba is a wild-type virus that belongs to the vesiculovirus genus of the *Rhabdoviridae* family. A double mutant (MG1) strain has been modified with M (L123W) and G (Q242R) protein mutations to attenuate its effect in normal cells, and improve its anti-cancer efficacy [305]. MG1 is an enveloped, single-stranded negative-sense RNA virus [306]. Interestingly, there have been no cases of virus-related illness reported in humans [307]. For this reason, MG1 is a potential agent of interest for therapeutic use [305]. Of note, MG1 virus uses the widespread low-density lipoprotein receptor (LDLR) to enter into target cells; LDLR is expressed by a variety of malignant cells, including ovarian and breast cancer cells [308]. MG1 is also capable of inducing anti-tumour immune response through the production of pro-inflammatory cytokines and activation of APC, NK cells and priming of anti-tumour T cells [309].

1.3.8 Herps simplex virus (HSV-1)

The *Herpesviridae* family is comprised of a vast number of enveloped, double-strand DNA viruses. These viruses are linked to a wide array of diseases that affect a variety of hosts. There are three subfamilies of herpesviruses, α, β, and γ and the key differences between each form is the replication cycle and host cell tropism. HSV-1 belongs to the Alpha-herpesvirus family [310]. HSV-1 infections are often characterised by the formation of skin lesions or blisters at the mucosal surfaces around the mouth, which normally heal after a period of two to four weeks [310]. Interestingly, HSV-1 has been modified to delete infected cell protein (ICP) 34.5 gene to attenuate its infection in normal cells while enhancing

its replication in malignant cells [311]. Importantly, oncolytic HSV-1 utilises herpesvirus entry mediator (HVEM) and nectin-1 receptors to penetrate into the target cells [312]. Several cancer cells express nectin-1 receptors including, colorectal cancer cells [313], melanoma cells [314], and squamous carcinoma cell [315]. HSV-1 showed potent oncolytic activity in several human tumour cell lines including, pancreatic and melanoma cells [316]. Moreover, significant reduction of tumour size in mice bearing A20 lymphoma tumours was observed in response to HSV-1 treatment, along with a significant increase in CD8+ T cells [317].

1.4 The Role of apoptotic modulators in OVs immunotherapy

1.4.1 Smac mimetics and OV immunotherapy

The combined application of Smac mimetics with OVs have revealed widespread efficiency with remarkable effect, which has been attributed to the production of elevated levels of localised TNF-α during OV infection [318]. For example, Dobson *et.al* demonstrated synergy between LCL161 and vesicular stomatitis virus (VSVΔ51-GFP) *in vitro* in Rhabdomyosarcoma (RMS) cell lines, where cell death was TNF-α-dependent. Moreover, the combination significantly inhibited the tumour growth of 76-9 syngeneic mice, extended survival, and cured 12.5% of the animals [318]. Furthermore, according to Cai *et al.* LCL161 enhanced the oncolytic efficacy of alphavirus (M1) *in vitro, in vivo* and *ex vivo* causing cell death in hepatocellular carcinoma cell lines and colorectal carcinoma cell lines. Herein, cell death was associated with the induction of pro-inflammatory cytokines (e.g., IL-8, IL-1A and TRAIL). In addition, LCL161 caused an increase in M1 replication, where aggregation of viral protein caused endoplasmic reticulum stress-mediated apoptosis [319].

Significantly, Beug *et al*. also demonstrated that breast carcinoma (EMT6 cells) and Glioblastoma (SNB75 cells) cells secreted IFN-β, TRAIL and TNF-α in response to VSVΔM51 treatment, which in combination with LCL161 potentiated cell death; IFN-β was responsible for the production of TRAIL and TNF-α, which acted synergistically with LCL161 to enhance cell killing. *In vivo*, the combination of LCL161 with VSVΔM51 decreased tumour burden and enhanced survival compared to mice treated with single agent therapy and a dependence on TNF-α production was reported [320]. Another study by Beug *et al*. reported that VSVΔM51-TNF-α, when used in combination with LCL161, improved the survival rate of mice and reduced tumour growth compared to LCL161 alone and unarmed VSVΔ51 in breast carcinoma (EMT6 cells) and Glioblastoma (SNB75 cells) *in vivo* models. This effect was attributed to a breakdown in tumour vasculature due to elevated levels of TNF-α. Also, the release of TNF-α from VSVΔM51-TNF-α infected cells enhanced cytokine-induced bystander-killing of cancerous cells [321].

Interestingly, Kim *et al*. reported that VSVΔM51 stimulated a pro-inflammatory environment which increased infiltration of T-cells and enhanced therapy; VSVΔM51 treatment prior to LCL161 was required because LCL161 abrogated both VSVΔM51 infection and cytokine secretion if delivered first. LCL161 as monotherapy also indirectly re-activated exhausted T-cells in immunocompetent Balb/c mice bearing orthotopic EMT6 breast carcinoma by modulating TAM (polarization); TAM polarisation resulted in the accumulation of pro-inflammatory cytokines (MCP-1, MIP-2, RANTES, IFN-γ and IL-1) and reduced the immunosuppressive cytokines (IL-4 and IL-10) within the TME. Collectively, the combination of LCL161 and VSVΔM51, reduced breast carcinoma tumour burden *in vivo* and this was dependent on T-cell cytotoxicity [322]. Surprisingly, TNF-α-

mediated tumour killing was not required for the anti-tumour response *in vivo.* However, the efficacy of LCL161 and VSVΔM51 was further enhanced by the addition of αPD-1, which caused tumour regression in 90% of the tumour bearing mice, suggesting a role for T cells [322].

1.4.2 BH3 mimetics and OV immunotherapy

To date, only a handful of studies have been carried out investigating the combination of BH3 mimetics and OVs. One study by Tumilasci *et al.* showed that the BH3 mimetic, EM20-25, could be used to overcome CLL resistance to VSV-AV1 oncolysis. The combination of these two agents caused cell death in primary *ex vivo* CLL cells and increased apoptosis in B-lymphoma cell lines by blocking BCL-2 interaction with BAX and sensitizing cells to VSV-AV1 oncolytic stress [323]. Additionally, to overcome the resistance of CLL cells to VSV-mediated oncolysis, Samuel *et al.* combined obatoclax (GX15-070; BCL-2 inhibitor) with VSV. The combination synergistically increased death of primary CLL samples, and inhibited tumour growth in A20 B-lymphoma bearing mice. The combination triggered the activation of BAX, and cytochrome *c* release which led to apoptosis [324]. Furthermore, the combination of GX15-070 with poxviral vaccinia (rV) decreased the viability of adenocarcinoma mouse cells *in vitro* which was dependent on ER stress-induced apoptosis. Interestingly, rV treatment prior to GX15-070 enhanced the activation of CD8 T-cells, reduced the activity of T_{regs}, and significantly reduced pulmonary tumour nodules in mice bearing lung adenocarcinoma cells (LL2) [325]. Sarkar *et al.* also demonstrated that the combination of an adenovirus, AD.tCCN1-CTV-m7, that expressed IL-24, with MCL-1 inhibitor (BI-97D6), sensitized oncolysis-resistant prostate cancer cell lines to IL-24, which caused ER stress and induced apoptosis. Importantly, the

combination significantly suppressed tumour growth and enhanced apoptosis in Hi-myc prostate cancer transgenic mice [326].

1.5 Conclusion

Taken together, the immune system plays a vital role in reducing the risk of developing cancer and removing of cancerous cells. As described above, many studies have shown that OVT has the ability to effectively exploit the immune system to enhance anti-tumour immune responses. In addition, several studies have demonstrated the multifactorial activity of Smac/ BH3 mimetics in facilitating immune responses against tumours, with the possibility for combined OV therapy to boost the host anti-tumour immune responses. As shown previously, Smac/ BH3 mimetics can enhance OV bystander cytokine killing, modulate the TME and help prime T cell responses in a variety of cancer types and models.

1.6 Hypothesis and aims

To date, the efficacy of SMAC mimetics in combination with OV has been previously reported for Rhabdoviruses-induced inflammation; however, no data is currently available regarding different OV in combination with SMAC mimetics, or the role for this strategy in the context of AML. Therefore, the hypotheses for this project were: 1) that apoptotic modulators (BH3/SMAC mimetics) will potentiate OV efficacy in AML, and 2) that different apoptotic modulators (or OV) will preferentially target different AML subtypes. To test these hypotheses the following aims were devised.

1) Examine the cytokine profile of PBMC-conditioned media after treatment with different OV.
2) Test the cytotoxic effects of OV-induced pro-inflammatory cytokines against AML cell lines.
3) Establish whether Smac/ BH3 mimetics can potentiate OV-induced bystander-cytokine killing in AML cell lines.
4) Determine whether Smac/ BH3 mimetics could be used to potentiate NK cell mediated killing and/or direct oncolysis.
5) Validate the efficacy of Smac/ BH3 mimetic in combination with OV *in vivo* and in AML patient samples.

Chapter 2：Material and methods

2.1 Cell culture

All cells were maintained at 37°C in a humidified environment containing 5% CO_2 in a CO_2 incubator with continuous UV decontamination (Sanyo). Cells were cultured in Corning® Costar® and Nunc® tissue culture flasks (25 cm^3, 75 cm^3, and 150 cm^3). For collecting and washing cells, 15 mL or 50 mL sterile polypropylene tubes (BD Falcon) or 25 mL sterile plastic 'Universal' containers (Sterilin®) were used. For the appropriate experiments, cells were seeded in 6-, 24-, 48- and 96-well plates (Corning® Costar®, Nunc®, and Sterilin®). Suspension cells were passaged every 3-4 days by adding appropriate volume of cell suspension to fresh media, at an appropriate split ratio. Adherent cell lines were washed with sterile phosphate buffered saline (PBS, made using Dulbecco's A PBS tablets in dH2O [Oxoida]), followed by the addition of trypsin at 37°C (10x stock diluted 1:10 in Hanks' Balanced Salt Solution (HBSS), both Sigma-Aldrich). Unless otherwise indicated, cells were centrifuged at 400g for 5 minutes at room temperature (RT) using an Eppendorf 5810 centrifuge. Using Nuaire Class II Microbiological Safety Cabinets, all tissue culture was conducted under aseptic conditions. Trypan blue (0.2 percent in PBS, Sigma-Aldrich) and an Improved Neubauer haemocytometer was used to count viable cells. All cell lines were regularly tested and verified to be free of mycoplasma contamination.

2.2 Cell lines

An overview of all cells and their culture media is provided in Table 2-1. Unless otherwise noted, all culture media was purchased from Sigma-Aldrich and contained 10% foetal calf serum (FCS, Gibco), which was heat-inactivated for 30

minutes at 56^{o}C before being used. Sigma-Aldrich was also a source for other supplements such as L-glutamine, 2-β mercaptoethanol and penicillin/streptomycin. Table 2-1 provides an overview of primary growth media. In all experiments, cells were resuspended at 1x10^{6} cells/mL, unless otherwise stated.

Table 2-1: Cell lines and culture media

	Cell line	Cell type/ FAB classification	Species	Culture medium
AML cell lines	KG-1	Myelogenous (M6)	Human	1% L-glutamine containing Rosewell Park Memorial Institute-1640 (RPMI-1640)+ 10% FCS
	THP-1	Monocyte (M5)	Human	RPMI-1640 + 10% FCS
	Kasumi-1	Myeloblast (M2)	Human	RPMI-1640 + 10% FCS
	HL-60	Promyeloblast (M2)	Human	RPMI-1640 + 10% FCS
	C1498	Lymphoblast	Mouse	1% L-glutamine containing Dulbecco's modified eagles medium (DMEM) + 10% FCS
Adherent cell lines	Mel-624	Melanoma	Human	DMEM + 10%FCS
	Vero	Normal epithelial cells	Monkey	DMEM + 10%FCS
Peripheral blood mononuclear cells (PBMC)		Healthy PBMC	Human	RPMI-1640 + 10% FCS
CD14+ Monocytes		Healthy monocytes	Human	RPMI-1640 + 10% FCS
Primary AML		PBMC from AML patient sample	Human	RPMI-1640 + 20% FCS
Splenocytes		Immune cells	Mouse	DMEM + 5% FCS + 2 mM L-glutamine + 50 µM 2β-mercaptoethanol+ 1% penicillin/streptomycin

2.3 Cryopreservation

Cells were collected and pelleted by centrifugation. Following that, cell pellets were re-suspended in freezing medium (90% FCS; 10% dimethyl sulphoxide (DMSO, Sigma-Aldrich)), and then aliquoted into 1 mL cryovials (Nunc®) and placed at -80˚C. Cryovials were transported to liquid nitrogen the next day for long term storage. To recover the cells, they were first rapidly thawed in a water bath heated to 37˚C and placed in fresh culture medium (10 times excess). Cells were subsequently harvested by centrifugation before being resuspended in fresh culture medium and transferred to tissue culture flasks.

2.4 PBMC

2.4.1 Isolation of human PBMCs using density gradient separation

Blood was obtained from National Health Service Blood and Transplant (NHSBT) apheresis cones which were processed in accordance with institutional protocols. Firstly, blood was diluted 1:2 in HBSS, 30 mL aliquots were layered on top of 15 mL Lymphoprep© (Alere Ltd.) and then centrifuged at 800g for 25 minutes without a brake. The white cell layer was subsequently isolated using a Pasteur pipette with a broad tip (Alpha laboratories Ltd.). Isolated cells were washed with 50 mL of HBSS and centrifuged for 10 minutes at 400g, followed by a further wash with 50 mL of HBSS and centrifugation at 300g for five minutes. For all experiments, PBMCs were resuspended at a concentration of 2 x 10^6 cells/mL in RPMI-1640 supplemented with 10% FCS.

2.4.2 PBMC-conditioned medium (CM)

PBMC-CM was generated by seeding PBMCs at a density of 2 x 10^6 cells/mL and then treating them with either 0, 0.1 or 1 pfu/cell OVs. After incubation for 48 hours, PBMC were removed by centrifugation at 400g for 5 minutes and the culture medium supernatant was then placed in the freezer at -20 °C until needed. To inactivate OV within the CM, for all experiments the CM was subjected to UV irradiation as detailed below (section 2.14).

2.4.3 CD14 cells separation using Magnetic cell sorting

To isolate human monocytes and macrophages, CD14 selections were carried out using either freshly isolated PBMC or PBMC that had been previously cryopreserved in freezing medium. PBMC were resuspended in 50 mL of MACS buffer (PBS; 1% FCS; 2 mM EDTA), centrifuged at 300g for 5 minute and resuspended in 80 µL of MACS buffer containing 20 µL CD14 MACS microbeads (Miltenyi Biotec Ltd.) per 1x10^7 cells. PBMC were incubated for 15 minutes at 4℃, centrifuged at 300g for 10 minutes, washed in an excess volume of MACS solution, and then re-suspended in 500 µL of MACS buffer per 1x10^8 cells. Before applying the labelled cells to the MACS® LS separation column, the LS column was placed in the magnetic stand and prepared by washing with 3 mL MACS buffer (manufactured by Miltenyi Biotech). To eliminate any non-labelled cells from the column, it was washed 3 times with 3 mL of MACS buffer. After removing the column from the magnetic stand, CD14+ cells were removed by flushing with 5 mL MACS buffer and resuspended at a concentration of 1x10^6 cells/mL in RPMI-1640 supplemented with 10% FCS.

2.5 Harvest and processing of spleens

St. James's Biological Services (SBS) provided female C57BL/6 mice aged 6 to 8 weeks. Animal spleens were removed, placed in transport medium (HBSS; 1% HEPES; 0.2% aprontinin (Nordic pharma)) and processed immediately. Spleens were disaggregated by passing them through a 70 µm cell strainer (BD Falcon) into splenocyte medium (Table 2-1) before centrifugation. In order to lyse red blood cells, splenocytes were re-suspended in 5 mL of ACK buffer (0.15 M ammonium chloride; 10 mM KHCO3; 0.1 mM EDTA, pH 7.2-7.4) per spleen for two minutes. After adding cold splenocyte media, the cells were centrifuged for five minutes at 400g. The cells were subsequently resuspended in a warm splenocyte medium, filtered using a 70 µm cell strainer, and pelleted by centrifugation. After the cell pellet was washed a further two times in pre-warmed splenocyte media, the splenocytes were counted and resuspended in splenocyte media at $2x10^6$ cells/mL and used within experiments.

2.6 Primary AML patient samples

Patients diagnosed with AML at St. James's University Hospital, Leeds, United Kingdom, provided peripheral blood from which primary leukemic blast cells were isolated. The cohort included samples from a range of subtypes of AML. The PBMC fraction, which included leukemic blasts, was isolated as stated above (Section 2.4.1) and resuspended in RPMI-1640 supplemented with 20% FCS; all primary AML cells were used immediately in experiments. In all samples, patient PBMCs were used at a cell density of 2×10^6 cells/mL. All patients provided written informed permission in compliance with the local institution's ethical review and approval, ethics number 06/Q1206/106. For some primary AML

samples, PBMC-CM was generated in the same manner as described in Section 2.4.2

2.7 Oncolytic viruses

Dearing strain Reovirus type 3 was obtained from Oncolytics Biotech Inc and the *Kuykendall* strain CVA21 was purchased from ATCC and propagated in-house using Mel-624 cells (section 2.13.1). BioVex provided the type 1 HSV-1 modified virus (HSV1716) and Turnstone Biologics provided Maraba virus (MG-1) vectors which were used to propagate MG-1 “in-house’’ using Vero cells. MG-1 was propagated by Dr Jennings and provided for use in the experiments. Long-term storage of CVA21, reovirus, MG1 and HSV-1 stock was at -80^{o}C. Aliquots were used directly after thawing, except for Reovirus, which was stored for a maximum of 14 days at 4°C.

2.8 Cell treatments

2.8.1 SMAC and BH3 mimetics

SMAC (LCL161 and BV-6) or BH3 mimetics (ABT199 and ABT263) (all purchased from Selleckchem) were reconstituted in DMSO at a concentration of 10mM and stored at -80°C. For cell viability and combination treatment experiments, cells were treated with either SMAC or BH3 mimetics at concentrations ranging from 0.01µM to 10µM for either 48 or 72 hours.

2.8.2 OVs

AML patient samples, AML cell lines and PBMC were treated with MOI of virus at 0.1 and 1 pfu/cell. Cells and supernatants were taken at different time points post-treatment to assess cell viability (section 2.10.1), cytokine/chemokine production (Section2.12.1 and 2.12.2), and to generate CM (Section 2.4.2).

2.8.3 Recombinant cytokine treatments

2.8.3.1 Human cytokine treatments

Human recombinant cytokines, IFN-α, IFN-γ, or TNF-α (all R&D Systems) were reconstituted in sterile PBS containing 0.1% bovine serum albumin (BSA), at a concentration of 100 µg/mL for IFN-α and IFN-γ, and 10 µg/mL for TNF-α and stored at -20°C. AML cell lines were treated with recombinant cytokines either alone or in combination with BV-6 or ABT199 prior to flow cytometric evaluation of cell viability (Section2.10.1). Cells were either left untreated or treated with IFN-α and TNF-α at concentrations of 500, 1000, and 2000 pg/mL, or IFN-γ at concentrations of 250, 500, and 1000 pg/mL either alone or in combination (Low concentrations were 500 pg/mL IFN-α, 500pg/mL TNF-α plus 250 pg/mL IFN-γ, intermediate concentrations were 1000 pg/mL IFN-α, 1000pg/mL TNF-α plus 500 pg/mL IFN-γ and high concentration were 2000 pg/mL IFN-α, 2000pg/mL TNF-α plus 1000 pg/mL IFN-γ).

2.8.3.2 Murine cytokine treatments

IFN-α or TNF-α (both BioLegend) were provided in a reconstituted form at a concentration of 2000 ug/mL. C1498 cells were treated for 48 hours with recombinant mouse cytokines at doses of 100, 500, or 1000 pg/mL alone, or in

combination with either BV-6 or ABT199, before cell viability was determined by flow cytometry (section 2.10.1).

2.8.4 Measurement of the effect of ZVAD on cell death

To confirm that cell death occurred via apoptosis, a pan-caspase inhibitor, z-VAD-FMK (zVAD), was used. AML cell lines were seeded at $1x10^6$ cells/mL and treated with 50µM or 100µM zVAD and incubated at 37°C for 1hr prior to the addition of PBMC-CM (± reovirus treatment) alone or in combination with Smac or BH3 mimetics or further 72 hrs. Cell viability was assessed using Live/Dead flow cytometry (section 2.10.1).

2.9 Cell tracker staining

Using DMSO, a 5mM stock solution Cell Tracker™ (Invitrogen) Green CMFDA was produced. A working dilution of 2.5 µM was made using prewarmed serum-free RPMI-1640, and cells were stained at a concentration of $1x10^6$ cells /mL for 30 minutes at 37°C. After that, the cells were washed 2 times in 10 mL RPMI-1640 supplemented with 10% FCS before being used, as appropriate.

2.10 Flow cytometry analysis

All flow cytometry experiments were carried out using a 6-laser Cytoflex LX (Beckman Coulter). CytExpert software was used to analyse the data. Information for all antibodies used in this study can be found in Table 2-2.

2.10.1 Cell viability assessment using Live/Dead discrimination staining kit

The viability of cells was determined using the LIVE/DEAD® Fixable Yellow Dead Cell Stain Kit (Invitrogen). Cells (± required treatments) were collected into 5 mL FACS tubes (BD Falcon) diluted in PBS, then centrifuged at 400 g for 5 minutes.

Each cell sample was subsequently incubated in 500 µL of staining mix (LIVE/DEAD dye diluted 1:1000 in PBS) for 30 minutes in the dark at a temperature of 4°C. Following this, cells were washed with 2 mL PBS and then fixed with 300 µL 1% paraformaldehyde (PFA) (diluted in PBS). Cells were stored at 4°C until acquisition by flow cytometry and all samples were acquired within 5 days.

2.10.2 Cell phenotyping

For flow cytometry analysis, $5x10^5$-10^6 cells were collected, placed in 5mL FACS tubes, and washed in 1 mL of FACS buffer (PBS, 1% FCS, 0.1% sodium azide). The cell pellet was resuspended in the residual volume of FACS buffer and fluorescently conjugated antibodies, relevant to each experiment, were added according to Table 2-2. For example, for NK cell phenotyping, CD69 expression was measured on NK cells using CD3, CD56 and CD69, or CD3, CD56 and the appropriate isotype control. CD45 was used to identify leucocytes within AML patient PBMC. After a 30 minutes incubation period in the dark at a temperature of 4°C, cells were washed with 2 mL FACS buffer and fixed in 300 µL 1% PFA. Cells were stored at 4°C until acquisition by flow cytometry and all samples were acquired within 5 days.

2.10.3 Flow cytometry-based killing assay

Cell tracker green solution was used to stain target AML cell lines as indicated in section 2.9. PBMC were either left untreated or treated with reovirus at 1pfu/cell for 48 hours. After the PBMC had been treated with OV, they were cultured with cell-tracker-labelled target cells at a ratio of 25:1 for 5 hours at 37°C. Following two washes with 2mL PBS, cells were stained with LIVE/DEAD® dye as described in section 2.10.1, and placed at 4°C in the dark for 30 minutes. Cells

were subsequently washed with 1 mL PBS and then re-suspended in 300 µL 1% PFA. The percentage of dead cell-tracker-labelled target cells was determined using flow cytometry. Figure 2-1 illustrates the gating strategy used.

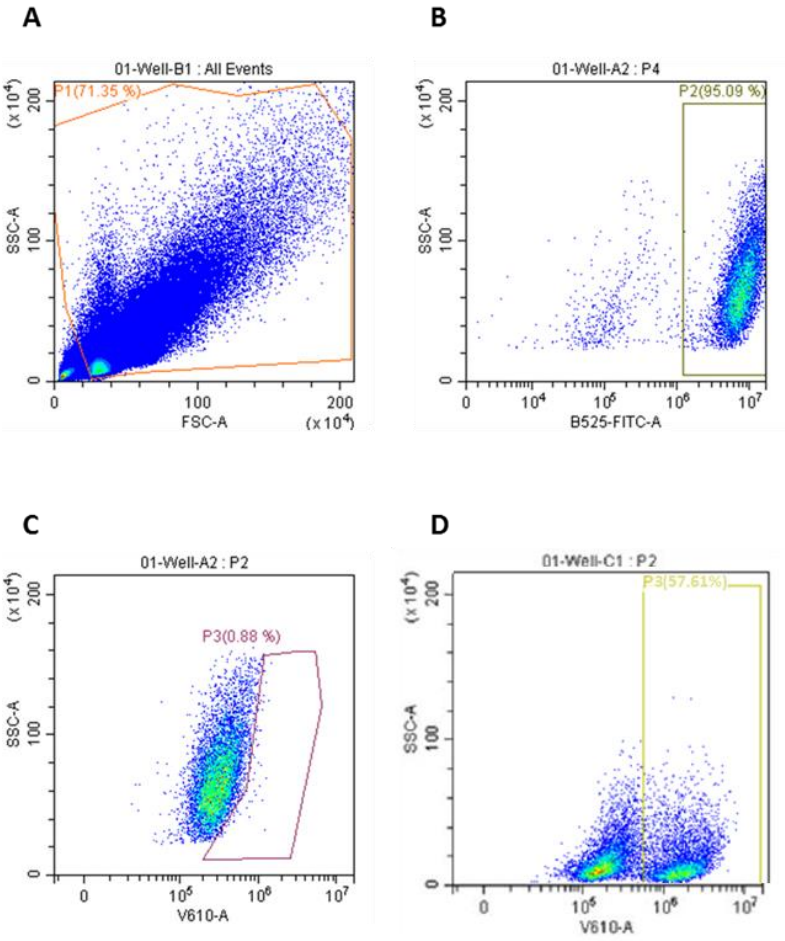

Figure 2-1: Gating strategy used to identify cell tracker-labelled target cells and quantify dead cells. PBMC were treated with OV and co-cultured with cell-tracker green labelled THP-1 cells. The percentage of dead target cells was determined by (A) Excluding cellular debris from THP-1 cells using a forward scatter-area (FSC-A) – side scatter-area (SSC-A) dot plot (gate Pl). (B) Gating on cell-tracker green labelled target cells using a B525-FITC-A channel vs-side SSC-A dot plot (gate P2). (C) To identifying live vs. dead cell populations, cell-tracker positive cells were interrogated using the V619-A LIVE/DEAD channel. THP-1 cells without PBMC co-culture were used to generate a gate which excluded live cells (gate P3). (D) shows a population of dead cells following co-culture with OV-treated PBMC; after gating on P3 the percentage of dead cells was determined.

Table 2-2: Flow cytometry antibodies

Target	Fluorochrome	Volume added	Origin	clone	Supplier
IgG control	PE	5 µL	mouse	SK7	Biolegend
CD3	PerCP	5 µL	mouse	W264/56	Biolegend
CD56	eFluor450	2 µL	mouse	TULY56	Miltenyi Biotec
CD69	PE	5 µL	mouse	FN50	Biolegend
CD45	FITC	2 µL	mouse	REA293	Miltenyi Biotec

PE: phycoerythrin, PerCP: peridinin chlorophyll protein complex, FITC: fluorescein isothiocyanate.

2.11 Measurement of caspase-3/7 activation

Caspase-3 and -7 activation was determined using CellEvent™ Caspase-3/7 Green Flow Cytometry Assay Kit (Thermofisher). AML cell lines (THP-1) were seeded at $1x10^6$ cells/mL and treated with PBMC-CM (± reovirus treatment) alone or in combination with the Smac mimetic, BV-6, for 7, 24 or 72 hrs. THP-1 cells were harvested and resuspended in 1mL PBS prior to the addition of 1µL caspase-3/7 green detection reagent, followed by 25 mins incubation at 37°C. 100 µl of DMSO was added to SYTOX™ AADvanced™ Dead Cell vial to reconstitute it at 1mM. 1 µl of SYTOX™ AADvanced™ Dead Cell was subsequently added to each sample and incubated at 37°C for 5 mins, samples were analysed by flow cytometry without washing or fixing.

2.12 Cytokine detection

2.12.1 Enzyme linked immunosorbent assay (ELISA)

Flat bottom 96 wells Nunc Maxisorp plated were coated with optimised dilutions of capture antibodies diluted in coating buffer (100nM $NaHCO_3$ in ddH2O) or PBS (Table 2-3 and Table 2-4). The plates were then covered with foil and incubated at 4℃ overnight. Using the Skan Washer 300 (Molecular Devices), antibody-coated plates were washed 3 times with PBST (0.05 % TWEEN®20 (Sigma Aldrich) in PBS). After two hours at RT, 200 µL of the blocking solution (10% FCS in PBS) was added for 2 hours at RT. After 3 more PBS-T washes, 100 µL of each of the recombinant protein standards and sample supernatants were added to the plates in triplicate. Halving serial dilutions of the recombinant standards were carried out (Table 2-5) to generate standard curves for each cytokine. The loaded plates were then covered with foil, placed at 4℃, and left overnight. After that, the plates were washed with PBS-T 6 times using the Skan washer 300, before addition of biotinylated detection antibodies diluted in blocking solution (Table 2-3 and Table 2-4). The plates were then incubated for two hours at RT. After washing the plates 6 times with PBS-T, 100 µL of extravidin-alkaline phosphatase (ALP) conjugate (Sigma), which had been diluted 1:5000 with PBS-T, was added to each well and incubated at RT for one hour. After washing the plates with PBS-T and ddH2O, each 3 times, 100 µL of substrate solution (p-nitrophenyl phosphate (Sigma) at a concentration of 1 mg/mL in 0.2 M TRIS buffer (Sigma)) was added. The plates were then left to develop in the dark for 10 to 30 minutes, or longer if required. At a wavelength of 405 nm, optical densities were measured using a Multiskan EX plate reader.

Table 2-3: Human ELISA antibodies

Target molecule	Species of origin	Clone	Role	Dilution	Dilution buffer
IL-6	Rat	MQ2-13A5	Capture	1:500	100nM $NaHCO_3$ in ddH2O
IL-6	Rat	MQ2-39C3	Detection	1:500	10% FCS in PBS
IL-8	Mouse	G265-5	Capture	1:500	100nM $NaHCO_3$ in ddH2O
IL-8	Mouse	G265-8	Detection	1:500	10% FCS in PBS
IFN-α	Mouse	MT1/3/5	Capture	1:250	PBS
IFN-α	mouse	MT2/4/6	Detection	1:1000	10% FCS in PBS
IFN-γ	Mouse	NIB42	Capture	1:250	100nM $NaHCO_3$ in ddH2O
IFN-γ	Mouse	4S.B3	Detection	1:500	10% FCS in PBS
TNF-α	Mouse	Mab1	Capture	1:500	100nM $NaHCO_3$ in ddH2O
TNF-α	Mouse	68B3C5	Detection	1:1000	10% FCS in PBS
MCP-1	Mouse	5D3-F7	Capture	1:250	100nM $NaHCO_3$ in ddH2O
MCP-1	Mouse	5D3-F7	Detection	1:500	10% FCS in PBS

IL-6: eBioscience, and the rest of the antibodies BD Bioscience.

Table 2-4: Mouse ELISA antibodies

For IFN-α, a mouse IFN-α ELISA kit was used according to the manufacturer's instructions (Invitrogen).

Target Molecule	Species of origin	Role	Dilution	Coating buffer/blocking solution
IL2	Mouse	Capture	1:250	100nM $NaHCO_3$ in ddH2O
IL2	Mouse	Detection	1:500	10% FCS in PBS
IL12	Rat	Capture	1:250	100nM $NaHCO_3$ in ddH2O
IL12	Rat	Detection	1:500	10% FCS in PBS
IFN-γ	Rat	Capture	1:500	100nM $NaHCO_3$ in ddH2O
IFN-γ	Rat	Detection	1:500	10% FCS in PBS
CCL2	Mouse	Capture	1:500	PBS
CCL2	Mouse	Detection	1:60	10% FCS in PBS
TNF-α	Rat	Capture	1:500	PBS
TNF-α	Rat	Detection	1:250	10% FCS in PBS

Source: BD Biosciences

Table 2-5: ELISA cytokine standards

Cytokine	Species	Top standard concentration	Bottom standard concentration	Manufacturer
IL-6	Human	2000 pg/mL	31.25 pg/mL	BD Biosciences
IL-8	Human	500 pg/mL	31.25 pg/mL	BD Biosciences
IFN-α	Human	10000 pg/mL	156.25 pg/mL	BD Biosciences
IFN-γ	Human	4000 pg/mL	62.5 pg/mL	BD Biosciences
TNF-α	Human	2000 pg/mL	31.25 pg/mL	Biosource
MCP-1	Human	20 ng/mL	0.313 ng/mL	BD Biosciences
IFN-α	Mouse	2000 pg/mL	31.25 pg/mL	Invitrogen
IL2	Mouse	5000 pg/mL	78.125 pg/mL	R&D Systems
IL12	Mouse	10000 pg/mL	156.25 pg/mL	R&D Systems
IFN-γ	Mouse	10000 pg/mL	156.25 pg/mL	R&D Systems
CCL2	Mouse	5000 pg/mL	78.125 pg/mL	R&D Systems
TNF-α	Mouse	10000 pg/mL	156.25 pg/mL	R&D Systems

2.12.2 Magnetic bead-based multiplex immunoassay

Production of 9 different cytokines and chemokines was determined using a custom designed 9-plex Biorad multiplex assay (Bio-Rad Laboratories) and the assay was carried out following the manufacturer's instructions. Briefly, the assay plate was first loaded by antibody-conjugated magnetic beads and washed twice with the provided wash buffer (100 µL/well) using the Bio-plex hand-held magnetic washer provided by the clinical team. All the subsequent washes were also carried out using the hand-held magnetic washer. Using the recombinant standard controls provided, a 1 in 4 dilution series of recombinant standard was produced to generate an eight-point standard curve. Subsequently, 50 µL of each standard and sample were added to the assay plate in duplicate. In the dark, at RT, the plate was shaken at 850 rpm for 30 minutes and then washed 3 times with a 100 µL/ well washing buffer before addition of 25 µL of the prepared detection antibody mix. The plate was then incubated for 30 minutes at RT while being shaken at 850 rpm. Following this incubation, the plate was washed 3 times in wash buffer (100 µL/well), and then 50 µL/well of streptavidin-phycoerythrin (SA-PE) was added. This was followed by incubation on a plate shaker 850 rpm for 10 minutes at RT, in the dark. After subjecting the beads to 3 washes in wash buffer, they were resuspended in 125 µL of assay buffer per well prior to analysed using a Bio-Plex 100 plate reader and Bio-Plex Manager software (Bio-Rad Laboratories).

2.13 OV propagation and quantification

2.13.1 CVA21 propagation

Figure 2-2 shows CVA21 propagation process. Propagation of CVA21 was carried out using Mel-624 cells. Cells were seeded in 150 cm^3 (Corning) tissue culture flasks at $12.5x10^6$ cells in 20 mL and incubated overnight to adhere. When cells reached 80-90% confluency they were infected with CVA21 at 0.001 pfu/cell for 24 hours, and the supernatant was then harvested and filtered (65 µm). Filtered supernatants were then transferred into Thinwall polypropylene heat-sealed tubes (Beckman Coulter). Centrifugation was applied to pellet the CVA21 (150,000g setting at 4°C for 2 hours) using a SW45 rotor (Optima™ L-80 ultra-centrifuge, Beckman Coulter). Purification of CVA21 took place using OptiPrep™ (Sigma-Aldrich) density gradient centrifugation. Preparation of the gradients for OptiPrep™ was done with 3 distinct solutions (Table 2-6).

Table 2-6: Solutions for OptiPrep gradient

Solution 1	0.3 M Tris and 0.3 mM EDTA in 100 mL dH2O (pH 7.4)
Solution 2	0.5 mM EDTA, 0.1 M NaCl and 50 mM Tris in 100 mL dH2O (pH 7.4)
Solution 3	20 mL 60% OptiPrep and 5 mL solution 1

Solution 3 was diluted in solution 2 to get the OptiPrep concentrations outlined in Table 2-7

Table 2-7: Solution dilutions for OptiPrep gradient

Concentration (%)	Solution 2 (mL)	Solution 3 (mL)
15	7	3
23	6	4
28	4	6
35	3	7

Layering of the prepared solutions was then performed into Thinwall Ultra-Clear™ open-top tubes (Beckman Coulter), beginning with the 35% dilution, using 2.5 mL for each solution. This was carried out the night before they were required, and gradient tubes were placed at 4°C overnight. The collected viral pellet was layered on OPtiPrep gradient tubes, followed by centrifugation at 160,000g, 4°C for 1.5 hours using the SW41 Ti rotor. 1 mL solution which contained CVA21 was harvested from the correct interface, aliquoted and stored at - 80°C. Plaque assays on Mel-624 cells were used to determine the CVA21 concentration (section 2.13.1.1).

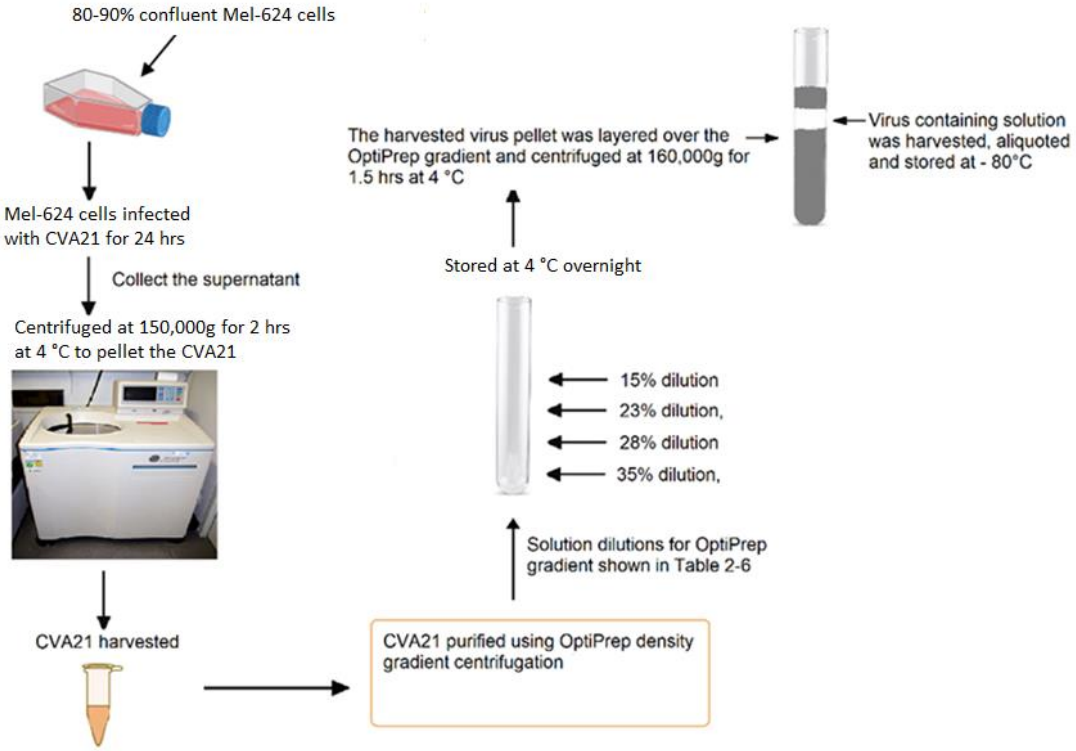

Figure 2-2: CVA21 propagation. Mel-624 cells were seeded in 150 cm^3 flasks and left to adhere overnight. Cells were then infected with 0.001 pfu/cell CVA21 for 24 hrs. The supernatants were harvested and filtered using a 0.65µm vacuum filtration unit. Filtered supernatants were then transferred into 94 mL thin wall polypropylene heat-sealed tubes and centrifuged at 150,000g for 2 hrs at 4°C. The virus was then harvested and purified using OptiPrep density gradient centrifugation.

2.13.1.1 CVA21 Plaque Assay

$6x10^5$ Mel-624 cells were seeded into each well of 6-well plate and left to adhere overnight. The next day, serum-free DMEM was used to create ten-fold serial dilutions of propagated virus. Culture medium was removed from each well and replaced with 500 µL serum-free DMEM per well, along with 100 µL of prepared virus dilutions. After a 2 hour incubation, serum-free DMEM was replaced with 2 mL 1:1 DMEM (20% FCS) and 1% Agarose in ddH2O (Agar, Sigma-Aldrich). After incubating for 24 hours, 1mL of 1% PFA was applied to each well and left

at RT for 30 minutes. The agarose was then removed by gentle washing with tap water before application of 1% methylene blue for 10 minutes. Viral plaques were then counted, and the pfu/mL calculated using the following calculation (number of plaques / dilution counted) x10. The concentration was determined as $3.5x10^8$ pfu/mL.

2.13.2 MG-1 Plaque Assay

MG-1 stock titre was determined using a similar protocol to above but using $7x10^5$ Vero cells instead of Mel-624 cells. The concentration of MG-1 was determined as $1x10^9$ pfu/mL.

2.13.3 Reovirus Plaque Assay

To quantify reovirus titre and determine the effectiveness of UV inactivation of reovirus stock and reovirus-CM, plaque assays were performed using L929 cells. $7x10^5$ L929 cells were seeded into each well of a 6-well plate and left to adhere for 24 hours at 37 °C. Reovirus-CM and stock reovirus (± UV inactivation) were diluted in serum free DMEM medium. Media was removed from L929 cells and replaced with 400 µL of DMEM serum free medium, followed by 100 µL of diluted viral samples in duplicate. The plates were incubated for 3 hours at 37°C and shaken regularly to ensure even distribution of the viral sample. After incubation, virus samples were removed and L929 cells were covered with 2 mL/well overlay media (2:1 ratio of DMEM complete medium mixed with 1.6% carboxymethylcellulose (CMC)). The plates were then incubated at 37°C for 72 hours. After removing the overlay media, the cells were washed twice with PBS and fixed with 1% PFA for 10minutes. After removing the fixative, the cells were stained for 5 minutes with 1% methylene blue. Plaques were then counted,

and the mean of duplicate wells was used to calculate viral titre using the formula below:

$$\text{pfu/mL} = \frac{\text{Average number of plaques}}{\text{Dilution}}$$

2.14 Ultraviolet (UV) irradiation of virus and CM

UV irradiation using a C-1000 UV CrossLinker (UVP) was used to inactivate virus stocks and prevent virus replication. An open 6-well plate and 1.5 mL aliquots were used for CM collected after OV treatment. An open 96-well plate and 50 µL aliquots were used to inactivate stock virus. Samples (stock virus or OV treated CM) were UV-treated for 2 minutes before being used in downstream assays.

2.15 ^{51}Chromium release assay

NK cell cytotoxicity was examined by the release of ^{51}Chromium (Cr). After harvesting $1x10^6$ target cells, they were labelled for one hour at 37°C with 100 µCi ^{51}Cr (PerkinElmer) in a 50 mL falcon tube. After labelling, the target cells were washed 3 times using 50 mL PBS each time and harvested by centrifugation. Cells were resuspended in 20 mL RPMI-1640 supplemented with 10% FCS at density of $5x10^4$ cells/ mL. The effector cells (PBMC±OV) were collected, counted and resuspended at $5x10^6$ cells/mL in RPMI and placed in triplicate to a 96-well round-bottom plate. A serial halving dilution was made in RPMI-1640 supplemented with 10% FCS to generate known effector:target (E:T) ratios, beginning at 100:1. Each well containing effector cells received $5x10^3$ ^{51}Cr labelled target cells, which were then co-cultured for 4 hours at 37°C with the effector cells. Spontaneous release was measured using separate plate where ^{51}Cr-labelled cells were placed in media which did not contain effector cells. For

maximum release, ^{51}Cr-labelled cells were placed in media contained 1 % Triton X (Sigma-Aldrich) to lyse target cells. After the 4 hours incubation at 37°C, the cells were pelleted at 400g for 5 minutes, and then 50 µL of the supernatant from each well was transferred to a Lumaplate (Perkin Elmer). Plates were dried overnight and the concentration of ^{51}Cr in the supernatant was then monitored using a Microbeta2 scintillation counter (PerkinElmer), and the percent of target cell lysis was determined using the following formula:

$$\%\text{Release} = 100 \times \frac{\text{(sample counts per minute (cpm) - spontaneous release cpm)}}{\text{(maximum release cpm - spontaneous release cpm)}}$$

2.16 *In vivo* models

All animal research was authorised by the University of Leeds's Local Ethical Review Committee and done under a project licence (PF0BA8592) issued by the UK Home Office. Debra Evans kindly administered all the injections. Charles River Laboratories supplied the CB17/Icr-*Prkdc*^{scid}/IcrIcoCrl (CB17) mice that were obtained between the ages of 6 and 10 weeks. Mice were kept in individually ventilated cages with a maximum of five mice per cage. All mice had access to water, nutrition, nesting material, and a regulated daylight cycle. At the end of each experimental, all animals were euthanized by cervical dislocation.

2.16.1 Xenograft AML model – subcutaneous injection (s.c)

On day 0, female CB17 mice aged 6–10 weeks were injected s.c with $5x10^6$ or $10x10^6$ THP-1 or KG-1 cells (delivered in 100 µL in PBS) (n=5 mice/group). The growth of the tumours was monitored twice a week. For therapy studies, $10x10^6$ cells were use and tumour growth was more reproducible. All treatments began when the tumours were palpable.

2.16.2 Therapy experiments

Mice implanted with THP-1 cells

On day 0, 32 female CB17 mice aged 6-10 weeks were injected s.c. with $10x10^6$ THP-1 cells (delivered in 100µL in PBS). On day 29, tumours were palpable in 21 mice; thus mice were randomly assigned into groups in order to ensure an equal number of tumour-bearing (and treatable) animals in each group (animal numbers/group are shown in Table 2-8). The treatment schedule consists of mice bearing treated i.t with $5x10^7$ pfu of UV-irradiated reovirus (diluted in 50 µL of PBS), then after 6 hours animals were subsequently treated i.p with 100 µL BV-6 (5mg/Kg); reconstituted 1mg/mL in NaCl. To confirm drug safety before administration to all animals, initially, only a couple of mice were treated with BV-6, and adverse reactions such as convulsions, laboured breathing and reduced mobility were monitored for ~30 mins. Treatments were subsequently administered twice weekly for 2 weeks as described in Table 2-8. Mice were monitored 3 times a week for weight loss, and tumour size was measured using callipers. Mice were euthanized when the tumour reached a maximum of 1.5 cm in any direction.

Table 2-8 THP-1 mice groups

Group	No of mice	Treatment
1	4	50 µl i.t PBS (morning) and 100 µl i.p NaCl vehicle control (afternoon) (Tuesday & Friday)
2	6	50 µl i.t UV-Reovirus ($5x10^7$ pfu in PBS) (Tuesday & Friday)
3	5	100 µl i.p BV-6 (5mg/kg in NaCl) (Tuesday & Friday)
4	6	50 µl i.t UV-reovirus ($5x10^7$ pfu in PBS; morning) and 100 µl i.p BV-6 (5mg/kg in NaCl; afternoon) (Tuesday & Friday)

Mice implanted with KG-1 cells

On day 0, 32 female CB17 mice aged 6-10 weeks were injected s.c. with $10x10^6$ KG-1 cells (delivered in 100µL in PBS). On day 17 after tumour implantation, tumours were palpable and treatments began. The treatment schedule consisted of mice being treated i.t with $5x10^7$ pfu of UV-inactivated reovirus in 50 µL of PBS first, then after 3 hours mice were subsequently treated i.p with 100 µL ABT199 (reconstituted at 100mM in DMSO) dissolved in PBS (1mg/kg). As mentioned above, to confirm drug safety before administration to all animals, only a couple of mice were treated with ABT-199, and adverse reactions such as convulsion, laboured breathing and reduced mobility were monitored for ~30 mins. Following assessment of safety, treatments were administered twice weekly for 2 weeks as described in Table 2-9. Mice were monitored 3 times a week for weight loss, and

tumour size was measured using callipers. Mice were euthanized when the tumour reached a maximum of 1.5 cm in any direction.

Table 2-9 KG-1 mice groups

Group	No of mice	Treatment
1	8	50 µl i.t PBS (morning) and 100 µl i.p DMSO + PBS vehicle control (afternoon) (Monday & Thursday)
2	8	50 µl i.t UV-Reovirus ($5x10^7$ pfuin PBS) (Monday & Thursday)
3	8	100 µl i.p ABT-199 (1mg/kg in PBS) (Monday & Thursday)
4	8	50 µl i.t UV-reovirus ($5x10^7$ pfuin PBS; morning) and 100 µl i.p ABT-199 (1mg/kg in PBS; afternoon) (Monday & Thursday)

2.17 Statistical analysis

Graph Pad Prism 8.0 was used for the statistical analysis of the data. P-values were obtained using either student's t-test with two-tailed distribution for comparing two groups, one-way analysis of variance (ANOVA), or two-way ANOVA with post-hoc testing was used when comparing three or more groups or combination treatment, respectively. Levels of statistical significance are as follows: *P≤0.05, **P≤0.01, ***P≤0.001, ****P≤0.0001, and the absence of a * indicates that the data obtained was not significant. The legends for each figure include information on the number of replicates and donors.

Chapter 3 : Smac/ BH3 mimetics potentiate cytokine-induced killing by OVs in AML

3.1 : Introduction

AML is a haematological malignancy that is currently incurable; therefore, developing new effective therapies is crucial. Several cytokines, most notably IL-2, IL-27 and type I IFNs, have been considered for the treatment of malignant disorders including AML [327, 328]; type I IFN promotes several mechanisms of cell death including direct apoptosis and indirect enhancement of phagocytic and cytotoxic mechanisms by immune effector cells [329]. Type I IFN also induces anti-tumour responses by disrupting tumour vasculature as well as causing maturation of DCs and activation of immune cells (e.g. NK cells and T cells) [330, 331]. Moreover, IFN-α (PEGylated IFN-2α) was approved by the FDA in 2011 for the adjuvant treatment of melanoma [332] and is currently in phase I/II trials for AML [329, 333], which when administered prophylactically produced relatively low rates of relapse [333].

A handful of OVs have been suggested as promising agents for AML treatment, including HSV-1 [285], reovirus [277], myxoma virus [278] and VSV [283]. However, only VSV-IFNβ-NIS has progressed to clinical trials [334]. As discussed in sections 1.2.3 and 1.4.1, Smac mimetics can synergize with OV treatment to enhance cancer cell death and suppress tumour growth in many malignancies [318-320]. The anti-cancer synergy between Smac mimetics and OV treatment was dependent on pro-inflammatory cytokines, such as TNF-α and IFN-α, secreted in response to OV infection [320, 322]. Moreover, OV treatment prior to Smac mimetic therapy was crucial to obtain synergistic responses [322]. In addition to Smac mimetics, several BH3 mimetics (e.g. GX15-070, EM20-25 and

BI-97D6) have also been reported to enhance tumour cell death when combined with OV treatment, such as VSV and adenovirus [335].

To date, the potential of OV treatment for AML remains relatively under investigated and the ability of Smac/ BH3 mimetics to potentiate OV therapy in AML has not been explored. Hence, the overarching aim of this study was to investigate whether Smac/ BH3 mimetics could be used to enhance OV efficacy in AML. The work outlined in this chapter focused on OV-induced cytokine mediated killing because of the known role of cytokines in AML therapy. Moreover, the ability of UV-inactivated OV to induce pro-inflammatory cytokines was also explored as a possible safer option for AML treatment, given the immunosuppressed nature of patients. Importantly, the efficacy of this combination was also explored using primary AML patient samples to better represent the heterogeneity of AML. Primary samples consisted of peripheral blood taken from patients diagnosed at St. James's University Hospital, Leeds, between April 2021 and March 2022, the age range of participants was between 20 and 88 years old, and both male and female donors were included.

The purpose of the work outlined in this chapter was to: (i) investigate the secretion of pro-inflammatory cytokines from healthy PBMCs in response to four molecularly distinct OVs (reovirus, MG1, CVA21 and HSV-1), (ii) examine pro-inflammatory cytokine-mediated killing of AML cells, (iii) investigate the ability of Smac/ BH3 mimetics to enhance OV-induced cytokine-mediated killing of AML cells, (iv) identify the cytokines responsible for killing and confirm the role of apoptosis, and (v) investigate the secretion of pro-inflammatory cytokines in response to UV-inactivated OV treatment to explore the potential use of UV-inactivated OV as a safer treatment option for immunosuppressed AML patients.

3.2 Pro-inflammatory cytokines secreted by OV

Since AML is a blood disorder and OV treatment would be administered via i.v injection, PBMCs would be the first point of contact for OV and act as the first line of defence against OV infection. However, molecularly distinct OV may induce different inflammatory profiles from PBMCs, due to engagement of diverse PRRs, hence, it was important to examine the cytokine profile induced in response to OV treatments.

The production of IFN-α, IFN-β, IFN-γ and TNF-α from healthy PBMCs donors (HD-PBMC) in response to reovirus, MG1, CVA21 or HSV-1 treatment (0.1 or 1 pfu/PBMC) for 48 hrs was examined by ELISA. A maximum dose of 1 pfu/PBMC was chosen because this dose would be achievable in patients; moreover, immune activation has been previously reported using these OV doses [258, 336-338]. PBMCs produced significant amounts of IFN-α in response to reovirus, MG1, CVA21 and HSV-1 treatments, with a maximum production of ~8000 pg/mL after treatment with 1 pfu/PBMC reovirus (Figure 3-1A). MG1 and HSV-1 treatment induced significant amounts of IFN-α (~7000 pg/mL) at both 0.1 and 1 pfu/cell (Figure 3-1A); however, no dose dependent increase was observed. CVA21 induced significant levels of IFN-α at 1 pfu/PBMC and overall produced lower levels than the other OV (~4000 pg/mL) (Figure 3-1A). These data demonstrate that all of the OV used were capable of stimulating IFN-α production. Using the top dose of each OV (1 pfu/PBMC), the production of IFN-β was also investigated. Significant levels of IFN-β were detected in response to reovirus and MG1 treatment, with an average of ~260 pg/mL and ~170 pg/mL, respectively (Figure 3-1B). No statistically significant amounts of IFN-β were detected (~50 pg/mL) in response to HSV-1 treatment, and CVA21 treatment did not induce detectable levels of IFN-β (Figure 3-1B).

Upon assessment of IFN-γ, production appeared to be induced after OV treatment, however, statistical significance was only reached following treatment with HSV-1, not the other OV, due to varied response across different PBMC donors (Figure 3-2). Overall, an average of ~1500 pg/mL IFN-γ was induced in response to reovirus and CVA21 (Figure 3-2), compared to only ~500 pg/mL following MG1 and HSV-1 treatment (Figure 3-2). The secretion of TNF-α was also varied between the viruses and no statistically significant increases were observed in response to any of the OV tested (Figure 3-3). However, levels did increase from a mean of ~5 pg/mL in untreated samples to ~70 pg/mL after treatment with 1 pfu/PBMC reovirus, and ~100 pg/mL after MG1 or HSV-1 treatment (Figure 3-3); values greater than 31.25 pg/mL are within the detection range of the TNF-α ELISA standard. By contrast, TNF-α secretion was not detected after CVA21 treatment (data not shown). Collectively, these data confirm that OVs can induce cytokine production from PBMC. However, the data presented also suggests that CVA21 may be less inflammatory than the other OV as secretion of IFN-α was lower, and IFN-β and TNF-α were not detected following CVA21 treatment.

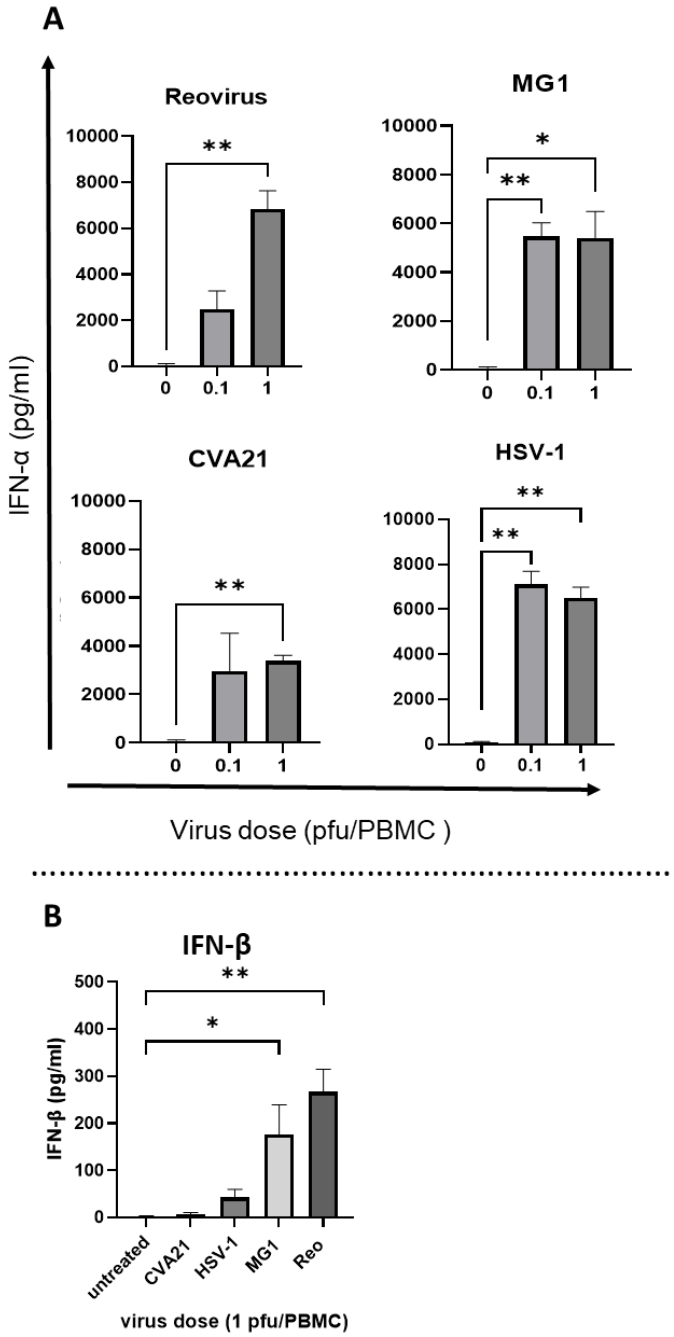

Figure 3-1: Type I IFN secretion in response to OV treatment. HD-PBMCs were treated with reovirus, MG1, CVA21 or HSV-1 for 48 hrs at 0, 0.1 or 1 pfu/PBMC. Supernatants were harvested and secretion of **A**: IFN-α and **B**: IFN-β was measured by ELISA. Error bars indicate mean + S.E.M for at least 3 individual PBMC donors. Statistical significance was performed using an unpaired one-way ANOVA and comparisons with untreated controls are shown. *= $p<0.05$, **=$p<0.01$.

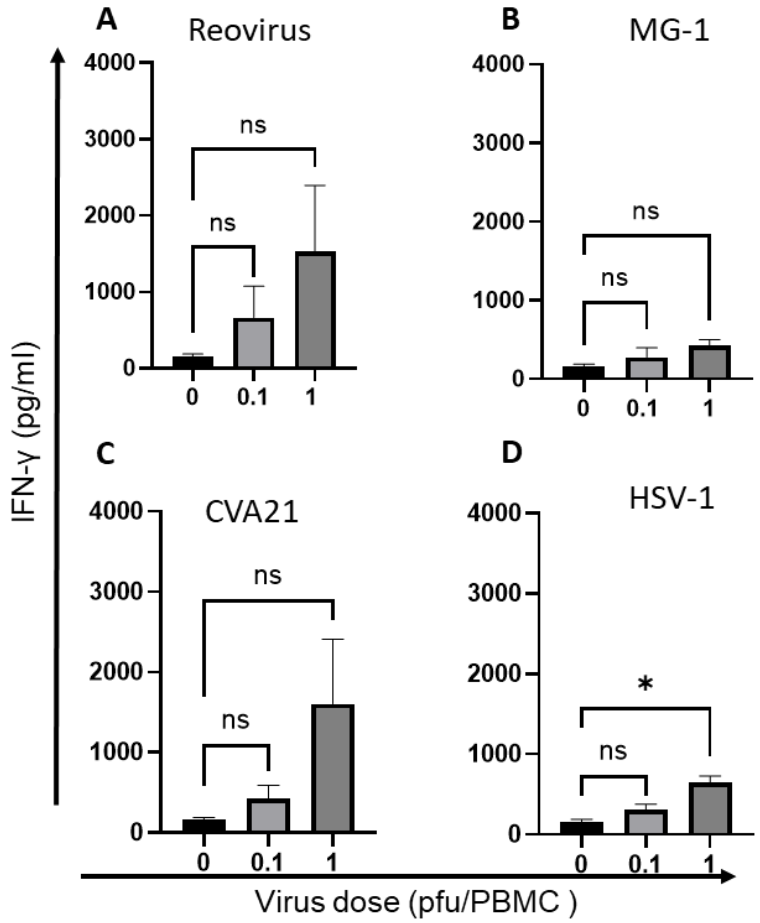

Figure 3-2: IFN-γ secretion in response to OV treatment. HD-PBMC were treated with OV for 48 hrs at 0, 0.1 or 1 pfu/PBMC; **A**: reovirus, **B**: MG1, **C**: CVA21, or **D**: HSV-1. Supernatants were harvested and secretion of IFN-γ was measured by ELISA. Error bars indicate mean + S.E.M for at least 3 individual PBMC donors. Statistical significance was performed using an unpaired one-way ANOVA and comparisons with untreated controls are shown. *= $p<0.05$.

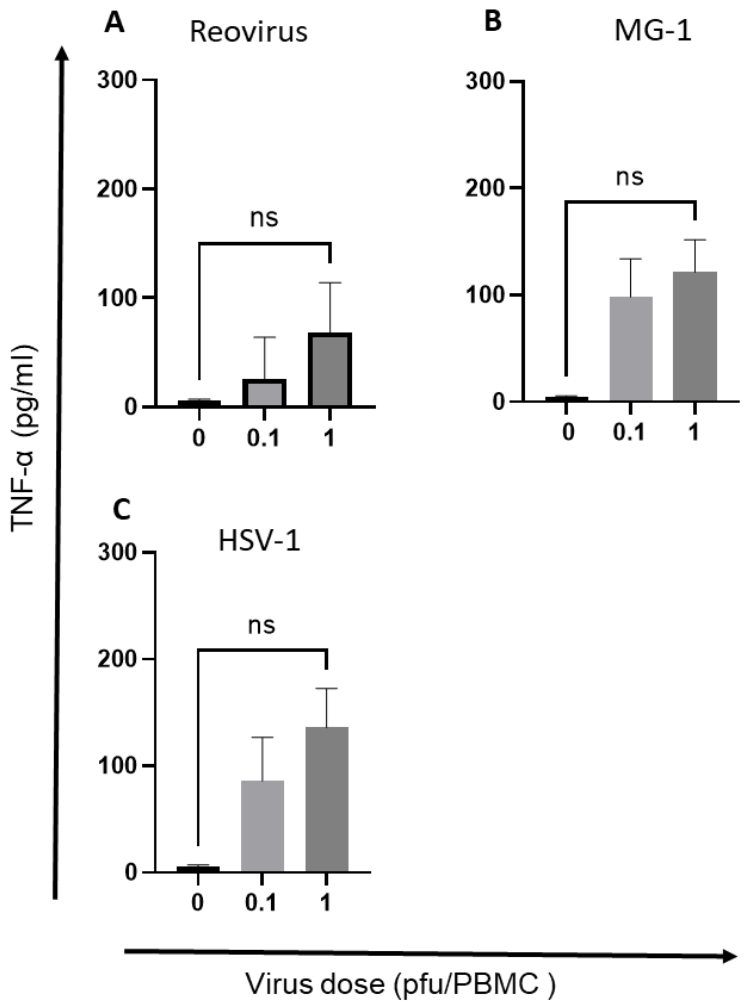

Figure 3-3: TNF-α secretion in response to OV treatment. HD-PBMC were treated with OV for 48 hrs at 0, 0.1 or 1 pfu/PBMC; **A**: reovirus, **B**: MG1, **C**: HSV-1. Supernatants were harvested and secretion of TNF-α was measured by ELISA. Error bars indicate mean + S.E.M for at least 3 individual PBMC donors. Statistical significance was performed using an unpaired one-way ANOVAs and comparisons with untreated controls are shown.

Given the variability of cytokine secretion in response to different OV treatment and between different PBMC donors, the secretion of these and additional cytokines were further analysed using multiplex immunoassay. Using this assay, the secretion of a wider range of pro-inflammatory cytokines (IFN-2α, IFN-γ, IP-10, TNF-α, TNF-β, TRAIL, IL-1β, RANTES and MCP-1) from HD-PBMC in response to OV was evaluated. PBMCs were treated with 0, 0.1 or 1 pfu/PBMC reovirus, MG1, CVA21 or HSV-1 for 48 hrs and the secretion of cytokines was examined. Interestingly, various levels of pro-inflammatory cytokines were observed in response to OV with the greatest levels observed in response to reovirus treatment. Reovirus induced significant amounts of IFN-2α, IP-10, TNF-α, TNF-β, TRAIL, IL-1β, RANTES and MCP-1; however, reovirus treatment did not induce statistically significant amounts of IFN-γ (Figure 3-4A, Figure 3-5A and Figure 3-6A). MG1 induced significant amounts of IFN-2α, IFN-γ, IP-10, TNF-α, TRAIL, IL-1β and MCP-1 but not statistically significant levels of TNF-β and RANTES (Figure 3-4B, Figure 3-5B and Figure 3-6B). For CVA21 treatment, significant amounts of IP-10, TNF-α, TNF-β, TRAIL and MCP-1 were secreted but there was no statistically significant increase in IFN-2α, IFN-γ, IL-1β and RANTES secretion (Figure 3-4C, Figure 3-5C and Figure 3-6C). While HSV-1 induced significant levels of IFN-2α, IP-10, TNF-α, TRAIL, IL-1β and MCP-1, HSV-1 treatment did not induce significant amounts of IFN-γ, TNF-β and RANTES (Figure 3-4D, Figure 3-5D and Figure 3-6D). Collectively, these results demonstrated that different OV induce a similar, but not identical, range of pro-inflammatory cytokines.

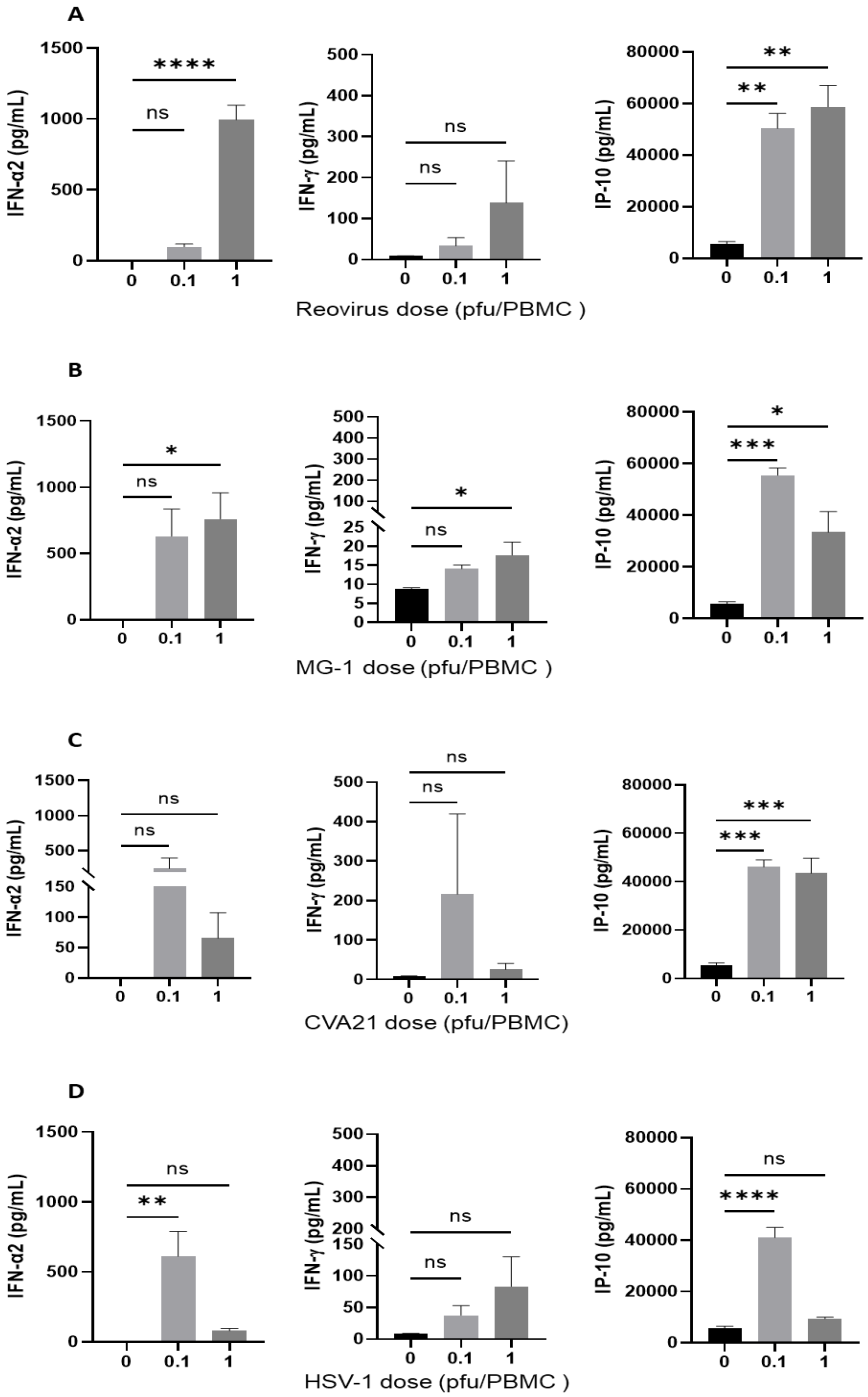

Figure 3-4: IFN-α, IFN-γ and IP-10 cytokine secretion from HD-PBMC in response to OV treatment. HD-PBMC were treated for 48 hrs with 0, 0.1 and 1 pfu/PBMC **A**: reovirus, **B**: MG1, **C**: CVA21, and **D**: HSV-1. Supernatants were harvested and secretion of IFN-α, IFN-γ and IP-10 was measured using a 9-multiplex immunoassay. Error bars indicate mean for n=3 independent PBMC donors, + S.E.M. Statistical significance was performed using an unpaired one-way ANOVAs and comparisons with untreated controls are shown. *=p<0.05, **=p<0.01, ***=p<0.005, ****=p<0.0001.

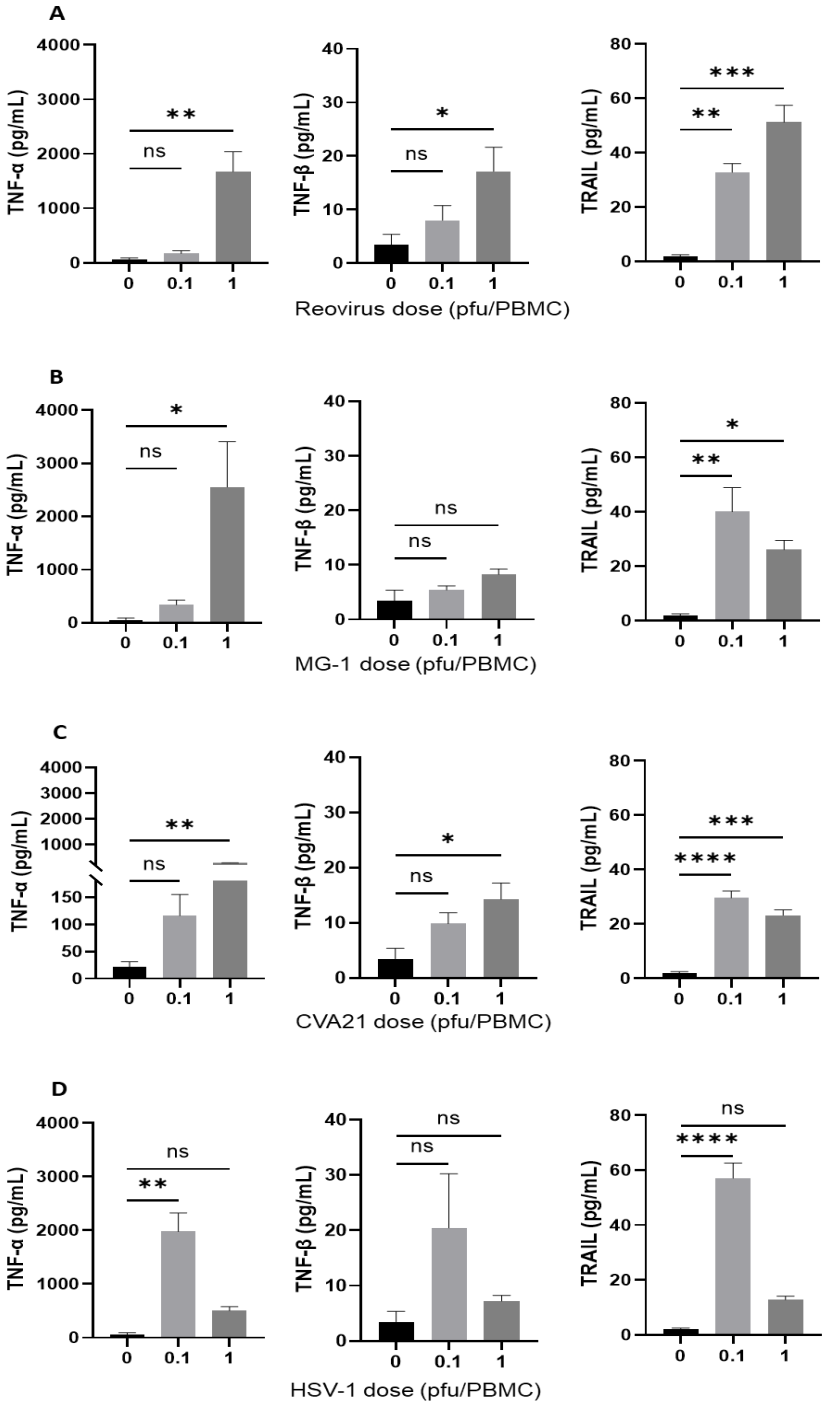

Figure 3-5: TNF-α, TNF-β and TRAIL cytokine secretion from HD-PBMC in response to OV treatment. HD-PBMC were treated for 48 hrs with 0, 0.1 and 1 pfu/PBMC **A**: reovirus, **B**: MG1, **C**: CVA21, and **D**: HSV-1. Supernatants were harvested and secretion of TNF-α, TNF-β and TRAIL was measured using a 9-multiplex immunoassay. Error bars indicate mean for n=3 independent PBMC donors, + S.E.M. Statistical significance was performed using an unpaired one-way ANOVAs and comparisons with untreated controls are shown. *=p<0.05, **=p<0.01, ***=p<0.005, ****=p<0.0001.

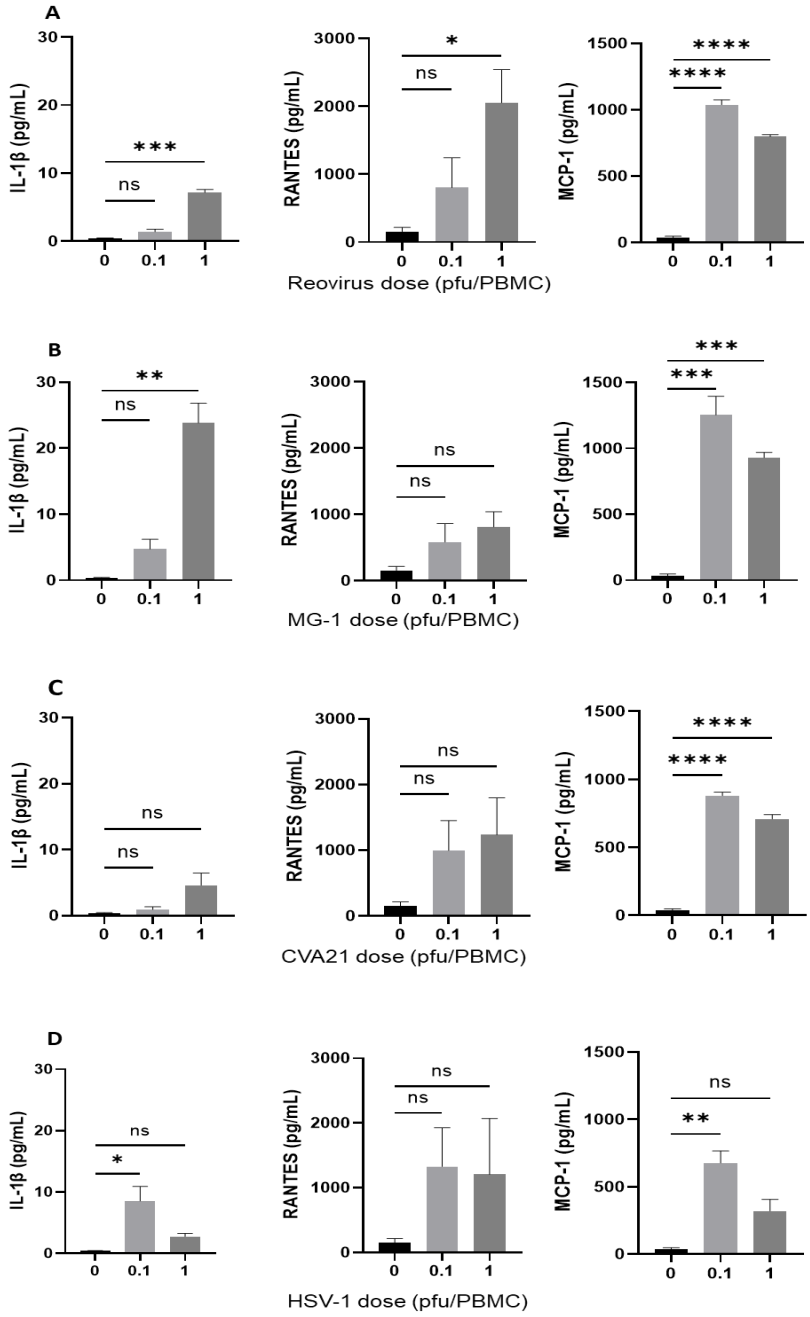

Figure 3-6: IL-1β, RANTES and MCP-1 cytokine secretion from HD-PBMC in response to OV treatment. HD-PBMC were treated for 48 hrs with 0, 0.1 and 1 pfu/PBMC **A**: reovirus, **B**: MG1, **C**: CVA21, and **D**: HSV-1. Supernatants were harvested and secretion of IL-1β, RANTES and MCP-1 was measured using a 9-multiplex immunoassay. Error bars indicate mean for n=3 independent PBMC donors, + S.E.M. Statistical significance was performed using an unpaired one-way ANOVAs and comparisons with untreated controls are shown. *=p<0.05, **=p<0.01, ***=p<0.005, ****=p<0.0001.

3.3 Cytotoxic effect of OV-induced cytokine production from PBMC

Given the range of cytotoxic cytokines produced by PBMC after OV treatment, we next sought to test the cytotoxic bystander killing effect of OV-induced cytokines. CM from PBMCs was collected and added to AML cell lines (1:1 dilution in fresh medium) for 72 or 96 hrs before assessment of cell viability using LIVE/DEAD flow cytometry or MTS assays (data not shown), respectively. Initially, MTS and LIVE/DEAD assays were compared to establish the most consistent assay to use in future experiments. LIVE/DEAD specifically quantifies the number of dead cells, unlike the MTS assay which will be affected by both cytostatic and cytotoxic effects, therefore, LIVE/DEAD assays were selected for use in all future studies.

PBMC were treated with 0, 0.1 or 1 pfu/PBMC OV for 48 hrs, the PBMC-CM was collected and then subjected to UV-irradiation to inactivate OV and prevent OV-induced direct oncolysis. All OV-CM collected after treatment with 1 pfu/PBMC induced a significant cytotoxic effect in THP-1 cells after 72 hrs, with cell death reaching ~20% (Figure 3-7A). In KG-1 cells, a significant cytotoxic effect was observed for reovirus-CM, HSV-1-CM and MG1-CM, but not CVA21-CM (Figure 3-7B). Whilst there appeared to be an increase in cell death after treatment with OV-CM in HL-60 cells, this was only significant with reovirus-CM (Figure 3-7C). Moreover, for Kasumi-1 cells, significant cell death was only induced in response to reovirus-CM and HSV-1-CM (Figure 3-7D).

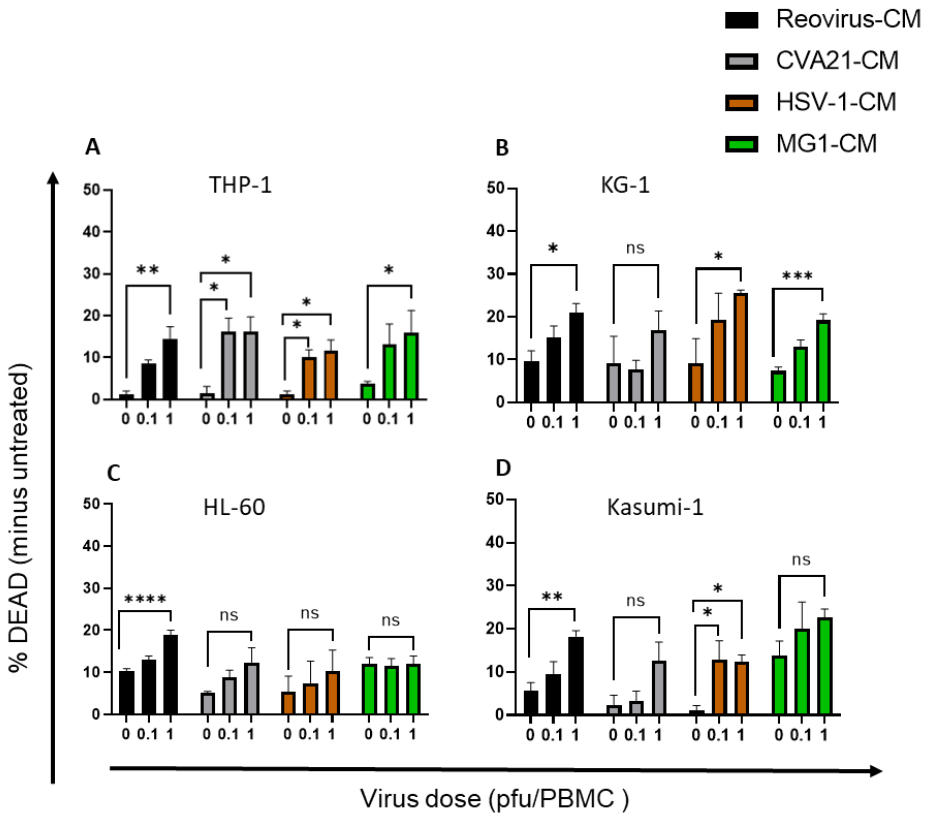

Figure 3-7: Cytotoxic effect of OV-induced pro-inflammatory cytokines on AML cell lines. AML cells were cultured in UV-inactivated PBMC-CM (± OV treatment) for 72 hrs and cell viability was measured using LIVE/DEAD flow cytometry. The percentage (%) of dead cells after treatment with Reovirus-PBMC-CM, CVA21-PBMC-CM, HSV-1-PBMC-CM and MG1-PBMC-CM is shown for **A**: THP-1 cells, **B**: KG-1 cells, **C**: HL-60 cells and **D**: Kasumi-1 cells. Data was normalised to remove spontaneous cell death observed in the absence of CM. Error bars indicate mean + S.E.M for at least 3 individual PBMC donors. Statistical significance was performed using unpaired one-way ANOVAs. *=p<0.05, **=p<0.01, ***=p<0.005, ****=p<0.0001.

3.4 Cytotoxicity of Smac and BH3 mimetics in AML cell lines and non-malignant cells

Having identified that OVs secrete a range of pro-inflammatory cytokines and that PBMC-CM was cytotoxic towards AML cell lines, albeit at variable levels and with <20% cytotoxicity observed, it was possible that apoptotic modulators (e.g. Smac/ BH3 mimetics) could be used to enhance extrinsic cytokine-mediated killing. Smac mimetics bind to IAPs, and BH3 mimetics binds to BCL-2 anti-apoptotic family members to facilitate apoptosis [128, 339]. However, to examine the potential interaction of combination treatment, it is necessary (and helpful) to use conditions that were not too toxic to cells when used as a single agent. To identify a sub-toxic dose of Smac and BH3 mimetics, increasing concentrations were applied to AML cell lines, and cell death was examined after 72 hrs using LIVE/DEAD assays. For the Smac mimetic, LCL161, a dose-dependent increase in cell death was observed with a maximum average of ~50% cell death in HL-60 cells and ~30% cell death in the other cell lines at the highest concentration used (20μM) (Figure 3-8A). In comparison, BV-6 (an alternative Smac mimetic) treatment also caused cell death in a dose-dependent manner, with a maximum of ~90% cell death observed in HL-60 and THP-1 cells, and ~65% cell death observed in KG-1 and Kasumi-1 cells at the highest concentration (20μM) (Figure 3-8B). ABT-199 (a BH3 mimetic) caused a dose-dependent increase in cell death in AML cell lines, with a maximum of ~90% cell death in HL-60 cells, ~80% in THP-1 and KG-1 cells, and ~60% in Kasumi-1 cells at the top concentration of 10μM (Figure 3-8C), similar data were also observed after ABT-263 treatment in all cell lines (Figure 3-8D). To aid comparisons across cell lines and drugs, Table 3-1 highlights the concentrations of each drug that induced a significant increase

in cell death for each cell line. Collectively, these data demonstrate that different AML cell lines had variable degrees of sensitivity to Smac and BH3 mimetics.

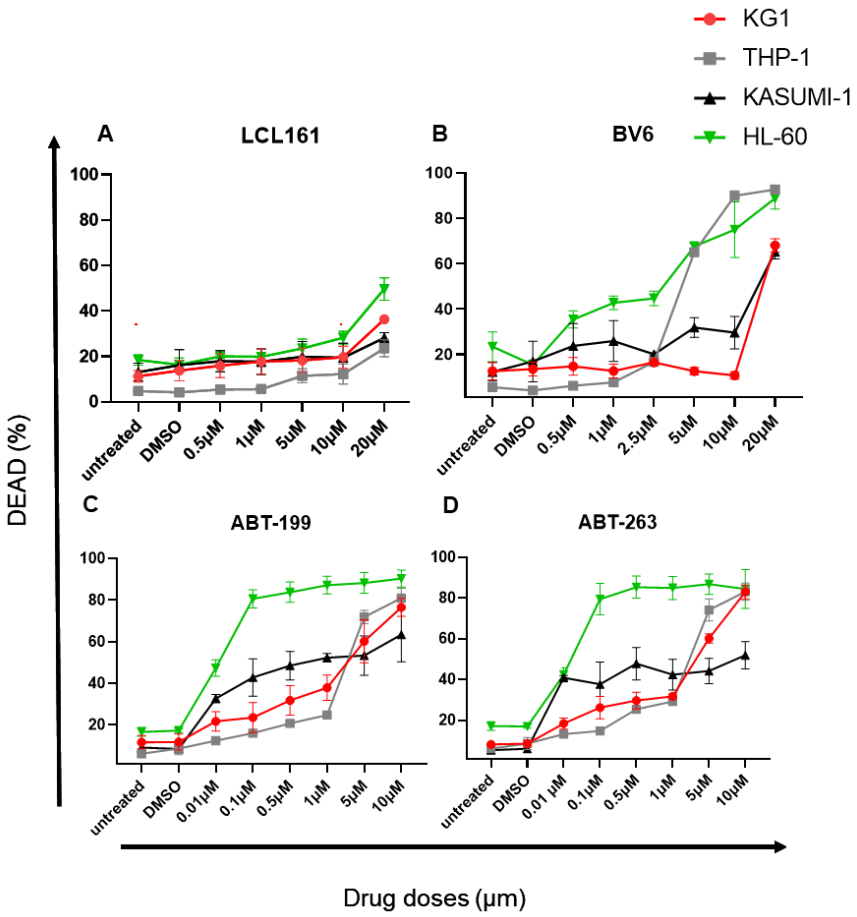

Figure 3-8: Direct cytotoxic effect of Smac/ BH3 mimetics on AML cell lines. AML cell lines (KG-1; red, THP-1; grey, Kasumi-1; black, HL-60; green) were treated with increasing doses of **A**: LCL161, **B**: BV-6, **C**: ABT-199 or **D**: ABT-263 for 72 hrs. Cell death was assessed using LIVE/DEAD flow cytometry. Data shows the mean percentage of cell death for n=3 independent experiment, ± SEM.

Table 3-1: Smac/ BH3 mimetics concentrations that caused significant cell death in AML cell lines.

Cell line	LCL161	BV-6	ABT-199	ABT-263
THP-1	20μM	5μM	5μM	1μM
KG-1	20μM	20μM	1μM	0.05μM
Kasumi-1	Not reached	20μM	5μM	0.05μM
HL-60	20μM	2.5μM	0.01μM	0.01μM

Considering the susceptibility of AML cell lines to both Smac and BH3 mimetics, alongside a desire to develop less toxic AML therapies, it was also important to examine the cytotoxic effect of these compounds on non-malignant healthy cells. To do this, cell death was investigated after treatment with increasing concentrations of LCL161, BV-6, ABT-199 or ABT-263 using HD-PBMC and non-malignant myeloid cells, namely CD14+ monocytes isolated from PBMC. Of note, an average of ~30%, ~40%, ~65% and ~80% cell death was observed in PBMC after treatment with LCL161, BV-6, ABT-199 and ABT-263, respectively, at the top dose (10 μM) (Figure 3-9A). A significant increase in PBMC cell death was not observed after treatment with LCL161 at any dose, but was observed after treatment with BV-6 at 5μM and 0.1 μM ABT-199 and ABT-263. Importantly, monocyte cell death was not observed after the treatment with either Smac or BH3 mimetics at any concentration used (Figure 3-9B).

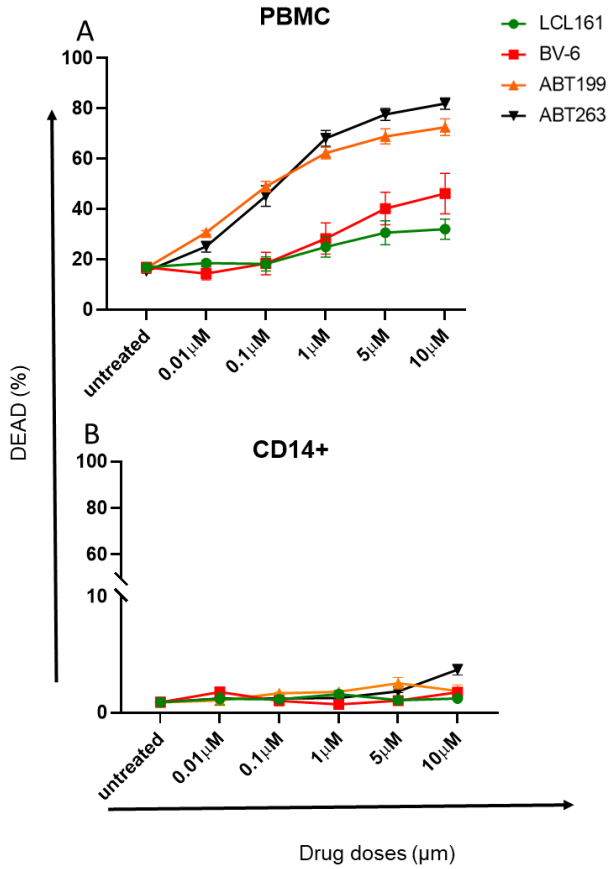

Figure 3-9: Direct cytotoxic effect of Smac and BH3 mimetics on healthy PBMCs and CD14+ monocytes. A: PBMC or **B**: CD14+ cells isolated from PBMC were treated with Smac or BH3 mimetics at increasing concentrations for 72 hrs. Cell death was assessed using LIVE/DEAD flow cytometry. The data shows the mean cell death ± S.E.M for n=3 independent PBMC donors.

Taken together, the varied responses of AML cells towards Smac or BH3 mimetic treatment suggested that different concentrations would be required for each cell line to use sub-toxic doses in combination treatment approaches. Table 3-2 illustrates the drug concentration selected for each cell line. Importantly, the selected drug concentrations did not cause a statistically significant increase in cell death in AML cell lines or healthy PBMC.

Table 3-2: Smac and BH3 mimetic doses selected for each AML cell line

Cell line	LCL161	BV-6	ABT-199	ABT-263
THP-1	10 µM	2.5 µM	0.01 µM	0.01 µM
KG-1	10 µM	1 µM	0.01 µM	0.01 µM
HL-60	10 µM	1 µM	0.01 µM	0.01 µM
Kasumi-1	10 µM	1 µM	Not determined	0.01 µM

3.5 Smac and BH3 mimetics potentiated the bystander killing of OV-CM on AML cells

Very little is currently known about the combination of Smac or BH3 mimetics and OV treatment in the context of AML. To evaluate the possibility of boosting the bystander cytotoxic effect of OV-CM using Smac or BH3 mimetics, AML cells were treated with Smac or BH3 mimetics (at specified doses depending on the cell line) immediately prior to the addition of PBMC-CM and cells were left for 72 hrs before cell death was evaluated using LIVE/DEAD. Initially, only LCL161 and ABT-263 were used, as LCL161 is the most studied Smac mimetic and because ABT-263 targets multiple anti-apoptotic BCL-2 family members. For THP-1 cells (Figure 3-10), in the absence of CM there was no significant increase in cell death following drug treatment, demonstrating that sub-toxic concentrations of drug were selected. However, as observed previously (Figure 3-7), OV treated PBMC-CM (reovirus, MG1, CVA21 and HSV-1) induced cell death as expected. When PBMC-CM (in the absence of OV treatment) was combined with 10 µM LCL161,

there was no significant enhancement in cell death. By contrast, when OV-treated PBMC-CM (OV-CM) was used, the addition of LCL161 significantly increased cell death when compared with OV-treated PBMC-CM alone. For example, for reovirus, LCL161 increased cell death (above PBMC-CM alone) by 15%, 25% and 30% when combined with 0, 0.1 and 1 pfu/PBMC-CM, respectively; for MG1, LCL161 increased cell death by 10%, 15% and 20% when combined with 0, 0.1 and 1 pfu/PBMC-CM, respectively; for CVA21, LCL161 increased cell death over PBMC-CM alone by ~10% and ~20% at 0, 0.1 or 1pfu/PBMC; and finally, for HSV-1, LCL161 enhanced cell death by 10%, 30% and 25% when combined with 0, 0.1 and 1 pfu/PBMC-CM, respectively (Figure 3-10). Interestingly, despite the slightly different cytokine profiles induced by different OVs, similar results were observed irrespective of the OV used. However, upon interrogation of data for all OV-CM, maximum cell death was observed when 1 pfu/PBMC reovirus-CM was used in combination with LCL161 (~55%), compared to only 40-46% for PBMC-CM collected after treatment with MG1, CVA21 or HSV-1.

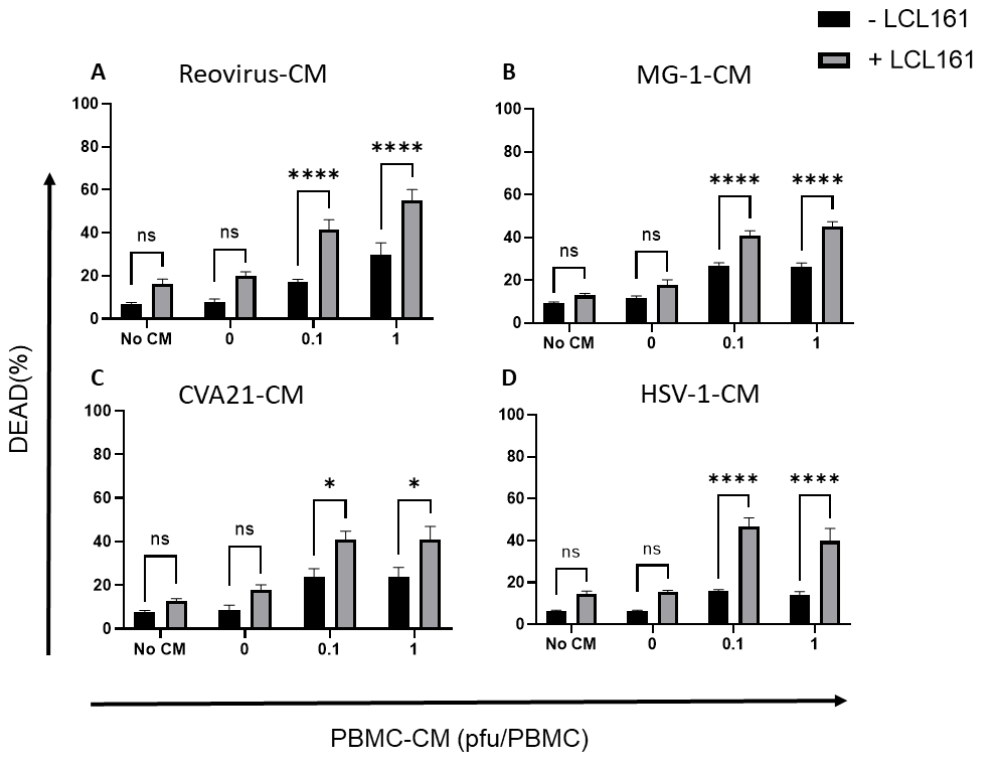

Figure 3-10: THP-1 cell death induced by LCL161 in combination with UV-irradiated PBMC-CM. THP-1 cells were treated with 10 µM LCL161 and UV-inactivated PBMC-CM (± OV treatment) for 72 hrs, and cell death was assessed using LIVE/DEAD flow cytometry. The mean percentage of dead cells after treatment with **A**: Reovirus-CM, **B**: MG1-CM, **C**: CVA21-CM and **D**: HSV-1-CM is shown from at least 3 individual PBMC donors, + S.E.M. Statistical significance was performed using a two-way ANOVA and significance between PBMC-CM alone and combination with LCL161 is shown. *=p<0.05, ****=p<0.0001.

Next, cytotoxic effect of ABT-263 (a BH3 mimetic) alone or in combination with OV-CM, was tested in THP-1 AML cells. Interestingly, THP-1 cell death was significantly enhanced when reovirus-CM, MG1-CM or HSV-1-CM (not CVA21-CM) was combined with 0.01 µM ABT-263; however, as expected, this was not observed when PBMC-CM was used in the absence of OV treatment. In contrast to the results obtained with LCL161, ABT-263 only enhanced cell death above OV-CM alone by ~15% irrespective of the doses of OV used e.g., 0.1 or 1 pfu/PBMC (Figure 3-11). Therefore, the data presented in Figure 3-10 and Figure 3-11 suggests that modulation of XIAP and CIAP by Smac mimetics has more of

pronounced effect on THP-1 cells, when used in combination with OV-treated PBMC-CM, than modulation of BCL-2 family members.

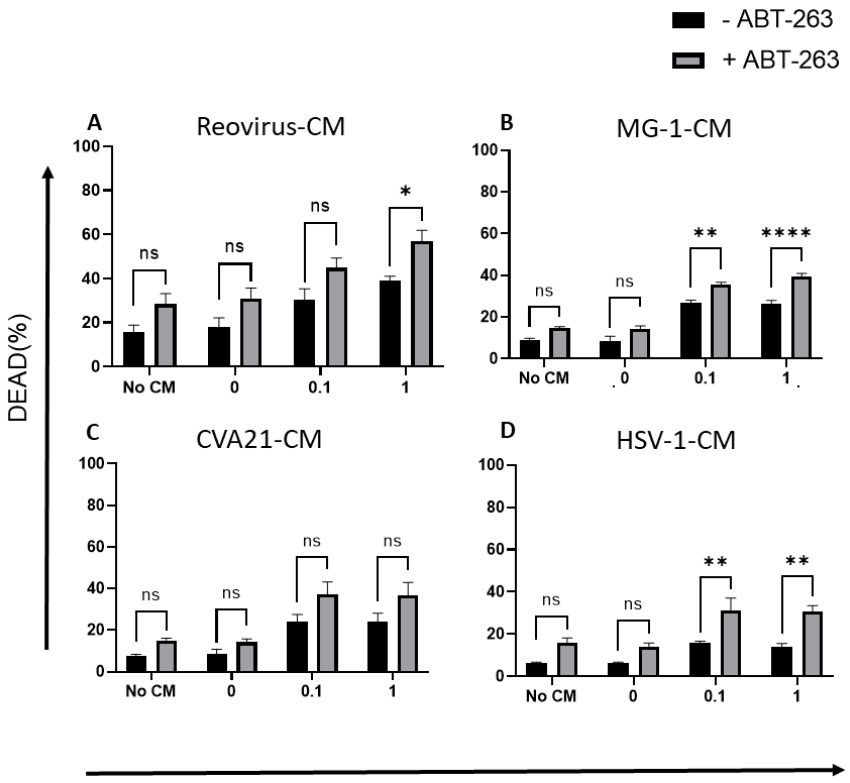

Figure 3-11: THP-1 cell death induced by ABT-263 in combination with UV-irradiated PBMC-CM. THP-1 cells were treated with 0.01 µM ABT-263 and UV-inactivated PBMC-CM (± OV treatment) for 72 hrs, and cell death was assessed using LIVE/DEAD flow cytometry. The mean percentage of dead cells after treatment with **A**: Reovirus-CM, **B**: MG1-CM, **C**: CVA21-CM and **D**: HSV-1-CM is shown for at least 3 individual PBMC donors, + S.E.M. Statistical significance was performed using a two-way ANOVA and significance between PBMC-CM alone and combination with ABT-263 is shown. *=p<0.05, **=p<0.01 and ****=p<0.0001.

To further demonstrate the importance of IAPs and/or BCL-2 family members in THP-1 cells, it was important to examine the efficacy of OV-CM in combination with alternative Smac and BH3 mimetics. However, given that the results for PBMC-CM collected after treatment with all four OV were similar, it seemed unnecessary to use all four OV. Based on the results obtained, reovirus and MG1 were selected for future experiments, because: (i) maximum cell death was usually observed with reovirus-CM, (ii) both reovirus and MG1 induced high levels of cytokines whilst levels induced by CVA21 were lower, and (iii) the most studied clinical route of HSV-1 is i.t, not i.v, which could restrict clinical translation in the context of AML.

THP-1 cells were treated with reovirus-CM or MG1-CM in combination with 2.5 µM BV-6 or 0.01 µM ABT-199 for 72 hrs before cell death was evaluated using LIVE/DEAD assay. Importantly, the combination of reovirus-treated PBMC-CM with 2.5 µM BV-6 significantly increased cell death when compared to reovirus-treated PBMC-CM alone. For example, BV-6 enhanced cell death by 5%, 30% and 35%, respectively, when compared to 0, 0.1 and 1 pfu/PBMC reovirus-CM alone (Figure 3-12A). Furthermore, upon combination with 0.01 µM ABT-199, ABT-199 only caused a significant increase in cell death, above PBMC-CM alone, when 1 pfu/PBMC reovirus-treated PBMC-CM was used; here, cell death was increased by ~18% (Figure 3-12A). Overall, similar trends were observed for MG1-CM, where BV-6 significantly enhanced cell death over MG1-treated PBMC-CM alone by ~30% at both doses (0.1 and 1 pfu/PBMC). Surprisingly, there was no enhancement in cell death following the combination of MG1-treated PBMC-CM and ABT-199 at either dose used (Figure 3-12B). Collectively, the data presented in Figure 3-10, Figure 3-11and Figure 3-12 suggest that XIAP and CIAP modulation exerts a more pronounced impact on

THP-1 cells than modulation of BCL-2 family members. Therefore, these data demonstrate that Smac mimetics could be used to potentiate OV-induced cytokine-mediated killing in THP-1 AML cells.

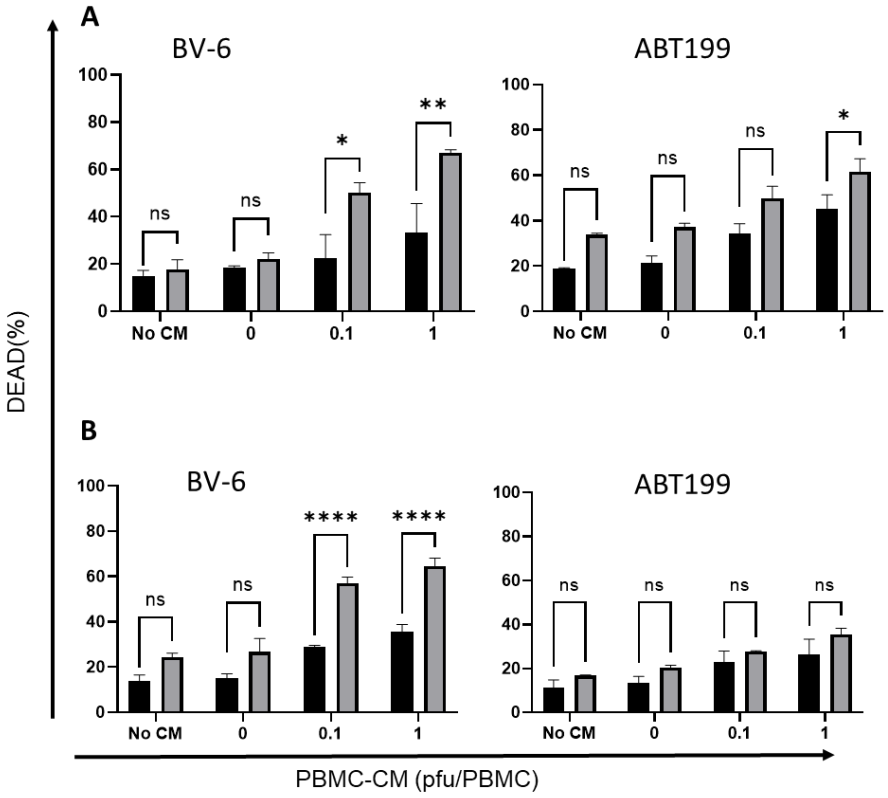

Figure 3-12: Cell death of THP-1 cells after treatment with BV-6 or ABT199 in combination with reovirus-treated or MG1-treated PBMC-CM. THP-1 cells were treated with 2.5 µM BV-6 or 0.01 µM ABT199 and UV-inactivated PBMC-CM (± OV treatment) for 72 hrs, and cell death was assessed using LIVE/DEAD flow cytometry. The mean percentage of dead cells after treatment with **A**: Reovirus-CM, **B**: MG1-CM is shown from at least 3 individual PBMC donors, + S.E.M. Statistical significance was performed using a two-way ANOVA, asterisks indicate comparison of the combination treatment in the presence (grey) and absence (black) of BV-6 or ABT-199, *=p<0.05, **=p<0.01 and ****=p<0.0001.

As mentioned previously in section 1.1.1, AML is a heterogeneous disease with multiple subtypes, therefore it was important to test the efficacy of this combination approach on different AML cell lines. To do this, KG-1, HL-60 and Kasumi-1 cells were treated with 10 µM LCL161, 1 µM BV-6, 0.01 µM ABT-199 or 0.01 µM ABT263 in combination with reovirus-CM or MG1-CM for 72 hrs and cell death was evaluated using LIVE/DEAD. As expected, reovirus-CM and MG1-CM induced death of KG-1 cells as shown previously (Figure 3-7). Moreover, the combination of PBMC-CM (in the absence of OV treatment) with LCL161, BV-6, ABT-199 or ABT263 did not cause a significant increase in cell death. By contrast, combining BH3 mimetics (ABT-199 and ABT-263), but not Smac mimetics (LCL161 and BV-6), with both reovirus-CM (Figure 3-13) or MG1-CM (see Appendix Figure 8-1) increased cell death over OV-treated PBMC-CM alone. For example, for reovirus-CM, neither of Smac mimetics (LCL161 or BV-6) induced significant cell death at any OV dose. However, ABT-199 caused a significant increase in cell death (~44%) over reovirus-CM alone at both 0.1 and 1 pfu/PBMC, and ABT-263 significantly enhanced cell death by ~21% when compared to 1 pfu/PBMC reovirus-CM alone (Figure 3-13A). Similar results were observed using MG1-treated PBMC-CM, with ABT-199 being the only drug to significantly enhance KG-1 cell death above that induced with MG1-treated PBMC-CM alone (See Appendix Figure 8-1). These data indicate that modulation of BCL-2 proteins, specifically BCL-2, has a more significant effect in KG-1 cells than modulation of XIAP and CIAP, therefore, ABT-199 could be used to enhance OV-induced cytokine-mediated cell death in KG-1 AML cells.

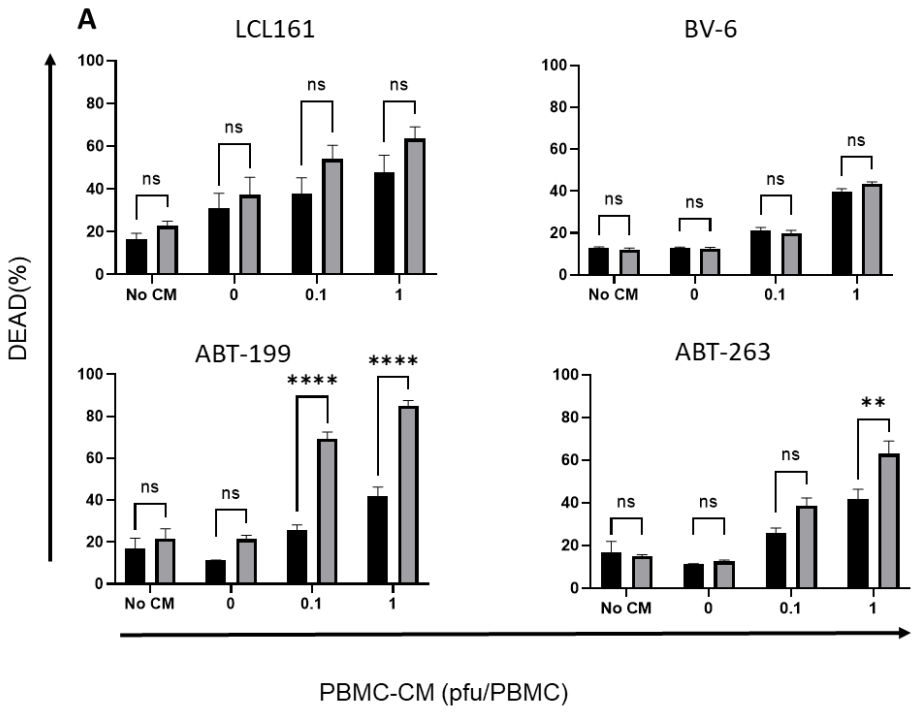

Figure 3-13: KG-1 cell death induced by Smac or BH3 mimetics in combination with UV-irradiated Reovirus-CM. KG-1 cells were treated with10 µM LCL161, 1µM BV-6, 0.01 µM ABT 199 or 0.01 µM ABT263 and UV-inactivated PBMC-CM (± reovirus treatment) for 72 hrs, and cell death was assessed using LIVE/DEAD flow cytometry. The mean percentage of dead cells after treatment with Reovirus-CM is shown from at least 3 individual PBMC donors, + S.E.M. Statistical significance was performed using two-way ANOVA analysis and asterisks indicate comparison of the combination treatment in the presence (grey) and absence (black) of drugs. **=p<0.01 and ****=p<0.0001.

In HL-60 cells (Figure 3-14), in the absence of reovirus-treated PBMC-CM, neither LCL161 or BV-6 induced significant cell death; however, cytotoxicity was observed for both ABT-199 and ABT-263 as shown previously (Figure 3-8 C and D). Importantly, addition of reovirus-treated PBMC-CM in combination with Smac mimetics enhanced cell death. For example, for reovirus-treated PBMC-CM, LCL161 significantly enhanced cell death by ~30% compared to 0.1 or 1 pfu/PBMC-CM alone; moreover, BV-6 was slightly more effective and increased

cell death over reovirus-treated PBMC-CM alone by ~30% and ~38%, respectively, when used in combination with 0.1 and 1 pfu/PBMC-CM. By contrast, ABT-199 increased cell death by ~20% as a single agent or when used in combination with PBMC-CM (with or without reovirus treatment) at all doses. Similarly, ABT-263 did not enhance death of HL-60 cells when used in combination with reovirus-treated PBMC-CM, over levels observed with ABT-263 alone or when used in combination with PBMC-CM collected in the absence of reovirus treatment (Figure 3-14A). Comparable results were obtained using MG1-treated PBMC-CM, with BV-6 being the most effective drug to significantly enhance HL-60 cell death above that observed for MG1-treated PBMC-CM alone (See Appendix Figure 8-2). Therefore, these data suggest that XIAP and CIAP modulation could be used to potentiate OV-induced cytokine-mediated bystander killing in HL-60 cells.

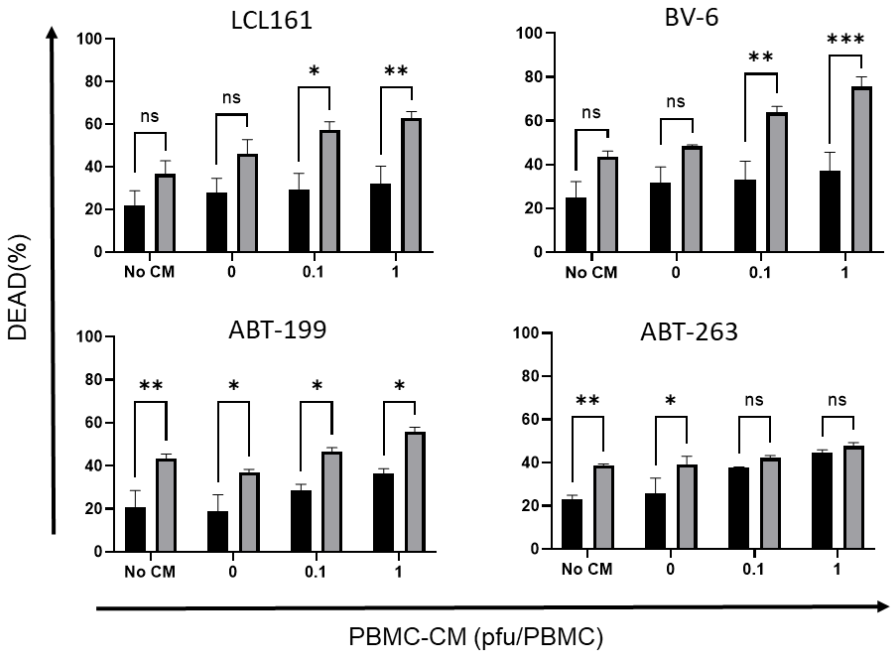

Figure 3-14: HL-60 cell death induced by Smac or BH3 mimetics in combination with UV-irradiated Reovirus-CM. HL-60 cells were treated with 10 µM LCL161, 1µM BV-6, 0.01 µM ABT 199 or 0.01 µM ABT263 and UV-inactivated PBMC-CM (± reovirus treatment) for 72 hrs, and cell death was assessed using LIVE/DEAD flow cytometry. The mean percentage of dead cells after treatment with Reovirus-CM is shown from at least 3 individual PBMC donors, + S.E.M. Statistical significance was performed using two-way ANOVA analysis and asterisks indicate comparison of the combination treatment in the presence (grey) and absence (black) of drugs. *=$p<0.05$, **=$p<0.01$ and ***=$p<0.005$

Upon assessment of Kasumi-1 AML cells, a significant (but low) increase in cell death was observed after LCL161, BV-6 or ABT-263 treatment as a monotherapy. In combination PBMC-CM, LCL161 increased cell death by ~23%, ~25% and ~30%, respectively, above 0, 0.1 and 1 pfu-PBMC reovirus-CM alone; BV-6 increased cell death (over PBMC-CM alone) by ~10% when combined with untreated 0pfu/PBMC-CM and 0.1 pfu/PBMC reovirus-treated CM, and ~20% when combined with 1 pfu/PBMC reovirus-treated CM; by contrast, ABT-263 only enhanced cell death by ~7% over PBMC-CM alone, irrespective of reovirus

treatment (Figure 3-15A). Similar results were observed using MG1-treated PBMC-CM, with LCL161 being the most effective agent at increasing cell death in Kasumi-1 cells above levels induced by MG1-CM alone (See Appendix Figure 8-3). ABT-199 was not tested in Kasumi-1 cells as no potentiation of cell death was observed with ABT-263 which inhibits BCL-2 as well as BCL-xL, and BCL-w. Collectively, these data suggest that neither Smac or BH3 mimetics are very effective at enhancing OV-induced cytokine mediated killing in Kasumi-1 cells.

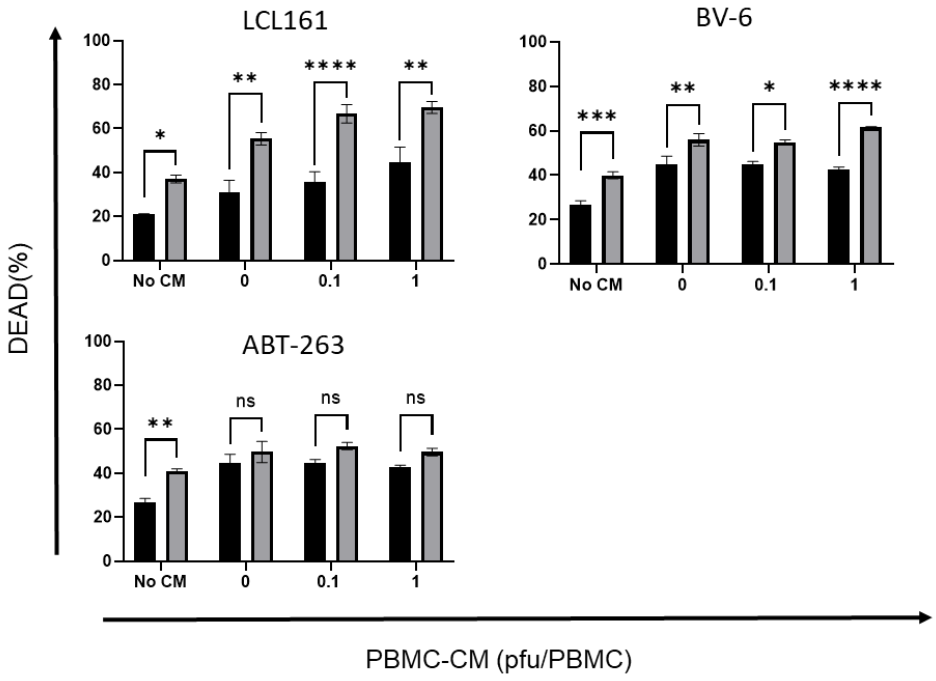

Figure 3-15: Kasumi-1 cell death induced by Smac or BH3 mimetics in combination with UV-irradiated Reovirus-CM. Kasumi-1 cells were treated with 10 µM LCL161, 1µM BV-6, or 0.01 µM ABT263 and UV-inactivated PBMC-CM (± rovirus treatment) for 72 hrs, and cell death was assessed using LIVE/DEAD flow cytometry. The mean percentage of dead cells after treatment with Reovirus-CM is shown from at least 3 individual PBMC donors, + S.E.M. Statistical significance was performed using two-way ANOVA analysis and asterisks indicate comparison of the combination treatment in the presence (grey) and absence (black) of drugs. *=p<0.05, **=p<0.01, ***=p<0.005, ****=p<0.0001.

Taken together, these results demonstrated that cell death in response to OV-CM was potentiated by different apoptotic modulators, depending on the AML cell line. Therefore, going forward, we chose the optimum drug for each cell line; BV-6 was selected for both THP-1 and HL-60 cells, whilst ABT-199 was selected for KG-1 cells; given the limited response observed in Kasumi-1 cells, we decided to exclude this cell line from future work.

3.6 Investigation the role of OV-induced cytokines in the killing of AML

Having identified that OV treatment induced a range of different pro-inflammatory cytokines, and that cytokine induced cell death could be potentiated by Smac/BH3 mimetics in AML cell lines, the potential importance of individual cytokines (induced upon OV treatment) was explored. Initially we focused on IFN-α, TNF-α and IFN-γ because of their known cytotoxic potential in AML and other malignancies [340-342], and because their efficacy in combination with Smac/BH3 mimetics has been previously reported [145, 146, 343].

AML cell lines were treated with IFN-α, TNF-α or IFN-γ alone or in combination with 2.5 μM BV-6 (THP-1 cells), 1μM BV-6 (HL-60 cells) or 0.01 μM ABT-199 (KG-1 cells) for 72 hrs before cell death was evaluated using LIVE/DEAD assay. BV-6 and ABT-199 were selected because they were identified in chapter 1 as the optimal drugs to potentiate cytotoxic effects in response to OV-treated PBMC-CM. Moreover, the doses of these human recombinant cytokines were selected to reflect the amounts secreted from HD-PBMC after OV treatment. For example, the IFN-α doses used were 500 pg/mL, 1000 pg/mL and 2000 pg/mL, where OV-treated PBMC secreted IFN-α levels ranging from ~300 pg/mL to ~1000 pg/mL, with the highest amount observed after reovirus treatment (Figure 3-4). Thus, the

doses used were similar to, or higher than, those that secreted after OV treatment.

In THP-1 cells, treatment with increasing doses of IFN-α (500 pg/mL, 1000 pg/mL or 2000 pg/mL) did not induce any significant toxicity. Moreover, although statistical significance was not observed, the combination of BV-6 with IFN-α increased cell death by ~20% over BV-6 treatment alone (Figure 3-16A). Treatment with IFN-γ alone (250 pg/mL, 500 pg/mL or 1000 pg/mL) did not enhance cell death, and combination with BV-6 did not increase cell death (Figure 3-16B). Similarly, treatment with TNF-α alone (500 pg/mL, 1000 pg/mL or 2000 pg/mL) did not cause any toxicity against THP-1 cells; however, combination with BV-6 significantly increased cell death (by ~26%) over BV-6 alone, at the highest dose (2000 pg/mL) (Figure 3-16C). Importantly, the combination of IFN-α and TNF-α increased cell death by 14% at the highest concentrations used. However, combination with BV-6 significantly enhanced cell death by ~41%, ~46% and ~51% at 500 pg/mL, 1000 pg/mL and 2000 pg/mL, respectively, over BV-6 alone (Figure 3-16D). Furthermore, the combination of IFN-γ, IFN-α and TNF-α treatment increased cell death by ~12% at the highest concentration, moreover, cell death was significantly increased by ~45 over BV-6 alone at low and intermediate concentrations, and ~56% at the highest cytokine concentrations used (Figure 3-16E). Collectively, maximum cell death was observed when the combination of IFN-α, TNF-α and IFN-γ was used, demonstrating a role for each cytokine. However, data suggest that IFN-α and TNF-α could play a more significant role.

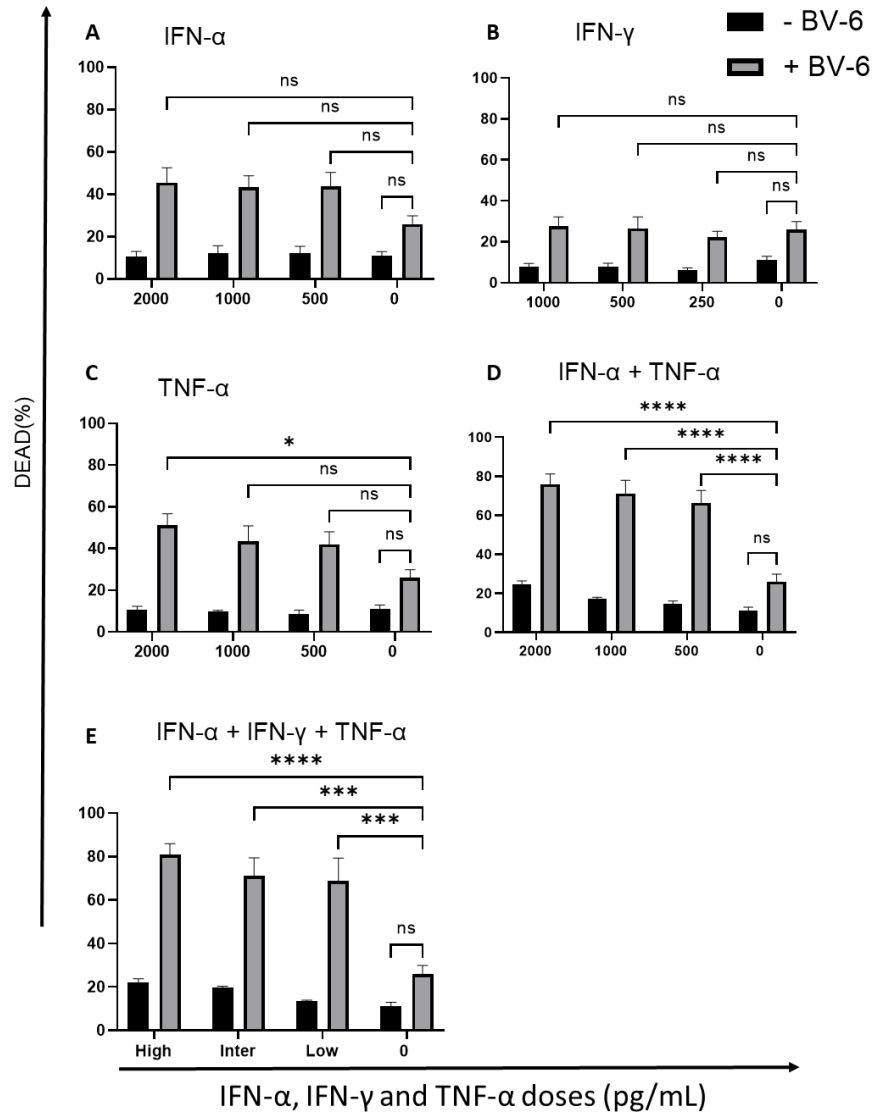

Figure 3-16: Cytotoxicity induced by human recombinant cytokines in combination with BV-6 in THP-1 AML cells. THP-1 cells were treated with 2.5 µM BV-6 and combined with: **A**: human recombinant IFN-α (0, 500,1000, 2000 pg/mL), **B**: human recombinant IFN-γ (0, 250, 500, 1000 pg/mL), **C**: human recombinant TNF-α (0, 500, 1000, 2000 pg/mL), **D**: combination of human recombinant IFN-α and TNF-α (each at 0, 500, 1000, 2000 pg/mL), **E**: combination of human recombinant IFN-α, IFN-γ and TNF-α (Low = 500 pg/mL IFN-α + 500pg/mL TNF-α + 250 pg/mL IFN-γ, Inter = 1000 pg/mL IFN-α + 1000pg/mL TNF-α + 500 pg/mL IFN-γ, High = 2000 pg/mL IFN-α + 2000pg/mL TNF-α + 1000 pg/mL IFN-γ) for 72 hrs. Cell death was measured by LIVE/DEAD flow cytometry. The mean percentage of dead cells after treatment is shown from 3 individual experiments, + S.E.M. Statistical significance was performed using two-way ANOVA analysis and asterisks indicate comparison of the combination treatment in the presence (grey) of BV-6 and human recombinant cytokine. *=p<0.05, ***=p<0.005, ****=p<0.0001.

Next, identical experiments were also carried out using HL-60 AML cells. HL-60 cells were treated with IFN-α at concentrations of 500 pg/mL, 1000 pg/mL, or 2000 pg/mL, and no significant cell death was observed in response to IFN-α treatment alone, or when combined with BV-6 (Figure 3-17A). Similarly, treatment with IFN-γ (250 pg/mL, 500 pg/mL, or 1000 pg/mL) did not induce significant cell death and this was not enhanced by the addition of BV-6 (Figure 3-17B). By contrast, whilst treatment with 500 pg/mL, 1000 pg/mL, or 2000 pg/mL TNF-α alone did not cause any significant increase in cell death, the addition of BV-6 enhanced cell death by ~25% over BV-6 treatment alone, at the highest concentration used (Figure 3-17C). Importantly, the combination of IFN-α and TNF-α in the absence of BV-6 did not induce significant cell death. However, BV-6 increased cell death by ~40% compared to BV-6 treatment alone across all the concentrations used (Figure 3-17D). Furthermore, the addition of IFN-γ to IFN-α and TNF-α alone did not induce significant toxicity in HL-60 cells. However, when BV-6 was added, cell death was increased by ~45% over BV-6 treatment alone across all concentrations used (Figure 3-17E).

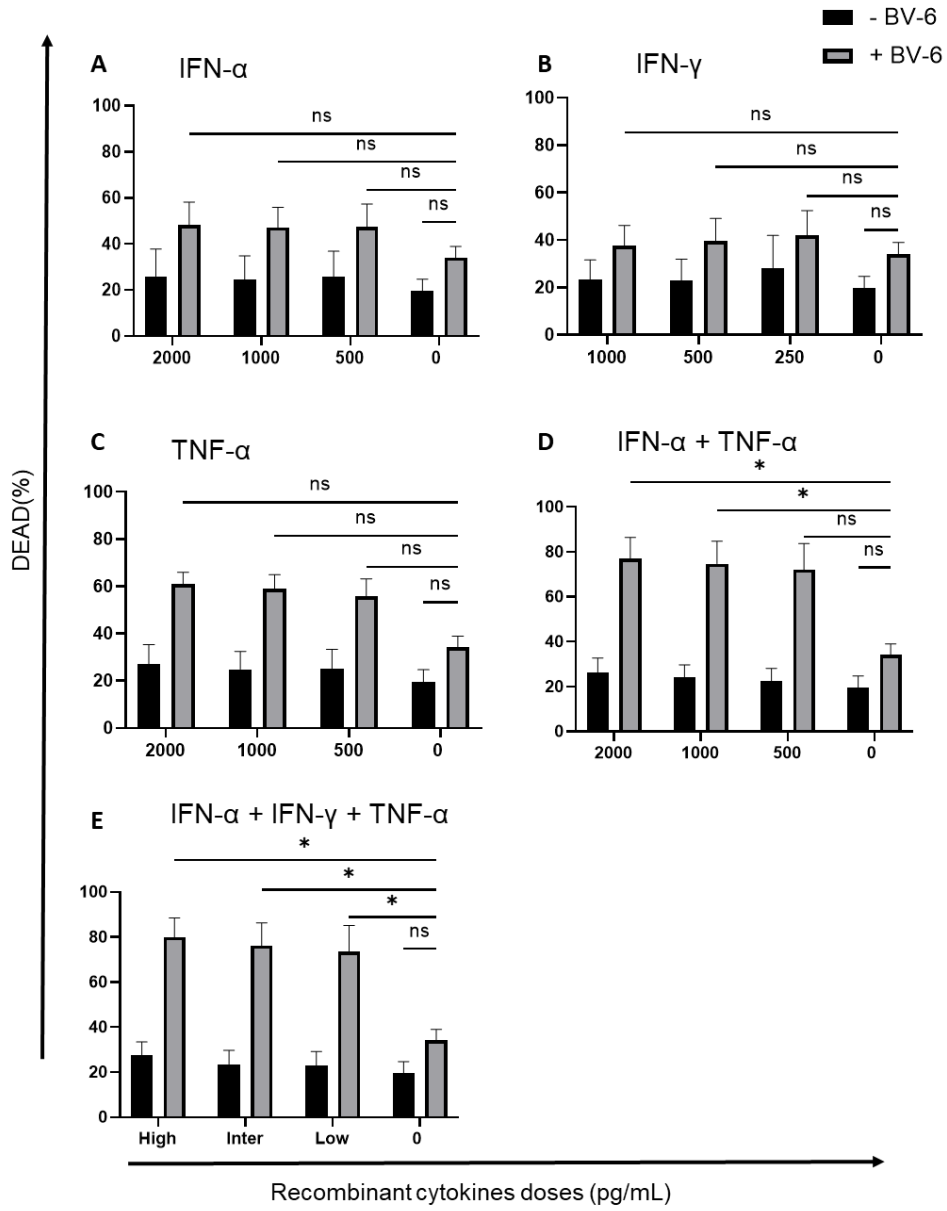

Figure 3-17: Cytotoxicity induced by human recombinant cytokines in combination with BV-6 in HL-60 AML cells. HL-60 cells were treated with 1 µM BV-6 and combined with: **A**: human recombinant IFN-α (0, 500,1000, 2000 pg/mL), **B**: human recombinant IFN-γ (0, 250, 500, 1000 pg/mL), **C**: human recombinant TNF-α (0, 500, 1000, 2000 pg/mL), **D**: combination of human recombinant IFN-α and TNF-α (each at 0, 500, 1000, 2000 pg/mL), **E**: combination of human recombinant IFN-α, IFN-γ and TNF-α (Low = 500 pg/mL IFN-α + 500pg/mL TNF-α + 250 pg/mL IFN-γ, Inter = 1000 pg/mL IFN-α + 1000pg/mL TNF-α + 500 pg/mL IFN-γ, High = 2000 pg/mL IFN-α + 2000pg/mL TNF-α + 1000 pg/mL IFN-γ) for 72 hrs. Cell death was measured by LIVE/DEAD flow cytometry. The mean percentage of dead cells after treatment is shown from 3 individual experiments, + S.E.M. Statistical significance was performed using two-way ANOVA analysis and asterisks indicate comparison of the combination treatment in the presence (grey) of BV-6 and human recombinant cytokine. *=$p<0.05$.

By contrast to THP-1 and HL-60 cells, KG-1 cells were more sensitive to cytokine treatment. For example, treatment with 500 pg/mL, 1000 pg/mL, or 2000 pg/mL IFN-α significantly increased cell death by ~20%, ~23% and ~28%, respectively. However, the addition of ABT-199 significantly enhanced cell death compared to ABT-199 alone (by ~44%) across all doses of IFN-α used (Figure 3-18A). By contrast, no cell death was observed when KG-1 cells were treated with 250 pg/mL, 500 pg/mL, or 1000 pg/mL IFN-γ, while the addition of ABT-199 increased cell death by ~25% above ABT-199 treatment alone at all of the concentrations used (Figure 3-18B). Surprisingly, treatment with 500 pg/mL, 1000 pg/mL, or 2000 pg/mL TNF-α did not increase cell death, and the addition of ABT-199 did not enhance KG-1 cell death in response to TNF-α treatment (Figure 3-18C). Unfortunately, the cytotoxic effect observed upon treatment with IFN-α and TNF-α treatment (and the subsequent addition of IFN-γ) made it difficult to accurately assess the effect of ABT-199 in this cell line (Figure 3-18D and E).

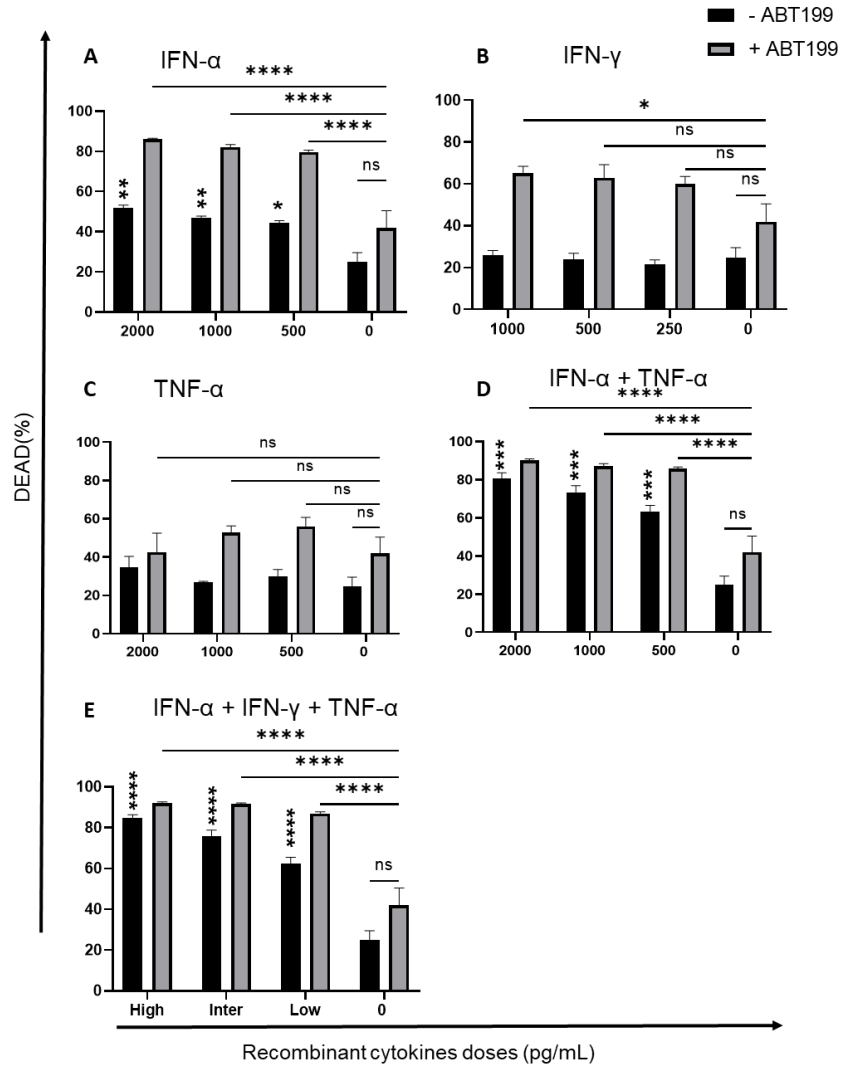

Figure 3-18: Cytotoxicity induced by human recombinant cytokines in combination with ABT-199 in KG-1 AML cells. KG-1 cells were treated with 0.01 µM ABT-199 and combined with: **A**: human recombinant IFN-α (0, 500,1000, 2000 pg/mL), **B**: human recombinant IFN-γ (0, 250, 500, 1000 pg/mL), **C**: human recombinant TNF-α (0, 500, 1000, 2000 pg/mL), **D**: combination of human recombinant IFN-α and TNF-α (each at 0, 500, 1000, 2000 pg/mL), **E**: combination of human recombinant IFN-α, IFN-γ and TNF-α (Low = 500 pg/mL IFN-α + 500pg/mL TNF-α + 250 pg/mL IFN-γ, Inter = 1000 pg/mL IFN-α + 1000pg/mL TNF-α + 500 pg/mL IFN-γ, High = 2000 pg/mL IFN-α + 2000pg/mL TNF-α + 1000 pg/mL IFN-γ) for 72 hrs. Cell death was measured by LIVE/DEAD flow cytometry. The mean percentage of dead cells after treatment is shown from 3 individual experiments, + S.E.M. Statistical significance was performed using two-way ANOVA analysis and asterisks above the lines indicate comparison of the combination treatment in the presence (grey) of ABT-199 and human recombinant cytokine. Asterisks above black bars indicate comparisons between recombinant cytokine treatment and untreated control cells. *=p<0.05, ***=p<0.005 and ****=p<0.0001.

Taken together, these data demonstrate differential sensitivity across AML cell lines towards cytokines-mediated killing. For THP-1 and HL-60 cells, none of the cytokines (IFN-γ to IFN-α and TNF-α) induced significant cell death as a single agent, or when combined. However, the addition of BV-6 increased cell death significantly in both cell lines. By contrast, KG-1 cells were more sensitive to cytokine-mediated killing; recombinant human IFN-α treatment when used in isolation induced significant cell death, and this was further potentiated when ABT-199 was added.

3.7 Mode of cell death following the combination of reovirus-treated PBMC-CM and Smac/ BH3 mimetics.

The data presented suggest a pivotal role for IFN-α and TNF-α for inducing AML cell death when combined with apoptotic modulators (Figure 3-16, Figure 3-17 and Figure 3-18). Several studies have shown that IFN-α and TNF-α induce cell death via apoptosis and as discussed in Sections 1.2.1 1.2.3 BV-6 binds to IAPs, whilst ABT-199 binds to BCL-2, to facilitate apoptosis. Hence, the induction of apoptosis was investigated. Initially, the functionality of the pan-caspase inhibitor z-VAD-FMK (zVAD) was tested using a positive control cell line, Mel-888 cells; reovirus induces cell death in Mel-888 cells via caspase dependent apoptosis which can be inhibited using zVAD [344]. Importantly, zVAD was able to abrogate reovirus killing in Mel-888 cells, as expected (See Appendix Figure 8-4), demonstrating the *in vitro* activity of this compound. Subsequently, THP-1 cells were treated with 50 μM zVAD for 1 hr followed by treatment with reovirus-treated PBMC-CM and BV-6 for 72 hrs before cell death was quantified using LIVE/DEAD. Importantly, in the absence of zVAD, as expected, 71% cell death was observed in response to the combination treatment. However, perhaps surprisingly, zVAD did not rescue or inhibit cell death induced by this combination

treatment (Figure 3-19A). To investigate this further, published literature [345] had suggested using zVAD at higher doses than those used in our initial assay (e.g. 100μM); thus, THP-1 cells were treated with 100 μM zVAD for 1 hr prior to addition of the combination therapy for further 72 hrs. In this experiment, a statistically significant reduction in cell death was observed when zVAD was added (Figure 3-19 B), although a significant increase in cell death was still observed. Similarly, when KG-1 cells were treated with 100 μM zVAD for 1 hr followed by treatment with ABT-199 and reovirus-treated PBMC-CM 24 hours, cell death was also significantly reduced in the presence of zVAD (data not shown).

Unexpectedly, zVAD did not completely abrogate cell death and the role for caspases and/or apoptosis remained inconclusive. Therefore, an alternative method of identifying a role for apoptosis was sought. In this regard, Walsh *et al*. have demonstrated that caspase-3 and -7 are activated during apoptosis [346], hence, the next step was to examine the activation of these caspases. THP-1 cells were treated with reovirus-treated PBMC-CM and BV-6 for 7, 24 or 72 hrs and activation of caspase-3/-7 was detected using caspase-3/7 green flow cytometry assay kit. Of note, no significant activation of caspase-3/7 was observed at the early time point of 7 hrs and the later time point of 72 hrs. However, importantly, there was significant increase in caspase-3/7 activation following 24 hrs treatment, suggesting an important role for apoptosis (Figure 3-20).

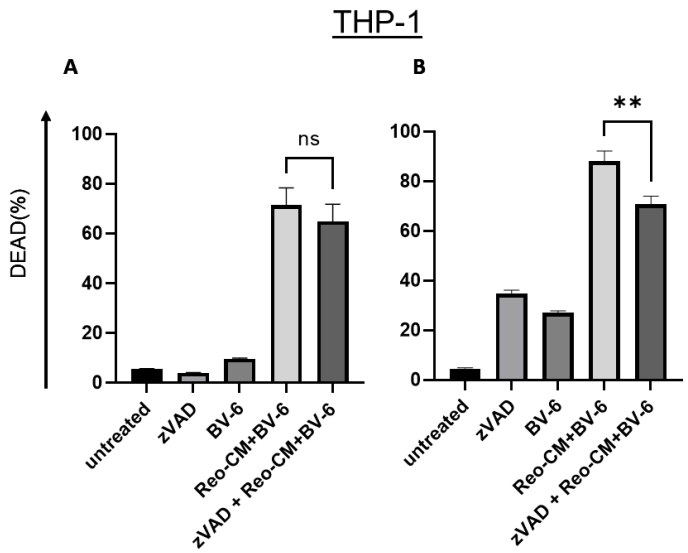

Figure 3-19: zVAD partially inhibits THP-1 cell death following treatment with Reovirus-treated PBMC-CM and BV-6. THP-1 cells were treated first with **A**: 50 µM or **B**: 100 µM zVAD for 1 hr then 2.5 µM BV-6 and UV-irradiated reovirus-CM were added for a further 72 hrs. Cell death was measured by LIVE/DEAD flow cytometry. The mean percentage of dead cells after treatment is shown for PBMC-CM generated from 3 individual donors, + S.E.M. Statistical significance was performed using an unpaired one-way ANOVA analysis. **=p<0.01.

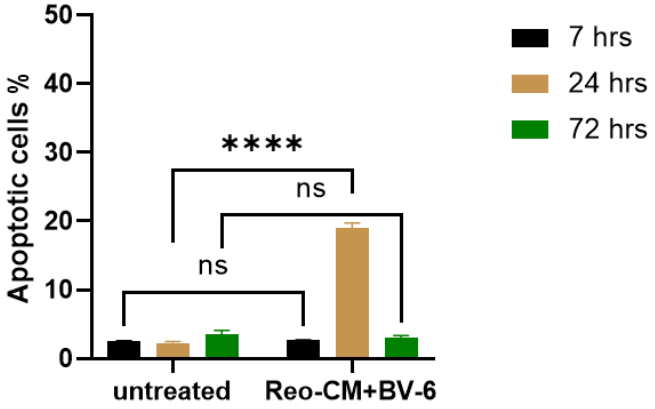

Figure 3-20: Caspase-3/7 activation in THP-1 cells after treatment with reovirus-CM combined with BV-6. THP-1 cells were treated with UV-irradiated reovirus-CM combined with 2.5 µM BV-6 for 7, 24 or 72 hrs. Cells were collected and stained with caspase-3/7 green flow cytometry stain. Apoptotic cells were quantified using flow cytometry. The mean percentage of apoptotic cells after treatment is shown from 3 individual PBMC donors, + S.E.M. Statistical significance was performed using one-way ANOVA analysis, ****=p<0.0001.

3.8 Efficacy of UV-inactivated OV in combination with apoptotic modulation

One potential concern of using OV in immunocompromised patients would be the possibility of a sustained infection due to a limited antiviral immune response, therefore the possibility of using UV-inactivated OV, instead of live virus, is an attractive possibility. To test this possibility, HD-PBMC were treated with 1pfu/PBMC UV-inactivated reovirus, MG1, CVA21 or 0.1 pfu/PBMC HSV-1 for 48 hrs and the secretion of pro-inflammatory cytokines (IFN-2α, TNF-α, MCP-1, TRAIL, IL-1β, IP-10, RANTES, TNF-β and IFN-γ) was evaluated using a multiplex immunoassay. While the fold increase in cytokine production was reduced compared to treatment with replicant competent OV (see Figure 3-4, Figure 3-5 and Figure 3-6 for absolute values and Appendix Figure 8-5), UV-irradiated OV were still able to induce the secretion of pro-inflammatory cytokines. For example, for UV-reovirus, the secretion of IFN-2α, TNF-α, MCP-1, TRAIL, IL-1β and IP-10 was observed but not RANTES, TNF-β and IFN-γ (Figure 3-21A); UV-MG1 induced the secretion of IFN-2α, MCP-1, TRAIL and IP-10 but not TNF-α, IL-1β, RANTES, TNF-β and IFN-γ (Figure 3-21B); UV-CVA21 induced IFN-2α, TNF-α, MCP-1, TRAIL and IP-10 but not IL-1β, RANTES, TNF-β and IFN-γ (Figure 3-21C); finally, UV-HSV-1 induced the secretion of IFN-2α, TNF-α, MCP-1, TRAIL, IP-10 and TNF-β but not IL-1β and IFN-γ (Figure 3-21D). Table 3-3 presents a comparison of the release of cytokines after treatment with UV-inactivated or live OV. Any value below 3-fold increase was considered as ‘’not secreted’’.

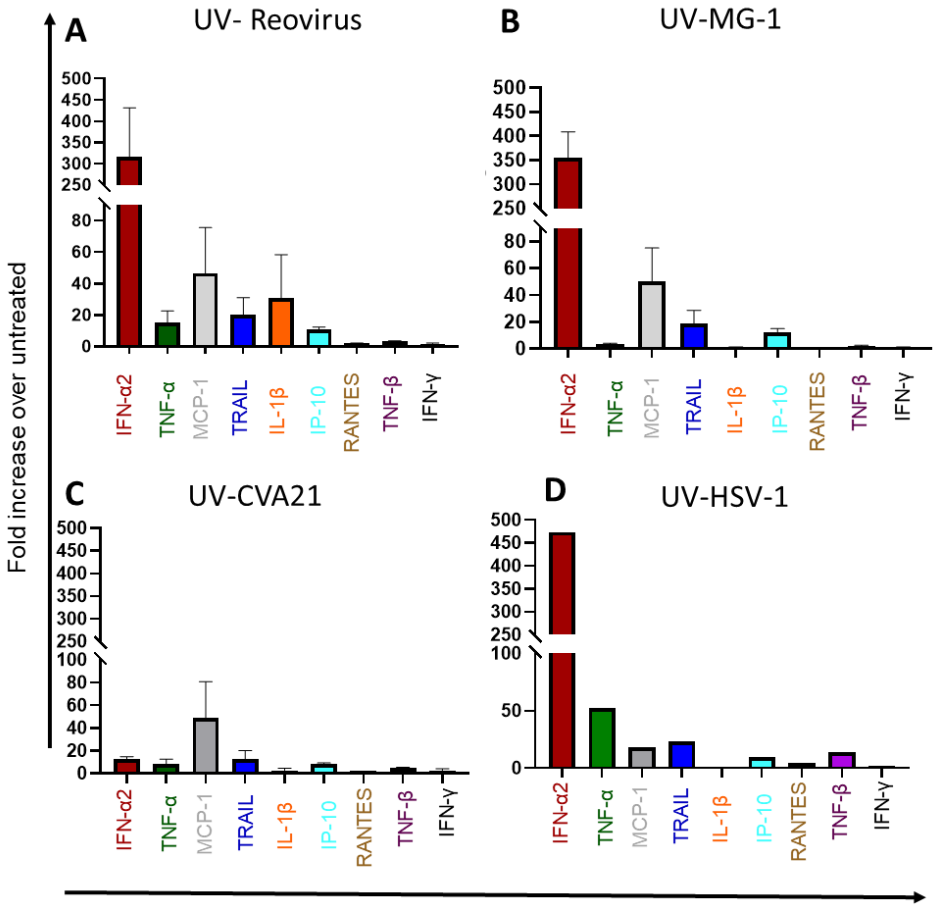

Figure 3-21: Pro-inflammatory cytokines secreted from HD-PBMC in response to UV-inactivated OV treatment. HD-PBMC were treated for 48 hrs with 1pfu/PBMC UV-inactivated **A**: Reovirus, **B**: MG1, **C**: CVA21 or **D**: 0.1pfu/PBMC HSV-1. Supernatants were harvested and secretion of pro-inflammatory cytokines was measured using a 9-multiplex immunoassay. The graph shows the mean fold change in pg/mL compared to untreated PBMCs for n=3 for reovirus and MG1, n=2 for CVA21, n=1 for HSV-1 independent PBMC donors, + S.E.M.

Table 3-3: Secretion of pro-inflammatory cytokines (pg/mL) from HD-PBMC in response to UV-inactivated or live OV

Cytokine	Live reovirus	UV reovirus	Live MG1	UV MG1	Live CVA21	UV CVA21	Live HSV-1	UV HSV-1
IFN-2α	993	316	761	354	65	12.8	79	473
TNF-α	1675	259	2553	63	286	150	504	1622
MCP-1	798	752	930	1220	709	700	320	710
TRAIL	51	27	26	25	23	16	12	60
IL-1β	7.1	16	42	1.2	4.6	2.4	2.7	5.9
IP-10	53047	47558	27820	43015	37859	33934	35401	41775
RANTES	2053	404	811	167	1236	435	1207	1099
TNF-β	17	5.2	8.3	3.3	14.2	7.9	7.2	16.9
IFN-γ	138	16.4	17	11.7	83	24	25	17

The data presented in Figure 3-21 and Table 3-3 demonstrates that UV-inactivated reovirus, and other OV, can induce a range of pro-inflammatory cytokines, however, as reovirus-CM collected after treatment with UV-inactivated virus contained both type I IFN-α and TNF-α, and a role for these cytokines had been previously defined (Figure 3-16D and Figure 3-17D), this agent was selected for further investigation. Initial studies sought to confirm the killing ability of the cytokines induced by UV-inactivated reovirus and determine whether the efficacy of this agent was enhanced when used in combination with Smac or BH3 mimetics. To do this, reovirus was UV-inactivated for 2 min before being applied to PBMCs for 48 hrs. CM was subsequently collected and added to THP-1 cells (1:1 dilution in fresh medium) in combination with 10 μM LCL161 for 72 hrs before evaluation of cell death using LIVE/DEAD assay. Surprisingly, the combination of UV-reovirus-treated PBMC-CM and LCL161 significantly increased cell death of THP-1 cells and levels were comparable to those induce with live-reovirus-treated

PBMC-CM. For live-reovirus-CM, LCL161 enhanced cell death (above PBMC-CM alone) by ~34% at both doses (0.1 and 1 pfu/PBMC reovirus-CM), while for UV-reovirus-CM, LCL161 enhanced cell death by ~35% at both doses (Figure 3-22). This experiment was done to compare the efficacy of replication-competent versus UV-inactivated reovirus, thus only THP-1 cells and LCL161 were used. These data demonstrate that both live and UV-inactivated reovirus-treated PBMC-CM can induce bystander cytokine-mediated killing in THP-1 cells, and that this can be potentiated using the Smac mimetic, LCL161.

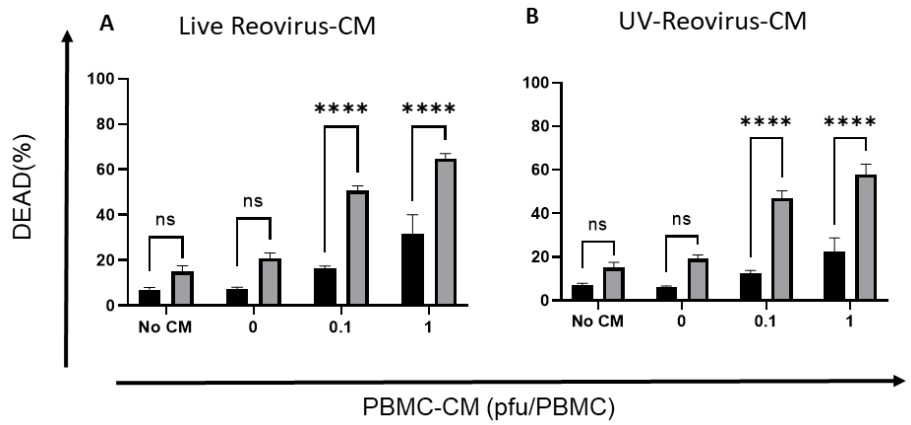

Figure 3-22: Cell death induced by LCL161 in combination with live or UV-irradiated Reovirus-CM. PBMCs were treated with Reovirus or UV-irradiated Reovirus for 48 hrs and the supernatant was collected. THP-1 cells were treated with 10 µM LCL161 and UV-inactivated PBMC-CM collected after treatment with live or UV-inactivated reovirus treatment for 72 hrs. Cell death was assessed using LIVE/DEAD flow cytometry. The mean percentage of dead cells after treatment with **A**: live-reovirus-CM, **B**: UV-reovirus-CM is shown from 3 individual PBMC donors, + S.E.M. Statistical significance was performed using two-way ANOVA analysis and asterisks indicate comparison of the combination treatment in the presence (grey) and absence (black) of LCL161. ****=p<0.0001.

3.9 Evaluate the efficacy of reovirus-treated PBMC-CM in combination with Smac/BH3 mimetics using AML patient samples

3.9.1 Secretion of pro-inflammatory cytokine from AML patient samples

As confirmed above (Section 3.2), HD-PBMC secreted large amounts of a range of pro-inflammatory cytokine in response to reovirus treatment. To determine whether a similar response was observed in primary AML patient samples, the secretion of IFN-α, IFN-γ and TNF-α was examined by ELISA. PBMC were isolated from AML patients and treated with 0. 0.1 or 1 pfu/PBMC live or UV-inactivated reovirus for 48 hrs before collection of supernatants. As expected, the magnitude of response to reovirus treatment was variable between patients, however, there was a significant increase in the secretion of IFN-α (~7800 pg/mL) in response to 1 pfu reovirus treatment (Figure 3-23A). additionally, although there was no statistically significant increase in IFN-α secretion after treatment with UV-inactivated reovirus, an average of ~4000 pg/mL was observed in response to treatment with 1 pfu/PBMC UV-inactivated reovirus (Figure 3-23A). IFN-γ was also secreted with an average of ~360 pg/mL and ~620 pg/mL after 0.1 and 1 pfu/PBMC live reovirus, respectively, and ~105 pg/mL and 415 pg/mL after treatment with 0.1 and 1 pfu/PBMC UV-inactivated reovirus, respectively (Figure 3-23B). By contrast, TNF-α was not detected in response to treatment with live or UV-inactivated reovirus at any of the doses used (data not shown).

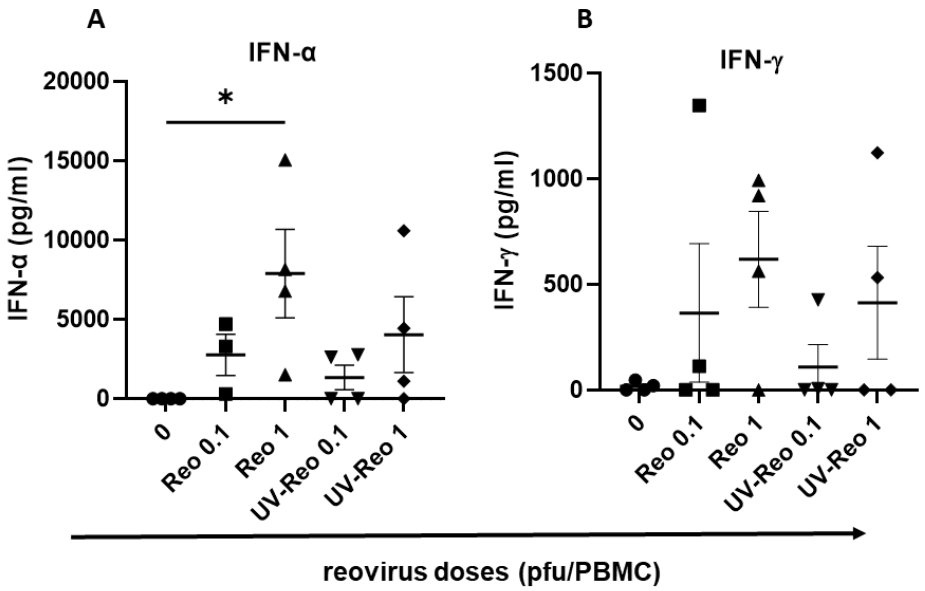

Figure 3-23: Pro-inflammatory cytokine secretion from AML patient samples in response to Reovirus or UV-inactivated Reovirus treatment. PBMC were isolated from AML patient samples and treated for 48 hrs with 0, 0.1 or 1 pfu/PBMC live or UV-inactivated reovirus. Supernatants were harvested and secretion of **A**: IFN-α or **B**: IFN-γ was measured by ELISA. Error bars indicate mean + S.E.M for 4 individual PBMC AML donors. Statistical significance was performed using a one-way ANOVA and comparisons with untreated controls are shown. *= $p<0.05$.

3.9.2 Efficacy of reovirus-treated PBMC-CM in combination with Smac/ BH3 mimetics against primary AML cells

Having identified the efficacy of reovirus treatment in combination with Smac/ BH3 mimetics in AML cell lines and that AML patient samples induced pro-inflammatory cytokines, it was important to examine the efficacy of reovirus-treated HD-PBMC-CM and AML-generated PBMC-CM in combination with Smac or BH-3 mimetics using AML patient samples.

As demonstrated above (and in Appendix Figure 8-5), live reovirus treatment resulted in a higher production of cytokines from HD-PBMC and AML patient

samples than UV-inactivated reovirus (section 3.8). Therefore, live reovirus was chosen to evaluate the effectiveness of the combination strategy on primary AML patient samples. For AML-generated PBMC-CM, AML-PBMC were left untreated or treated with 1pfu/PBMC reovirus for 48 hrs prior to collection of CM. Next, PBMC were isolated from AML patient samples (AML-PBMC) and treated with reovirus-treated PBMC-CM (collected from HD-PBMC or AML-generated PBMC-CM) in combination with 1 µM LCL161, 0.1 µM BV-6 or 0.001 µM ABT-199 for 48 hrs and cell death was evaluated using LIVE/DEAD flow cytometry. Interestingly, the response to the combination therapy varied between patient samples. For example, for one patient sample (AML-96) that responded to this combination treatment, ~26%, ~17% and ~10% cell death was observed after treatment with LCL161, BV-6 and ABT-199 alone, respectively. Moreover, when PBMC-CM (in the absence of reovirus treatment) was combined with LCL161, BV-6 or ABT-199, no enhancement in cell death was observed over drug alone. However, by contrast, upon addition of reovirus-treated HD-PBMC-CM or AML-generated PBMC-CM (1pfu/PBMC) cell death was increased when compared with untreated PBMC-CM alone. For example, LCL161 increased cell death by ~37%; BV-6 increased cell death by ~17%, and ABT-199 did not enhance cell death at all (Figure 3-24A and B). By contrast Figure 3-24C and D illustrates data obtained for a different AML patient (AML-95) that did not respond to any drug, alone or in combination with reovirus-treated HD-PBMC-CM or AML-generated PBMC-CM. Interestingly, AML-100 responded to ABT-199 but did not respond to LCL161 or BV-6, here, ABT-199 increased cell death above reovirus-treated HD-PBMC-CM or AML-generated PBMC-CM alone by ~16% and ~13%, respectively (Figure 3-24E and F). Collectively, 5 out of 10 patients responded to the combination treatment, with two patients responding to LCL161, two patients responding to

both Smac mimetics (LCL161 and BV-6), and one patient responding to ABT-199. An overview of the AML patient samples used along with those that responded or did not respond to the combination treatment approach is shown in Table 3-4. Collectively, all patients that responded to HD-PBMC-CM and Smac/ BH3 mimetics responded to PBMC-CM generated from AML patient samples.

Interestingly, upon inspection of patient data, all patient samples that demonstrated enhanced killing in response to Smac mimetics had NPM1 or FLT3 mutations. By contrast, the patient sample that required the BH3 mimetic, ABT-199, had GATA2 and KRAS mutations, which were not observed in the other patients.

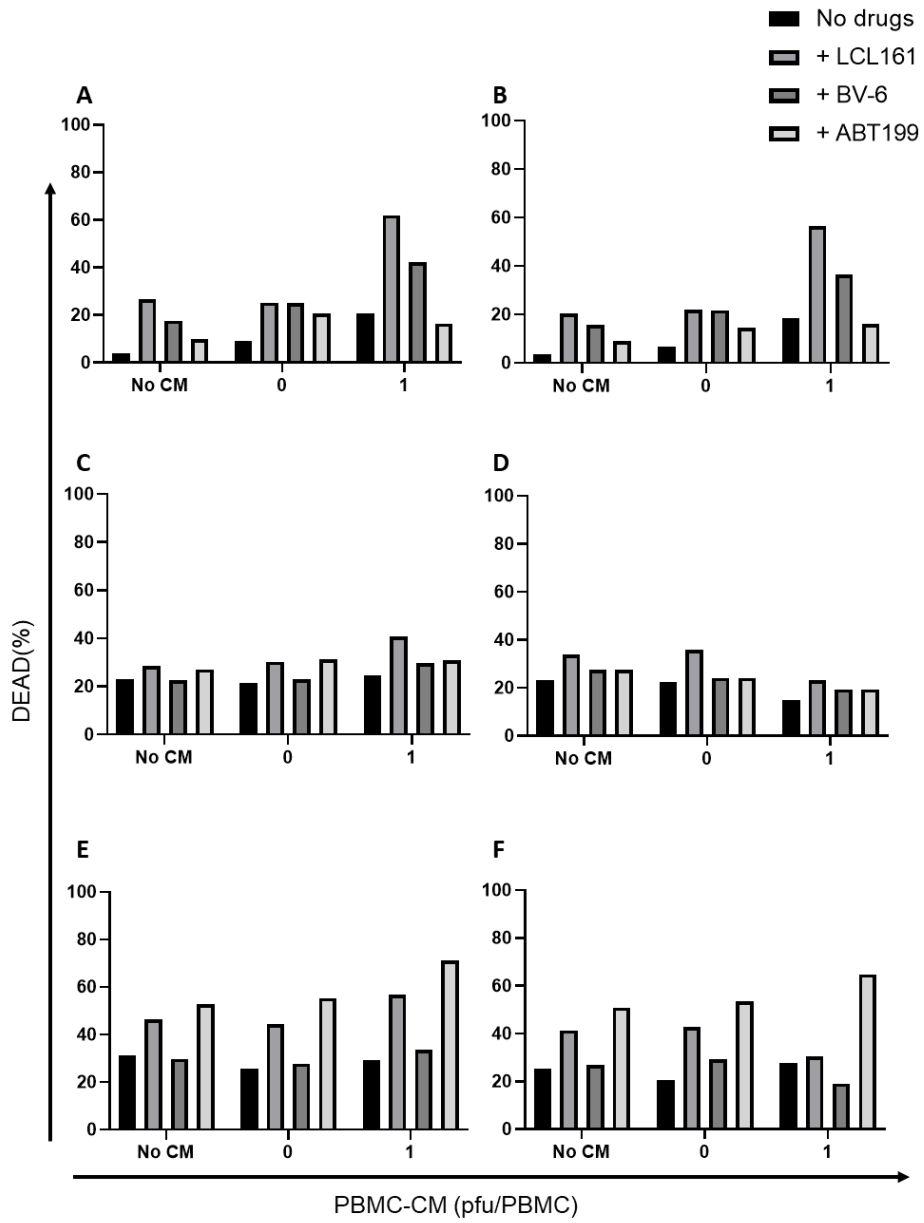

Figure 3-24: Primary AML cell death induced by Smac or BH3 mimetics in combination with UV-irradiated PBMC-CM ± reovirus treatment. AML-PBMC were treated with 1 μM LCL161, 0.1 μM BV-6 or 0.001 μM ABT-199 in the presence or absence of UV-inactivated HD-PBMC-CM (**A**, **C** and **E**) or AML-generated PBMC-CM (**B**, **D** and **F**) (± reovirus treatment) for 48 hrs, and cell death was assessed using LIVE/DEAD flow cytometry. The mean percentage of dead cells after treatment with drugs and PBMC-CM (± reovirus treatment) is shown for representative **A** and **B**: responding (AML-92) to Smac mimetics, **C** and **D**: non-responding (AML-95) and **E** and **F**: responding (AML-100) to ABT-199 AML patient samples.

Table 3-4: AML patient samples responsive to the combination of Smac/ BH3 mimetics and reovirus-CM

AML ID	Age/ Years	RES to LCL161	RES to BV-6	RES to ABT-199	Mutations	Time point of sample	Treatments
AML 92	54	Yes	Yes	No	NPM1, FLT3 and DNMT3A	Diagnosis	Started AML19 trial.
AML 93	66	No	No	No	MDS-related changes (NRAS, RUNX1VUS, TET2 and U2AF1	Relapse	Previously had FLAMSA-Bu allograft, then Azacitadine prior to this relapse, then Venetoclax and Azacitadine. RIP Aug 2021
AML 94	46	Yes	No	No	DNMT3A, FLT3, IDH1, KMT2C (MLL3)VUS NPM1	Diagnosis	Started AML19 trial, relapsed and started venetoclax and azacitadine, then gilteritinib, allograft in Nov 2022.
AML 95	53	No	No	No	AML with MDS-related changes	Diagnosis	Received one cycle of liposomal Duanorubicin + Cytarabine, then refractory, so 1 cycle FLAG-Ida, to which also refractory. RIP Oct 2021
AML 96	75	Yes	No	No	FLT3, IDH2 and SRSF2	Diagnosis	Started venotoclax and azacitadine.
AML 97	51	No	No	No	AML t(8;21)(q22;q22) and FLT3	Diagnosis	Started AML19 trial.
AML 98	22	No	No	No	CEBPA, CUX1VUS NF1VUS WT1	Diagnosis	Started AML19 trial, Proceeded to allograft in Dec 2022.
AML 99	62	Yes	Yes	No	DNMT3A, FLT3 and NPM1	Diagnosis	Started DA for 2 cycles, then Azacitadine and Venetocax 2 cycles, then gilteritinib. RIP Sept 2022
AML 100	49	No	No	Yes	CEBPA, GATA2 and KRAS	Diagnosis	Started DA + gemtuzumab for 4 cycles.
AML 101	84	No	No	No	FLT3, NRAS, TET2 and WT1	Diagnosis	Venetocloax and Azacitadine. RIP after 1 cycle

Daunorubicin and ara-C (DA), Responded (RES). Details of the AML19 trial can be found in the appendix (additional information)

3.10 Discussion

This chapter has: (i) confirmed the secretion of pro-inflammatory cytokines in response to reovirus, MG1, CVA21 and HSV-1 treatment from HD-PBMC, (ii) demonstrated that OV-CM have anti-AML activity, (iii) Smac and/ or BH3 mimetics are cytotoxic against AML cells at higher doses, and (iv) demonstrated that the combination of OV-CM and Smac and/or BH3 mimetics can work together to enhance AML cell death. Furthermore, a potential role for both IFN-α and TNF-α was identified, alongside a partial dependence on caspase activation. Importantly for the development of a safer OV-based treatment, the ability of UV-inactivated reovirus to induce the secretion of pro-inflammatory cytokines was also confirmed, together with their cytotoxic potential when combined with LCL161 on THP-1 cells. Finally, these data confirmed that: (i) live and UV-inactivated reovirus could induce the secretion of pro-inflammatory cytokines from AML patient samples, and (ii) combined treatment with reovirus-treated PBMC-CM and Smac/BH3 mimetics could enhance cytotoxicity in primary AML patient samples; although responses varied across AML patient samples.

All OVs tested were able to induce pro-inflammatory cytokines from PBMCs (Figure 3-4), however, cytokine levels varied depending on the OV used. This could reflect the fact that different OV receptors may be required for viral entry and/or recognition by PBMCs. For example, Muller *et.al*. demonstrated that plasmacytoid DC (pDC) express ICAM-1 and that pDC in isolation from PBMCs produced significant amounts of IFN-α after CVA21 treatment, moreover, the secretion of IFN-α was abrogated when pDC were depleted from PBMCs [258]. Whilst monocytes also express ICAM-1, they were not required for IFN-α production following CVA21 treatment, therefore, alternative factors such as the expression and engagement of relevant PRRs are also likely to play a role. By

contrast, HSV induced the secretion of type I IFN from HD-PBMC, which has previously been reported to be dependent on CD14+ monocytes [338]. Similarly, reovirus has also been reported to induce IFN-α from PBMCs in a monocyte-dependent manner; e.g., IFN-α production was lost when monocytes were removed from PBMC [259]. Comparison between the ELISA pan-IFNs (Figure 3-1) and multiplex assay (IFN-2α) (Figure 3-4A) show discrepancies in values, suggesting that OV induced a range of type I IFNs, not just IFN-2α. Importantly, it has been reported that IFN-α subtypes (IFN-α IFN-α1, -2a, -2b, -4a, -4b, -5, -6, -7 and -8) have different potency [347], however, IFN-2α and 2b have been tested in clinical trials [329].

PRRs regulate the secretion of various levels of cytokines after OV treatment. For example, MDA-5 and RIG-I are pivotal sensors of reovirus [348], while RIG-I and myeloid differentiation primary response 88 (MYD88) detect MG1 infection [306]. Coxsackieviruses can be recognised by RIG-I, MDA-5, TLR7 and TLR 8 [349-351], and HSV-1 can be detected by TLR2, TLR9 and HVEM [352]. Binding to these different PRRs will trigger a variety of signalling pathways (e.g. NF-κB and IFN signalling pathway), causing the secretion of a various pro-inflammatory cytokines. A dependence on different immune cell subsets and distinct PRRs is likely to be responsible for the slightly altered repertoire of cytokines produced in response to each OV.

Importantly, pro-inflammatory cytokines secreted in response to OV treatment induced bystander cytokine killing of AML cell lines (Figure 3-7), and this has been reported previously. For example, Muller *et al*. demonstrated that CVA21-treated PBMC induced pro-inflammatory cytokines which induced cell death in both MM and AML cell lines (Kasumi-1, KG-1 and HL-60) [258]. Moreover,

reovirus-treated PBMC-CM has also been reported to induce significant cell death of MM cell lines [336].

Several cytokines secreted in response to OV treatment (Figure 3-4) have been reported to have an anti-tumour effect on AML cells, including IFN-α, TNF-α and IL-1β [353-355]. As demonstrated above, IFN-α production is induced by all OV tested and this cytokine has been tested for the treatment of AML, and other malignancies [342, 356]. Interestingly, OVs have been modified to express cytokines to enhance the induction of anti-tumour activity within the TME. An example for this is adenovirus, which has been engineered to express TRAIL (zA4); zA4 induced significant apoptosis in AML cell lines (THP-1 and MV4-11) and inhibited the proliferation of primary patient samples [280]. Moreover, VSV-IFN-β induced death of NSCLC cells and reduced tumour growth of H2009-bearing mice [357]. Importantly, IFN-β promotes specificity by inhibiting VSV replication within healthy cells, has direct anti-cancer effects, and is able to enhance DC-driven anti-tumour T-cell immune responses [358].

IFN-γ is critical for adaptive CTL activation and proliferation and is secreted in high quantities following antigen recognition by CTL, as well as by NK cells and Th1 $CD4^+$ T cells [359, 360]. Thus, the induction of IFN-γ following OV treatment could facilitate the generation of tumour-specific CTLs; indeed, the ability of CVA21 to induce AML specific CTLs has been reported [258].

Interestingly, Binder *et al*. reported that TNF-α promotes tumour growth, proliferation, tumour angiogenesis and can increase chemoresistance in AML [361]. However, the combination of TNF-α with agents that inhibit NFkB activation could sensitize cancer cells to apoptosis [362], as is suggested by the data presented herein. Moreover, TRAIL was also secreted in response to OV

treatments (Figure 3-5) and it has been reported to have a cytotoxic effect against cancer cells.

IAPs (e.g. XIAP and cIAP2) are expressed in AML cell lines and primary samples [363], and overexpression of IAPs has been associated with poor prognosis and a reduced CR rate in AML patients [364]. Moreover, BCL-2 anti-apoptotic proteins have also been reported to be overexpressed in AML and BCL-2 mRNA expression was identified in 65% of 119 AML patients [364]. Therefore, these anti-apoptotic pathways may play a key role in the ability of AML cells to evade apoptosis. Importantly, the bivalent variation of Smac mimetics have elevated cytotoxic effects compared to their structurally associated monovalent IAP antagonists [134]. Of note, it has been reported that BV-6 was more effective in degrading cIAP1, than LCL161 [365] because of the differences in chemical structure; LCL161 consist of a single N-terminal amino acid binding motif, whereas BV-6 consist of two binding motifs [133]. Safferthal *et al*. showed that both LCL161 and BV-6 antagonise IAPs and induced cell death in AML cell lines, and in apoptosis-resistant patient derived AML blasts [366]. Moreover, BV-6 induced degradation of both cIAP1 and cIAP2 and sensitised a range of cancer cells (MM, human colorectal adenocarcinoma, fibrosarcoma, cervical carcinoma and T-cell lymphoma cell lines) to TNF-α and TRAIL-dependent apoptosis [367]. IL-1β also induced upon OV treatment can cause activation of NFkB and produced TNF-α in a panel of cancer cells (originated from breast, colon, bone, central nervous system, ovaries, lung, pancreas, and skin) which causes apoptosis when combined with the Smac mimetic (SM-164) [368]. Furthermore, pre-clinical studies in different cancer types, including childhood acute leukaemia and CLL have shown that Smac mimetics can sensitise cancer cells to cell death in response to various cytotoxic stimuli, such as TRAIL, TNF-α, γ-irradiation or

chemotherapies (e.g. alkylating agents such as dacarbazine and temozolomide) [145, 146].

In accordance with our data (Figure 3-8), Shi *et al*. have also proven that targeting BCL-2 using ABT-199 can induce apoptosis in AML cells. In addition, ABT-199 was effective against chemotherapy-resistant AML cells, which had down-regulated BCL-2 and MCL-1 levels and increased expression of Bax [369]. Moreover, the BCL-2 inhibitor, cpm-1285, induced apoptosis in AML cell lines, and inhibited the growth of human myeloid leukaemia cells in immunodeficient mice [204].

Importantly, HD-PBMC cells showed a dose-dependent response when treated with LCL161, BV-6 ABT-199 or ABT-263 (Figure 3-9) with significant cell death observed when higher doses were used. However, healthy monocytes isolated from PBMCs were resistant to the drugs. Death observed within PBMC could reflect that fact that lymphocytes account for 70–90% of PBMC [370], and that BH3 mimetics (ABT-199 and ABT-263) in particular have been reported to cause death of lymphocytes, specifically B cells, but not monocytes [371]. Similarly, an alternative BCL-2 inhibitor, cpm-1285, caused low level cell death on healthy human PBMC [204]. Importantly, LCL161 or birinapant did not induce significant cell death in normal colorectal, aortic endothelial or corneal epithelial cells [319]. Moreover, a phase II clinical trial study showed that LCL161 was safe and well tolerated. In this study, LCL161 was given to myelofibrosis patients orally at a dose of 1500mg/ week. In all 50 patients (median age 60 years), 64% observed no adverse effects, 46% reported fatigue, dizziness and vertigo, whilst only 4- 6% developed thrombocytopenia and anaemia [162]. In addition, ABT-199 was well tolerated at dose of 800mg daily in AML patients recruited to a phase II study.

However, common adverse events associated with ABT-199 were diarrhoea, vomiting, neutropenia and hypokalaemia [90]. With regards to ABT-263 safety, a phase IIa study of 26 lymphoma patients reported that all patients experienced some adverse events; 38% thrombocytopenia, 30% neutropenia, and two patients experienced serious adverse events [185].

Several studies have demonstrated that the efficacy of Smac or BH3 mimetics could be potentiated when combined with other agents. In this project, the combination of OV-CM with Smac or BH3 mimetics significantly increased AML cell death (Figure 3-10, Figure 3-11,

Figure 3-12, Figure 3-13, Figure 3-14 and Figure 3-15). Previous studies have demonstrated a synergistic effect between Smac mimetics and OVs treatments and importantly this synergy was documented to be relay on the production of cytokines following OV treatment, in particular; TRAIL, IL-1A, IL-8 [319], and TNF-α [320]. Furthermore, Cai *et al*. demonstrated that LCL161 enhanced M1-bystander killing of hepatocellular and colorectal carcinoma cell lines in a cytokine-dependent manner (e.g. TRAIL, IL-1A and IL-8) [319]. Breast carcinoma (EMT6 cells) and Glioblastoma (SNB75 cells) cells also induced IFN-β, TRAIL and TNF-α in response to VSVΔM51 treatment, which in combination with LCL161 decreased tumour burden and enhanced survival in tumour bearing mice, as compared to single agent therapy [320]. To our knowledge combination of ABT-199 or ABT-263 with OV has not previously been reported.

Interestingly, work with recombinant cytokines demonstrated that KG-1 cells were susceptible to IFN-α treatment alone, however, this was not consistent with levels of cell death observed after treatment with OV-treated PBMC-CM. This could reflect the range of pro-inflammatory cytokines secreted after OV treatment and

the interaction between these signalling events. For example, OV-CM contains the IFN-α signalling inhibitor, IL-1β, which could inhibit cell death induced by type I IFNs [372]. Limited studies have previously reported the efficacy of the combination of human recombinant cytokines with Smac or BH3 mimetics in AML. However, BV-6 co-treatment with IFN-α can induce the upregulation of TNF-α and stimulate death of AML cells, which was dependent on TNF-α/TNFR1 signalling [373]. Moreover, Roesler *et al*. demonstrated that BV-6 in combination with IFN-α synergistically triggered apoptosis in multiple solid tumour cell lines (colon carcinoma, glioblastoma, pancreatic carcinoma, rhabdomyosarcoma and Ewing sarcoma) and this was also TNF-α and TRAIL-mediated [374]. Furthermore, Hao and Tang demonstrated that combination of Smac mimetic (AZD5582) and IFN-γ (but not IFN-α or TNF-α) induced death of H1975 NSCLC cells in a TNF-α autocrine-dependent manner [343]. In addition, Petersen *et al*. demonstrated that the Smac mimetic (named compound 2) in combination with either TRAIL or TNF-α led to synergistic activation of caspases and induced apoptosis in NSCC (HCC44, MDA-MB-231 and SK MEL-5 cell lines) both *in vitro* and *in vivo* [120, 127]. The combination of SM-164 with TRAIL, as well as other death-inducing inflammatory cytokines, (e.g., TNFα) also led to synergistic cytotoxicity when tested *in vitro* on various cancer cell lines (breast, prostate, and colon cancer) [142]. Additionally, TNF-α and TRAIL synergized with the Smac mimetic, AEG40730, to promote cell death in RMS cell lines (RH36, RH41 and Kym-1), activate caspase-3/-7, and suppress tumour growth in a Kym-1 xenograft model [375].

The work presented in section 3.7, demonstrated a role for apoptosis for AML cell death, as supported by reduced cell death in the presence of zVAD and activation of caspase -3/7. The importance of apoptosis was initially examined using zVAD,

which is an irreversible inhibitor of caspase-3, -6 and -7. However, although zVAD treatment was able to reduce cell death, death in THP-1 cells remined high (70%). One possible explanation for this could be because of the long incubation-time, thus additional time points could have been investigated. However, it could also be due to activation of alternative death pathways (e.g. necroptosis) when apoptosis is inhibited. Indeed, in colorectal adenocarcinoma (HT29 cell line), zVAD blocked caspase -8 activity to inhibit apoptosis, but necroptosis was triggered [376], demonstrating the complex interplay between these two significant death pathways. Previous work has also confirmed a role for apoptosis in both cytokine-mediated killing when used alone or in combination with Smac/BH3 mimetics; LCL161 and TRAIL treatment induced apoptosis and cleaved caspase-3, -7 and -8 in breast cancer cell lines (MDA-MB-368 and CAMA-1) [377]. Moreover, the combination of AZD5582 with TNF-α significantly decreased the number of gallbladder cancer cells (SGC-996 and NOZ) via apoptosis, which was demonstrated by increased cleavage of both caspase-8 and caspase-3, compared to either of the treatment alone [378].

To date, several clinical studies have tested the efficacy of OV in the context of haematological malignancies, in particular MM and cutaneous T-cell lymphoma (CTCL). A study published in 2005 treated a total of 16 T-cell lymphoma patients (i.t) with live MV (patients were pre-treated with IFN-a to control virus spread), which was well tolerated, therefore, CTCLs could be promising target for MV-based therapy [379]. In a phase I trial, 32 MM patients were treated (i.v) with MV-NIS, which effectively targeted MM, increased T-lymphocyte cytotoxicity, and was capable of replicating before being cleared by the immune system [380]. Moreover, a recent study published in 2022 by Cook *et al*. demonstrated that i.v. treatment with VSV-IFNβ-NIS, which is engineered to induce IFN-β, was well

tolerated in all patients including one AML patient. Importantly, 5 of 7 patients with T-cell lymphoma responded to the treatment and tumour regression was reported. Pre-existing cytopenia was reported for the AML patient and this was more profound after virus infusion [334].

Some OV in preclinical and clinical development are naturally occurring pathogens without safety modifications, e.g. reovirus and CVA21, and they have potential to cause mild infection in healthy individuals. However, in AML patients, this could be problematic due to reduced innate immunity. Investigations using UV-inactivated OV, as a safer treatment option for AML patients has yielded some promising results in this study. For example, Figure 3-21 demonstrated that UV-inactivated OV can induce pro-inflammatory cytokines, however, this appeared more pronounced when UV-inactivated reovirus was used compared to the other OV tested. Moreover, LCL161 potentiated cell death induced using PBMC-CM collected after treatment with UV-inactivated reovirus, and these results were also comparable to levels observed using PBMC-CM collected after treatment with live (replication-competent) reovirus (Figure 3-22). This was consistent with previous work from our laboratory which showed that both replication competent and UV-inactivated reovirus acted similarly in their ability to induce type I IFN and activate innate NK cell anti-tumour immunity in the context of CLL [259]. In addition, both replication-competent and UV-inactivated reovirus have the ability to mature DC [260], activate NK cells [259] and prime tumour-specific cytotoxic T lymphocyte [381]. Therefore, this suggests that UV-inactivated reovirus could stimulate additional effector mechanisms to reduce AML burden, if it was successfully translated into AML early phase clinical trials in combination with apoptotic modulators. Similar results have also been observed for alternative RNA viruses, such as respiratory syncytial virus (RSV),

where both live and UV-inactivated RSV induced the secretion of cytokines including, RANTES, IL1-a, CXCL8 and CXCL10 [382]. Other groups have also considered using UV-inactivated OV, namely HSV-1, as a safer option for the treatment of AML patients. This paper demonstrated that UV-inactivated HSV-1 could activate NK cells and kill both AML cell lines and AML primary blasts [285].

LCL161, BV-6 and ABT-199 appeared to potentiate the cytotoxic effect of reovirus-treated PBMC-CM in some but not all primary AML patient samples. The varied response observed in primary AML is most likely due to the heterogeneity of this disease and preliminary data obtained suggests a possible role for FLT3, NPM1 and/or DNMT3A in the response to Smac mimetics and KRAS for ABT-199 (Table 3-4). FLT3 mutations occur in 27% of AML patients aged over 65 and regulate cell cycle and proliferation. FLT3 mutations are associated with a high white blood cell count, but they do not impact upon complete remission rates in AML patients. However, FLT3 mutations are linked to an increased risk of relapse and a low overall survival [383]. Importantly, synergistic responses with extrinsic apoptotic stimuli (TRAIL and CD95L) used in combination with BV-6 have been previously reported in AML patient samples harbouring FLT3 mutations [384]. Herein, FLT3 mutations were correlated with increased RIPK expression, where RIPK activity is regulated by IAP (cIAP1/2) and can promote necroptosis. Thus, binding of cIAPs by BV-6 acts to release RIPK and promote cell death via apoptosis or necroptosis. These data support our observation regarding the potential importance of FLT3 mutations for predicting response to Smac mimetics and OV-generated PBMC-CM [384]. There is also further evidence to suggest that FLT3 mutations may affect the activity of apoptotic modulators. For example, one study found that FLT3 mutations can lead to an increase in the expression of BCL-2 family protein (MCL1) in primary AML blasts [385]. This could explain

why ABT-199, which targets BCL-2 but not MCL1, did not potentiate cell death in primary samples from patients with FLT3 mutations. Importantly, cell line information regarding mutational status suggests a more complex network of interactions, as FLT-3 mutations have not been reported in THP-1 cells, which responded to LCL-161 and BV-6.

NPM1 mutations are detected in 35% of AML patients and a high number of AML patients carry both NPM1 and FLT3 mutations. NPM1 mutations are linked with increased overall survival and a high complete remission rate. However, these effects are lost when FLT3 mutations are presents [383]. In line with our study, NPM1 mutations were prevalent in BV-6-senstive compared to BV-6-resistant primary AML samples [158].

DNMT3A mutations are found in 20% of AML patients and are linked with DNA methylation, which is associated with a poor outcome in AML [386]. Interestingly, sensitivity to the combination of BCL-2 and MCL-1 targeting was observed in AML patients harbouring RUNX1 mutations (11 out of 15 cases), DNMT3A mutations (10 out of 16 cases), or ASXL1 mutations (7 out of 14 cases) [69]. Therefore, DNMT3A mutations could play a role in apoptosis resistance and warrant further exploration in future work relating to Smac/BH3 mimetics (or other apoptotic modulators) and OV.

As illustrated above, one patient sample responded to reovirus-treated PBMC-CM and ABT-199, which was harbouring CEBPA and GATA2 mutations. In line with this finding, Bisaillon *et al*. reported that a strong association between ABT-199 sensitivity and mutations in GATA2, CEBPA, KMT2D, RAD21, STAG2, NPM-1, IDH1/2 and SMC1A. By contrast resistance to ABT-199 was associated with mutations in RUNX1, TET2, TP53, PTPN11 and JAK2 [387].

Having identified that the combination of reovirus-treated PBMC-CM and Smac or BH3 mimetics can induce cell death in AML cells, the next step was to examine whether Smac/BH3 mimetics can enhance alternative OV mechanisms of cell death in AML. This will be explored in the next chapter.

Chapter 4：The ability of Smac and BH3 mimetics to enhance alternative mechanisms

4.1 Introduction

Previous studies have demonstrated the efficacy of reovirus-direct oncolysis in the context of AML. For example, it has been shown that AML cell lines (e.g. THP-1, KG-1, Kasumi-1, ML-1 and HL-60 cells) express JAM-A, the reovirus entry receptor on their surface and were susceptible to reovirus oncolysis [277, 388]. Cai *et.al.* also showed that LCL161 enhanced M1 virus replication in a colorectal carcinoma cell line (HCT116) and induced significant cell death [319]. Moreover, the BH3 mimetic, EM20-25, worked synergistically with VSV-AV1 to overcome apoptosis-resistance in CLL patient samples and increased cleavage of caspase -3 and -7; however, EM20-25 did not increase VSV-AV1 replication [323]. Another BH3 mimetic, obatoclax, was shown to increase VSV-direct oncolysis in CLL cells *in vitro* [324].

NK cell-mediated killing is a novel immunotherapeutic approach that has emerged for AML in recent years. This approach is dependent on evading immune suppression within the TME and activating NK cells to attack malignant cells [389]. In the context of AML, NK cell anti-tumour immunity using adoptive cell transfer is still at the initial stage and is being developed to enhance their therapeutic efficacy [390]. For example, a first human clinical trial of CAR NK92 cells, in three refractory or relapsed AML patients demonstrated that CAR NK92 cells can be infused at doses up to 5 billion cells per patient without causing serious adverse effects [391, 392]. Importantly, BV-6 has been shown to increase NK cell cytotoxicity and sensitise Rhabdomyosarcoma cell lines (RD and RH30) to NK cell-mediated killing [393]. A recent study by Sarchen *et.al*. also showed

that sub-toxic doses (< 1μM) of apoptotic modulators can enhance NK cell-mediated killing of paediatric cancer spheroids (osteosarcoma and neuroblastoma). Specifically, A1331852 (a BCL-xL inhibitor) and S63845 (a MCL-1 inhibitor) enhanced the cytotoxicity of NK cells and reduced spheroids size whilst no effect was reported for ABT-199 [394].

As demonstrated in chapter 1, Smac and BH3 mimetics enhanced cytokine-mediated bystander killing and increased cell death. However, as OV use a range of effector mechanisms to induce anti-cancer effects, the aim of this chapter was to; (i) examine direct-oncolysis-mediated AML cell death in combination with Smac/ BH3 mimetics; and (ii) investigate whether Smac/ BH3 mimetics could be used to potentiate NK cell-mediated cytotoxicity in AML.

4.2 The ability of BH3/ Smac mimetics to enhance reovirus-mediated direct oncolysis in AML cell lines

Previous work demonstrated that AML cell lines (THP-1, HL-60 and KG-1 cells) express JAM-A receptors and were susceptible to reovirus-induced cell death [277, 388]. Reovirus can induce cell death (oncolysis) via apoptosis in cancer cells [344, 395, 396], thus, the ability of apoptotic modulators (Smac or BH3 mimetics) to enhance reovirus-direct oncolysis was examined. To do this, THP-1, HL-60 and KG-1 cells were treated with reovirus for 24 hrs (to allow infection) followed with Smac and/or BH3 mimetics for a further 48 hrs, cell death was subsequently evaluated using LIVE/DEAD. As expected, reovirus induced death of THP-1 cells in a dose dependent manner. However, when reovirus was combined with 10 μM LCL161, a significant increase in cell death as observed at 0.1 pfu/cell which increased by ~13% above reovirus treatment alone (Figure 4-1A). Similarly, BV-6 also significantly increased reovirus-induced cell death by

~32% and ~15% when combined with 0.1 and 1 pfu/cell reovirus, respectively (Figure 4-1B). For ABT-199 and ABT-263, in the absence of reovirus, both drugs alone induced a statistically significant increase in cell death (~10-13%) which was slightly increased to ~17-19% when used in combination with 0.1 pfu/cell reovirus (Figure 4-1C and Figure 4-1D). Collectively, these data suggests that Smac mimetics, in particular BV-6, could be used to enhance cell death in response to lower doses of reovirus.

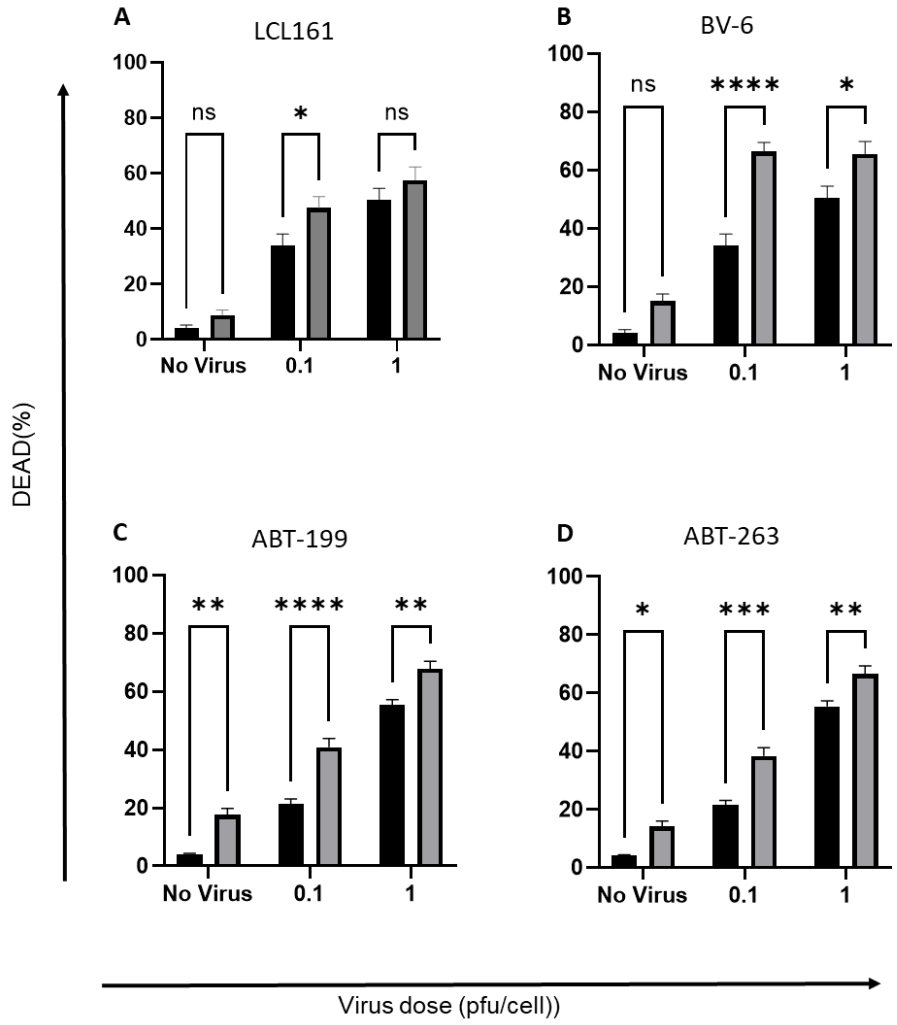

Figure 4-1: Reovirus oncolysis in THP-1 cells treated alone or in combination with Smac or BH3 mimetics. THP-1 cells were treated with 0, 0.1 or 1 pfu/cell reovirus for 24 hrs followed by **A**: 10 µM LCL161, **B**: 2.5 µM BV-6, **C**: 0.01 µM ABT-199, **D**: 0.01µM ABT-263 for 48 hrs. Cell death was assessed using LIVE/DEAD flow cytometry. The mean percentage of dead cells after treatment is shown from at least 3 experiments, + S.E.M. Statistical significance was performed using two-way ANOVA and show comparisons in the presence (grey) or absence (black) of drug. *=p<0.05, **=p<0.01, ***=p<0.005 and ****=p<0.0001.

Next, HL-60 cells were treated as above. As expected, reovirus induced death of HL-60 cells although levels were lower than those observed for THP-1 cells. However, there was no significant increase in cell death when HL-60 cells were treated with Smac mimetics (LCL161 and BV-6) alone, or in response to reovirus when used in combination with LCL161 (Figure 4-2A). By contrast, combining BV-6 with reovirus caused a significant increase in cell death (~16%) over reovirus alone at 1 pfu/cell (Figure 4-2B). Significant cytotoxicity was observed for both ABT-199 and ABT-263 as a single agent treatment. For example, ABT-199 increased cell death by ~18% as a monotherapy; however, there was no significant increase in cell death when used in combination with reovirus at both doses (Figure 4-2C). Similarly, ABT-263 increased cell death by ~16% as a single agent treatment but did not enhance reovirus-induced death at either of the doses used (Figure 4-2D).

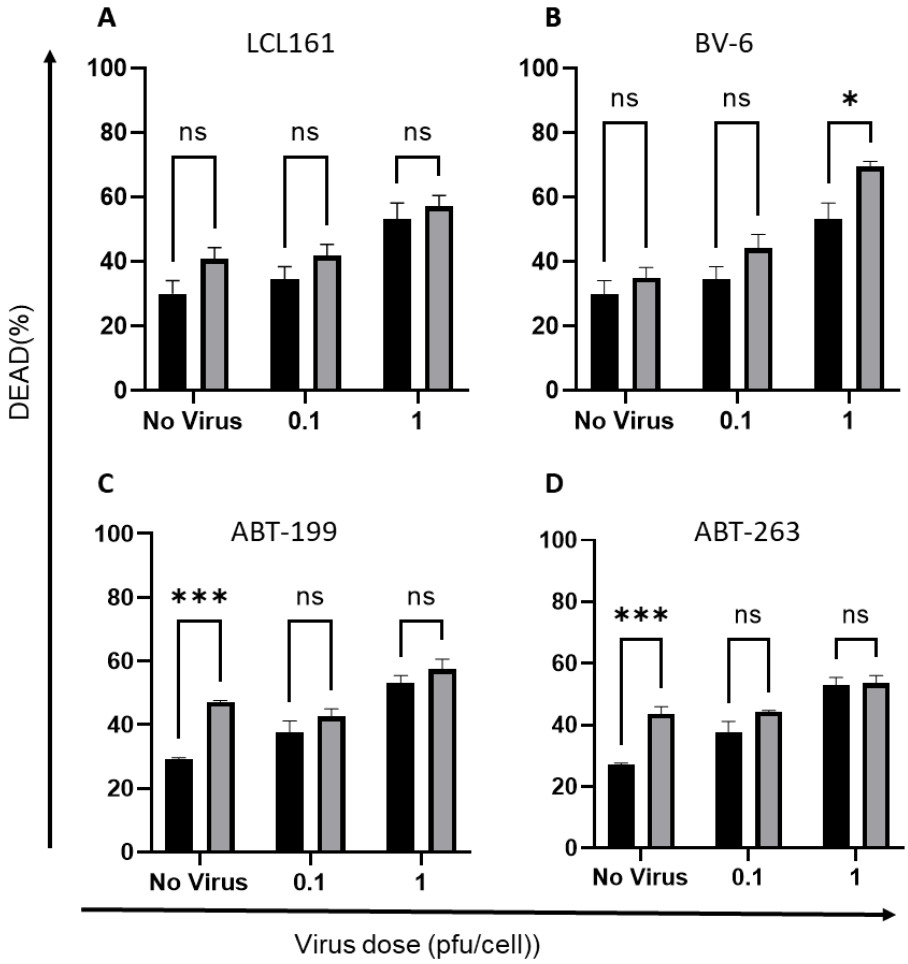

Figure 4-2: Reovirus direct oncolysis in HL-60 cells treated alone or in combination with Smac or BH3 mimetics. HL-60 cells were treated with 0, 0.1 or 1 pfu/cell reovirus for 24 hrs followed by **A**: 10 µM LCL161, **B**: 1 µM BV-6, **C**: 0.01 µM ABT-199, **D**: 0.01µM ABT-263 for 48 hrs. Cell death was assessed using LIVE/DEAD flow cytometry. The mean percentage of dead cells after treatment is shown from at least 3 experiments, + S.E.M. Statistical significance was performed using two-way ANOVA analysis and show comparisons in the presence (grey) or absence (black) of drug. *=p<0.05 and ***=p<0.005.

In KG-1 cells, reovirus induced cell death at 1 pfu/cell, as expected based on previous literature [277]; none of the drugs induced significant cell death as a single agent. The combination of reovirus and LCL161 significantly increased cell death by ~10% above reovirus alone at 1 pfu/cell (Figure 4-3A) and there was no enhancement of reovirus-induced death in combination with either BV-6 or ABT-263 (Figure 4-3B and Figure 4-3D). By contrast, ABT-199 significantly enhanced KG-1 cell death (by ~25%) over reovirus alone at 1 pfu/cell (Figure 4-3C), Collectively, these results suggest that reovirus-induced direct oncolysis could be potentiated by apoptotic modulators, depending on the AML cell line. Similar to the results observed in chapter 1, BV-6 was the most effective agent in both THP-1 and HL-60 cells, and ABT-199 enhanced reovirus oncolysis in KG-1 cells.

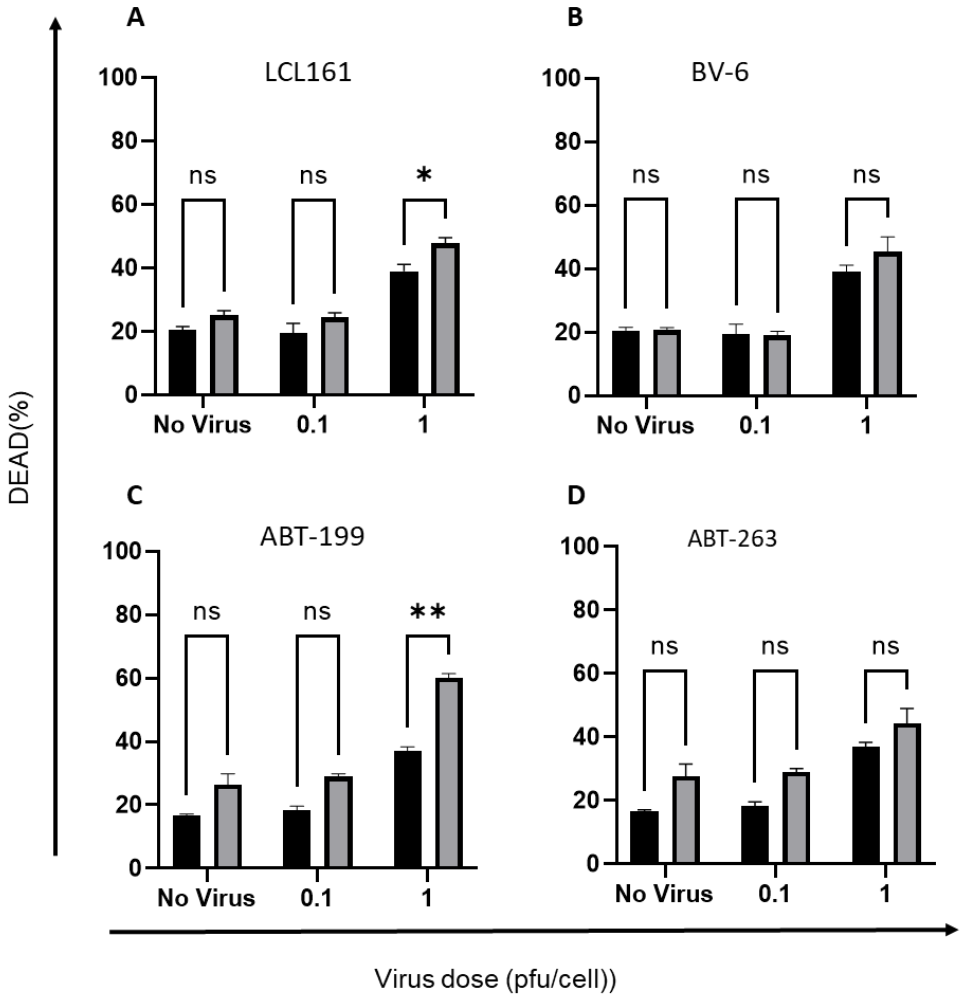

Figure 4-3: Reovirus direct oncolysis in KG-1 cells treated alone or in combination with Smac or BH3 mimetics. KG-1 cells were treated with 0, 0.1 or 1 pfu/cell reovirus for 24 hrs followed by **A**: 10 µM LCL161, **B**: 1 µM BV-6, **C**: 0.01 µM ABT-199, **D**: 0.01µM ABT-263 for 48 hrs. Cell death was assessed using LIVE/DEAD flow cytometry. The mean percentage of dead cells after treatment is shown from at least 3 experiments, + S.E.M. Statistical significance was performed using two-way ANOVA analysis and show comparisons in the presence (grey) or absence (black) of drug. *=$p<0.05$ and **=$p<0.01$.

4.2.1 Efficacy of UV-inactivated reovirus in combination with Smac/ BH3 mimetics

As shown in chapter 1, UV-reovirus induced a range of pro-inflammatory cytokines from HD-PBMC and UV-reovirus-CM was cytotoxic to AML cell lines. Moreover, previous literature published by Hall et al., reported that reovirus treatment of AML cell lines can induce the production of inflammatory cytokines. Therefore, to determine whether reovirus replication was required for AML cell death, or if cell death was due to reovirus-induced cytokines following infection, cell death was investigated using UV-inactivated (replication incompetent) reovirus, alone or in combination with Smac/ BH3 mimetics. Reovirus was UV-inactivated for 2 minutes and applied to AML cell lines for 24 hrs followed by 10 µM LCL161, 1 µM BV-6 (2.5 µM for THP-1 cells), 0.01 µM ABT-199 or ABT-263 for a further 48 hrs. Perhaps surprisingly, UV-inactivated reovirus induced cell death in THP-1 cells, however, no significant cell death was observed in response to LCL161 or BV-6 treatment. Interestingly, LCL161 significantly increased cell death (by ~10% and ~20%) over UV-inactivated reovirus treatment alone at 0.1 and 1 pfu/cell, respectively (Figure 4-4A). Moreover, BV-6 also enhanced cell death in response to UV-inactivated reovirus by ~23% and ~35% at 0.1 and 1 pfu/cell, respectively (Figure 4-4B). Both ABT-199 and ABT-263 induced significant cell death as a monotherapy by ~15%, and this was increased to ~23-~25% (less than 10%) in the presence of 1 pfu/cell UV-inactivated reovirus (Figure 4-4C and D).

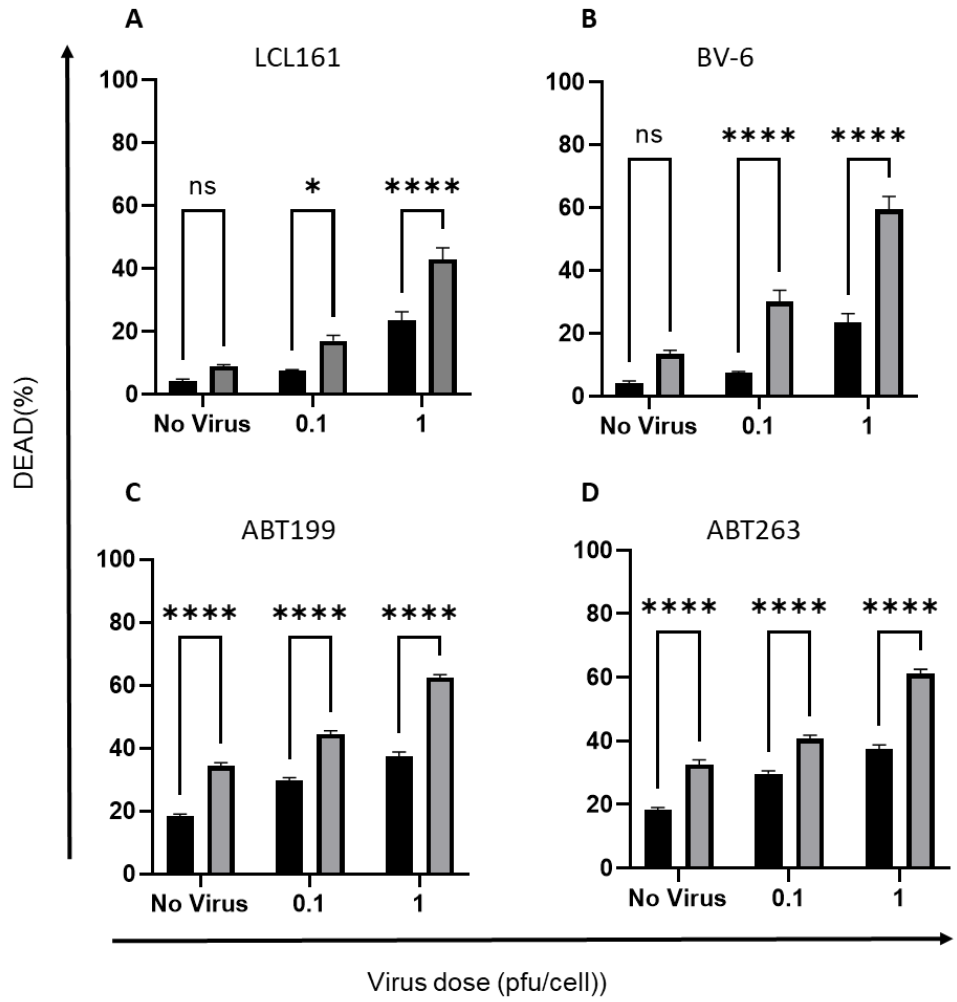

Figure 4-4: Cell death of THP-1 cells after treatment with Smac or BH3 mimetics in combination with UV-inactivated Reovirus. THP-1 cells were treated with 0, 0.1 or 1 pfu/cell UV-inactivated reovirus for 24 hrs followed by **A**: 10 µM LCL161, **B**: 2.5 µM BV-6, **C**: 0.01 µM ABT-199, **D**: 0.01µM ABT-263 for 48 hrs. Cell death was assessed using LIVE/DEAD flow cytometry. The mean percentage of dead cells after treatment is shown from at least 3 experiments, + S.E.M. Statistical significance was performed using two-way ANOVA analysis and show comparisons in the presence (grey) or absence (black) of drug. *=p<0.05 and ****=p<0.0001.

Similarly, for HL-60 cells both LCL161 and BV-6 significantly enhanced cell death. For example, LCL161 increased cell death by ~15% and ~20% over UV-inactivated reovirus alone at 0.1 and 1 pfu/cell, respectively, (Figure 4-5A); and by ~15% (0.1 pfu/cell) and ~27% (1 pfu/cell) for BV-6 (Figure 4-5B). By contrast, ABT-199 and ABT-263 did not significantly increased cell death over that observed for single agent treatment at any doses reovirus used (Figure 4-5C and D).

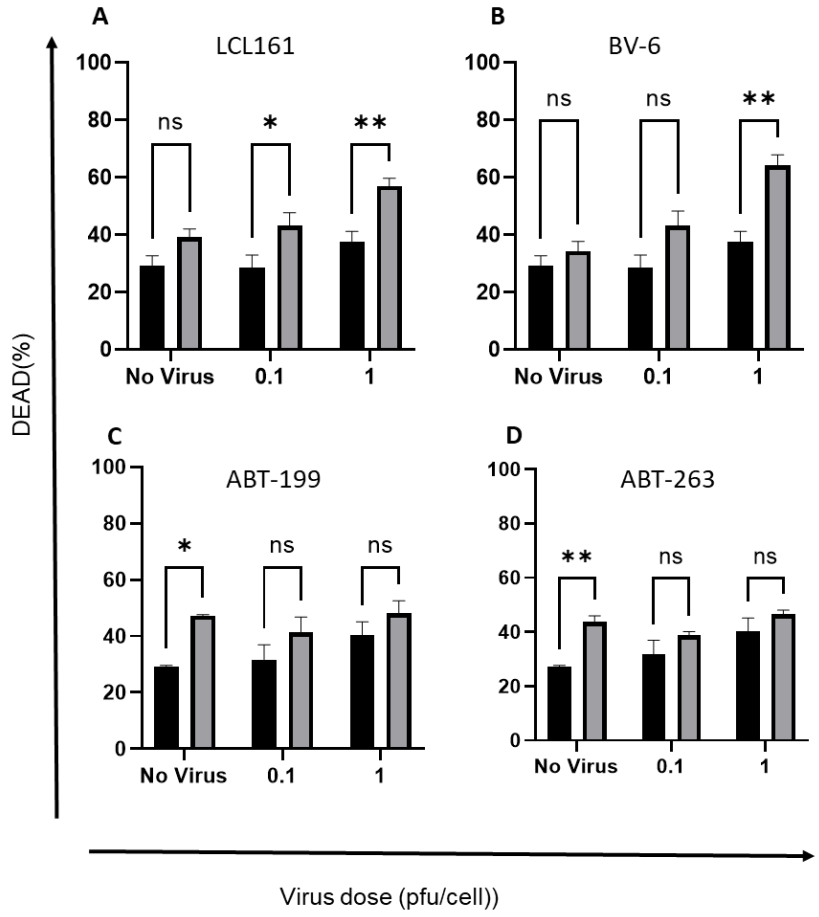

Figure 4-5: Cell death of HL-60 cells after treatment with Smac or BH3 mimetics alone or in combination with UV-inactivated Reovirus. HL-60 cells were treated with 0, 0.1 or 1 pfu/cell UV-inactivated reovirus for 24 hrs followed by **A**: 10 µM LCL161, **B**: 1 µM BV-6, **C**: 0.01 µM ABT-199, **D**: 0.01µM ABT-263 for 48 hrs. Cell death was assessed using LIVE/DEAD flow cytometry. The mean percentage of dead cells after treatment is shown from at least 3 experiments, + S.E.M. Statistical significance was performed using two-way ANOVA analysis and show comparisons in the presence (grey) or absence (black) of drug. *=p<0.05 and **=p<0.01.

Taken together, Smac mimetics were able to potentiate cell death induced by UV-inactivated reovirus, suggesting that viral replication was not required for cell death and that another mechanism was responsible. Therefore, given the role for cytokine-mediated killing (outlined in chapter 1), the production of cytokines from reovirus treated cell lines (± UV-inactivation) was investigated.

4.3 Pro-inflammatory cytokines secreted by reovirus from AML cell lines

The above data confirmed that reovirus and UV-inactivated reovirus induced cell death to AML cell lines and that cell death induced by UV-inactivated reovirus could be potentiated by the addition of Smac mimetics in both THP-1 and HL-60 cells. Next, the secretion of pro-inflammatory cytokines in response to live or UV-inactivated reovirus treatment was examined. THP-1, HL-60 and KG-1 cells were treated with live or UV-inactivated reovirus for 48 hrs and the secretion of IFN-α, IFN-γ and TNF-α was measured by ELISA. Interestingly, THP-1 cells secreted significant levels of IFN-α (130 pg/mL) in response to live reovirus treatment and 30 pg/mL in response to UV-inactivated reovirus at 1 pfu/cell (Figure 4-6A). Low levels of TNF-α were observed (~25 pg/mL) after treatment with 1 pfu/cell live reovirus but not UV-inactivated virus (Figure 4-6B) and IFN-γ was not detected in response to any treatment (data not shown). For KG-1 and HL-60 cells there was no significant enhancement of IFN-α and IFN-γ, this was often below the ELISA detection limit (Table 2-5, Figure 4-6E and F).

As demonstrated above, the levels of IFN-α and TNF-α detected after reovirus treatment were low, and in some cases below of the detection range for ELISA. Therefore, preliminary experiments aimed to test the ability of AML-secreted cytokines (following reovirus treatment) to kill AML cells in the presence or absence of Smac/BH3 mimetics THP-1 cells were treated with 1 pfu/cell live or UV-inactivated reovirus for 48 hrs and the supernatant was collected (THP-1-CM). THP-1 cells were subsequently treated with THP-1-CM in combination with 2.5 μM BV-6 for 72 hrs and the cell death was evaluated using LIVE/DEAD assay. As expected, BV-6 as a single agent increased cell death by ~16%. Interestingly, this preliminary experiment demonstrated that the combination of THP-1-CM and

BV-6 increased cell death by ~37% (live reovirus) and ~27% (UV-inactivated reovirus) over THP-1-CM alone (see Appendix Figure 8-6). Collectively, these data suggest that Smac/BH3 mimetics: (i) do not potentiate direct reovirus oncolysis (as similar levels of cell death were observed with both Live and UV-inactivated reovirus), and (ii) act to enhance AML-derived cytokine-mediated killing in response to reovirus treatment.

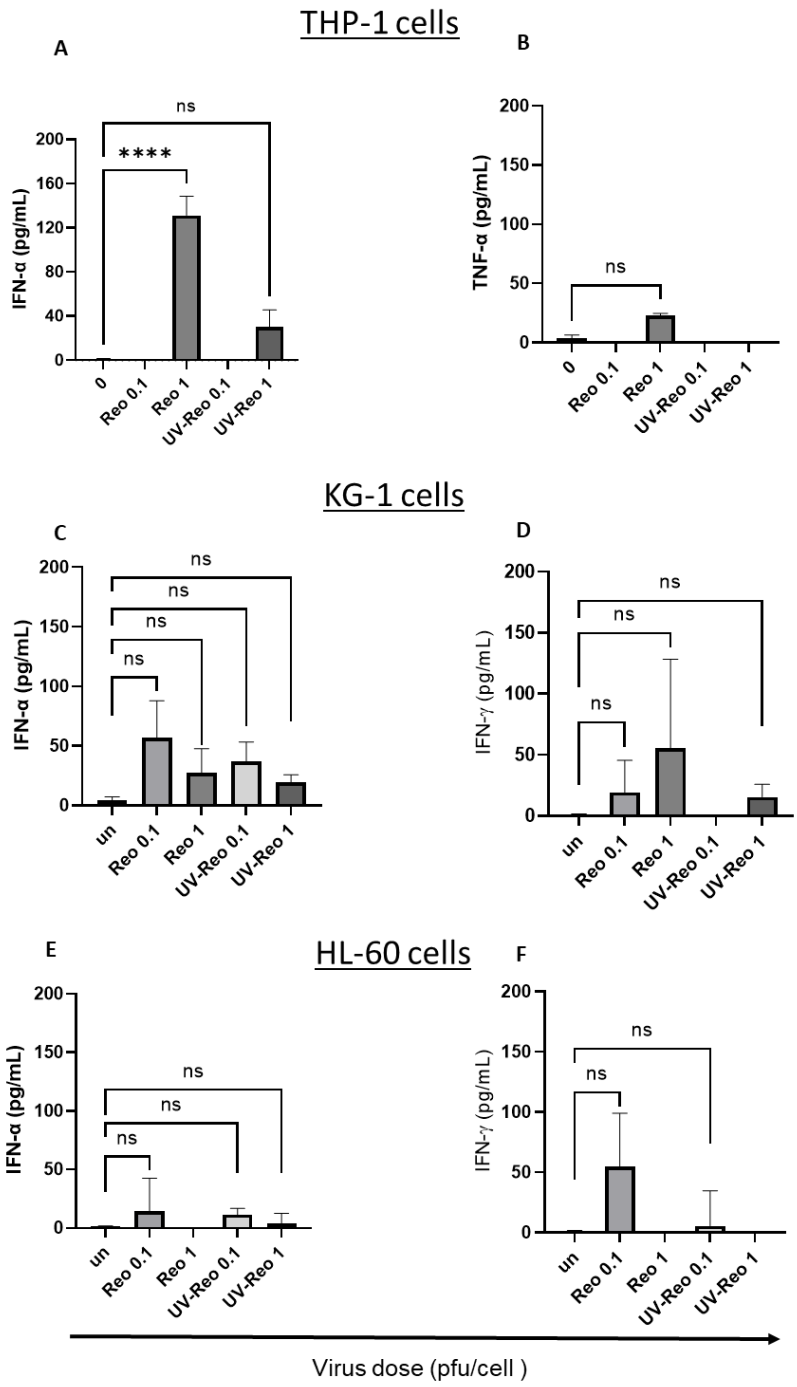

Figure 4-6: IFN-α and IFN-γ cytokine secretion from AML cell lines in response to live or UV-inactivated Reovirus treatment. THP-1, KG-1 and HL-60 cells were treated for 48 hrs at 0, 0.1 or 1 pfu/cell reovirus or UV-inactivated reovirus. Supernatants were harvested and secretion of **A**, **C** and **E**: IFN-α2, **B**: TNF-α, **D** and **F**: IFN-γ was measured by ELISA. Error bars indicate mean + S.E.M for 3 individual experiments. Statistical significance was performed using an unpaired one-way ANOVA and comparisons with untreated controls are shown. ****=p<0.0001.

4.4 Reovirus-mediated activation of NK cell cytotoxicity against AML cell lines

The production of pro-inflammatory cytokines, particularly type I IFN, plays an important role in the maturation, activation and function of NK cells [397]. Thus, the capability of reovirus to activate NK cells and enhance their cytotoxicity against AML cells was investigated. PBMCs were isolated from healthy donors and treated with 0 or 1 pfu/PBMC reovirus, or UV-inactivated reovirus, for 48 hrs, and the activation of NK cells (as determined by CD69 expression) was examined using flow cytometry.

As shown in Figure 4-7, the expression of CD69 was significantly upregulated in response to reovirus treatment, indicative of NK cell activation. As expected, UV-inactivated reovirus treatment also significantly boosted the expression of CD69. For example, following 1 pfu/ PBMC reovirus treatment ~70% of NK cells expressed CD69, and ~60% with UV-inactivated reovirus; however, there was a small but significant decrease in NK cell activation following treatment with UV-inactivated reovirus compared to live reovirus (Figure 4-7).

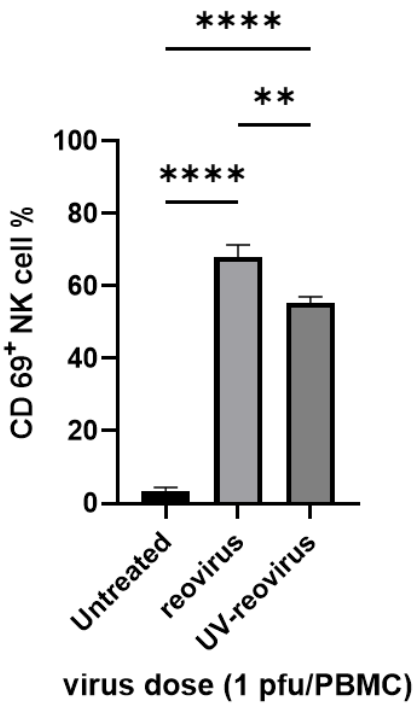

Figure 4-7: Activation of NK cells in healthy PBMC following Reovirus treatment. PBMCs isolated from healthy donors were treated with 1 pfu/PBMC live or UV-inactivated reovirus for 48 hrs. NK cell activation was measured by CD69 expression on CD3-CD56+ NK cells by flow cytometry. Error bars indicate mean + S.E.M for 6 PBMC donors. Statistical significance was performed using an unpaired one-way ANOVA. **=p<0.01 and ****=p<0.0001.

Next, the cytotoxicity of reovirus-activated NK cells was tested in combination with Smac or BH3 mimetics. HD-PBMC were treated with 0 or 1 pfu/PBMC reovirus for 48 hrs to activate NK cells. PBMC were subsequently harvested and co-cultured with target cells (THP-1) for 5 hrs, which were pre-treated with 2.5 µM BV-6 for 24 hrs. The ability of this combination approach to kill the target cells was evaluated using a ^{51}Cr release assay. Importantly, killing of THP-1 target cells was significantly enhanced when co-cultured with reovirus-treated PBMC and cell death reached ~30% at the top effector:target ratio (Figure 4-8). Unfortunately, BV-6 treatment did not enhance cell death over reovirus treatment

alone (Figure 4-8A). Given reversible nature of BV-6 it was possible that maintaining BV-6 in the culture medium during the co-culture would be more effective. Therefore, the experiment was repeated where target THP-1 cells were pre-treated with BV-6 for 24 hrs and co-cultured with reovirus-treated PBMC for 5 hrs in the presence of BV-6. Similar to previous results, ~29% cell death was observed in response to reovirus-treated PBMC, and no enhancement was observed when BV-6 was added (Figure 4-8B). Collectively, these data indicate that reovirus can activate NK cells to kill AML cells; however, apoptotic modulators, such as BV-6, do not significantly abrogate or enhance NK cell-mediated killing.

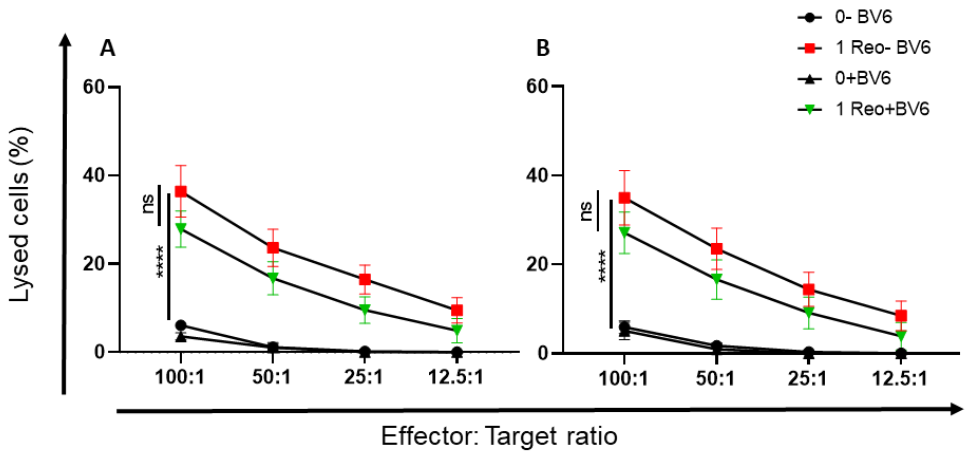

Figure 4-8: NK cell-mediated killing of THP-1 target cells in the presence or absence of BV-6. HD-PBMC were treated with 0 or 1pfu/PBMC Reovirus for 48 hrs. THP-1 cells were treated with 2.5 µM BV-6 for 24 and labelled with ^{51}Cr for 1 hour prior to washing. ^{51}Cr-labelled THP-1 cells (±BV-6 treatment) were **A**: co-cultured with PBMC in the absence of BV-6 or **B**: maintained in BV-6 upon co-culture PBMC (±reovirus) for 5 hrs. THP-1 cell lysis was evaluated using a chromium release assay at various effector:target ratios. Error bars indicate mean + S.E.M for 6 PBMC donors. Statistical significance was performed using a two-way ANOVA. ns indicates comparison of the presence (green) and absence (red) of BV-6 and Reovirus-PBMC.

Figure 4-7 demonstrated the ability of live and UV-inactivated reovirus to activate NK cells from HD; however, it was important to confirm this observation using AML patient NK cells. PBMC were isolated from AML patients and treated with both live and UV-inactivated reovirus for 48 hrs. CD69 expression was upregulated on AML patient NK cells in response to live and UV-inactivated reovirus (Figure 4-9). For example, ~50% of NK cells expressed CD69 after treatment with 0.1 pfu/PBMC live reovirus, which increased to ~70% following 1 pfu/PBMC. For UV-inactivated reovirus, ~40% and 60% of NK cell expressed CD69 in response to 0.1 and 1 pfu/PBMC, respectively (Figure 4-9). These data confirm that reovirus can stimulate NK cell activation in AML patient samples, which could lead to NK cell killing of AML blasts. However, unfortunately NK cell-mediated killing is unlikely to be enhanced by apoptotic modulation based on results presented in Figure 4-8.

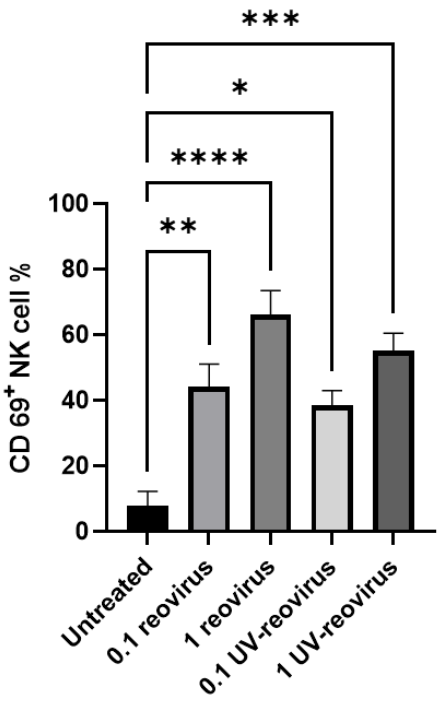

Figure 4-9: Activation of NK cells from AML patient samples following treatment with live or UV-inactivated Reovirus. PBMCs were isolated from AML patients and treated with 0.1 or 1 pfu/PBMC live or UV-inactivated reovirus for 48 hrs. NK cell activation was measured by CD69 expression on CD3-CD56+ cells by flow cytometry. Error bars indicate mean + S.E.M for 6 patients PBMC donors. Statistical significance was performed using a one-way ANOVA and comparisons with untreated controls are shown. *= $p<0.05$, **=$p<0.01$, ***=$p<0.005$ and ****=$p<0.0001$

4.5 Discussion

This chapter evaluated reovirus as a direct oncolytic agent in AML cell lines and the ability of Smac or BH3 mimetics to potentiate the efficacy of reovirus oncolysis. AML cell lines were susceptible to reovirus-direct oncolytic treatment in agreement with a previous study which showed that reovirus can replicate in, and kill, AML cell lines (THP-1, KG-1, Kasumi-1 and ML-1) [277]. Moreover, Schwarts *et.al* also demonstrated that reovirus could reduce AML cell viability and induced apoptosis in 8 different AML cell lines [398]. Furthermore, the combination of reovirus and azacytidine worked synergistically to enhance cell death, compared to either treatment alone, an approach that was also confirmed using primary AML samples [398].

The effectiveness of using reovirus in combination with Smac/BH3 mimetics has not been studied previously. However, it is important to note that previous literature has suggested that the timing of each treatment is crucial, as synergy with the OV VSVΔM51 was only seen when the OV was administered prior to Smac mimetic treatment. However, it was postulated that if the treatment schedule was reversed Smac-induced immune cytokines create an antiviral state before OV treatment, thus, reducing viral replication within the tumour [322]. Several studies have demonstrated that BH3 mimetics (EM20-25 and GX15-070) could be used to overcome CLL resistance to VSV-AV1 oncolysis. The combination of these agents caused cell death in primary *ex vivo* CLL cells and increased apoptosis in B-lymphoma cell lines by blocking BCL-2 interaction with BAX and sensitizing cells to VSV-AV1 oncolytic stress [323, 324]. Moreover, combination of ABT-263 with M1 virus inhibited Bcl-xL and caused M1-induced up-regulation of Bak, subsequently, this enhanced apoptosis in both liver and bladder cancer cells [399].

In this study, the initial data obtained suggested reovirus-direct oncolysis could be enhanced by BV-6 in THP-1 cells (Figure 4-1) and ABT-199 in KG-1 cells (Figure 4-3). However, subsequent data suggested that this effect may be due to the release of reovirus-induced pro-inflammatory cytokines, and this was confirmed using UV-inactivated reovirus which also induced AML cell death when combined with Smac/BH3 mimetics (Figure 4-4 and Figure 4-5). Pivotally, UV-inactivated reovirus induced pro-inflammatory cytokines from HD-PBMC (Figure 3-21) and primary AML samples (Figure 3-23). Batenchuk et al. demonstrated that UV-inactivated VSV induced immunogenic cell death in acute lymphoblastic leukaemia cell line (L1210) and primary patient samples and induced a range of pro-inflammatory cytokines (IL-2, IL-4, MCP-1, MIP-1α and RANTES) from peripheral blood L1210 cells-bearing mice [400]. In addition, Prestwich *et al*. also reported that UV-inactivated reovirus stimulates and primes anti-tumour immunity [381].

Hall *et al*. reported that reovirus was able to generate IFN-α and RANTES from AML cells [277]. A previous study by Errington *et al*. showed that reovirus can induce the secretion of a variety of cytokines from melanoma cells, including Mip-1α, Mip-1β, IL-6, IL8, IL10, and RANTES, which can lead to the bystander killing of nearby melanoma cells [344]. Moreover, Beug *et al*. also demonstrated that breast carcinoma (EMT6 cells) and Glioblastoma (SNB75 cells) cells induced IFN-β, TRAIL and TNF-α in response to VSVΔM51 treatment, which in combination with LCL161 potentiated cell death; IFN-β was responsible for the production of TRAIL and TNF-α which acted synergistically with LCL161 to enhance cell killing [320]. Therefore, this literature supports the notion that death of AML cell lines, in response to reovirus -BV-6/ABT-199 treatment, could be

mediated by cytokines, rather than viral replication and reovirus-induced apoptosis.

The work presented herein demonstrated that both live and UV-inactivated reovirus treatment can activate NK cells from HD-PBMC and AML-PBMC. Hall *et al*. showed that reovirus-treated PBMC activated NK cells and enhanced their degranulation against AML cell lines (Kas, THP-1, KG-1 and ML-1) [277]. Moreover, reovirus-activated NK cells have been shown to kill a range of tumour cell types including MM cells [336], CLL primary samples [259], melanoma cells [401] and colorectal cancer cells (DLD-1) [402]. Importantly, Parrish et al. reported that UV-inactivated reovirus induced the secretion of IFN-α from PBMC isolated from CLL patients and activated NK cells [259]. Moreover, UV-inactivated reovirus has the ability to mature DC [260], and prime tumour-specific cytotoxic T lymphocyte [381]. Similarly, UV-inactivated HSV-1 can also activate NK cells to kill AML cell lines and AML primary blasts [285].

The work presented in this chapter suggests that Smac mimetics did not enhance NK cell-mediated killing of AML cell lines (Figure 4-8). This is in contrast to a previous study by Fischer *et al*. who isolated NK cells using immunomagnetic negative selection and demonstrated that pre-treatment of target RD and RH30 cell lines (Rhabdomyosarcoma) with BV-6 for 24 hrs and co-culture with IL-2-activated NK cells (E10:T1) significantly increase cell death, which was mainly TNF-α dependent and partially NK cell-mediated [393]. An additional study also reported that LCL161 treatment increased MICA and MICB expression, NKG2D activatory ligands, and enhanced the susceptibility of Hodgkin lymphoma cell lines to NK cell killing in NKG2D-dependent manner; up-regulation of MICA and MICB was due to DNA damage upon LCL161 treatment [403]. Furthermore, a

study showed that A1331852 (a BCL-xL inhibitor) and S63845 (a MCL-1 inhibitor) enhanced the cytotoxicity of NK cells and reduced spheroids size, whilst no effect was reported for ABT-199 [394].

Interestingly, whilst we have not had the opportunity to evaluate the ability of Smac/BH3 mimetics to enhance the generation of AML-specific T cells in the presence of reovirus, a role for adaptive anti-tumour immunity has previously been reported for Smac mimetics. The Smac mimetic, SM83, triggered the secretion of TNF-α, IFN-γ and IL-1β and killed ascitic ovarian carcinoma (IGROV-1 cells) and murine sarcoma (MethA cells) *in vivo*, and prolonged mouse survival. Importantly, MethA-bearing animals were resistant to tumour rechallenge, indicating that SM83 treatment developed an adaptive anti-tumour response [404]. In addition, Kim *et al*. demonstrated that LCL161 treatment reinvigorates exhausted CD8+ T cells within immunosuppressed tumours and when combined with VSVΔM51, reduced breast carcinoma tumour burden *in vivo* and this was dependent on T-cell cytotoxicity [322]. Moreover, the combination of recombinant poxviral vaccinia (rV) treatment with GX15-070 enhanced the activation of CD8+ T-cells, reduced the activity of T_{regs}, and significantly reduced pulmonary tumour nodules in LL2-bearing mice [325].

Chapter 5：Investigate the efficacy of OV and apoptotic modulators using an *in vivo* model

5.1 Introduction

The data outlined in the previous chapters provided evidence that reovirus or UV-inactivated reovirus in combination with Smac or BH3 mimetics can kill AML cell lines and primary AML samples more effectively than single agent treatment. To ensure clinically relevant results, it was important to evaluate the cytotoxicity of this combination approach in an *in vivo* model of AML. Throughout the literature, immunocompetent and immunodeficient mouse models have been used to study of AML. Immunocompetent mice are used to understand how the immune system responds to leukemic cells and test novel immunotherapies [283, 405], while immunodeficient mice can display severe combined immunodeficiency (SCID), where both B and T lymphocytes are impaired [406]; immunodeficient SCID mice allow the growth of human cells, including AML cell lines. The most established immunocompetent model of AML is the C1498 model which grows in C57BL/6 mice and has been used in systemic and flank tumour models. An example, mesenchymal stem cell (MSCs) carrying reovirus triggered an immune response in C1498- bearing immunocompetent mice (C57BL/6) and inhibited tumour growth [407]. Several studies have also demonstrated the use of SCID mice in the context of AML. Li *et al*. demonstrated the anti-leukemic activity of SGNCD123A (an antibody–drug conjugate) using KG-1 and MOLM-13-bearing SCID mice [408]. Wang *et al*. also reported that zA4 enhanced anti-tumour activity in THP-1 xenograft model using immunodeficient (nude) mice [280]. A complication if using SCID mice to test OV-based therapies is the fact that the immune system is unable to mount and effective anti-viral immune response and neutralise the virus, this can lead to unacceptable toxicities in treated animals.

However, to combat this, UV-irradiated OV can be used. For example, reovirus-treated, HCC-bearing immunodeficient mice developed toxicity. However, to avoid this, reovirus was UV-inactivated, which significantly inhibited tumour growth to levels comparable with those observed with live reovirus [409].

Overall, the main aim of this chapter was to identify the most appropriate *in vivo* model to use to investigate the efficacy of OV in combination with Smac or BH3 mimetics and test the efficacy of this combination strategy *in vivo*.

5.2 Efficacy of reovirus in combination with Smac/ BH3 mimetics *in vivo* model

Having demonstrated that Smac and BH3 mimetics have potentiated OV-induced cytokine killing on AML cell lines and some primary AML patient samples, the next step was to validate the efficacy of this combination treatment approach using an *in vivo* model. To do this, it was necessary to establish the most appropriate model. Given the important role for OV-induced cytokines from immune cell populations, we Initially tested the applicability of the syngeneic immunocompetent AML mouse cells, C1498. The C1498 syngeneic mouse model of AML maintains features of human pathology and harbours different subclones with genomic and immunogenic diversity. However, the genotype of C1498 cells and clonal heterogeneity have not been fully characterized [410].

5.2.1 Cytotoxicity of Smac/ BH3 mimetics on C1498

Initially, to identify a sub-toxic dose of LCL161, BV-6 and ABT-199 to use on C1498 cells, increasing concentrations were applied and cell death was examined after 48 hrs using LIVE/DEAD flow cytometry. For LCL161, a dose-dependent increase in cell death was observed with a maximum average of ~20% cell death at the highest concentration used (10μM). BV-6 treatment also caused

cell death in a dose-dependent manner, with a maximum of ~22% cell death observed at the highest concentration (10μM). ABT-199 was the most toxic agent, with a maximum of ~35% cell death at the highest concentration (10μM) (Figure 5-1). These data demonstrate that C1498 had variable degrees of sensitivity to Smac and BH3 mimetics and significant cell death was observed at the highest concentration for all drugs, therefore, 5 μM of each drug was selected for use in subsequent experiments as this was the highest dose that did not significantly increase cell death.

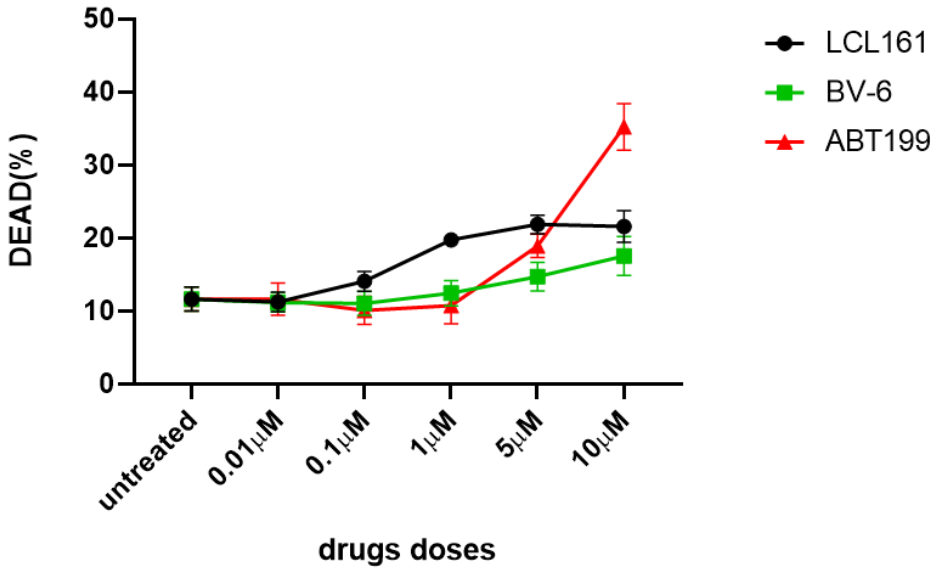

Figure 5-1: Direct cytotoxic effect of Smac/ BH3 mimetics on C1498 cells. C1498 cells were treated with increasing doses of LCL161 (black), BV-6 (green) or ABT-199 (red) for 48 hrs. Cell death was assessed using LIVE/DEAD flow cytometry. Data shows the mean percentage of cell death for n=3 independent experiment, ± SEM.

5.2.2 Efficacy of reovirus in combination with Smac/ BH3 mimetics

Having identified the sub-toxic doses of Smac and BH3 mimetics, the next step was to test the cytotoxicity of the combination of reovirus and Smac/ BH3 mimetics on C1498 cells. To do this, reovirus-CM was generated by treating mouse spleens with 0 or 1 pfu/cell reovirus for 48 hrs before the CM was collected (splenocyte-CM) and UV-irradiated to inactivate remaining reovirus particles. C1498 cells were subsequently treated with UV-inactivated splenocyte-CM (collected ± reovirus treatment) alone or in combination with 5 μM LCL161, BV-6 or ABT-199 for 48 hrs, and cell death was examined using LIVE/DEAD. Unfortunately, cytokine-mediated killing was not observed in C1498 cells, and cell death was not enhanced when reovirus-treated splenocyte-CM was used in combination with LCL161, BV6 or ABT-199 (Figure 5-2).

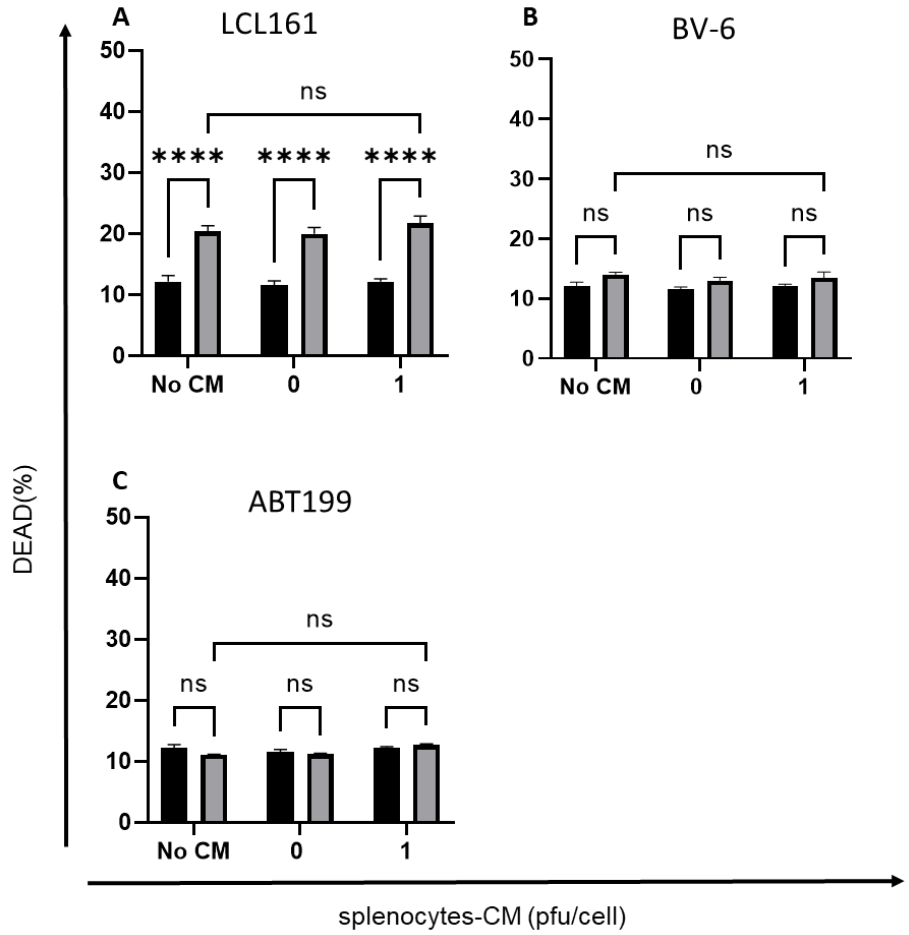

Figure 5-2: C1498 cell death induced by Smac or BH3 mimetics in combination with splenocyte-CM ± reovirus treatment. C1498 cells were treated with UV-inactivated splenocyte-CM (± reovirus treatment) for 48 hrs in the presence or absence of 5 µM Smac (LCL161 and BV-6) or BH3 mimetic (ABT-199) and cell death was assessed using LIVE/DEAD flow cytometry. The mean percentage of dead cells after treatment with 5 µM **A**: LCL161, **B**: BV-6 and **C**: ABT-199 is shown, where splenocyte-CM was collected from n=3 mice, + S.E.M. Statistical significance was performed using two-way ANOVA and indicate comparison between (black bar) splenocyte-CM alone and (grey bar) combination with drugs. *=p<0.05, ****=p<0.0001.

5.2.3 Pro-inflammatory cytokines secreted from splenocytes after reovirus treatment

Given that splenocyte-CM collected after reovirus treatment did not induce death in C1498 cells, alone or in combination with Smac/ BH3 mimetics, it was important to determine whether splenocytes from C57BL/6 responded to reovirus treatment, thus, the cytokine profile induced from mouse spleens following reovirus treatment was examined. To do this, splenocytes were treated with 0 or 1 pfu/cell reovirus for 48 hrs and the secretion of murine IFN-α, IFN-γ, TNF-α, CCL2, IL-2 and IL-12 was evaluated by ELISA. Importantly, splenocytes secreted statistically significant levels of IFN-α (~62 pg/mL) (Figure 5-3A) in response to reovirus treatment; the secretion of IL-2, IFN-γ, TNF-α, CCL2 and IL-12 was not detected (data not shown).

Given the low level of cytokine production from splenocytes treated with reovirus *in vitro*, the suitability of this syngeneic model to test the efficacy of reovirus in combination with Smac or BH3 mimetics remained unclear.

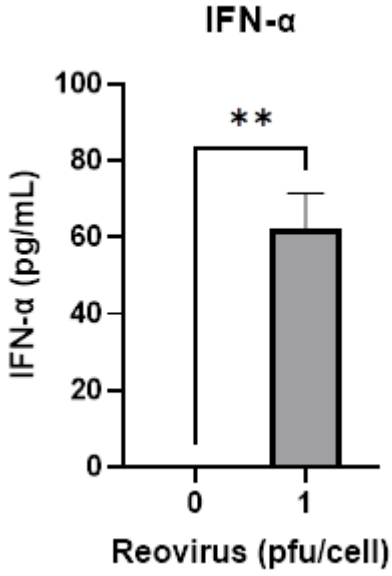

Figure 5-3: IFN-α secretion from murine splenocytes following Reovirus treatment. Splenocytes were harvested from C57BL/6 mice and left untreated or treated with 1 pfu/cell reovirus for 48 hrs. Supernatants were harvested and secretion of IFN-α was measured by ELISA. Error bars indicate mean + S.E.M for 3 spleens. Statistical significance was performed using unpaired t-test. ** = $p<0.01$.

5.2.4 Efficacy of BV-6/ ABT-199 and recombinant cytokine to induce C1498 cell death

Having shown that mouse spleens secreted less pro-inflammatory cytokines (Section 5.2.3) as compared to human PBMC (Section 3.2), it was possible that the syngeneic C1498 AML model would not be suitable to test the efficacy of reovirus in combination with Smac/ BH3 mimetics for the treatment of AML. However, it was also possible that spleen did not encompass the relevant immune cell population to respond to reovirus, thus limiting the response observed. Therefore, given the role for recombinant cytokines (IFN-α and TNF-α) when combined with BV-6 or ABT-199 (identified in Section 3.6), the cytotoxic effect of murine IFN-α and TNF-α, alone or in combination with BV-6 or ABT199,

was investigated to further evaluate the suitability of this model. C1498 cells were treated with increasing dose of recombinant murine IFN-α or TNF-α, alone or in combination with 5 μM BV-6 or ABT-199 for 48 hrs, and cell death was evaluated using LIVE/DEAD. Figure 5-4 shows that BV-6 did not increase C1498 cell death when combined with IFN-α at any dose (Figure 5-4A). Moreover, whilst addition of BV-6 to TNF-α (100 pg/mL, 500 pg/mL or 1000 pg/mL) did increase C1498 cell death, this was only by ~7% over BV-6 alone and at the highest concentration used (Figure 5-4B). Additionally, by contrast to results described in section 3.6, the combination of IFN-α and TNF-α did not cause any significant toxicity; and whilst addition of BV-6 did increase cell death, this effect was low and only reached ~8% at the highest cytokine concentrations (Figure 5-4C). Unfortunately, similar results were also observed for ABT-199 (data not shown).

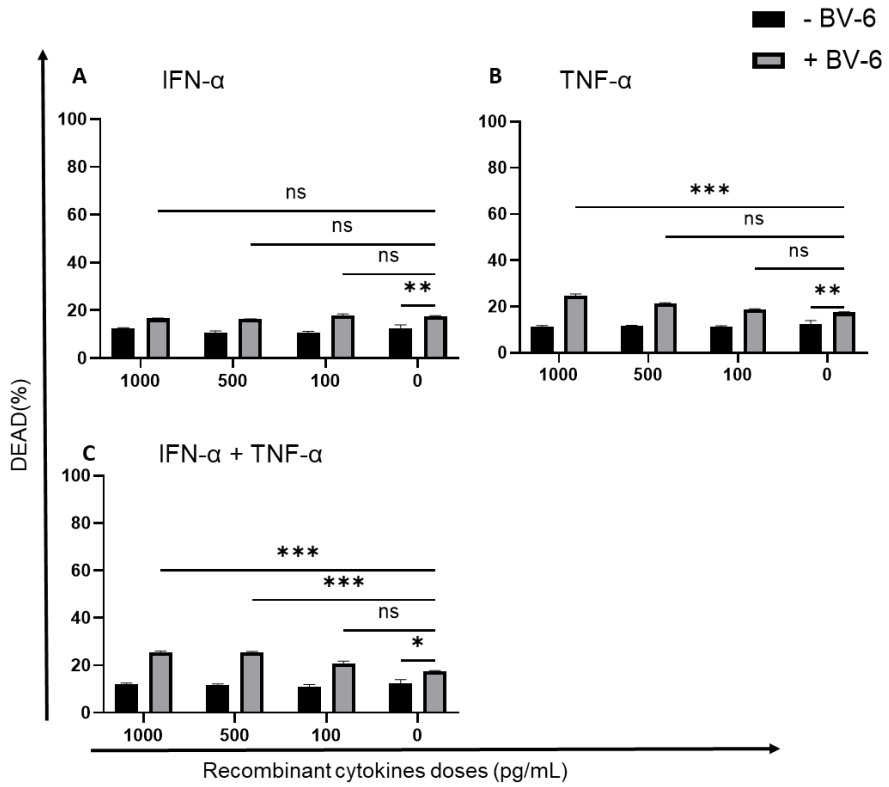

Figure 5-4: Cytotoxicity induced by mouse recombinant cytokines in combination with BV-6 in C1498 cells. C1498 cells were treated with 5 µM BV-6 in combination with **A**: IFN-α (0, 100, 500, 1000 pg/mL), **B**: TNF-α (0, 100, 500, 1000 pg/mL) and **C**: Combination of IFN-α and TNF-α (0, 100, 500, 1000 pg/mL) for 48 hrs and cell death was measured by flow cytometry. The mean percentage of dead cells after treatment is shown from 3 individual experiments, + S.E.M. Statistical significance was performed using a two-way ANOVA, asterisks indicate comparison of the combination treatment in the presence (grey) and absence (black) of BV-6 and recombinant cytokine. *=$p<0.05$, **=$p<0.01$ and ***=$p<0.005$,

Taken together, these data demonstrate that the syngeneic C1498 model of AML would not be suitable to test the efficacy of the previously identified reovirus combination therapy. This is because limited cytokines were secreted in response to reovirus treatment and C1498 cells were less responsive to cytokine-mediated killing, either alone or in combination with Smac/BH3 mimetics.

5.3 Optimisation of AML cell density protocol for use in xenograft models

Given the disappointing results demonstrated in section 5.2, it was decided to examine the combination of reovirus and Smac/ BH3 mimetics using previously published xenograft models of AML, which utilised both THP-1 and KG-1 cells. Specifically, we reasoned that these models may be suitable because of the data illustrated in section 4.3 which demonstrated (i) that reovirus treatment was capable of inducing cytokine secretion directly from AML cell lines (e.g. THP-1, HL-60 and KG-1 cells; Figure 4-6), and (ii) that Smac/ BH3 mimetics could increase cytokine-mediated killing, where the cytokines were produced from reovirus-treated THP-1/ KG-1 cell lines.

Initially, an experiment was performed to optimise the cell seeding density of THP-1 and KG-1 cells in CB17 SCID mice, and to monitor tumour growth to establish appropriate treatment schedules. Four groups, each containing four CB17 SCID mice, were injected s.c with either (i) $5x10^6$ THP-1 cells (group 1), (ii) $10x10^6$ THP-1 cells (group 2), (iii) $5x10^6$ KG-1 cells (group 3) or (iv) $10x10^6$ KG-1 cells (group 4), based on previously published literature [408, 411, 412], and tumour growth was monitored. Figure 5-5 illustrates tumour growth for each animal within each group. Tumour growth in THP-1 bearing mice was slower in group 1, compared to group 2. In addition, no tumour growth was observed in one mouse (mouse 2) in group 1, whilst all animals developed tumours in group 2 (Figure 5-5A and B). Importantly, tumour growth in group 2 was more consistent and all animals developed tumour (Figure 5-5B). Unfortunately, no tumour growth was observed in any of the mice in group 3, injected with $5x10^6$ KG-1 cells (data not shown). However, tumour growth was observed in all KG-1 injected mice in

group 4 (Figure 5-5C). Collectively, it appeared that a seeding density of $10x10^6$ for THP-1 and KG-1 cells would be optimum to use for further experiments.

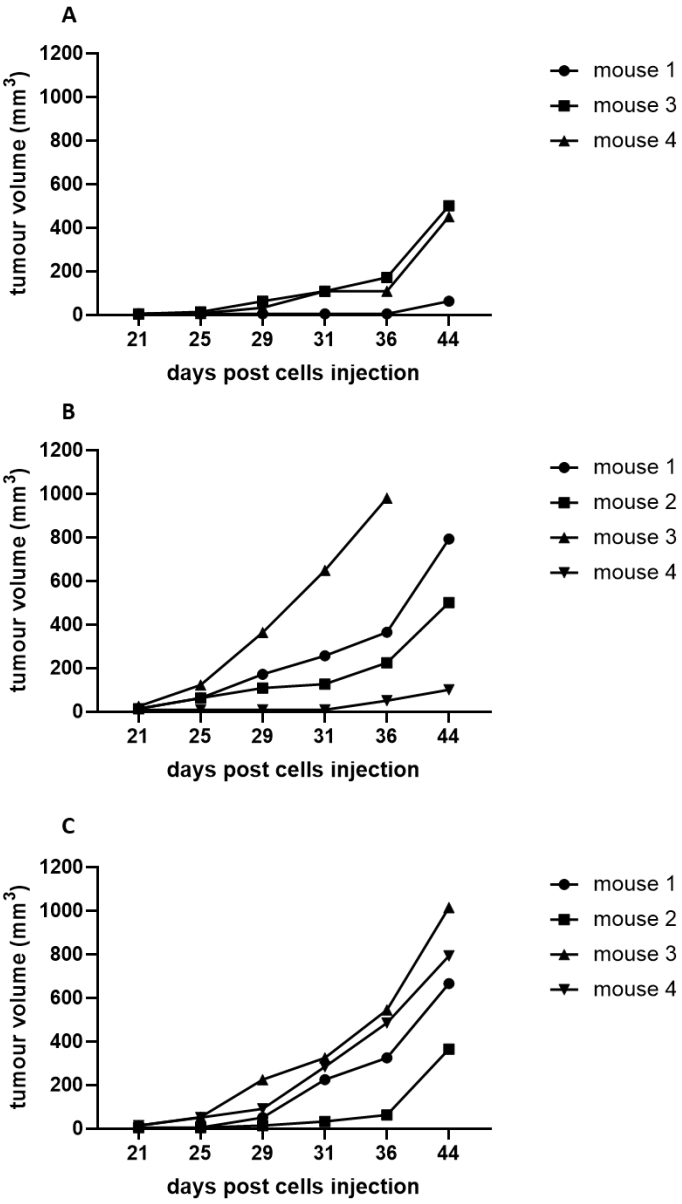

Figure 5-5: THP-1 and KG-1 tumour growth in SCID mice. Six to ten weeks old female CB17 SCID mice were injected s.c with human AML cell lines at different seeding density. THP-1 cells were injected s.c at density of **A**: $5x10^6$ and **B**: $10x10^6$ cells in each mouse (n=4 mice/group). **C**: KG-1 cells were injected s.c at density of $10x10^6$ cells in each mouse (n=4). Tumour growth was monitored using callipers and tumour volume was calculated (tumour volume= length* width*width/2).

5.3.1 Efficacy of UV-inactivated reovirus and Smac/ BH3 mimetics on xenograft model

Having identified the cell density for use in THP-1 and KG-1 xenograft models, the next step was to evaluate the efficacy of UV-inactivated reovirus alone or in combination with Smac/BH3 mimetics. However, as SCID mice have a deficient immune system, UV-inactivated reovirus was used to eliminate the risk of reovirus replication and reduce the possibility of virus-associated adverse events. A total of 64 CB17 SCID mice were injected s.c with either $10x10^6$ THP-1 or KG-1 cells (32 mice for each AML cell line). For tumour treatment, i.t delivery of UV-inactivated reovirus was chosen to produce pro-inflammatory cytokines within the TME, i.p delivery of BV-6 (5 mg/kg) and ABT-199 (1 mg/kg) was used based on previously published literature [413, 414]. Treatments started when tumours where palpable (day 17 for KG-1 mice and day 29 for THP-1 mice post-tumour seeding) and treatments were administrated for two weeks and given twice each week.

5.3.1.1 Efficacy of UV-inactivated reovirus and ABT-199 on KG-1 cells-bearing mice

KG-1-bearing mice were either left untreated or treated i.t with UV-inactivated reovirus followed with i.p injection of ABT-199 3 hrs post reovirus treatment (treatments were administered Monday and Thursday for 2 weeks); a period of 3 hrs was selected based on the half-life of ABT-199 (19-26hrs). Figure 5-6 illustrates the treatment schedule and Table 5-1 provides details for each treatment group. Figure 5-7 shows the tumour growth for each animal within each group. Figure 5-7 demonstrates that tumour growth varied between mice, even with treatment groups, and no obvious effects of treatment were observed. However, as tumour sizes varied slightly at the beginning of the treatment

regimen, tumour growth rate was calculated to more accurately compare tumour growth between each group. Tumour growth from the start of treatment to 3 days after last treatment was administered is shown in Figure 5-8A. Unfortunately, no statistically significant decrease in tumour growth was observed in any of the treatment groups when compared to the vehicle control. Moreover, looking to the survival of the mice (Figure 5-8B), no significant differences were observed. All mice treated with UV-inactivated reovirus as a single treatment were culled by day 58, compared to day 49 in vehicle-treated mice, while both ABT-199 treated mice and the combination treated mice had to be culled by day 46, as the tumour size reached its humane endpoint of 1.5 cm in any direction (Figure 5-8B).

Figure 5-6: Schematic diagram demonstrating the *in vivo* treatment schedule. 32 female CB 17 SCID mice were injected with $10x10^6$ KG-1 cells s.c. on day 0. From day 17 post tumour seeding, UV-inactivated reovirus (or DMSO+PBS vehicle) treatment ($5x10^7$ pfu) was injected i.t and ABT-199 (1mg/kg) was delivered i.p. ABT-199 was delivered 3 hrs post-treatment with UV-inactivated reovirus. Four injections were administered, and mice were culled when the tumour reached 1.5 cm in any direction.

Table 5-1: KG-1 cells-implanted mice treatments for each group

Group	No of mice	Treatment
1	8	50 µl i.t PBS (morning) and 100 µl i.p vehicle control (afternoon) (Monday & Thursday)
2	8	50 µl i.t UV-Reovirus ($5x10^7$ pfu in PBS) (Monday & Thursday)
3	8	100 µl i.p ABT-199 (1mg/kg) diluted in PBS (Monday & Thursday)
4	8	50 µl i.t UV-reovirus (morning) and 100 µl i.p ABT-199 (afternoon) (Monday & Thursday)

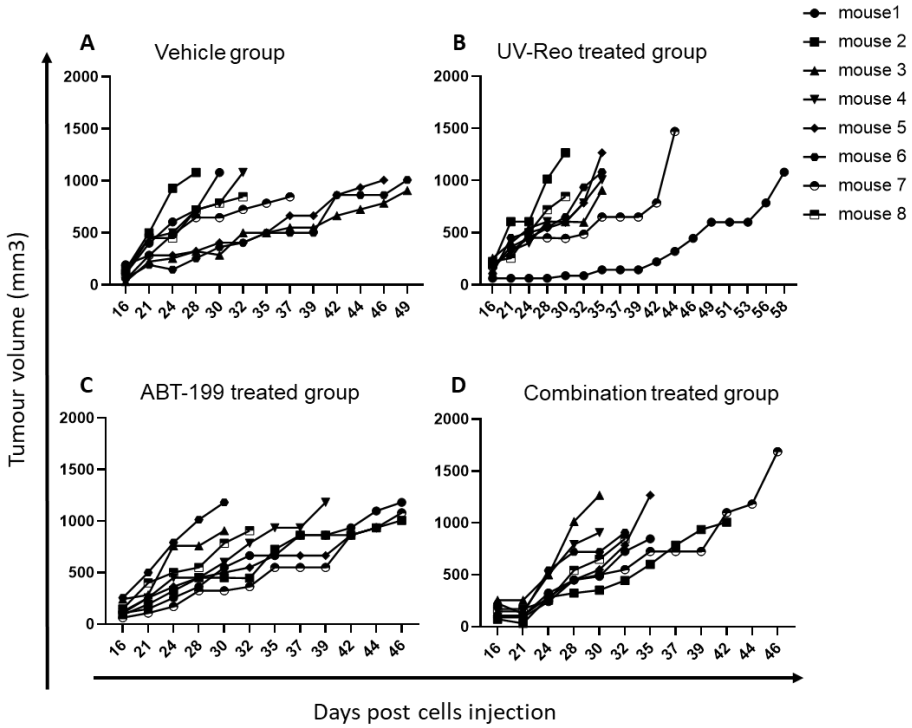

Figure 5-7: KG-1-bearing mice tumour growth after treatment with UV-inactivated reovirus in combination with ABT-199. On day 0, 32 female CB 17 SCID mice (6-10 weeks old) were injected s.c with $10x10^6$ KG-1 cells (100µl in PBS). Treatment started on day 17 post tumour seeding and mice were treated twice a week for 2 weeks with **A**: 50 µl i.t PBS and 100 µl i.p vehicle control (group 1), **B**: 50 µl i.t $5x10^7$ pfu UV-inactivated Reovirus in PBS (group 2), **C**: 100 µl i.p 1 mg/kg ABT-199 (group 3), and **D**: 50 µl i.t UV-inactivated Reovirus (delivered 3 hrs prior to ABT-199 treatment) and 100 µl i.p ABT-199 (group 4). Tumour growth was monitored using callipers and tumour volume was calculated. Mice were euthanized when the tumour reached 1.5 cm in any direction.

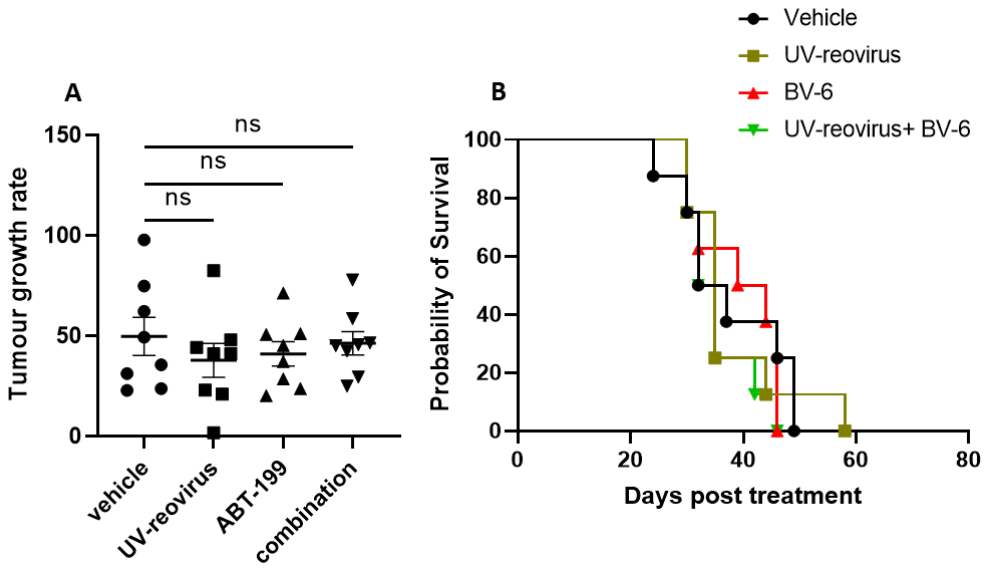

Figure 5-8: Tumour growth rate and survival of KG-1-bearing mice after treatment with UV-inactivated reovirus alone or in combination with ABT-199. 32 female CB 17 SCID mice were injected s.c with $10x10^6$ KG-1 cells (in 100 µl PBS) in each mouse, and treatment started 17 days after KG-1 cells were implanted and was delivered twice a week for 2 weeks. Mice were treated with 50 µl i.t PBS and 100 µl i.p vehicle control (group1), 50 µl i.t $5x10^7$ pfu i.t UV-inactivated Reovirus in PBS (group 2), 100 µl i.p 1 mg/kg ABT-199 (group 3), and 50 µl i.t UV-inactivated reovirus (delivered 3 hrs prior to ABT-199 treatment) and 100 µl i.p ABT-199 (group 4). **A**: The tumour growth rate was calculated by subtracting the tumour volume at the start of treatment from the tumour volume measured 3 days after treatment had ended (divided by the number of days). **B**: Survival of KG-1-bearing mice is shown using a Kaplan Meier curve. Statistical significance was performed using an unpaired one-way ANOVA and comparisons with vehicle controls are shown.

5.3.1.2 Efficacy of UV-inactivated reovirus and BV-6 on THP-1 cells-bearing mice

THP-1-bearing mice were either left untreated or treated i.t with UV-inactivated reovirus followed with i.p injection of BV-6, 6 hrs post-reovirus treatment (treatments were administered Tuesday and Friday for 2 weeks), 6 hrs was selected based on previous literature using OV in combination with LCL161. Figure 5-9 illustrates the treatment schedule and Table 5-2 provides details for each treatment group. Figure 5-10 shows the tumour growth for each animal within each group. Unfortunately, tumour size varied significantly at the start of the treatment regimen, with no tumours being detected in 11 mice; moreover, tumour growth varied between animals making it difficult to accurately assess the impact of treatment. Therefore, tumour growth rate was calculated to more accurately compare tumour growth between each treatment group. Tumour growth from start of treatment to 3 days after treatment administration is shown in Figure 5-11A. Unfortunately, no statistical significant decrease in tumour growth was observed in any of the treatment groups when compared to the vehicle control. Moreover, looking to the survival rate of the mice (Figure 5-11B), no statistically significant differences were observed. However, mice treated with the combination treatment survived up to day 73, compared to day 67 in vehicle-treated mice; mice treated with UV-inactivated reovirus and BV-6 as monotherapy were culled by day 71 (Figure 5-11B).

Unfortunately, using xenograft immunodeficient *in vivo* models, we were unable to confirm the *in vivo* efficacy of OV therapy alone, or in combination with Smac or BH3 mimetics.

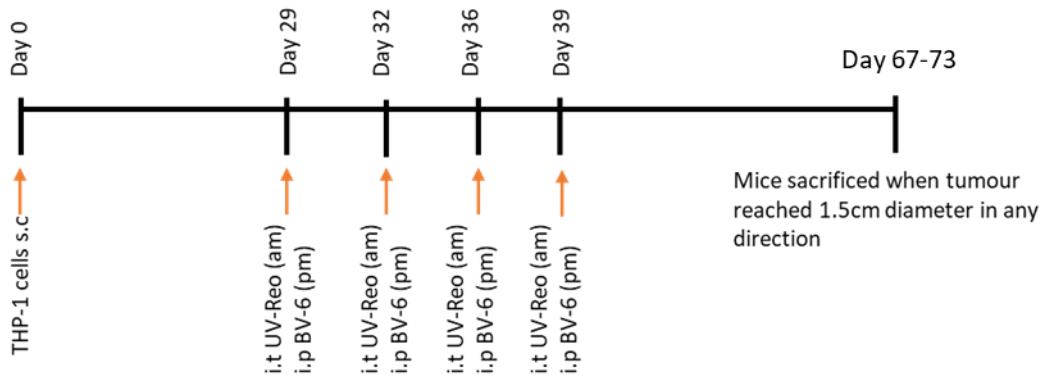

Figure 5-9: Schematic diagram demonstrating the *in vivo* treatment schedule. 32 female CB 17 SCID mice were injected with $10x10^6$ THP-1 cells s.c. on day 0. From day 29 post tumour seeding, UV-inactivated reovirus (or PBS vehicle) treatment ($5x10^7$ pfu) was injected i.t and BV-6 (5mg/kg) was delivered i.p. BV-6 was delivered 6 hrs post-treatment with UV-inactivated reovirus. Four injections were administered before mice were euthanized when the tumour reached 1.5 cm in any direction.

Table 5-2: THP-1 cells-bearing mice treatments for each group

Group	No of mice	Treatment
1	4	50 µl i.t PBS (morning) and 100 µl i.p vehicle control (afternoon) (Tuesday & Friday)
2	6	50 µl i.t UV-Reovirus ($5x10^7$ pfu in PBS) (Tuesday & Friday)
3	5	100 µl i.p BV-6 (5mg/kg) diluted in NaCl (Tuesday & Friday)
4	6	50 µl i.t UV-reovirus (morning) and 100 µl i.p BV-6 (afternoon) (Tuesday & Friday)

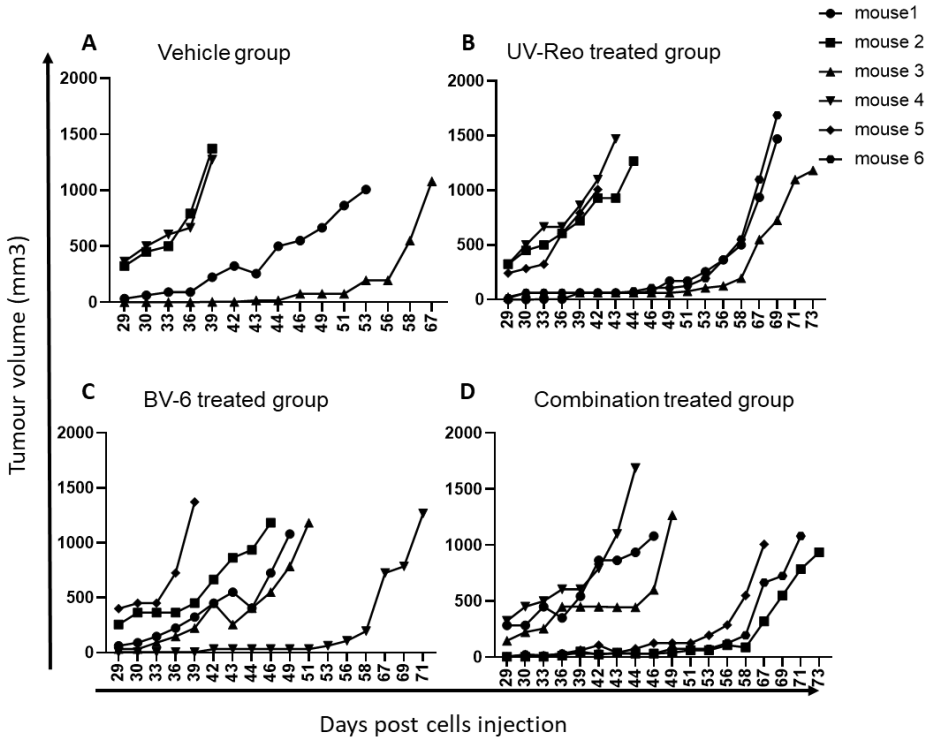

Figure 5-10: THP-1-bearing mice tumour growth after treatment with UV-inactivated reovirus in combination with BV-6. On day 0, 32 female SCID mice were injected s.c with $10x10^6$ THP-1 cells (100µl in PBS). Treatment started on day 29 post tumour seeding and mice were treated twice a week for 2 weeks with **A**: 50 µl i.t PBS and 100 µl i.p vehicle control (group 1), **B**: 50 µl $5x10^7$ pfu i.t UV-inactivated Reovirus in PBS (group 2), **C**: 100 µl i.p 5 mg/kg BV-6 (group 3), and **D**: 50 µl i.t UV-inactivated Reovirus (delivered 6 hrs prior to BV-6 treatment) and 100 µl i.p BV-6 (group 4). Tumour growth was monitored using callipers and tumour volume was calculated. Mice were euthanized when the tumour reached 1.5 cm in any direction.

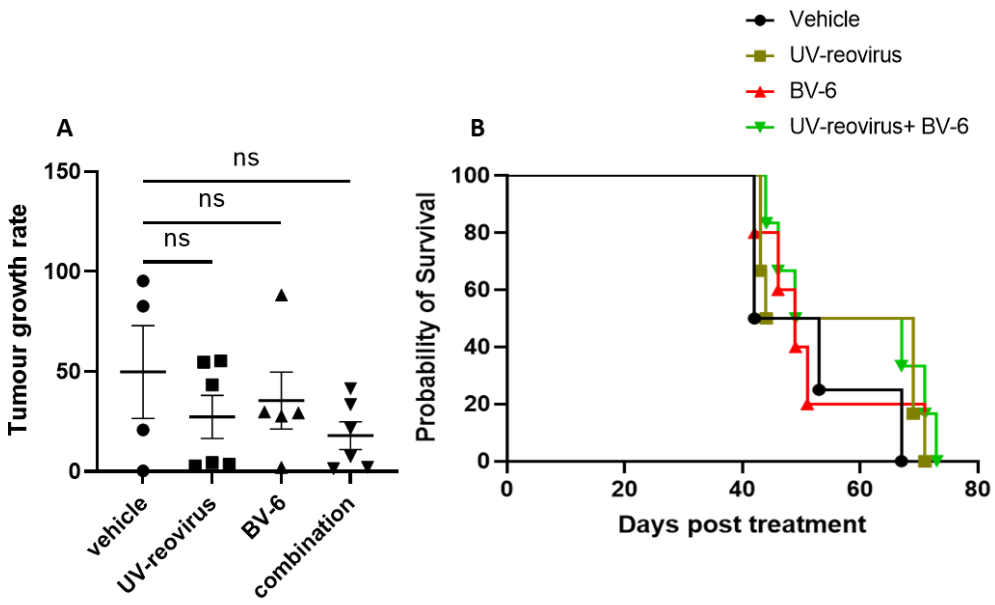

Figure 5-11: Tumour growth rate and survival of THP-1-bearing mice after treatment with UV-inactivated reovirus alone or in combination with BV-6. 32 female CB 17 SCID mice were injected s.c with $10x10^6$ THP-1 cells (in 100 µl PBS) in each mouse, and treatment started 29 days after THP-1 cells were implanted and was delivered twice a week for 2 weeks. Mice were treated with 50 µl i.t PBS and 100 µl i.p vehicle control (group1), 50 µl i.t 5x107 pfu i.t UV-inactivated Reovirus in PBS (group 2), 100 µl i.p 5 mg/kg BV-6 (group 3), and 50 µl i.t UV-inactivated reovirus (delivered 6 hrs prior to BV-6 treatment) and 100 µl i.p BV-6 (group 4). **A**: The tumour growth rate was calculated by subtracting the tumour volume at the start of treatment from the tumour volume measured 3 days after treatment had ended (divided by the number of days). **B**: Survival of THP-1-bearing mice is shown using a Kaplan Meier curve. Statistical significance was performed using an unpaired one-way ANOVA and comparisons with vehicle controls are shown.

5.4 Discussion

This chapter has examined the possible use of a syngeneic C1498 AML mouse model to test the efficacy of reovirus-drug combinations and evaluated the efficacy of UV-inactivate reovirus treatment in combination with BV-6 or ABT-199 in THP-1 or KG-1-bearing immunodeficient mice.

As demonstrated in chapters 3 and 4, the efficacy of reovirus treatment combined with Smac or BH3 mimetics was dependent on cytokine-mediated killing. Disappointingly, reovirus treatment induced low levels of cytokine production from splenocytes *in vitro*, and when combined with Smac or BH3 mimetics, no enhancement of C1498 cell death was observed (Figure 5-4), hence the C1498 model of AML was deemed not suitable to examine the combination treatment.

Interestingly, it has previously been reported that C1498 cells are sensitive to reovirus treatment *in vitro* [407], where C1498 cells were treated with 1 pfu/cell reovirus for 24, 48 and 72 hrs, and cell death was evaluated using Trypan blue. Interestingly, ~35% and 85% cells were infected with reovirus after 48 and 72 hrs treatment, respectively. In addition, these data also demonstrated that human umbilical cord mesenchymal stem cells (hUC-MSCs) could be loaded with reovirus (MSC-reovirus), to combat anti-reovirus neutralizing antibodies, and that this strategy could effectively trigger an anti-tumour immune responses and inhibit tumour growth in C1498-bearing immunocompetent mice [407]. Unexpectedly, in this project, reovirus treatment (1 pfu/cell) did not induce C1498 cell death after 48 or 72 hrs using LIVE/DEAD (data not shown). Ultimately, this project did not use C1498 model due to insensitivity to cytokine-mediated killing, irrespective of apoptotic modulation. However, as Wang *et al*. demonstrated that reovirus was able to activate an anti-tumour immune response when

administered *in vivo*, this suggests that reovirus may have been able to activate immunity and inflammation in C57BL6 mice. Thus, it is possible that an *in vivo* assessment of reovirus in combination with Smac/BH3 mimetics may have yielded some promising results if this model was explored further.

As demonstrated in Figure 4-6, THP-1 and KG-1 induced pro-inflammatory cytokines following UV-inactivated reovirus treatment; moreover, cell death was potentiated by Smac/BH3 mimetics. Therefore, we sought to test the efficacy of this combination using xenograft mouse models. Tumour growth of THP-1 was varied between mice, and in some cases tumours did not grow. The variation observed in this study, compared to previously published results could be due to the differences in genetic background of the mice [415]. Rahman *et al*. reported that subcutaneous injection of $5x10^6$ THP-1 cells were used to generate tumours in NOD-SCID mice (6-8 weeks old), where tumour growth was detected after 6 days post-seeding [416]. A previous study by Mashima *et al*. also demonstrated that THP-1 cells ($5x10^6$) administered intravenously into severe immunodeficient NOG mice spread throughout the body within 21 days [417]. Moreover, another study by Wang *et al*. reported that only $1x10^6$ THP-1 cells were required for tumour growth (3-4 weeks) in NOD-SCID mice, when injected intravenously [418].

The fact that THP-1 tumours did not grow uniformly in CB17 SCID mice, suggests that perhaps another AML *in vivo* model would have been more suitable to test the efficacy of the combination treatment. Interestingly, a recent study by Wang *et al*. used male BALB/c nude mice (3-4 weeks old), where THP-1 cells ($1x10^7$) were injected s.c or i.v, and the mice were treated with i.v adenovirus (zA4) when tumours reached 100-200 mm^3, or THP-1 cells constituted between 15-20% of

the murine PBMC. In this model, zA4 treatment suppressed leukaemia progression and significantly reduced tumour size compared to control animals. However, it was also observed that the virus accumulated in the liver and spleen [280]. Another study also used male BALB/c nude mice (6 weeks old), here, U937 AML cells were injected s.c and tumours were treated with a combination of measles and mumps virus when tumours reached 5-10 mm. I.t, administration of OV slowed tumour development and prolonged mice survival compared to single agent-virus treatment or untreated animals [275, 284].

Zhang *et.al* utilised a xenograft model of lymphoma by s.c injection of ~$5x10^6$ cells into immunodeficient NSG mice. Here, ABT-199 treatment administered i.p (1mg/kg) suppressed tumour growth. However, when combined with SDS-1-021, a synthetic rocaglate, tumour growth was abolished with only small residual disease observed [413]. A recent study published in 2022, by Li *et al*., reported that ABT-199 (100mg/kg; delivered intragastric) had no significant effect on the survival of immunodeficient NSG mice bearing MOLM-13 AML tumours. However, the combination of all-trans retinoic acid (ATRA) with ABT-199 prolonged animal survival and reduced tumour burden [419]. Moreover, when OCL-AML3 cells ($5x10^6$) were injected s.c into NOD-SCID mice, ABT-199 (administered by oral gavage; 50mg/kg/day), had little effect on tumour burden. However, the combination of ABT-199 with homoharringtonine (HTT) inhibited tumour growth and progression [369]

Unfortunately, the *in vivo* work presented herein did not confirm the efficacy of the OV-drug combination approach. However, Beug *et al*. reported the efficacy of similar approach using EMT6 cells injected into the mammary fat pad of immunocompetent mice (BALB/c; 6 weeks old). When tumours reached

~100mm^3, mice were treated with 50mg/kg LCL161 orally and i.v injection of VSVΔM51. LCL161 as a single agent decreased tumour growth rate and modestly prolonged survival, whereas VSVΔM51 treatment did not decrease tumour growth. By contrast, the combination of VSVΔM51 and LCL161 suppressed tumour growth and cured ~40% of EMT6-bearing mice, and this death was type I IFN and TNF-α-dependent [320]. Moreover, another study by Sarkar *et al.* demonstrated that the combination of an adenovirus, AD.tCCN1-CTV-m7 (express mda-7/IL-24 cytokine; administered by i.v) with the MCL-1 inhibitor, BI-97D6, (3mg/kg; delivered by i.p) suppressed tumour growth and enhanced apoptosis in immunocompetent Hi-myc prostate cancer transgenic mice, this was dependent on mda-7/IL-24-mediated apoptosis, which was enhanced by BI-97D6 [326].

Kim *et al*. also demonstrated that the combination of VSVΔM51 (administered by i.v) followed with LCL161 (50mg/kg delivered by oral gavage) after 6 hrs induced tumour regression in EMT6-bearing immunocompetent mice (BALB/c), which was dependent on $CD8^+$ T cells [322]. Moreover, recombinant poxviral vaccinia (rV) treatment prior to GX15-070 enhanced the activation of CD8 T-cells, reduced the activity of T_{regs}, and significantly reduced pulmonary tumour nodules in LL2-bearing mice (C57BL/6) [325]. Furthermore, to establish an AML model, Shen *et al*. implanted C1498.GFP cells by i.v injection into C57BL/6 mice. After 14 days, mice were treated with VSV-mIFNβ-NIS (delivered i.v) or anti-PD-L1 (delivered i.p) or a combination of these agents. Virus treatment or anti-PD-L1 treatment significantly prolonged the survival of mice compared to isotype controls, and the combination of these agents was superior to either of the treatments alone. Importantly, depletion of CD8 and NK cells resulted in loss of the anti-tumor response and animal survival was not significant when compared to the control.

Depletion of CD4 T-cells did not significantly affect the combination therapy in this model [283]. Collectively, these results suggest that alternative *in vivo* AML model would be useful to further evaluate the efficacy of reovirus treatment in combination with Smac and/or BH3 mimetics. Thus, future work should aim to further optimise xenograft mouse models, test the efficacy of this combination approach in C1498 syngeneic animal, or identify alternative *in vivo* models that could be suitable. Using patient-derived xenograft in immunodeficient mice could be a possibility, and would provide a more accurate representation of human disease.

Chapter 6 Conclusion and future work

6.1 Conclusions

The results presented within this study demonstrated that molecularly distinct OVs (reovirus, MG1, CVA21 and HSV-1) induced similar levels of pro-inflammatory cytokine from HD-PBMC. Moreover OV-CM collected after OV treatment induced a significant cytotoxic effect towards AML cell lines. Perhaps as expected given the heterogeneity of AML, different AML cell lines had variable degrees of sensitivity to Smac and BH3 mimetics treatment. Therefore, different concentrations were selected for each cell line, as illustrated in Table 3-2, to reduce drug-associated toxicities. Importantly, isolated monocytes from HD-PBMC were resistant to Smac/BH3 mimetics treatment, suggesting that this approach may be well-tolerated in patients.

The combination of OV-treated PBMC-CM with Smac mimetics (LCL161 and BV-6) induced significant THP-1 and HL-60 cell death. While combination of OV-treated PBMC-CM with the BH3 mimetic (ABT-199) induced significant KG-1 cell death. Importantly, data presented suggests a role for both IFN-α and TNF-α, which was confirmed using human recombinant cytokines.

Importantly, to aid the development of a potentially safer and well-tolerated therapeutic strategy, this work has also shown that UV-inactivated OV can induce pro-inflammatory cytokines from both HD-PBMC and patient-derived primary AML samples. Pivotally, PBMC-CM collected after treatment with UV-inactivated reovirus induced significant THP-1 cell death in combination with Smac mimetic (LCL161), and levels were comparable to those observed when PBMC-CM was collected after treatment with live, replicant-competent, reovirus.

Given the heterogenicity of the disease, primary AML patient samples secreted various levels of pro-inflammatory cytokine after reovirus treatment. Moreover, AML patient samples displayed a varied response against the combination therapy approach, with 5 out of 10 patients responding to either of Smac or BH3 mimetics when used in combination with reovirus-treated -PBMC-CM.

Smac/BH3 mimetics did not appear to enhance reovirus-direct oncolysis in AML cell lines. However, both live and UV-inactivated reovirus resulted in pro-inflammatory cytokine secretion from AML cell lines. Moreover, AML-derived cytokine killing could be potentiated by apoptotic modulation, for example, both live and UV-inactivated reovirus could be used to enhance THP-1 cell death in combination with the Smac mimetic (BV-6).

Importantly, both live and UV-inactivated reovirus could be used to activate NK cells within PBMC isolated from healthy donors and AML patient samples. In addition, reovirus-activated NK cells induced significant cell death in AML target cells (THP-1). Unfortunately, Smac mimetics did not potentiate NK cell-mediated killing; however, they did not impede NK cell killing, suggesting that alternative OV effector mechanism would remain, despite the presence of drug.

Unfortunately, reovirus-treated splenocytes-CM did not induce the death of C1498 cells as a single treatment or in combination with Smac/BH3 mimetics. Therefore, THP-1- and KG-1-bearing CB17 SCID mice were used. Disappointingly, the combination of UV-inactivated reovirus with Smac/BH3 mimetics did not validate the efficacy of this combination approach *in vivo*.

6.2 Future work

The work presented in this project has highlighted the potential for OV to be used in combination with apoptotic modulators as a treatment option for AML. However, to build on these promising findings it would be important to (i) confirm the secretion of pro-inflammatory cytokine following OV treatment in a wider range of primary AML samples, and (ii) demonstrate the possibility of bystander cytokine killing in additional primary samples, alone or in combination with Smac or BH3 mimetics. Ultimately, this would aid the development of a more personalised treatment approach that is stratified towards patients more likely to respond. Additionally, the expression of JAM-A on AML cells and immune cells should be also investigated after treatment with Smac/BH3 mimetics and *in vitro* testing with AML patient samples should be expanded to explore the potential of UV-inactivated reovirus.

The data presented suggest a role for both IFN-α and TNF-α in mediating AML cell death, confirmed using human recombinant cytokines; however, this warrants further exploration and validation. This could be done using cytokine specific blocking antibodies or using siRNA knockdown for IFN-α and TNF-α receptor.

Interestingly, the work presented suggested that apoptotic modulators do not abrogate NK cell killing, however, the effect of these agents on alternative OV effector mechanisms should also be explored. For example, what is the effect of these drugs on reovirus (OV) activation DC and/or the ability of OV to prime AML specific T cells.

In this study, reovirus-treated PBMC-CM combined with Smac/BH3 mimetics induced AML cell death *in vitro*. Unfortunately, this was not observed using AML xenograft CB17 SCID mice models. Therefore, alternative experiments to identify

the efficacy of this combination approach *in vivo* are required, for example, we consider using alternative immunocompetent cancer models, more reproducible xenograft models (e.g., grown in NSG mice) or develop humanised mouse models of AML.

Overall, this study demonstrates a comprehensive evaluation of the efficacy of OV combined with Smac/BH3 mimetic treatment for AML. This establishes the foundation for further study, with the goal of finding novel therapeutic options for AML patients.

Chapter 7 References

1. Döhner, H., D.J. Weisdorf, and C.D. Bloomfield, *Acute Myeloid Leukemia.* N Engl J Med, 2015. **373**(12): p. 1136-52.
2. Döhner, H., et al., *Diagnosis and management of acute myeloid leukemia in adults: recommendations from an international expert panel, on behalf of the European LeukemiaNet.* Blood, 2010. **115**(3): p. 453-74.
3. Yamamoto, J.F. and M.T. Goodman, *Patterns of leukemia incidence in the United States by subtype and demographic characteristics, 1997-2002.* Cancer Causes Control, 2008. **19**(4): p. 379-90.
4. CancerResearchUK, *Acute myeloid leukaemia (AML) statistics. Available from: https://www.cancerresearchuk.org/health-professional/cancer-statistics/statistics-by-cancer-type/leukaemia-aml#heading-One*. 2022.
5. Thein, M.S., et al., *Outcome of older patients with acute myeloid leukemia: an analysis of SEER data over 3 decades.* Cancer, 2013. **119**(15): p. 2720-7.
6. Yanada, M. and T. Naoe, *Acute myeloid leukemia in older adults.* Int J Hematol, 2012. **96**(2): p. 186-93.
7. Alter, B.P., et al., *Malignancies and survival patterns in the National Cancer Institute inherited bone marrow failure syndromes cohort study.* Br J Haematol, 2010. **150**(2): p. 179-88.
8. Loomis, D., et al., *Identifying occupational carcinogens: an update from the IARC Monographs.* Occup Environ Med, 2018. **75**(8): p. 593-603.
9. Shallis, R.M., et al., *Epidemiology of acute myeloid leukemia: Recent progress and enduring challenges.* Blood Rev, 2019. **36**: p. 70-87.
10. Granfeldt Østgård, L.S., et al., *Epidemiology and Clinical Significance of Secondary and Therapy-Related Acute Myeloid Leukemia: A National Population-Based Cohort Study.* J Clin Oncol, 2015. **33**(31): p. 3641-9.
11. Bennett, J.M., et al., *Proposals for the classification of the acute leukaemias. French-American-British (FAB) co-operative group.* Br J Haematol, 1976. **33**(4): p. 451-8.
12. *Acute Myeloid Leukemia (AML) Subtypes*. 2022 10/2022 [cited 2023 02/03]; Available from: https://www.healthline.com/health/leukemia/aml-subtypes.
13. Arber, D.A., et al., *The 2016 revision to the World Health Organization classification of myeloid neoplasms and acute leukemia.* Blood, 2016. **127**(20): p. 2391-405.
14. Sabattini, E., et al., *WHO classification of tumours of haematopoietic and lymphoid tissues in 2008: an overview.* Pathologica, 2010. **102**(3): p. 83-7.
15. Moarii, M. and E. Papaemmanuil, *Classification and risk assessment in AML: integrating cytogenetics and molecular profiling.* Hematology Am Soc Hematol Educ Program, 2017. **2017**(1): p. 37-44.
16. Hanahan, D., *Hallmarks of Cancer: New Dimensions.* Cancer Discov, 2022. **12**(1): p. 31-46.
17. de Oliveira Lisboa, M., et al., *Chromosomal Instability in Acute Myeloid Leukemia.* Cancers (Basel), 2021. **13**(11).
18. Soyfer, E.M. and A.G. Fleischman, *Inflammation in Myeloid Malignancies: From Bench to Bedside.* J Immunother Precis Oncol, 2021. **4**(3): p. 160-167.

19. Korn, C. and S. Méndez-Ferrer, *Myeloid malignancies and the microenvironment.* Blood, 2017. **129**(7): p. 811-822.
20. Tettamanti, S., et al., *Catch me if you can: how AML and its niche escape immunotherapy.* Leukemia, 2022. **36**(1): p. 13-22.
21. Garrido, F., et al., *Natural history of HLA expression during tumour development.* Immunol Today, 1993. **14**(10): p. 491-9.
22. Bai, R., et al., *Mechanisms of Cancer Resistance to Immunotherapy.* Front Oncol, 2020. **10**: p. 1290.
23. Mehta, R.S., et al., *NK cell therapy for hematologic malignancies.* Int J Hematol, 2018. **107**(3): p. 262-270.
24. Kochan, G., et al., *Role of non-classical MHC class I molecules in cancer immunosuppression.* Oncoimmunology, 2013. **2**(11): p. e26491.
25. Sordo-Bahamonde, C., et al., *Mechanisms of Apoptosis Resistance to NK Cell-Mediated Cytotoxicity in Cancer.* Int J Mol Sci, 2020. **21**(10).
26. Bates, D.J. and L.D. Lewis, *Manipulating the apoptotic pathway: potential therapeutics for cancer patients.* Br J Clin Pharmacol, 2013. **76**(3): p. 381-95.
27. Gupta, P., et al., *Fas ligand expression in the bone marrow in myelodysplastic syndromes correlates with FAB subtype and anemia, and predicts survival.* Leukemia, 1999. **13**(1): p. 44-53.
28. Strand, S., et al., *Lymphocyte apoptosis induced by CD95 (APO-1/Fas) ligand-expressing tumor cells--a mechanism of immune evasion?* Nat Med, 1996. **2**(12): p. 1361-6.
29. Owen-Schaub, L.B., et al., *Fas and Fas ligand interactions suppress melanoma lung metastasis.* J Exp Med, 1998. **188**(9): p. 1717-23.
30. Koyama, S., N. Koike, and S. Adachi, *Expression of TNF-related apoptosis-inducing ligand (TRAIL) and its receptors in gastric carcinoma and tumor-infiltrating lymphocytes: a possible mechanism of immune evasion of the tumor.* J Cancer Res Clin Oncol, 2002. **128**(2): p. 73-9.
31. Chamuleau, M.E., et al., *High TRAIL-R3 expression on leukemic blasts is associated with poor outcome and induces apoptosis-resistance which can be overcome by targeting TRAIL-R2.* Leuk Res, 2011. **35**(6): p. 741-9.
32. Riccioni, R., et al., *TRAIL decoy receptors mediate resistance of acute myeloid leukemia cells to TRAIL.* Haematologica, 2005. **90**(5): p. 612-24.
33. Bodmer, J.L., et al., *TRAIL receptor-2 signals apoptosis through FADD and caspase-8.* Nat Cell Biol, 2000. **2**(4): p. 241-3.
34. Zhou, J.-d., et al., *BCL2 overexpression: clinical implication and biological insights in acute myeloid leukemia.* Diagnostic Pathology, 2019. **14**(1): p. 68.
35. de Charette, M. and R. Houot, *Hide or defend, the two strategies of lymphoma immune evasion: potential implications for immunotherapy.* Haematologica, 2018. **103**(8): p. 1256-1268.
36. Ekert, P.G., et al., *DIABLO promotes apoptosis by removing MIHA/XIAP from processed caspase 9.* J Cell Biol, 2001. **152**(3): p. 483-90.
37. Boddu, P., et al., *SMAC mimetics as potential cancer therapeutics in myeloid malignancies.* 2019. **185**(2): p. 219-231.
38. Lynch, M.A., et al., *Responsiveness to transforming growth factor-beta (TGF-beta)-mediated growth inhibition is a function of membrane-bound TGF-beta type II receptor in human breast cancer cells.* Gene Expr, 2001. **9**(4-5): p. 157-71.

39. Seoane, J., *Escaping from the TGFbeta anti-proliferative control.* Carcinogenesis, 2006. **27**(11): p. 2148-56.
40. Chen, W., et al., *Conversion of peripheral CD4+CD25- naive T cells to CD4+CD25+ regulatory T cells by TGF-beta induction of transcription factor Foxp3.* J Exp Med, 2003. **198**(12): p. 1875-86.
41. Jewett, A. and H.C. Tseng, *Tumor induced inactivation of natural killer cell cytotoxic function; implication in growth, expansion and differentiation of cancer stem cells.* J Cancer, 2011. **2**: p. 443-57.
42. Kaliński, P., et al., *IL-12-deficient dendritic cells, generated in the presence of prostaglandin E2, promote type 2 cytokine production in maturing human naive T helper cells.* J Immunol, 1997. **159**(1): p. 28-35.
43. Gabrilovich, D., et al., *Vascular endothelial growth factor inhibits the development of dendritic cells and dramatically affects the differentiation of multiple hematopoietic lineages in vivo.* Blood, 1998. **92**(11): p. 4150-66.
44. Kim, R., M. Emi, and K. Tanabe, *Cancer immunosuppression and autoimmune disease: beyond immunosuppressive networks for tumour immunity.* Immunology, 2006. **119**(2): p. 254-64.
45. Berendt, M.J. and R.J. North, *T-cell-mediated suppression of anti-tumor immunity. An explanation for progressive growth of an immunogenic tumor.* J Exp Med, 1980. **151**(1): p. 69-80.
46. Kobayashi, N., et al., *FOXP3+ regulatory T cells affect the development and progression of hepatocarcinogenesis.* Clin Cancer Res, 2007. **13**(3): p. 902-11.
47. Curiel, T.J., et al., *Specific recruitment of regulatory T cells in ovarian carcinoma fosters immune privilege and predicts reduced survival.* Nat Med, 2004. **10**(9): p. 942-9.
48. Bates, G.J., et al., *Quantification of regulatory T cells enables the identification of high-risk breast cancer patients and those at risk of late relapse.* J Clin Oncol, 2006. **24**(34): p. 5373-80.
49. Meireson, A., M. Devos, and L. Brochez, *IDO Expression in Cancer: Different Compartment, Different Functionality?* Front Immunol, 2020. **11**: p. 531491.
50. Grossman, W.J., et al., *Human T regulatory cells can use the perforin pathway to cause autologous target cell death.* Immunity, 2004. **21**(4): p. 589-601.
51. Mougiakakos, D., et al., *Regulatory T cells in cancer.* Adv Cancer Res, 2010. **107**: p. 57-117.
52. Kryczek, I., et al., *Cutting edge: induction of B7-H4 on APCs through IL-10: novel suppressive mode for regulatory T cells.* J Immunol, 2006. **177**(1): p. 40-4.
53. Vinogradov, S., G. Warren, and X. Wei, *Macrophages associated with tumors as potential targets and therapeutic intermediates.* Nanomedicine (Lond), 2014. **9**(5): p. 695-707.
54. Noy, R. and J.W. Pollard, *Tumor-associated macrophages: from mechanisms to therapy.* Immunity, 2014. **41**(1): p. 49-61.
55. Cencini, E., et al., *The Role of Tumor-Associated Macrophages in Hematologic Malignancies.* 2021. **13**(14): p. 3597.
56. Malek, E., et al., *Myeloid-derived suppressor cells: The green light for myeloma immune escape.* Blood Rev, 2016. **30**(5): p. 341-8.
57. Bronte, V., et al., *L-arginine metabolism in myeloid cells controls T-lymphocyte functions.* Trends Immunol, 2003. **24**(6): p. 302-6.

58. Ochoa, J.B., et al., *Effects of L-arginine on the proliferation of T lymphocyte subpopulations.* JPEN J Parenter Enteral Nutr, 2001. **25**(1): p. 23-9.
59. Olivares-Hernández, A., et al., *Resistance to Immune Checkpoint Inhibitors Secondary to Myeloid-Derived Suppressor Cells: A New Therapeutic Targeting of Haematological Malignancies.* J Clin Med, 2021. **10**(9).
60. Rashidi, A. and G.L. Uy, *Targeting the microenvironment in acute myeloid leukemia.* Curr Hematol Malig Rep, 2015. **10**(2): p. 126-31.
61. Wilson, A. and A. Trumpp, *Bone-marrow haematopoietic-stem-cell niches.* Nat Rev Immunol, 2006. **6**(2): p. 93-106.
62. Weisberg, E., et al., *Stromal-mediated protection of tyrosine kinase inhibitor-treated BCR-ABL-expressing leukemia cells.* Mol Cancer Ther, 2008. **7**(5): p. 1121-9.
63. Zarrinkar, P.P., et al., *AC220 is a uniquely potent and selective inhibitor of FLT3 for the treatment of acute myeloid leukemia (AML).* Blood, 2009. **114**(14): p. 2984-92.
64. Sison, E.A. and P. Brown, *The bone marrow microenvironment and leukemia: biology and therapeutic targeting.* Expert Rev Hematol, 2011. **4**(3): p. 271-83.
65. Ladikou, E.E., et al., *Acute Myeloid Leukaemia in Its Niche: the Bone Marrow Microenvironment in Acute Myeloid Leukaemia.* Curr Oncol Rep, 2020. **22**(3): p. 27.
66. Walter, R.B., et al., *High expression of the very late antigen-4 integrin independently predicts reduced risk of relapse and improved outcome in pediatric acute myeloid leukemia: a report from the children's oncology group.* J Clin Oncol, 2010. **28**(17): p. 2831-8.
67. Yang, X., A. Sexauer, and M. Levis, *Bone marrow stroma-mediated resistance to FLT3 inhibitors in FLT3-ITD AML is mediated by persistent activation of extracellular regulated kinase.* Br J Haematol, 2014. **164**(1): p. 61-72.
68. Estey, E.H., *Acute myeloid leukemia: 2021 update on risk-stratification and management.* Am J Hematol, 2020. **95**(11): p. 1368-1398.
69. Papaemmanuil, E., et al., *Genomic Classification and Prognosis in Acute Myeloid Leukemia.* N Engl J Med, 2016. **374**(23): p. 2209-2221.
70. Ley, T.J., et al., *Genomic and epigenomic landscapes of adult de novo acute myeloid leukemia.* N Engl J Med, 2013. **368**(22): p. 2059-74.
71. Patel, J.P., et al., *Prognostic relevance of integrated genetic profiling in acute myeloid leukemia.* N Engl J Med, 2012. **366**(12): p. 1079-89.
72. Lagunas-Rangel, F.A., et al., *Acute Myeloid Leukemia-Genetic Alterations and Their Clinical Prognosis.* Int J Hematol Oncol Stem Cell Res, 2017. **11**(4): p. 328-339.
73. De Kouchkovsky, I. and M. Abdul-Hay, *'Acute myeloid leukemia: a comprehensive review and 2016 update'.* Blood Cancer Journal, 2016. **6**(7): p. e441-e441.
74. Coombs, C.C., M. Tavakkoli, and M.S. Tallman, *Acute promyelocytic leukemia: where did we start, where are we now, and the future.* Blood Cancer J, 2015. **5**(4): p. e304.
75. Döhner, H., et al., *Diagnosis and management of AML in adults: 2017 ELN recommendations from an international expert panel.* Blood, 2017. **129**(4): p. 424-447.

76. Burnett, A., M. Wetzler, and B. Löwenberg, *Therapeutic advances in acute myeloid leukemia.* J Clin Oncol, 2011. **29**(5): p. 487-94.
77. Moiseev, I., et al., *Graft-versus-Host Disease Prophylaxis with Post-Transplantation Bendamustine in Patients with Refractory Acute Leukemia: A Dose-Ranging Study.* Transplant Cell Ther, 2021. **27**(7): p. 601.e1-601.e7.
78. Schlenk, R.F., *Post-remission therapy for acute myeloid leukemia.* Haematologica, 2014. **99**(11): p. 1663-70.
79. Schlenk, R.F., et al., *Relapsed/refractory acute myeloid leukemia: any progress?* Curr Opin Oncol, 2017. **29**(6): p. 467-473.
80. Schlenk, R.F., S. Jaramillo, and C. Müller-Tidow, *Improving consolidation therapy in acute myeloid leukemia - a tough nut to crack.* Haematologica, 2018. **103**(10): p. 1579-1581.
81. Daver, N., et al., *New directions for emerging therapies in acute myeloid leukemia: the next chapter.* Blood Cancer J, 2020. **10**(10): p. 107.
82. Palmieri, R., et al., *Therapeutic Choice in Older Patients with Acute Myeloid Leukemia: A Matter of Fitness.* Cancers (Basel), 2020. **12**(1).
83. Daver, N., et al., *Targeting FLT3 mutations in AML: review of current knowledge and evidence.* Leukemia, 2019. **33**(2): p. 299-312.
84. Stone, R.M., et al., *Midostaurin plus Chemotherapy for Acute Myeloid Leukemia with a FLT3 Mutation.* N Engl J Med, 2017. **377**(5): p. 454-464.
85. Montalban-Bravo, G. and C.D. DiNardo, *The role of IDH mutations in acute myeloid leukemia.* Future Oncol, 2018. **14**(10): p. 979-993.
86. Liu, X. and Y. Gong, *Isocitrate dehydrogenase inhibitors in acute myeloid leukemia.* Biomark Res, 2019. **7**: p. 22.
87. Stein, E.M., et al., *Molecular remission and response patterns in patients with mutant-IDH2 acute myeloid leukemia treated with enasidenib.* Blood, 2019. **133**(7): p. 676-687.
88. Konopleva, M. and A. Letai, *BCL-2 inhibition in AML: an unexpected bonus?* Blood, 2018. **132**(10): p. 1007-1012.
89. Andreeff, M., et al., *Expression of Bcl-2-related genes in normal and AML progenitors: changes induced by chemotherapy and retinoic acid.* Leukemia, 1999. **13**(11): p. 1881-92.
90. Konopleva, M., et al., *Efficacy and Biological Correlates of Response in a Phase II Study of Venetoclax Monotherapy in Patients with Acute Myelogenous Leukemia.* Cancer Discov, 2016. **6**(10): p. 1106-1117.
91. DiNardo, C.D., et al., *Venetoclax combined with decitabine or azacitidine in treatment-naive, elderly patients with acute myeloid leukemia.* Blood, 2019. **133**(1): p. 7-17.
92. Belardelli, F., et al., *Interferon-alpha in tumor immunity and immunotherapy.* Cytokine Growth Factor Rev, 2002. **13**(2): p. 119-34.
93. Anguille, S., et al., *Interferon-α in acute myeloid leukemia: an old drug revisited.* Leukemia, 2011. **25**(5): p. 739-48.
94. Diamond, M.S., et al., *Type I interferon is selectively required by dendritic cells for immune rejection of tumors.* J Exp Med, 2011. **208**(10): p. 1989-2003.
95. Boddu, P., et al., *The emerging role of immune checkpoint based approaches in AML and MDS.* Leuk Lymphoma, 2018. **59**(4): p. 790-802.
96. Ansell, S.M., et al., *PD-1 blockade with nivolumab in relapsed or refractory Hodgkin's lymphoma.* N Engl J Med, 2015. **372**(4): p. 311-9.

97. Kadia, T.M., et al., *Nivolumab (Nivo) maintenance (maint) in high-risk (HR) acute myeloid leukemia (AML) patients.* 2018. **36**(15_suppl): p. 7014-7014.
98. Albring, J.C., et al., *PD-1 checkpoint blockade in patients with relapsed AML after allogeneic stem cell transplantation.* Bone Marrow Transplantation, 2017. **52**(2): p. 317-320.
99. Giannopoulos, K., *Targeting Immune Signaling Checkpoints in Acute Myeloid Leukemia.* J Clin Med, 2019. **8**(2).
100. Chao, M.P., et al., *Therapeutic Targeting of the Macrophage Immune Checkpoint CD47 in Myeloid Malignancies.* Front Oncol, 2019. **9**: p. 1380.
101. Hanahan, D. and R.A. Weinberg, *The hallmarks of cancer.* Cell, 2000. **100**(1): p. 57-70.
102. Vogelstein, B. and K.W. Kinzler, *Cancer genes and the pathways they control.* Nat Med, 2004. **10**(8): p. 789-99.
103. Reed, J.C., *Apoptosis-targeted therapies for cancer.* Cancer Cell, 2003. **3**(1): p. 17-22.
104. Opferman, J.T. and S.J. Korsmeyer, *Apoptosis in the development and maintenance of the immune system.* Nat Immunol, 2003. **4**(5): p. 410-5.
105. Evan, G.I. and K.H. Vousden, *Proliferation, cell cycle and apoptosis in cancer.* Nature, 2001. **411**(6835): p. 342-8.
106. Ghavami, S., et al., *Apoptosis and cancer: mutations within caspase genes.* J Med Genet, 2009. **46**(8): p. 497-510.
107. Jäger, U., et al., *Follicular lymphomas' BCL-2/IgH junctions contain templated nucleotide insertions: novel insights into the mechanism of t(14;18) translocation.* Blood, 2000. **95**(11): p. 3520-9.
108. Mannhold, R., S. Fulda, and E. Carosati, *IAP antagonists: promising candidates for cancer therapy.* Drug Discov Today, 2010. **15**(5-6): p. 210-9.
109. Nikkhoo, A., et al., *Smac mimetics as novel promising modulators of apoptosis in the treatment of breast cancer.* J Cell Biochem, 2019. **120**(6): p. 9300-9314.
110. Vucic, D. and W.J. Fairbrother, *The inhibitor of apoptosis proteins as therapeutic targets in cancer.* Clin Cancer Res, 2007. **13**(20): p. 5995-6000.
111. Shapiro, P.J., et al., *Regulation of the Drosophila apoptosome through feedback inhibition.* Nat Cell Biol, 2008. **10**(12): p. 1440-6.
112. Hunter, A.M., E.C. LaCasse, and R.G. Korneluk, *The inhibitors of apoptosis (IAPs) as cancer targets.* Apoptosis, 2007. **12**(9): p. 1543-68.
113. Mace, P.D., S. Shirley, and C.L. Day, *Assembling the building blocks: structure and function of inhibitor of apoptosis proteins.* Cell Death Differ, 2010. **17**(1): p. 46-53.
114. Chesi, M., et al., *IAP antagonists induce anti-tumor immunity in multiple myeloma.* Nat Med, 2016. **22**(12): p. 1411-1420.
115. Fulda, S. and D. Vucic, *Targeting IAP proteins for therapeutic intervention in cancer.* Nat Rev Drug Discov, 2012. **11**(2): p. 109-24.
116. Imoto, I., et al., *Expression of cIAP1, a target for 11q22 amplification, correlates with resistance of cervical cancers to radiotherapy.* Cancer Res, 2002. **62**(17): p. 4860-6.
117. Zender, L., et al., *Identification and validation of oncogenes in liver cancer using an integrative oncogenomic approach.* Cell, 2006. **125**(7): p. 1253-67.

118. Bashyam, M.D., et al., *Array-based comparative genomic hybridization identifies localized DNA amplifications and homozygous deletions in pancreatic cancer.* Neoplasia, 2005. **7**(6): p. 556-62.
119. Fulda, S., *Tumor resistance to apoptosis.* Int J Cancer, 2009. **124**(3): p. 511-5.
120. Petersen, S.L., et al., *Autocrine TNFalpha signaling renders human cancer cells susceptible to Smac-mimetic-induced apoptosis.* Cancer Cell, 2007. **12**(5): p. 445-56.
121. Samuel, T., et al., *Distinct BIR domains of cIAP1 mediate binding to and ubiquitination of tumor necrosis factor receptor-associated factor 2 and second mitochondrial activator of caspases.* J Biol Chem, 2006. **281**(2): p. 1080-90.
122. Rathore, R., et al., *Overcoming chemotherapy drug resistance by targeting inhibitors of apoptosis proteins (IAPs).* Apoptosis, 2017. **22**(7): p. 898-919.
123. Li, J., et al., *Human ovarian cancer and cisplatin resistance: possible role of inhibitor of apoptosis proteins.* Endocrinology, 2001. **142**(1): p. 370-80.
124. Tamm, I., et al., *Expression and prognostic significance of IAP-family genes in human cancers and myeloid leukemias.* Clin Cancer Res, 2000. **6**(5): p. 1796-803.
125. Ramp, U., et al., *XIAP expression is an independent prognostic marker in clear-cell renal carcinomas.* Hum Pathol, 2004. **35**(8): p. 1022-8.
126. LaCasse, E.C., et al., *IAP-targeted therapies for cancer.* Oncogene, 2008. **27**(48): p. 6252-75.
127. Bai, L., D.C. Smith, and S. Wang, *Small-molecule SMAC mimetics as new cancer therapeutics.* Pharmacol Ther, 2014. **144**(1): p. 82-95.
128. Tenev, T., et al., *The Ripoptosome, a signaling platform that assembles in response to genotoxic stress and loss of IAPs.* Mol Cell, 2011. **43**(3): p. 432-48.
129. Gaither, A., et al., *A Smac mimetic rescue screen reveals roles for inhibitor of apoptosis proteins in tumor necrosis factor-alpha signaling.* Cancer Res, 2007. **67**(24): p. 11493-8.
130. Varfolomeev, E., et al., *IAP antagonists induce autoubiquitination of c-IAPs, NF-kappaB activation, and TNFalpha-dependent apoptosis.* Cell, 2007. **131**(4): p. 669-81.
131. Schütze, S., V. Tchikov, and W. Schneider-Brachert, *Regulation of TNFR1 and CD95 signalling by receptor compartmentalization.* Nat Rev Mol Cell Biol, 2008. **9**(8): p. 655-62.
132. Marschall, V. and S. Fulda, *Smac mimetic-induced upregulation of interferon-β sensitizes glioblastoma to temozolomide-induced cell death.* Cell Death Dis, 2015. **6**(9): p. e1888.
133. Sun, H., et al., *Design of small-molecule peptidic and nonpeptidic Smac mimetics.* Acc Chem Res, 2008. **41**(10): p. 1264-77.
134. Mitsuuchi, Y., et al., *Bivalent IAP antagonists, but not monovalent IAP antagonists, inhibit TNF-mediated NF-κB signaling by degrading TRAF2-associated cIAP1 in cancer cells.* Cell Death Discov, 2017. **3**: p. 16046.
135. Fulda, S., *Promises and Challenges of Smac Mimetics as Cancer Therapeutics.* Clin Cancer Res, 2015. **21**(22): p. 5030-6.
136. Sun, H., et al., *Design, synthesis, and characterization of a potent, nonpeptide, cell-permeable, bivalent Smac mimetic that concurrently targets both the BIR2 and BIR3 domains in XIAP.* J Am Chem Soc, 2007. **129**(49): p. 15279-94.

137. Nikolovska-Coleska, Z., et al., *Interaction of a cyclic, bivalent smac mimetic with the x-linked inhibitor of apoptosis protein.* Biochemistry, 2008. **47**(37): p. 9811-24.
138. Zobel, K., et al., *Design, synthesis, and biological activity of a potent Smac mimetic that sensitizes cancer cells to apoptosis by antagonizing IAPs.* ACS Chem Biol, 2006. **1**(8): p. 525-33.
139. Benetatos, C.A., et al., *Birinapant (TL32711), a bivalent SMAC mimetic, targets TRAF2-associated cIAPs, abrogates TNF-induced NF-κB activation, and is active in patient-derived xenograft models.* Mol Cancer Ther, 2014. **13**(4): p. 867-79.
140. Foster, F.M., et al., *Targeting inhibitor of apoptosis proteins in combination with ErbB antagonists in breast cancer.* Breast Cancer Res, 2009. **11**(3): p. R41.
141. Langdon, C.G., et al., *SMAC mimetic Debio 1143 synergizes with taxanes, topoisomerase inhibitors and bromodomain inhibitors to impede growth of lung adenocarcinoma cells.* Oncotarget, 2015. **6**(35): p. 37410-25.
142. Lu, J., et al., *Therapeutic potential and molecular mechanism of a novel, potent, nonpeptide, Smac mimetic SM-164 in combination with TRAIL for cancer treatment.* Mol Cancer Ther, 2011. **10**(5): p. 902-14.
143. Brands, R.C., et al., *Cytotoxic effects of SMAC-mimetic compound LCL161 in head and neck cancer cell lines.* Clin Oral Investig, 2016. **20**(9): p. 2325-2332.
144. Beug, S.T., et al., *Smac mimetics synergize with immune checkpoint inhibitors to promote tumour immunity against glioblastoma.* Nat Commun, 2017. **8**.
145. Fakler, M., et al., *Small molecule XIAP inhibitors cooperate with TRAIL to induce apoptosis in childhood acute leukemia cells and overcome Bcl-2-mediated resistance.* Blood, 2009. **113**(8): p. 1710-22.
146. Löder, S., et al., *RIP1 is required for IAP inhibitor-mediated sensitization of childhood acute leukemia cells to chemotherapy-induced apoptosis.* Leukemia, 2012. **26**(5): p. 1020-9.
147. Chauhan, D., et al., *Targeting mitochondrial factor Smac/DIABLO as therapy for multiple myeloma (MM).* Blood, 2007. **109**(3): p. 1220-7.
148. Chromik, J., et al., *Smac mimetic primes apoptosis-resistant acute myeloid leukaemia cells for cytarabine-induced cell death by triggering necroptosis.* Cancer Lett, 2014. **344**(1): p. 101-109.
149. Carter, B.Z., et al., *Synergistic targeting of AML stem/progenitor cells with IAP antagonist birinapant and demethylating agents.* J Natl Cancer Inst, 2014. **106**(2): p. djt440.
150. Lalaoui, N., et al., *Targeting p38 or MK2 Enhances the Anti-Leukemic Activity of Smac-Mimetics.* Cancer Cell, 2016. **30**(3): p. 499-500.
151. Brumatti, G., et al., *The caspase-8 inhibitor emricasan combines with the SMAC mimetic birinapant to induce necroptosis and treat acute myeloid leukemia.* Sci Transl Med, 2016. **8**(339): p. 339ra69.
152. Amaravadi, R.K., et al., *A Phase I Study of the SMAC-Mimetic Birinapant in Adults with Refractory Solid Tumors or Lymphoma.* Mol Cancer Ther, 2015. **14**(11): p. 2569-75.
153. Tolcher A, P.K., Patnaik A, Fairbrother W, Wong H, Budha N, et al., *Phase I study of safety and pharmacokinetics (PK) of GDC-0917, an antagonist of inhibitor of apoptosis (IAP) proteins in patients (Pts) with refractory solid tumors or lymphoma. .* j Clin Oncol 31,2013, 2013.

154. Sikic BI, E.S., Gallant G, Burris HA, Camidge DR, Covelas AD, et al., *armocokinetics (PK), and pharmacodynamics (PD) of HGS1029, an inhibitor of apoptosis protein (IAP), in patients (Pts.) with advanced solid tumors: results of a phase I study.* J Clin Oncol 29,2011, 2011.
155. Sikic, B.I., et al., *Safety, pharmacokinetics (PK), and pharmacodynamics (PD) of HGS1029, an inhibitor of apoptosis protein (IAP) inhibitor, in patients (Pts) with advanced solid tumors: Results of a phase I study.* 2011. **29**(15_suppl): p. 3008-3008.
156. Hurwitz H, P.H., Smith D, Brill J, Vuagniaux G, Rouits E, et al., *First-in-human, pharmacokinetic (PK), and pharmacodynamics (PD) phase I study of Debio1143 (AT-406) in patients with advanced cancer: Final results. .* J Clin Oncol 32:5s, 2014, 2014.
157. Infante, J.R., et al., *Phase I dose-escalation study of LCL161, an oral inhibitor of apoptosis proteins inhibitor, in patients with advanced solid tumors.* J Clin Oncol, 2014. **32**(28): p. 3103-10.
158. Lueck, S.C., et al., *Smac mimetic induces cell death in a large proportion of primary acute myeloid leukemia samples, which correlates with defined molecular markers.* Oncotarget, 2016. **7**(31): p. 49539-49551.
159. Carter, B.Z., et al., *XIAP antisense oligonucleotide (AEG35156) achieves target knockdown and induces apoptosis preferentially in CD34+38- cells in a phase 1/2 study of patients with relapsed/refractory AML.* Apoptosis, 2011. **16**(1): p. 67-74.
160. Yang, L., et al., *LCL161, a SMAC-mimetic, Preferentially Radiosensitizes Human Papillomavirus-negative Head and Neck Squamous Cell Carcinoma.* Mol Cancer Ther, 2019. **18**(6): p. 1025-1035.
161. Bardia, A., et al., *Paclitaxel With Inhibitor of Apoptosis Antagonist, LCL161, for Localized Triple-Negative Breast Cancer, Prospectively Stratified by Gene Signature in a Biomarker-Driven Neoadjuvant Trial.* J Clin Oncol, 2018: p. Jco2017748392.
162. Pemmaraju, N., et al., *Final results of a phase 2 clinical trial of LCL161, an oral SMAC mimetic for patients with myelofibrosis.* Blood Adv, 2021. **5**(16): p. 3163-3173.
163. Juergens, R.A., et al., *A dose-finding study of the SMAC mimetic Debio 1143 when given in combination with avelumab to patients with advanced solid malignancies.* 2019. **37**(15_suppl): p. 2599-2599.
164. Pedrazzoli, A.B.A., et al., *560P Safety and efficacy of Debio 1143, an antagonist of inhibitor of apoptosis proteins (IAPs), in combination with nivolumab in a phase Ib/II trial in patients (pts) failing prior PD-1/PD-L1 treatment.* Annals of Oncology, 2020. **31**: p. S483.
165. Schilder, R.J., et al., *Determination of the recommended phase II dose of birinapant in combination with pembrolizumab: Results from the dose-escalation phase of BPT-201.* 2019. **37**(15_suppl): p. 2506-2506.
166. Noonan, A.M., et al., *Pharmacodynamic markers and clinical results from the phase 2 study of the SMAC mimetic birinapant in women with relapsed platinum-resistant or -refractory epithelial ovarian cancer.* Cancer, 2016. **122**(4): p. 588-597.
167. Bunch, K.P., et al., *Pharmacodynamic biomarkers from phase II study of the SMAC (Second Mitochondrial-Derived Activator of Caspases)-mimetic birinapant (TL32711; NSC 756502) in relapsed platinum-resistant epithelial ovarian cancer (EOC), primary peritoneal cancer (PPC), or fallopian tube cancer (FTC) (NCT01681368).* 2014. **32**(15_suppl): p. 5585-5585.

168. Gomez-Bougie, P., et al., *BH3-mimetic toolkit guides the respective use of BCL2 and MCL1 BH3-mimetics in myeloma treatment.* Blood, 2018. **132**(25): p. 2656-2669.
169. Adams, J.M. and S. Cory, *The Bcl-2 apoptotic switch in cancer development and therapy.* Oncogene, 2007. **26**(9): p. 1324-37.
170. Glab, J.A., M. Doerflinger, and H. Puthalakath, *BH3-only proteins: the thorny end of the ER stress response.* Cell Death Dis, 2017. **8**(6): p. e2889.
171. Shamas-Din, A., et al., *BH3-only proteins: Orchestrators of apoptosis.* Biochim Biophys Acta, 2011. **1813**(4): p. 508-20.
172. Haneef, J., et al., *Bax translocation mediated mitochondrial apoptosis and caspase dependent photosensitizing effect of Ficus religiosa on cancer cells.* PLoS One, 2012. **7**(7): p. e40055.
173. D'Alessio, M., et al., *Oxidative Bax dimerization promotes its translocation to mitochondria independently of apoptosis.* Faseb j, 2005. **19**(11): p. 1504-6.
174. McArthur, K., et al., *BAK/BAX macropores facilitate mitochondrial herniation and mtDNA efflux during apoptosis.* Science, 2018. **359**(6378).
175. Klener, P., et al., *BH3 Mimetics in Hematologic Malignancies.* Int J Mol Sci, 2021. **22**(18).
176. Loriot, Y., et al., *Radiosensitization by a novel Bcl-2 and Bcl-XL inhibitor S44563 in small-cell lung cancer.* Cell Death Dis, 2014. **5**(9): p. e1423.
177. Adam, A., et al., *A Dual Bcl-2/xL Inhibitor Induces Tumor Cell Apoptosis in a Hematopoietic Xenograft Model.* Blood, 2014. **124**(21): p. 5304-5304.
178. Ye, L., et al., *The small-molecule compound BM-1197 inhibits the antiapoptotic regulators Bcl-2/Bcl-xL and triggers apoptotic cell death in human colorectal cancer cells.* Tumour Biol, 2015. **36**(5): p. 3447-55.
179. Kotschy, A., et al., *The MCL1 inhibitor S63845 is tolerable and effective in diverse cancer models.* Nature, 2016. **538**(7626): p. 477-482.
180. Leverson, J.D., et al., *Potent and selective small-molecule MCL-1 inhibitors demonstrate on-target cancer cell killing activity as single agents and in combination with ABT-263 (navitoclax).* Cell Death Dis, 2015. **6**(1): p. e1590.
181. Tao, Z.F., et al., *Discovery of a Potent and Selective BCL-XL Inhibitor with in Vivo Activity.* ACS Med Chem Lett, 2014. **5**(10): p. 1088-93.
182. Kline, M.P., et al., *ABT-737, an inhibitor of Bcl-2 family proteins, is a potent inducer of apoptosis in multiple myeloma cells.* Leukemia, 2007. **21**(7): p. 1549-60.
183. Tse, C., et al., *ABT-263: a potent and orally bioavailable Bcl-2 family inhibitor.* Cancer Res, 2008. **68**(9): p. 3421-8.
184. Zhang, H., et al., *Bcl-2 family proteins are essential for platelet survival.* Cell Death Differ, 2007. **14**(5): p. 943-51.
185. de Vos, S., et al., *Safety and efficacy of navitoclax, a BCL-2 and BCL-X(L) inhibitor, in patients with relapsed or refractory lymphoid malignancies: results from a phase 2a study.* Leuk Lymphoma, 2021. **62**(4): p. 810-818.
186. Parry, N., H. Wheadon, and M. Copland, *The application of BH3 mimetics in myeloid leukemias.* Cell Death Dis, 2021. **12**(2): p. 222.
187. Souers, A.J., et al., *ABT-199, a potent and selective BCL-2 inhibitor, achieves antitumor activity while sparing platelets.* Nat Med, 2013. **19**(2): p. 202-8.

188. Corcoran, R.B., et al., *447PD - Phase I/II study of combined BCL-XL and MEK inhibition with navitoclax (N) and trametinib (T) in KRAS or NRAS mutant advanced solid tumours.* Annals of Oncology, 2019. **30**: p. v164.
189. Bertino, E.M., et al., *Phase IB Study of Osimertinib in Combination with Navitoclax in EGFR-mutant NSCLC Following Resistance to Initial EGFR Therapy (ETCTN 9903).* Clinical Cancer Research, 2021. **27**(6): p. 1604-1611.
190. Pemmaraju, N., et al., *Trial in Progress: Phase Ib/II Study of Bcl-2/Bcl-Xl Inhibitor Pelcitoclax (APG-1252) in Patients with Myelofibrosis (MF) That Progressed after Initial Therapy.* Blood, 2020. **136**: p. 15-16.
191. Wei, A.H., et al., *Venetoclax Combined With Low-Dose Cytarabine for Previously Untreated Patients With Acute Myeloid Leukemia: Results From a Phase Ib/II Study.* J Clin Oncol, 2019. **37**(15): p. 1277-1284.
192. Roberts, A.W., et al., *Targeting BCL2 with Venetoclax in Relapsed Chronic Lymphocytic Leukemia.* N Engl J Med, 2016. **374**(4): p. 311-22.
193. Le Gouill, S., et al., *A NEW BCL-2 INHIBITOR (S55746/BCL201) AS MONOTHERAPY IN PATIENTS WITH RELAPSED OR REFRACTORY NON-HODGKIN LYMPHOMA: PRELIMINARY RESULTS OF THE FIRST-IN-HUMAN STUDY.* 2017. **35**(S2): p. 47-48.
194. Casara, P., et al., *S55746 is a novel orally active BCL-2 selective and potent inhibitor that impairs hematological tumor growth.* Oncotarget, 2018. **9**(28): p. 20075-20088.
195. Sun, M., et al., *A Phase 1 Study to Evaluate the Safety, Pharmacokinetics (PK) and Pharmacodynamics (PD) of Lisaftoclax (APG-2575), a Novel BCL-2 Inhibitor (BCL-2i), in Patients (pts) with Certain Relapsed or Refractory (R/R) Hematologic Malignancies (HMs).* Blood, 2021. **138**: p. 3730.
196. Ailawadhi, S., et al., *First-in-human study of lisaftoclax (APG-2575), a novel BCL-2 inhibitor (BCL-2i), in patients (pts) with relapsed/refractory (R/R) CLL and other hematologic malignancies (HMs).* 2021. **39**(15_suppl): p. 7502-7502.
197. Tolcher, A.W., et al., *A first-in-human study of mirzotamab clezutoclax as monotherapy and in combination with taxane therapy in relapsed/refractory solid tumors: Dose escalation results.* 2021. **39**(15_suppl): p. 3015-3015.
198. Halilovic, E., et al., *Abstract 4477: MIK665/S64315, a novel Mcl-1 inhibitor, in combination with Bcl-2 inhibitors exhibits strong synergistic antitumor activity in a range of hematologic malignancies.* Cancer Research, 2019. **79**(13_Supplement): p. 4477-4477.
199. Maragno, A.L., et al., *Abstract 4482: S64315 (MIK665) is a potent and selective Mcl1 inhibitor with strong antitumor activity across a diverse range of hematologic tumor models.* Cancer Research, 2019. **79**(13_Supplement): p. 4482-4482.
200. Tron, A.E., et al., *Discovery of Mcl-1-specific inhibitor AZD5991 and preclinical activity in multiple myeloma and acute myeloid leukemia.* Nat Commun, 2018. **9**(1): p. 5341.
201. DiNardo, C.D., et al., *Azacitidine and Venetoclax in Previously Untreated Acute Myeloid Leukemia.* N Engl J Med, 2020. **383**(7): p. 617-629.
202. Lauria, F., et al., *High bcl-2 expression in acute myeloid leukemia cells correlates with CD34 positivity and complete remission rate.* Leukemia, 1997. **11**(12): p. 2075-8.

203. Bensi, L., et al., *Bcl-2 oncoprotein expression in acute myeloid leukemia.* Haematologica, 1995. **80**(2): p. 98-102.
204. Wang, J.L., et al., *Cell permeable Bcl-2 binding peptides: a chemical approach to apoptosis induction in tumor cells.* Cancer Res, 2000. **60**(6): p. 1498-502.
205. Wang, J.L., et al., *Structure-based discovery of an organic compound that binds Bcl-2 protein and induces apoptosis of tumor cells.* Proc Natl Acad Sci U S A, 2000. **97**(13): p. 7124-9.
206. Pallis, M., Y.M. Zhu, and N.H. Russell, *Bcl-x(L) is heterogenously expressed by acute myeloblastic leukaemia cells and is associated with autonomous growth in vitro and with P-glycoprotein expression.* Leukemia, 1997. **11**(7): p. 945-9.
207. Letai, A., et al., *Antiapoptotic BCL-2 is required for maintenance of a model leukemia.* Cancer Cell, 2004. **6**(3): p. 241-9.
208. Choudhary, G.S., et al., *MCL-1 and BCL-xL-dependent resistance to the BCL-2 inhibitor ABT-199 can be overcome by preventing PI3K/AKT/mTOR activation in lymphoid malignancies.* Cell Death Dis, 2015. **6**(1): p. e1593.
209. Pollyea, D.A., et al., *Venetoclax for AML: changing the treatment paradigm.* Blood Adv, 2019. **3**(24): p. 4326-4335.
210. Pan, R., et al., *Selective BCL-2 inhibition by ABT-199 causes on-target cell death in acute myeloid leukemia.* Cancer Discov, 2014. **4**(3): p. 362-75.
211. Chan, S.M., et al., *Isocitrate dehydrogenase 1 and 2 mutations induce BCL-2 dependence in acute myeloid leukemia.* Nat Med, 2015. **21**(2): p. 178-84.
212. Vo, T.T., et al., *Relative mitochondrial priming of myeloblasts and normal HSCs determines chemotherapeutic success in AML.* Cell, 2012. **151**(2): p. 344-55.
213. Wei, A.H., et al., *Venetoclax plus LDAC for newly diagnosed AML ineligible for intensive chemotherapy: a phase 3 randomized placebo-controlled trial.* Blood, 2020. **135**(24): p. 2137-2145.
214. Ma, J., et al., *Inhibition of Bcl-2 Synergistically Enhances the Antileukemic Activity of Midostaurin and Gilteritinib in Preclinical Models of FLT3-Mutated Acute Myeloid Leukemia.* Clin Cancer Res, 2019. **25**(22): p. 6815-6826.
215. Moujalled, D.M., et al., *Combining BH3-mimetics to target both BCL-2 and MCL1 has potent activity in pre-clinical models of acute myeloid leukemia.* Leukemia, 2019. **33**(4): p. 905-917.
216. Kelly, E. and S.J. Russell, *History of oncolytic viruses: genesis to genetic engineering.* Mol Ther, 2007. **15**(4): p. 651-9.
217. Dock, G.J.T.A.J.o.t.M.S., *The influence of complicating diseases upon leukaemia.* 1904. **127**(4): p. 563.
218. Toda, M., et al., *Herpes simplex virus as an in situ cancer vaccine for the induction of specific anti-tumor immunity.* Hum Gene Ther, 1999. **10**(3): p. 385-93.
219. Greiner, S., et al., *The highly attenuated vaccinia virus strain modified virus Ankara induces apoptosis in melanoma cells and allows bystander dendritic cells to generate a potent anti-tumoral immunity.* Clin Exp Immunol, 2006. **146**(2): p. 344-53.

220. Stojdl, D.F., et al., *Exploiting tumor-specific defects in the interferon pathway with a previously unknown oncolytic virus.* Nat Med, 2000. **6**(7): p. 821-5.
221. Shafren, D.R., et al., *Oncolysis of human ovarian cancers by echovirus type 1.* Int J Cancer, 2005. **115**(2): p. 320-8.
222. Lorence, R.M., P.A. Rood, and K.W. Kelley, *Newcastle disease virus as an antineoplastic agent: induction of tumor necrosis factor-alpha and augmentation of its cytotoxicity.* J Natl Cancer Inst, 1988. **80**(16): p. 1305-12.
223. Hashiro, G., P.C. Loh, and J.T. Yau, *The preferential cytotoxicity of reovirus for certain transformed cell lines.* Arch Virol, 1977. **54**(4): p. 307-15.
224. Moehler, M., et al., *Effective infection, apoptotic cell killing and gene transfer of human hepatoma cells but not primary hepatocytes by parvovirus H1 and derived vectors.* Cancer Gene Ther, 2001. **8**(3): p. 158-67.
225. Shafren, D.R., et al., *Systemic therapy of malignant human melanoma tumors by a common cold-producing enterovirus, coxsackievirus a21.* Clin Cancer Res, 2004. **10**(1 Pt 1): p. 53-60.
226. Reddy, P.S., et al., *Seneca Valley virus, a systemically deliverable oncolytic picornavirus, and the treatment of neuroendocrine cancers.* J Natl Cancer Inst, 2007. **99**(21): p. 1623-33.
227. Grote, D., et al., *Live attenuated measles virus induces regression of human lymphoma xenografts in immunodeficient mice.* Blood, 2001. **97**(12): p. 3746-54.
228. Martuza, R.L., et al., *Experimental therapy of human glioma by means of a genetically engineered virus mutant.* Science, 1991. **252**(5007): p. 854-6.
229. Bergmann, M., et al., *A genetically engineered influenza A virus with ras-dependent oncolytic properties.* Cancer Res, 2001. **61**(22): p. 8188-93.
230. McCart, J.A., et al., *Systemic cancer therapy with a tumor-selective vaccinia virus mutant lacking thymidine kinase and vaccinia growth factor genes.* Cancer Res, 2001. **61**(24): p. 8751-7.
231. Fueyo, J., et al., *A mutant oncolytic adenovirus targeting the Rb pathway produces anti-glioma effect in vivo.* Oncogene, 2000. **19**(1): p. 2-12.
232. Breitbach, C.J., et al., *Oncolytic vaccinia virus disrupts tumor-associated vasculature in humans.* Cancer Res, 2013. **73**(4): p. 1265-75.
233. Ilkow, C.S., et al., *Reciprocal cellular cross-talk within the tumor microenvironment promotes oncolytic virus activity.* Nat Med, 2015. **21**(5): p. 530-6.
234. Kaufman, H.L., F.J. Kohlhapp, and A. Zloza, *Oncolytic viruses: a new class of immunotherapy drugs.* Nat Rev Drug Discov, 2015. **14**(9): p. 642-62.
235. Anderson, B.D., et al., *High CD46 receptor density determines preferential killing of tumor cells by oncolytic measles virus.* Cancer Res, 2004. **64**(14): p. 4919-26.
236. Newcombe, N.G., et al., *Enterovirus capsid interactions with decay-accelerating factor mediate lytic cell infection.* J Virol, 2004. **78**(3): p. 1431-9.
237. Kirn, D., *Clinical research results with dl1520 (Onyx-015), a replication-selective adenovirus for the treatment of cancer: what have we learned?* Gene Ther, 2001. **8**(2): p. 89-98.

238. Dmitriev, I., et al., *An adenovirus vector with genetically modified fibers demonstrates expanded tropism via utilization of a coxsackievirus and adenovirus receptor-independent cell entry mechanism.* J Virol, 1998. **72**(12): p. 9706-13.
239. Kanerva, A., et al., *Targeting adenovirus to the serotype 3 receptor increases gene transfer efficiency to ovarian cancer cells.* Clin Cancer Res, 2002. **8**(1): p. 275-80.
240. Sadler, A.J. and B.R. Williams, *Structure and function of the protein kinase R.* Curr Top Microbiol Immunol, 2007. **316**: p. 253-92.
241. Strong, J.E., et al., *The molecular basis of viral oncolysis: usurpation of the Ras signaling pathway by reovirus.* Embo j, 1998. **17**(12): p. 3351-62.
242. Coffey, M.C., et al., *Reovirus therapy of tumors with activated Ras pathway.* Science, 1998. **282**(5392): p. 1332-4.
243. He, B., M. Gross, and B. Roizman, *The gamma(1)34.5 protein of herpes simplex virus 1 complexes with protein phosphatase 1alpha to dephosphorylate the alpha subunit of the eukaryotic translation initiation factor 2 and preclude the shutoff of protein synthesis by double-stranded RNA-activated protein kinase.* Proc Natl Acad Sci U S A, 1997. **94**(3): p. 843-8.
244. Levy, D.E., I.J. Marié, and J.E. Durbin, *Induction and function of type I and III interferon in response to viral infection.* Curr Opin Virol, 2011. **1**(6): p. 476-86.
245. Rojas, M., C.F. Arias, and S. López, *Protein kinase R is responsible for the phosphorylation of eIF2alpha in rotavirus infection.* J Virol, 2010. **84**(20): p. 10457-66.
246. Moore, A.E., *The destructive effect of the virus of Russian Far East encephalitis on the transplantable mouse sarcoma 180.* Cancer, 1949. **2**(3): p. 525-34.
247. Anthony, S.J., et al., *A strategy to estimate unknown viral diversity in mammals.* mBio, 2013. **4**(5): p. e00598-13.
248. Moore, A.E., *Effect of inoculation of the viruses of influenza A and herpes simplex on the growth of transplantable tumors in mice.* Cancer, 1949. **2**(3): p. 516-24.
249. Garber, K., *China approves world's first oncolytic virus therapy for cancer treatment.* J Natl Cancer Inst, 2006. **98**(5): p. 298-300.
250. Balachandran, S. and G.N. Barber, *Defective translational control facilitates vesicular stomatitis virus oncolysis.* Cancer Cell, 2004. **5**(1): p. 51-65.
251. Fiola, C., et al., *Tumor selective replication of Newcastle disease virus: association with defects of tumor cells in antiviral defence.* Int J Cancer, 2006. **119**(2): p. 328-38.
252. Hummel, J.L., E. Safroneeva, and K.L. Mossman, *The role of ICP0-Null HSV-1 and interferon signaling defects in the effective treatment of breast adenocarcinoma.* Mol Ther, 2005. **12**(6): p. 1101-10.
253. Symons, J.A., A. Alcamí, and G.L. Smith, *Vaccinia virus encodes a soluble type I interferon receptor of novel structure and broad species specificity.* Cell, 1995. **81**(4): p. 551-60.
254. Diaz, R.M., et al., *Oncolytic immunovirotherapy for melanoma using vesicular stomatitis virus.* Cancer Res, 2007. **67**(6): p. 2840-8.
255. Bhat, R., et al., *Enhancement of NK cell antitumor responses using an oncolytic parvovirus.* Int J Cancer, 2011. **128**(4): p. 908-19.

256. Schirrmacher, V., et al., *Newcastle disease virus activates macrophages for anti-tumor activity.* Int J Oncol, 2000. **16**(2): p. 363-73.
257. Prestwich, R.J., et al., *Tumor infection by oncolytic reovirus primes adaptive antitumor immunity.* Clin Cancer Res, 2008. **14**(22): p. 7358-66.
258. Müller, L.M.E., et al., *Plasmacytoid dendritic cells orchestrate innate and adaptive anti-tumor immunity induced by oncolytic coxsackievirus A21.* J Immunother Cancer, 2019. **7**(1): p. 164.
259. Parrish, C., et al., *Oncolytic reovirus enhances rituximab-mediated antibody-dependent cellular cytotoxicity against chronic lymphocytic leukaemia.* Leukemia, 2015. **29**(9): p. 1799-810.
260. Errington, F., et al., *Reovirus activates human dendritic cells to promote innate antitumor immunity.* J Immunol, 2008. **180**(9): p. 6018-26.
261. Woller, N., et al., *Oncolytic viruses as anticancer vaccines.* Front Oncol, 2014. **4**: p. 188.
262. Nguyen, K.B., et al., *Coordinated and distinct roles for IFN-alpha beta, IL-12, and IL-15 regulation of NK cell responses to viral infection.* J Immunol, 2002. **169**(8): p. 4279-87.
263. Paolini, R., et al., *NK cells and interferons.* Cytokine Growth Factor Rev, 2015. **26**(2): p. 113-20.
264. Sato, K., et al., *Antiviral response by natural killer cells through TRAIL gene induction by IFN-alpha/beta.* Eur J Immunol, 2001. **31**(11): p. 3138-46.
265. Zamai, L., et al., *Natural killer (NK) cell-mediated cytotoxicity: differential use of TRAIL and Fas ligand by immature and mature primary human NK cells.* J Exp Med, 1998. **188**(12): p. 2375-80.
266. Chaurasiya, S., Y. Fong, and S.G. Warner, *Oncolytic Virotherapy for Cancer: Clinical Experience.* Biomedicines, 2021. **9**(4).
267. Macedo, N., et al., *Clinical landscape of oncolytic virus research in 2020.* J Immunother Cancer, 2020. **8**(2).
268. Alberts, P., et al., *The advent of oncolytic virotherapy in oncology: The Rigvir® story.* Eur J Pharmacol, 2018. **837**: p. 117-126.
269. Liang, M., *Oncorine, the World First Oncolytic Virus Medicine and its Update in China.* Curr Cancer Drug Targets, 2018. **18**(2): p. 171-176.
270. Donnelly, O.G., et al., *Recent clinical experience with oncolytic viruses.* Curr Pharm Biotechnol, 2012. **13**(9): p. 1834-41.
271. Adair, R.A., et al., *Cell carriage, delivery, and selective replication of an oncolytic virus in tumor in patients.* Sci Transl Med, 2012. **4**(138): p. 138ra77.
272. Senzer, N.N., et al., *Phase II clinical trial of a granulocyte-macrophage colony-stimulating factor-encoding, second-generation oncolytic herpesvirus in patients with unresectable metastatic melanoma.* J Clin Oncol, 2009. **27**(34): p. 5763-71.
273. Xia, Z.J., et al., *[Phase III randomized clinical trial of intratumoral injection of E1B gene-deleted adenovirus (H101) combined with cisplatin-based chemotherapy in treating squamous cell cancer of head and neck or esophagus].* Ai Zheng, 2004. **23**(12): p. 1666-70.
274. Warner, S.G., M.P. O'Leary, and Y. Fong, *Therapeutic oncolytic viruses: clinical advances and future directions.* Curr Opin Oncol, 2017. **29**(5): p. 359-365.
275. Innao, V., et al., *Oncolytic Viruses and Hematological Malignancies: A New Class of Immunotherapy Drugs.* Curr Oncol, 2020. **28**(1): p. 159-183.

276. Maurer, S., et al., *Suicide gene-armed measles vaccine virus for the treatment of AML.* Int J Oncol, 2019. **55**(2): p. 347-358.
277. Hall, K., et al., *Reovirus-mediated cytotoxicity and enhancement of innate immune responses against acute myeloid leukemia.* Biores Open Access, 2012. **1**(1): p. 3-15.
278. Madlambayan, G.J., et al., *Acute myeloid leukemia targeting by myxoma virus in vivo depends on cell binding but not permissiveness to infection in vitro.* Leuk Res, 2012. **36**(5): p. 619-24.
279. Kim, M., et al., *Myxoma virus targets primary human leukemic stem and progenitor cells while sparing normal hematopoietic stem and progenitor cells.* Leukemia, 2009. **23**(12): p. 2313-7.
280. Wang, Z., et al., *Enhancing the antitumor activity of an engineered TRAIL-coated oncolytic adenovirus for treating acute myeloid leukemia.* Signal Transduct Target Ther, 2020. **5**(1): p. 40.
281. Lei, W., et al., *Enhancing therapeutic efficacy of oncolytic vaccinia virus armed with Beclin-1, an autophagic Gene in leukemia and myeloma.* Biomed Pharmacother, 2020. **125**: p. 110030.
282. Meng, H.T., et al., *Homoharringtonine acts synergistically with SG235-TRAIL, a conditionally replicating adenovirus, in human leukemia cell lines.* Acta Pharmacol Sin, 2009. **30**(11): p. 1529-36.
283. Shen, W., et al., *Immunovirotherapy with vesicular stomatitis virus and PD-L1 blockade enhances therapeutic outcome in murine acute myeloid leukemia.* Blood, 2016. **127**(11): p. 1449-58.
284. Zhang, L.F., et al., *Combination of vaccine-strain measles and mumps virus synergistically kills a wide range of human hematological cancer cells: Special focus on acute myeloid leukemia.* Cancer Lett, 2014. **354**(2): p. 272-80.
285. Samudio, I., et al., *UV-inactivated HSV-1 potently activates NK cell killing of leukemic cells.* Blood, 2016. **127**(21): p. 2575-86.
286. Rosen, L., et al., *Observations on a newly recognized virus (Abney) of the reovirus family.* Am J Hyg, 1960. **71**: p. 258-65.
287. Lemay, G., *Transcriptional and translational events during reovirus infection.* Biochem Cell Biol, 1988. **66**(8): p. 803-12.
288. Barton, E.S., et al., *Junction adhesion molecule is a receptor for reovirus.* Cell, 2001. **104**(3): p. 441-51.
289. Sugano, Y., et al., *Junctional adhesion molecule-A, JAM-A, is a novel cell-surface marker for long-term repopulating hematopoietic stem cells.* Blood, 2008. **111**(3): p. 1167-72.
290. Kyula, J.N., et al., *Oncolytic reovirus type 3 (Dearing) as a novel therapy in head and neck cancer.* Expert Opin Biol Ther, 2012. **12**(12): p. 1669-78.
291. Smakman, N., et al., *Sensitization to apoptosis underlies KrasD12-dependent oncolysis of murine C26 colorectal carcinoma cells by reovirus T3D.* J Virol, 2005. **79**(23): p. 14981-5.
292. Berger, A.K., et al., *Viral RNA at Two Stages of Reovirus Infection Is Required for the Induction of Necroptosis.* J Virol, 2017. **91**(6).
293. Ikeda, Y., et al., *Reovirus oncolysis in human head and neck squamous carcinoma cells.* Auris Nasus Larynx, 2004. **31**(4): p. 407-12.
294. Rossmann, M.G., et al., *Structure of a human common cold virus and functional relationship to other picornaviruses.* Nature, 1985. **317**(6033): p. 145-53.

295. Hyypiä, T., et al., *Pathogenetic differences between coxsackie A and B virus infections in newborn mice.* Virus Res, 1993. **27**(1): p. 71-8.
296. Xiao, C., et al., *Interaction of coxsackievirus A21 with its cellular receptor, ICAM-1.* J Virol, 2001. **75**(5): p. 2444-51.
297. Shafren, D.R., et al., *Coxsackievirus A21 binds to decay-accelerating factor but requires intercellular adhesion molecule 1 for cell entry.* J Virol, 1997. **71**(6): p. 4736-43.
298. Hopkins, A.M., A.W. Baird, and A. Nusrat, *ICAM-1: targeted docking for exogenous as well as endogenous ligands.* Adv Drug Deliv Rev, 2004. **56**(6): p. 763-78.
299. Au, G.G., et al., *Oncolytic Coxsackievirus A21 as a novel therapy for multiple myeloma.* Br J Haematol, 2007. **137**(2): p. 133-41.
300. Molica, S., et al., *Expression on leukemic cells and serum circulating levels of intercellular adhesion molecule-1 (ICAM-1) in B-cell chronic lymphocytic leukemia: implications for prognosis.* Leuk Res, 1995. **19**(8): p. 573-80.
301. Johnson, J.P., et al., *De novo expression of intercellular-adhesion molecule 1 in melanoma correlates with increased risk of metastasis.* Proc Natl Acad Sci U S A, 1989. **86**(2): p. 641-4.
302. Maeda, K., et al., *Expression of intercellular adhesion molecule-1 and prognosis in colorectal cancer.* Oncol Rep, 2002. **9**(3): p. 511-4.
303. Heicappell, R., et al., *Cell surface expression and serum levels of intercellular adhesion molecule-1 in renal cell carcinoma.* Urol Res, 1994. **22**(1): p. 9-15.
304. Schwaeble, W., et al., *De novo expression of intercellular adhesion molecule 1 (ICAM-1, CD54) in pancreas cancer.* Int J Cancer, 1993. **53**(2): p. 328-33.
305. Brun, J., et al., *Identification of genetically modified Maraba virus as an oncolytic rhabdovirus.* Mol Ther, 2010. **18**(8): p. 1440-9.
306. Pol, J.G., et al., *Development and applications of oncolytic Maraba virus vaccines.* Oncolytic Virother, 2018. **7**: p. 117-128.
307. Travassos da Rosa, A.P., et al., *Carajas and Maraba viruses, two new vesiculoviruses isolated from phlebotomine sand flies in Brazil.* Am J Trop Med Hyg, 1984. **33**(5): p. 999-1006.
308. Tong, J.G., et al., *Evidence for differential viral oncolytic efficacy in an in vitro model of epithelial ovarian cancer metastasis.* Mol Ther Oncolytics, 2015. **2**: p. 15013.
309. Jonker, D.J., et al., *Phase I study of oncolytic virus (OV) MG1 maraba/MAGE-A3 (MG1MA3), with and without transgenic MAGE-A3 adenovirus vaccine (AdMA3) in incurable advanced/metastatic MAGE-A3-expressing solid tumours: CCTG IND.214.* 2017. **35**(15_suppl): p. e14637-e14637.
310. Kramer, T. and L.W. Enquist, *Directional spread of alphaherpesviruses in the nervous system.* Viruses, 2013. **5**(2): p. 678-707.
311. Randazzo, B.P., et al., *Herpes simplex virus 1716, an ICP 34.5 null mutant, is unable to replicate in CV-1 cells due to a translational block that can be overcome by coinfection with SV40.* J Gen Virol, 1997. **78 (Pt 12)**: p. 3333-9.
312. Conner, J., F.J. Rixon, and S.M. Brown, *Herpes simplex virus type 1 strain HSV1716 grown in baby hamster kidney cells has altered tropism for nonpermissive Chinese hamster ovary cells compared to HSV1716 grown in vero cells.* J Virol, 2005. **79**(15): p. 9970-81.

313. Tampakis, A., et al., *Nectin-1 Expression in Colorectal Cancer: Is There a Group of Patients with High Risk for Early Disease Recurrence?* Oncology, 2019. **96**(6): p. 318-325.
314. Schwertner, B., et al., *Nectin-1 Expression Correlates with the Susceptibility of Malignant Melanoma to Oncolytic Herpes Simplex Virus In Vitro and In Vivo.* Cancers (Basel), 2021. **13**(12).
315. Yu, Z., et al., *Nectin-1 expression by squamous cell carcinoma is a predictor of herpes oncolytic sensitivity.* Mol Ther, 2007. **15**(1): p. 103-13.
316. Liu, B.L., et al., *ICP34.5 deleted herpes simplex virus with enhanced oncolytic, immune stimulating, and anti-tumour properties.* Gene Ther, 2003. **10**(4): p. 292-303.
317. Moesta, A.K., et al., *Local Delivery of OncoVEX(mGM-CSF) Generates Systemic Antitumor Immune Responses Enhanced by Cytotoxic T-Lymphocyte-Associated Protein Blockade.* Clin Cancer Res, 2017. **23**(20): p. 6190-6202.
318. Dobson, C.C., et al., *Oncolytic virus synergizes with Smac mimetic compounds to induce rhabdomyosarcoma cell death in a syngeneic murine model.* Oncotarget, 2017. **8**(2): p. 3495-3508.
319. Cai, J., et al., *Selective replication of oncolytic virus M1 results in a bystander killing effect that is potentiated by Smac mimetics.* Proc Natl Acad Sci U S A, 2017. **114**(26): p. 6812-6817.
320. Beug, S.T., et al., *Smac mimetics and innate immune stimuli synergize to promote tumor death.* Nat Biotechnol, 2014. **32**(2): p. 182-90.
321. Beug, S.T., et al., *Combination of IAP Antagonists and TNF-α-Armed Oncolytic Viruses Induce Tumor Vascular Shutdown and Tumor Regression.* Mol Ther Oncolytics, 2018. **10**: p. 28-39.
322. Kim, D.S., et al., *Smac mimetics and oncolytic viruses synergize in driving anticancer T-cell responses through complementary mechanisms.* Nat Commun, 2017. **8**(1): p. 344.
323. Tumilasci, V.F., et al., *Targeting the apoptotic pathway with BCL-2 inhibitors sensitizes primary chronic lymphocytic leukemia cells to vesicular stomatitis virus-induced oncolysis.* J Virol, 2008. **82**(17): p. 8487-99.
324. Samuel, S., et al., *VSV oncolysis in combination with the BCL-2 inhibitor obatoclax overcomes apoptosis resistance in chronic lymphocytic leukemia.* Mol Ther, 2010. **18**(12): p. 2094-103.
325. Farsaci, B., et al., *Effect of a small molecule BCL-2 inhibitor on immune function and use with a recombinant vaccine.* Int J Cancer, 2010. **127**(7): p. 1603-13.
326. Sarkar, S., et al., *Therapy of prostate cancer using a novel cancer terminator virus and a small molecule BH-3 mimetic.* Oncotarget, 2015. **6**(13): p. 10712-27.
327. Lee, S. and K. Margolin, *Cytokines in cancer immunotherapy.* Cancers (Basel), 2011. **3**(4): p. 3856-93.
328. Ferretti, E., et al., *Targeting acute myeloid leukemia cells with cytokines.* J Leukoc Biol, 2012. **92**(3): p. 567-75.
329. Healy, F.M., et al., *Recent Progress in Interferon Therapy for Myeloid Malignancies.* Front Oncol, 2021. **11**: p. 769628.
330. Cauwels, A., et al., *A safe and highly efficient tumor-targeted type I interferon immunotherapy depends on the tumor microenvironment.* Oncoimmunology, 2018. **7**(3): p. e1398876.

331. Spaapen, R.M., et al., *Therapeutic activity of high-dose intratumoral IFN-β requires direct effect on the tumor vasculature.* J Immunol, 2014. **193**(8): p. 4254-60.
332. Herndon, T.M., et al., *U.S. Food and Drug Administration Approval: peginterferon-alfa-2b for the adjuvant treatment of patients with melanoma.* Oncologist, 2012. **17**(10): p. 1323-8.
333. Magenau, J.M., et al., *A Phase I/II Clinical Trial of Type 1 Interferon for Reduction of Relapse after HCT in High Risk AML.* Biology of Blood and Marrow Transplantation, 2019. **25**(3, Supplement): p. S12-S13.
334. Cook, J., et al., *Clinical activity of single-dose systemic oncolytic VSV virotherapy in patients with relapsed refractory T-cell lymphoma.* Blood Adv, 2022. **6**(11): p. 3268-3279.
335. Spiesschaert, B., et al., *Combining Oncolytic Viruses and Small Molecule Therapeutics: Mutual Benefits.* Cancers (Basel), 2021. **13**(14).
336. Müller, L.M.E., et al., *Reovirus-induced cell-mediated immunity for the treatment of multiple myeloma within the resistant bone marrow niche.* J Immunother Cancer, 2021. **9**(3).
337. Zhang, J., et al., *Maraba MG1 virus enhances natural killer cell function via conventional dendritic cells to reduce postoperative metastatic disease.* Mol Ther, 2014. **22**(7): p. 1320-1332.
338. Jennings, V.A., et al., *Potentiating Oncolytic Virus-Induced Immune-Mediated Tumor Cell Killing Using Histone Deacetylase Inhibition.* Mol Ther, 2019. **27**(6): p. 1139-1152.
339. Ni Chonghaile, T. and A. Letai, *Mimicking the BH3 domain to kill cancer cells.* Oncogene, 2008. **27 Suppl 1**(0 1): p. S149-57.
340. Schmiegel, W.H., et al., *Antiproliferative effects exerted by recombinant human tumor necrosis factor-alpha (TNF-alpha) and interferon-gamma (IFN-gamma) on human pancreatic tumor cell lines.* Pancreas, 1988. **3**(2): p. 180-8.
341. Jiang, H., et al., *Interferon-α as maintenance therapy can significantly reduce relapse in patients with favorable-risk acute myeloid leukemia.* Leukemia & Lymphoma, 2021. **62**(12): p. 2949-2956.
342. Mo, X.D., et al., *Interferon-α Is Effective for Treatment of Minimal Residual Disease in Patients with t(8;21) Acute Myeloid Leukemia After Allogeneic Hematopoietic Stem Cell Transplantation: Results of a Prospective Registry Study.* Oncologist, 2018. **23**(11): p. 1349-1357.
343. Hao, Q. and H. Tang, *Interferon-γ and Smac mimetics synergize to induce apoptosis of lung cancer cells in a TNFα-independent manner.* Cancer Cell Int, 2018. **18**: p. 84.
344. Errington, F., et al., *Inflammatory tumour cell killing by oncolytic reovirus for the treatment of melanoma.* Gene Ther, 2008. **15**(18): p. 1257-70.
345. Chen, D., et al., *Inhibition of Na+/K+-ATPase induces hybrid cell death and enhanced sensitivity to chemotherapy in human glioblastoma cells.* BMC Cancer, 2014. **14**(1): p. 716.
346. Walsh, J.G., et al., *Executioner caspase-3 and caspase-7 are functionally distinct proteases.* 2008. **105**(35): p. 12815-12819.
347. Moll, H.P., et al., *The differential activity of interferon-α subtypes is consistent among distinct target genes and cell types.* Cytokine, 2011. **53**(1): p. 52-9.
348. Abad, A.T. and P. Danthi, *Recognition of Reovirus RNAs by the Innate Immune System.* Viruses, 2020. **12**(6).

349. Triantafilou, K., et al., *Human cardiac inflammatory responses triggered by Coxsackie B viruses are mainly Toll-like receptor (TLR) 8-dependent.* Cell Microbiol, 2005. **7**(8): p. 1117-26.
350. Wang, J.P., et al., *Cutting Edge: Antibody-mediated TLR7-dependent recognition of viral RNA.* J Immunol, 2007. **178**(6): p. 3363-7.
351. Wang, J.P., et al., *MDA5 and MAVS mediate type I interferon responses to coxsackie B virus.* J Virol, 2010. **84**(1): p. 254-60.
352. Danastas, K., M. Miranda-Saksena, and A.L. Cunningham, *Herpes Simplex Virus Type 1 Interactions with the Interferon System.* 2020. **21**(14): p. 5150.
353. Rushworth, S.A. and D.J. MacEwan, *HO-1 underlies resistance of AML cells to TNF-induced apoptosis.* Blood, 2008. **111**(7): p. 3793-801.
354. Yang, J., et al., *IL-1β inhibits self-renewal capacity of dormant CD34⁺/CD38⁻ acute myelogenous leukemia cells in vitro and in vivo.* Int J Cancer, 2013. **133**(8): p. 1967-81.
355. Smits, E.L., S. Anguille, and Z.N. Berneman, *Interferon α may be back on track to treat acute myeloid leukemia.* Oncoimmunology, 2013. **2**(4): p. e23619.
356. Bekisz, J., et al., *Immunomodulatory effects of interferons in malignancies.* J Interferon Cytokine Res, 2013. **33**(4): p. 154-61.
357. Patel, M.R., et al., *Vesicular stomatitis virus expressing interferon-β is oncolytic and promotes antitumor immune responses in a syngeneic murine model of non-small cell lung cancer.* Oncotarget, 2015. **6**(32): p. 33165-77.
358. Medrano, R.F.V., et al., *Immunomodulatory and antitumor effects of type I interferons and their application in cancer therapy.* Oncotarget, 2017. **8**(41): p. 71249-71284.
359. Bhat, P., et al., *Interferon-γ derived from cytotoxic lymphocytes directly enhances their motility and cytotoxicity.* Cell Death Dis, 2017. **8**(6): p. e2836.
360. Ghanekar, S.A., et al., *Gamma interferon expression in CD8(+) T cells is a marker for circulating cytotoxic T lymphocytes that recognize an HLA A2-restricted epitope of human cytomegalovirus phosphoprotein pp65.* Clin Diagn Lab Immunol, 2001. **8**(3): p. 628-31.
361. Binder, S., M. Luciano, and J. Horejs-Hoeck, *The cytokine network in acute myeloid leukemia (AML): A focus on pro- and anti-inflammatory mediators.* Cytokine Growth Factor Rev, 2018. **43**: p. 8-15.
362. Wang, X. and Y. Lin, *Tumor necrosis factor and cancer, buddies or foes?* Acta Pharmacol Sin, 2008. **29**(11): p. 1275-88.
363. Steinwascher, S., et al., *Identification of a novel synergistic induction of cell death by Smac mimetic and HDAC inhibitors in acute myeloid leukemia cells.* Cancer Letters, 2015. **366**(1): p. 32-43.
364. Krawiec, K., et al., *Targeting Apoptosis in AML: Where Do We Stand?* Cancers (Basel), 2022. **14**(20).
365. Zinngrebe, J., et al., *Biomarker profile for prediction of response to SMAC mimetic monotherapy in pediatric precursor B-cell acute lymphoblastic leukemia.* 2020. **146**(11): p. 3219-3231.
366. Safferthal, C., K. Rohde, and S. Fulda, *Therapeutic targeting of necroptosis by Smac mimetic bypasses apoptosis resistance in acute myeloid leukemia cells.* Oncogene, 2017. **36**(11): p. 1487-1502.
367. El-Mesery, M., M.E. Shaker, and A. Elgaml, *The SMAC mimetic BV6 induces cell death and sensitizes different cell lines to TNF-α and TRAIL-*

induced apoptosis. Exp Biol Med (Maywood), 2016. **241**(18): p. 2015-2022.
368. Cheung, H.H., et al., *Smac mimetic compounds potentiate interleukin-1beta-mediated cell death.* J Biol Chem, 2010. **285**(52): p. 40612-23.
369. Shi, Y., et al., *The Basic Research of the Combinatorial Therapy of ABT-199 and Homoharringtonine on Acute Myeloid Leukemia.* Front Oncol, 2021. **11**: p. 692497.
370. Kleiveland, C.R., *Peripheral Blood Mononuclear Cells*, in *The Impact of Food Bioactives on Health: in vitro and ex vivo models*, K. Verhoeckx, et al., Editors. 2015, Springer International Publishing: Cham. p. 161-167.
371. Rohner, L., et al., *Impact of BH3-mimetics on Human and Mouse Blood Leukocytes: A Comparative Study.* Scientific Reports, 2020. **10**(1): p. 222.
372. Ivashkiv, L.B. and L.T. Donlin, *Regulation of type I interferon responses.* Nat Rev Immunol, 2014. **14**(1): p. 36-49.
373. Bake, V., et al., *Synergistic interaction of Smac mimetic and IFNα to trigger apoptosis in acute myeloid leukemia cells.* Cancer Lett, 2014. **355**(2): p. 224-31.
374. Roesler, S., et al., *Cooperative TRAIL production mediates IFNα/Smac mimetic-induced cell death in TNFα-resistant solid cancer cells.* Oncotarget, 2016. **7**.
375. Faye, M.D., et al., *IGF2BP1 controls cell death and drug resistance in rhabdomyosarcomas by regulating translation of cIAP1.* Oncogene, 2015. **34**(12): p. 1532-1541.
376. Groborz, K., et al., *Exploring the prime site in caspases as a novel chemical strategy for understanding the mechanisms of cell death: a proof of concept study on necroptosis in cancer cells.* Cell death and differentiation, 2020. **27**(2): p. 451-465.
377. Holmgren, C., et al., *Induction of Breast Cancer Cell Apoptosis by TRAIL and Smac Mimetics: Involvement of RIP1 and cFLIP.* 2022. **44**(10): p. 4803-4821.
378. Chen, M., et al., *Smac mimetic promotes TNF-α to induce apoptosis of gallbladder carcinoma cells.* Cellular Signalling, 2020. **72**: p. 109654.
379. Heinzerling, L., et al., *Oncolytic measles virus in cutaneous T-cell lymphomas mounts antitumor immune responses in vivo and targets interferon-resistant tumor cells.* Blood, 2005. **106**(7): p. 2287-2294.
380. Packiriswamy, N., et al., *Oncolytic measles virus therapy enhances tumor antigen-specific T-cell responses in patients with multiple myeloma.* Leukemia, 2020. **34**(12): p. 3310-3322.
381. Prestwich, R.J., et al., *Immune-mediated antitumor activity of reovirus is required for therapy and is independent of direct viral oncolysis and replication.* Clin Cancer Res, 2009. **15**(13): p. 4374-4381.
382. Glaser, L., et al., *Airway Epithelial Derived Cytokines and Chemokines and Their Role in the Immune Response to Respiratory Syncytial Virus Infection.* 2019. **8**(3): p. 106.
383. Kindler, T., D.B. Lipka, and T. Fischer, *FLT3 as a therapeutic target in AML: still challenging after all these years.* Blood, 2010. **116**(24): p. 5089-102.
384. Hillert, L.K., et al., *Targeting RIPK1 in AML cells carrying FLT3-ITD.* 2019. **145**(6): p. 1558-1569.

385. Wergeland, L., et al., *Pre-apoptotic response to therapeutic DNA damage involves protein modulation of Mcl-1, Hdm2 and Flt3 in acute myeloid leukemia cells.* Mol Cancer, 2007. **6**: p. 33.
386. Park, D.J., et al., *Characteristics of DNMT3A mutations in acute myeloid leukemia.* Blood Res, 2020. **55**(1): p. 17-26.
387. Bisaillon, R., et al., *Genetic characterization of ABT-199 sensitivity in human AML.* Leukemia, 2020. **34**(1): p. 63-74.
388. Moog-Lutz, C., et al., *JAML, a novel protein with characteristics of a junctional adhesion molecule, is induced during differentiation of myeloid leukemia cells.* Blood, 2003. **102**(9): p. 3371-3378.
389. Xu, J. and T. Niu, *Natural killer cell-based immunotherapy for acute myeloid leukemia.* Journal of Hematology & Oncology, 2020. **13**(1): p. 167.
390. Baragaño Raneros, A., C. López-Larrea, and B. Suárez-Álvarez, *Acute myeloid leukemia and NK cells: two warriors confront each other.* Oncoimmunology, 2019. **8**(2): p. e1539617.
391. Tang, X., et al., *First-in-man clinical trial of CAR NK-92 cells: safety test of CD33-CAR NK-92 cells in patients with relapsed and refractory acute myeloid leukemia.* Am J Cancer Res, 2018. **8**(6): p. 1083-1089.
392. Liu, S., et al., *NK cell-based cancer immunotherapy: from basic biology to clinical development.* Journal of Hematology & Oncology, 2021. **14**(1): p. 7.
393. Fischer, K., et al., *The Smac Mimetic BV6 Improves NK Cell-Mediated Killing of Rhabdomyosarcoma Cells by Simultaneously Targeting Tumor and Effector Cells.* Front Immunol, 2017. **8**: p. 202.
394. Särchen, V., et al., *Pediatric multicellular tumor spheroid models illustrate a therapeutic potential by combining BH3 mimetics with Natural Killer (NK) cell-based immunotherapy.* Cell Death Discovery, 2022. **8**(1): p. 11.
395. Clarke, P., et al., *Mechanisms of reovirus-induced cell death and tissue injury: role of apoptosis and virus-induced perturbation of host-cell signaling and transcription factor activation.* Viral Immunol, 2005. **18**(1): p. 89-115.
396. Maitra, R., et al., *Oncolytic reovirus preferentially induces apoptosis in KRAS mutant colorectal cancer cells, and synergizes with irinotecan.* Oncotarget, 2014. **5**(9): p. 2807-19.
397. Konjević, G.M., et al., *The role of cytokines in the regulation of NK cells in the tumor environment.* Cytokine, 2019. **117**: p. 30-40.
398. Schwartz, R.L., et al., *The Clinical Oncolytic Reovirus Formulation Reolysin Synergistically Augments the Anti-Leukemic Activity of Azacitidine.* Blood, 2021. **138**(Supplement 1): p. 3337-3337.
399. Tan, Y., et al., *Selective Antagonism of Bcl-xL Potentiates M1 Oncolysis by Enhancing Mitochondrial Apoptosis.* Hum Gene Ther, 2018. **29**(8): p. 950-961.
400. Batenchuk, C., et al., *Non-replicating rhabdovirus-derived particles (NRRPs) eradicate acute leukemia by direct cytolysis and induction of antitumor immunity.* Blood Cancer J, 2013. **3**(7): p. e123.
401. Steele, L., et al., *Pro-inflammatory cytokine/chemokine production by reovirus treated melanoma cells is PKR/NF-κB mediated and supports innate and adaptive anti-tumour immune priming.* Mol Cancer, 2011. **10**: p. 20.
402. Zhao, X., et al., *Natural Killer Cells Activated By Oncolytic Reovirus Enhance Cetuximab Mediated Antibody Dependent Cellular Cytotoxicity*

in an in Vitro and In Vivo Model of Colorectal Cancer. Blood, 2015. **126**(23): p. 3439-3439.
403. Sauer, M., et al., *Induction of the DNA damage response by IAP inhibition triggers natural immunity via upregulation of NKG2D ligands in Hodgkin lymphoma in vitro.* Biol Chem, 2013. **394**(10): p. 1325-31.
404. Lecis, D., et al., *Smac mimetics induce inflammation and necrotic tumour cell death by modulating macrophage activity.* Cell Death Dis, 2013. **4**(11): p. e920.
405. Lee, H.M., et al., *A Murine Immunocompetent Acute Myeloid Leukemia (AML) Model for Testing Immunotherapies.* Blood, 2020. **136**(Supplement 1): p. 3-4.
406. Skayneh, H., et al., *A Critical Review of Animal Models Used in Acute Myeloid Leukemia Pathophysiology.* Genes (Basel), 2019. **10**(8).
407. Wang, X., et al., *Mesenchymal stem cell carriers enhance antitumor efficacy induced by oncolytic reovirus in acute myeloid leukemia.* International Immunopharmacology, 2021. **94**: p. 107437.
408. Li, F., et al., *Characterization of SGN-CD123A, A Potent CD123-Directed Antibody-Drug Conjugate for Acute Myeloid Leukemia.* Mol Cancer Ther, 2018. **17**(2): p. 554-564.
409. Samson, A., et al., *Oncolytic reovirus as a combined antiviral and anti-tumour agent for the treatment of liver cancer.* Gut, 2018. **67**(3): p. 562-573.
410. Driss, V., et al., *Sub-clonal analysis of the murine C1498 acute myeloid leukaemia cell line reveals genomic and immunogenic diversity.* Immunol Lett, 2017. **192**: p. 27-34.
411. Wang, C., et al., *Effect of RNAi-induced down regulation of nuclear factor kappa-B p65 on acute monocytic leukemia THP-1 cells in vitro and vivo.* Molecular and Cellular Biochemistry, 2012. **359**(1): p. 125-133.
412. Liao, X.M., et al., *[Construction and Identification of Acute Myeloid Leukemia NOD/SCID Mouse Model by Tail Vein Injection of THP-1 Cells].* Zhongguo Shi Yan Xue Ye Xue Za Zhi, 2020. **28**(2): p. 424-429.
413. Zhang, X., et al., *Targeting translation initiation by synthetic rocaglates for treating MYC-driven lymphomas.* Leukemia, 2020. **34**(1): p. 138-150.
414. Simon, P.S., et al., *NF-κB functions as a molecular link between tumor cells and Th1/Tc1 T cells in the tumor microenvironment to exert radiation-mediated tumor suppression.* Oncotarget, 2016. **7**(17): p. 23395-415.
415. Morton, C.L. and P.J. Houghton, *Establishment of human tumor xenografts in immunodeficient mice.* Nature Protocols, 2007. **2**(2): p. 247-250.
416. Rahman, M.M., et al., *Co-regulation of NF-kappaB and inflammasome-mediated inflammatory responses by myxoma virus pyrin domain-containing protein M013.* PLoS Pathog, 2009. **5**(10): p. e1000635.
417. Mashima, K., et al., *Differential Localization and Invasion of Tumor Cells in Mouse Models of Human and Murine Leukemias.* Acta Histochem Cytochem, 2020. **53**(3): p. 43-53.
418. Wang, Y., et al., *Sorting, identification and enrichment of side population cells in THP-1 acute monocytic leukemia cells.* Oncol Rep, 2013. **29**(5): p. 1923-31.
419. Li, D., et al., *All-trans retinoic acid enhanced the antileukemic efficacy of ABT-199 in acute myeloid leukemia by downregulating the expression of S100A8.* International Immunopharmacology, 2022. **112**: p. 109182.

Chapter 8 :Appendix

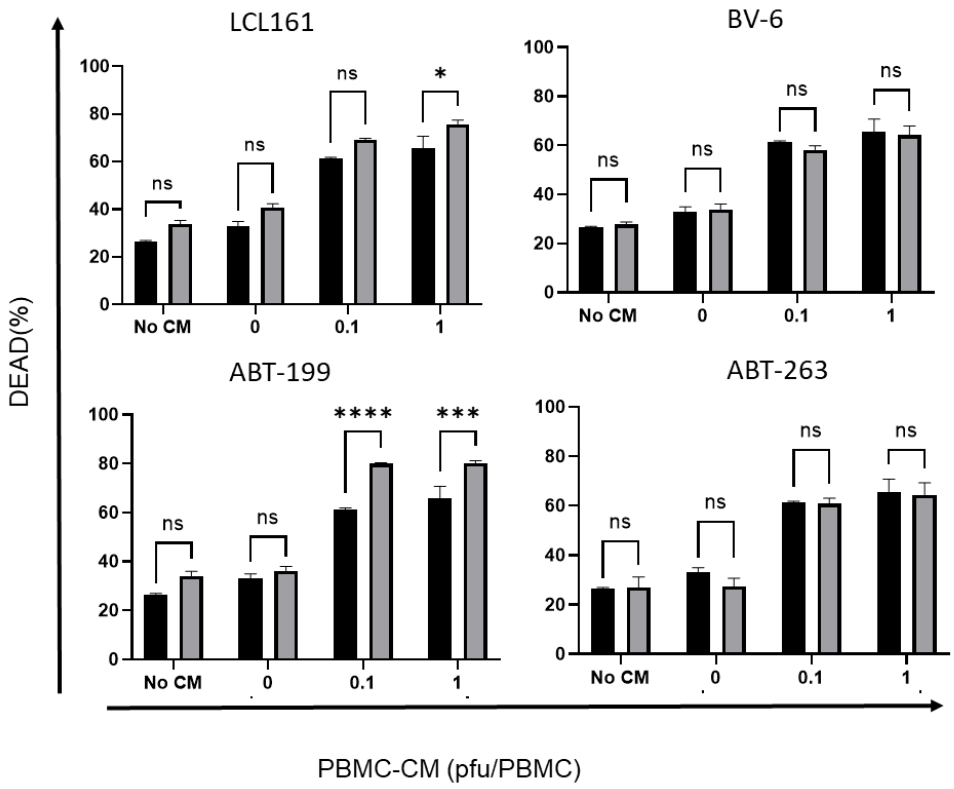

Figure 8-1: KG-1 cell death induced by Smac or BH3 mimetics in combination with UV-irradiated MG1-CM. KG-1 cells were treated with10 µM LCL161, 1µM BV-6, 0.01 µM ABT 199 or 0.01 µM ABT263 and UV-inactivated PBMC-CM (± OV treatment) for 72 hrs, and cell death was assessed using LIVE/DEAD flow cytometry. The mean percentage of dead cells after treatment with MG1-CM is shown from at least 3 individual PBMC donors, + S.E.M. Statistical significance was performed using two-way ANOVA analysis, asterisks indicate comparison of the combination treatment in the presence (grey) and absence (black) of drugs and MG1-CM. *=p<0.05, ***=p<0.005 and ****=p<0.0001.

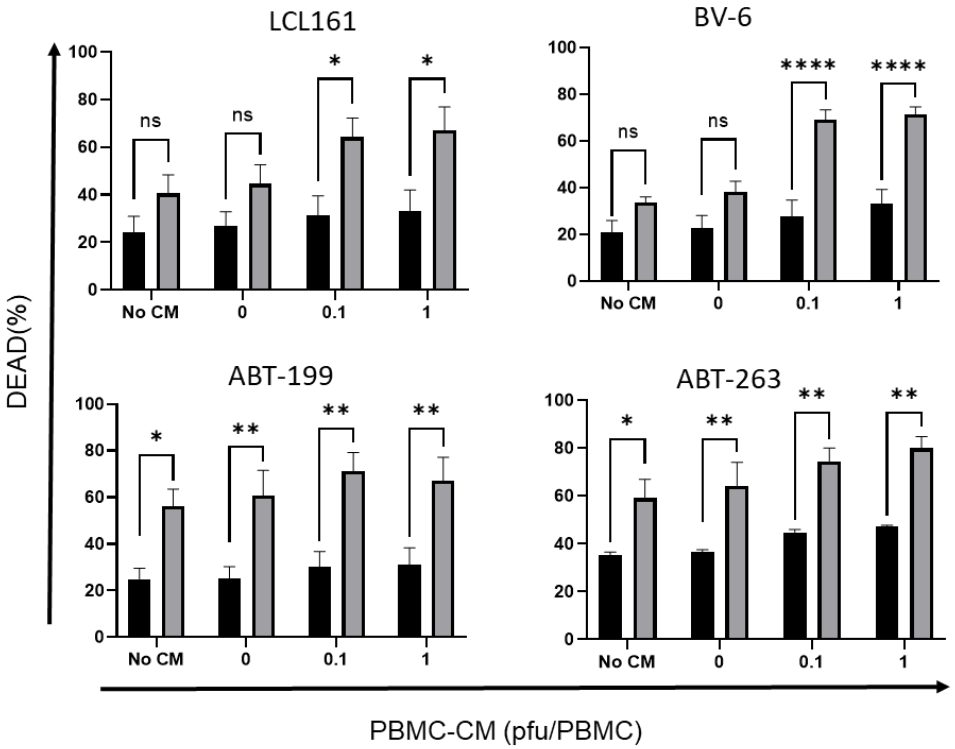

Figure 8-2: HL-60 cell death induced by Smac or BH3 mimetics in combination with UV-irradiated MG1-CM. HL-60 cells were treated with10 µM LCL161, 1µM BV-6, 0.01 µM ABT 199 or 0.01 µM ABT263 and UV-inactivated PBMC-CM (± OV treatment) for 72 hrs, and cell death was assessed using LIVE/DEAD flow cytometry. The mean percentage of dead cells after treatment with MG1-CM is shown from at least 3 individual PBMC donors, + S.E.M. Statistical significance was performed using two-way ANOVA analysis, asterisks indicate comparison of the combination treatment in the presence (grey) and absence (black) of drugs and MG1-CM. *=p<0.05, **=p<0.01and ****=p<0.0001.

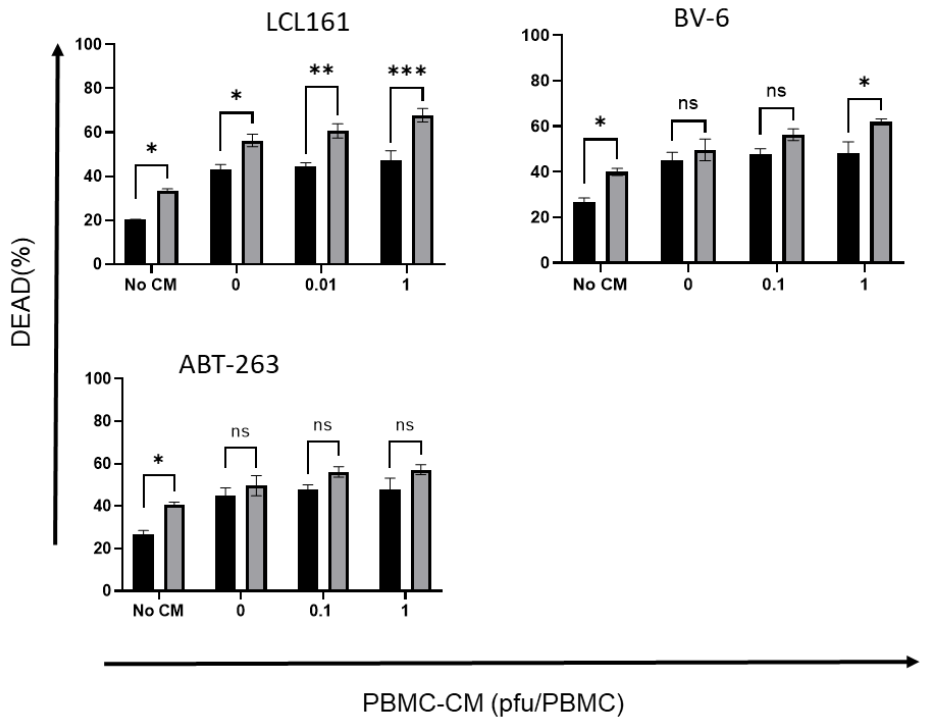

Figure 8-3: Kasumi-1 cell death induced by Smac or BH3 mimetics in combination with UV-irradiated MG1-CM. Kasumi-1 cells were treated with10 µM LCL161, 1µM BV-6, 0.01 or 0.01 µM ABT263 and UV-inactivated PBMC-CM (± OV treatment) for 72 hrs, and cell death was assessed using LIVE/DEAD flow cytometry. The mean percentage of dead cells after treatment with MG1-CM is shown from at least 3 individual PBMC donors, + S.E.M. Statistical significance was performed using two-way ANOVA analysis, asterisks indicate comparison of the combination treatment in the presence (grey) and absence (black) of drugs and MG1-CM. *=p<0.05, **=p<0.01, ***=p<0.005 and ****=p<0.0001.

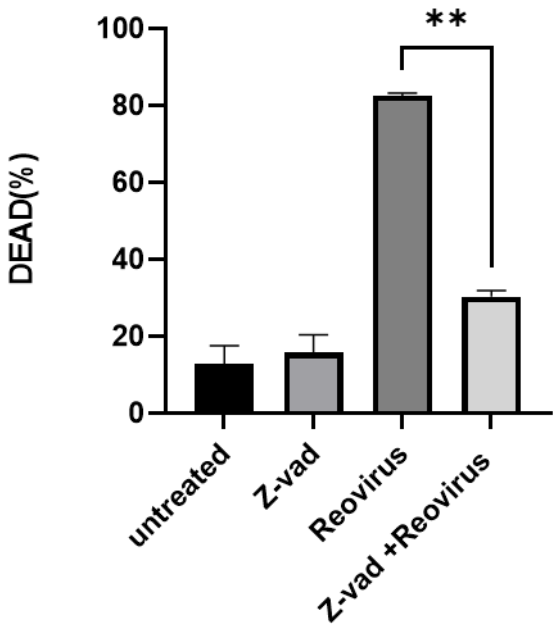

Figure 8-4: Mel-888 cells treated with zVAD and reovirus. Mel-888 cells were treated first with 100 µM zVAD for 1 hr then 10 pfu/cell reovirus was added for 72 hrs. Cell death was measured by flow cytometry. The mean percentage of dead cells after treatment is shown from 2 individual experiments, + S.E.M. Statistical significance was performed using one-way ANOVA analysis and asterisks indicate comparison of reovirus alone and zVAS+ reovirus. **=$p<0.01$

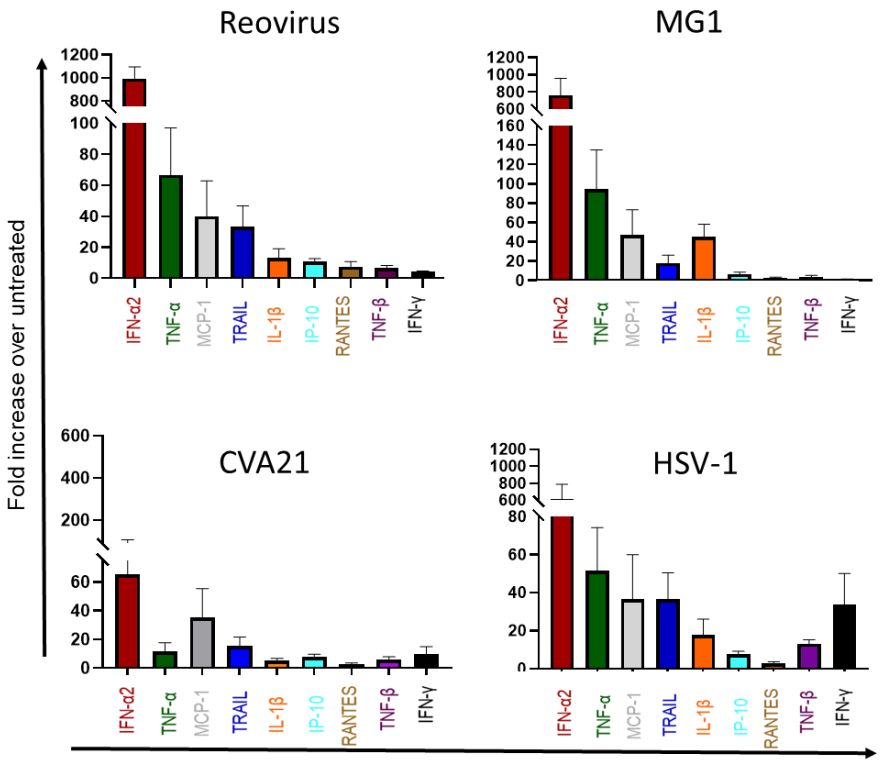

Figure 8-5: Pro-inflammatory cytokines secreted from HD-PBMC in response to OV treatment. HD-PBMC were treated for 48 hrs with 1pfu/PBMC UV-inactivated Reovirus, MG1, CVA21 or 0.1pfu/PBMC HSV-1. Supernatants were harvested and secretion of pro-inflammatory cytokines was measured using a 9-multiplex immunoassay. The graph shows the mean fold change in pg/mL compared to untreated PBMCs for n=3 independent PBMC donors, + S.E.M.

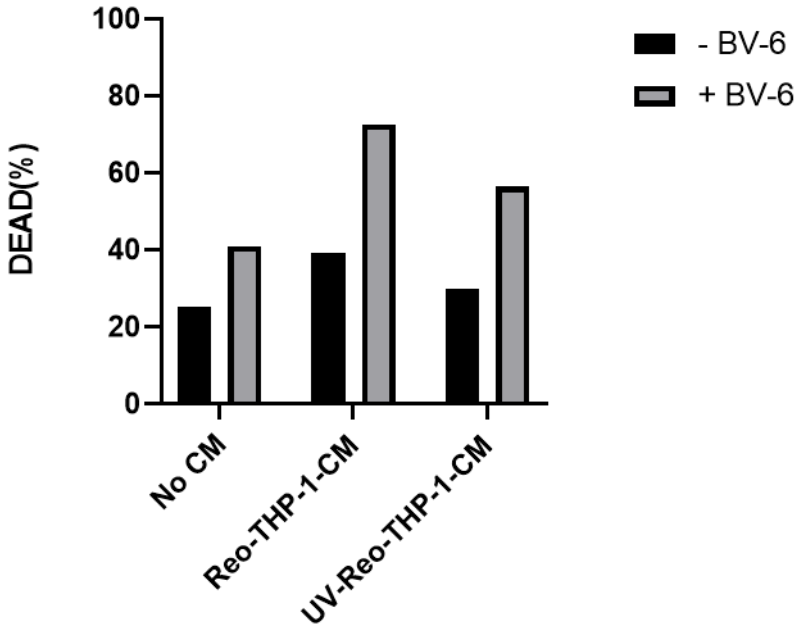

Figure 8-6: THP-1 cell death induced by BV-6 in combination with THP-1-CM. THP-1 cells were treated with 1 pfu/cell live or UV-inactivated reovirus for 48 hrs, then supernatant was collected. THP-1 cells were treated with 2.5 µM BV-6 and THP-1-CM for 72 hrs, and cell death was assessed using LIVE/DEAD flow cytometry. The mean percentage of dead cells is shown from one experiment.

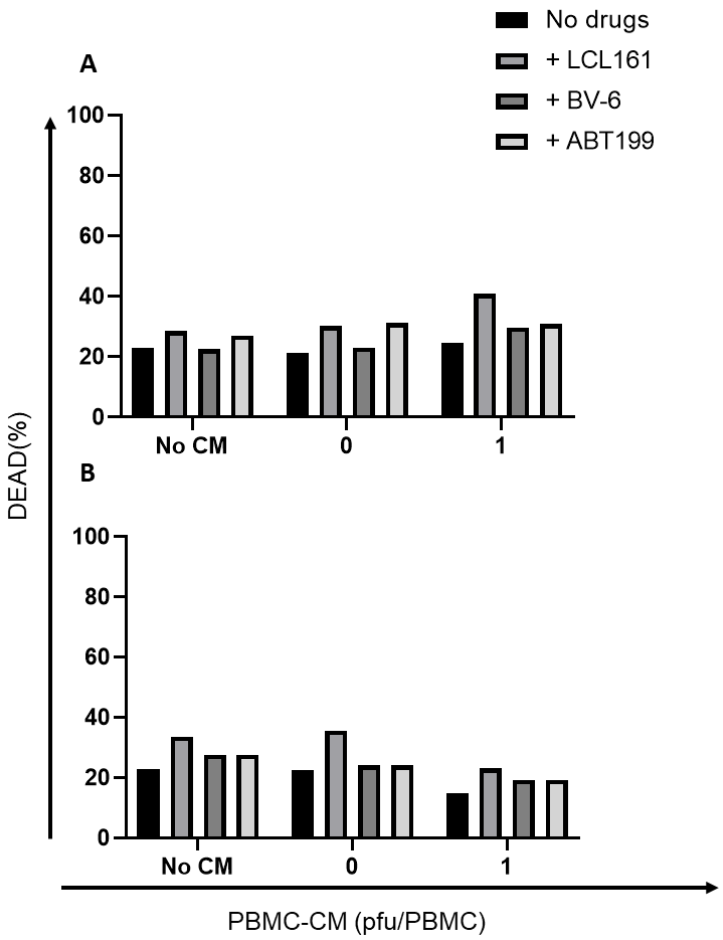

Figure 8-7: Primary AML cell death induced by Smac or BH3 mimetics in combination with UV-irradiated PBMC-CM ± reovirus treatment. AML-PBMC were treated with 1 µM LCL161, 0.1 µM BV-6 or 0.001 µM ABT-199 in the presence or absence of UV-inactivated HD-PBMC-CM (A)or AML-generated PBMC-CM (B) (± reovirus treatment) for 48 hrs, and cell death was assessed using LIVE/DEAD flow cytometry. The mean percentage of dead cells after treatment with drugs and PBMC-CM (± reovirus treatment) is shown for representative non-responding (AML-93) to drugs.

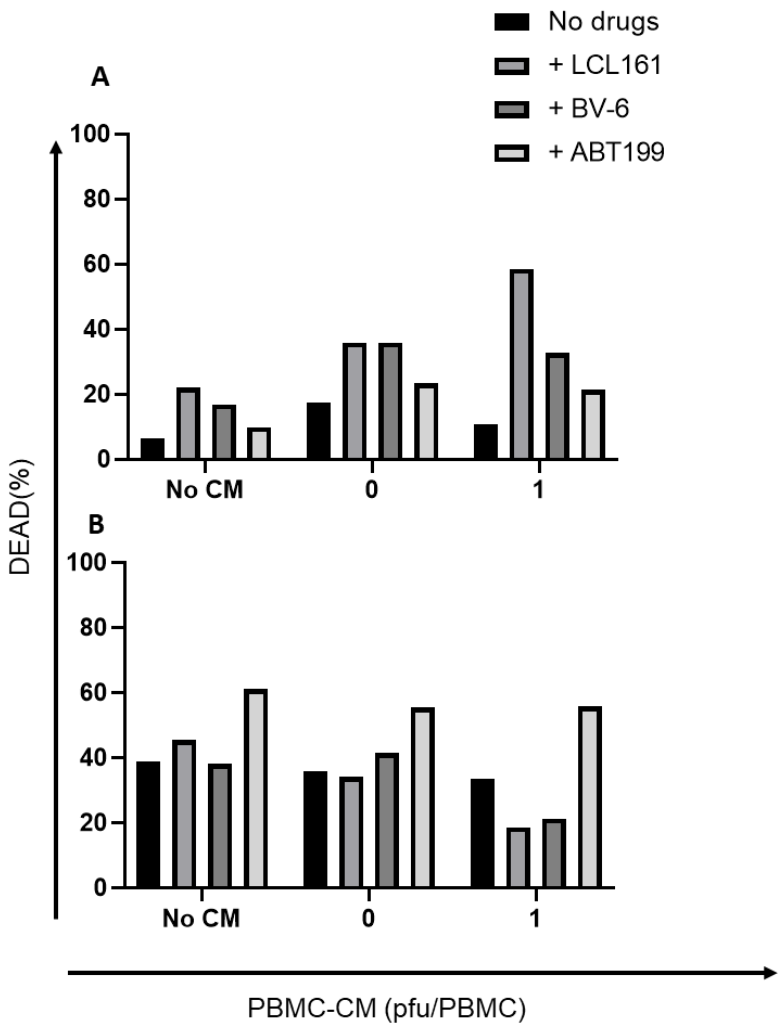

Figure 8-8: Primary AML cell death induced by Smac or BH3 mimetics in combination with UV-irradiated PBMC-CM ± reovirus treatment. AML-PBMC were treated with 1 µM LCL161, 0.1 µM BV-6 or 0.001 µM ABT-199 in the presence or absence of UV-inactivated HD-PBMC-CM (A)or AML-generated PBMC-CM (B) (± reovirus treatment) for 48 hrs, and cell death was assessed using LIVE/DEAD flow cytometry. The mean percentage of dead cells after treatment with drugs and PBMC-CM (± reovirus treatment) is shown for representative responding (AML-94) to LCL161.

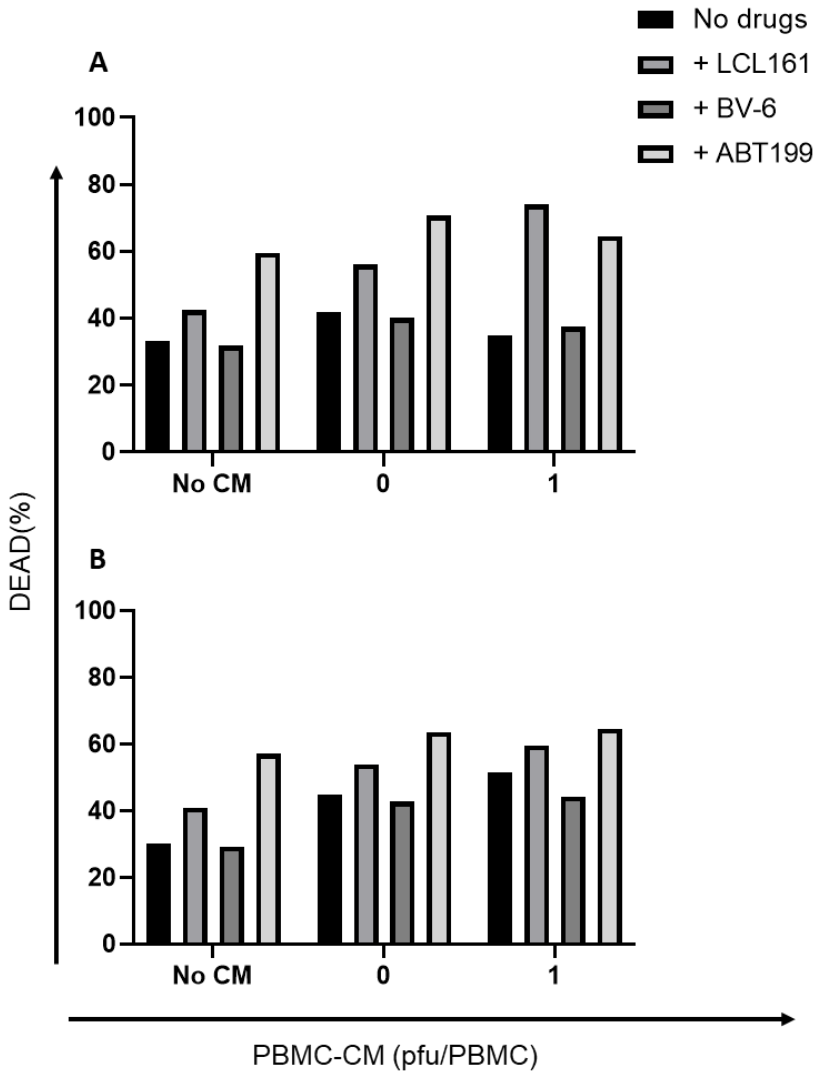

Figure 8-9: Primary AML cell death induced by Smac or BH3 mimetics in combination with UV-irradiated PBMC-CM ± reovirus treatment. AML-PBMC were treated with 1 µM LCL161, 0.1 µM BV-6 or 0.001 µM ABT-199 in the presence or absence of UV-inactivated HD-PBMC-CM (A)or AML-generated PBMC-CM (B) (± reovirus treatment) for 48 hrs, and cell death was assessed using LIVE/DEAD flow cytometry. The mean percentage of dead cells after treatment with drugs and PBMC-CM (± reovirus treatment) is shown for representative responding (AML-96) to Smac mimetic (LCL161).

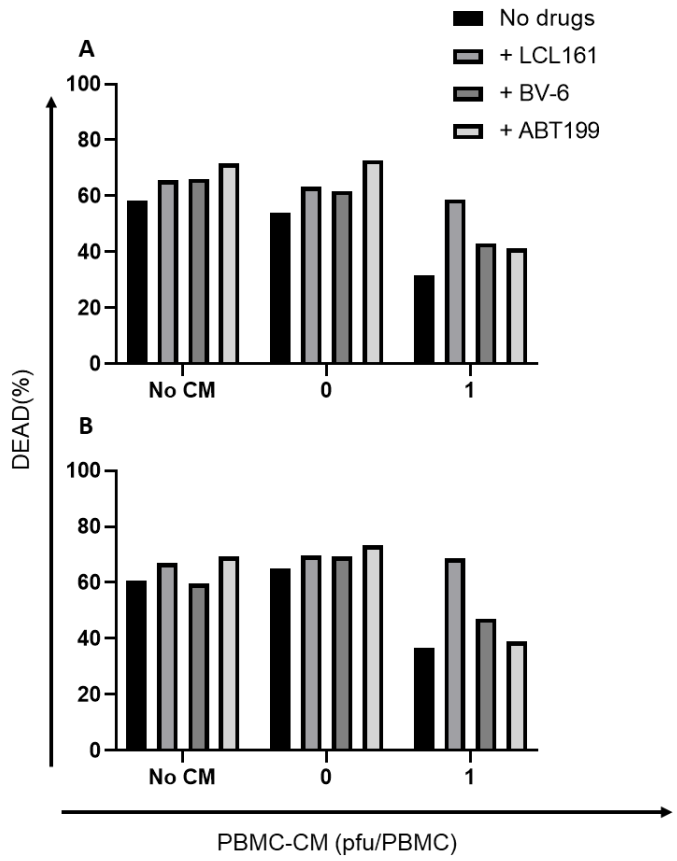

Figure 8-10: Primary AML cell death induced by Smac or BH3 mimetics in combination with UV-irradiated PBMC-CM ± reovirus treatment. AML-PBMC were treated with 1 µM LCL161, 0.1 µM BV-6 or 0.001 µM ABT-199 in the presence or absence of UV-inactivated HD-PBMC-CM (A)or AML-generated PBMC-CM (B) (± reovirus treatment) for 48 hrs, and cell death was assessed using LIVE/DEAD flow cytometry. The mean percentage of dead cells after treatment with drugs and PBMC-CM (± reovirus treatment) is shown for representative non-responding (AML-97) to the drugs.

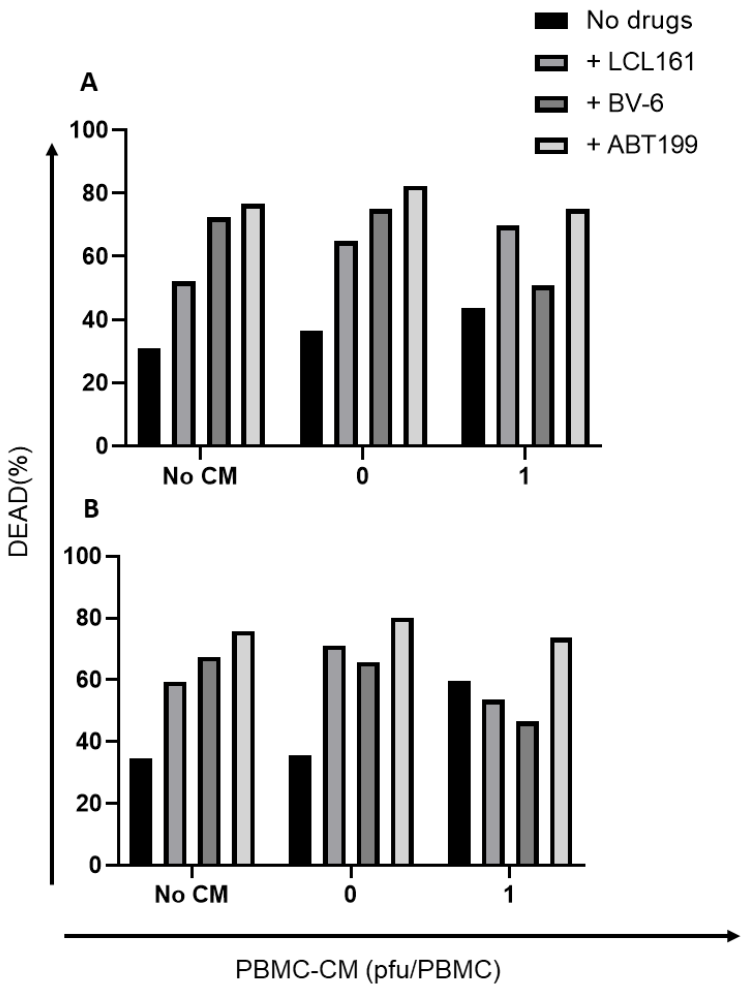

Figure 8-11: Primary AML cell death induced by Smac or BH3 mimetics in combination with UV-irradiated PBMC-CM ± reovirus treatment. AML-PBMC were treated with 1 µM LCL161, 0.1 µM BV-6 or 0.001 µM ABT-199 in the presence or absence of UV-inactivated HD-PBMC-CM (A)or AML-generated PBMC-CM (B) (± reovirus treatment) for 48 hrs, and cell death was assessed using LIVE/DEAD flow cytometry. The mean percentage of dead cells after treatment with drugs and PBMC-CM (± reovirus treatment) is shown for representative non-responding (AML-98) to the drugs.

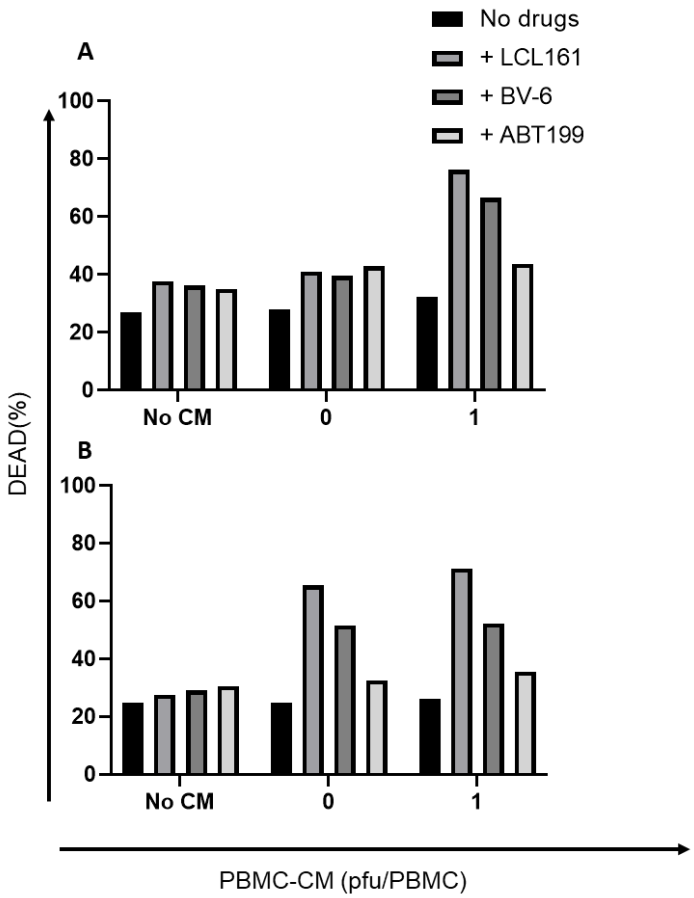

Figure 8-12: Primary AML cell death induced by Smac or BH3 mimetics in combination with UV-irradiated PBMC-CM ± reovirus treatment. AML-PBMC were treated with 1 µM LCL161, 0.1 µM BV-6 or 0.001 µM ABT-199 in the presence or absence of UV-inactivated HD-PBMC-CM (A)or AML-generated PBMC-CM (B) (± reovirus treatment) for 48 hrs, and cell death was assessed using LIVE/DEAD flow cytometry. The mean percentage of dead cells after treatment with drugs and PBMC-CM (± reovirus treatment) is shown for representative responding (AML-99) to Smac mimetics.

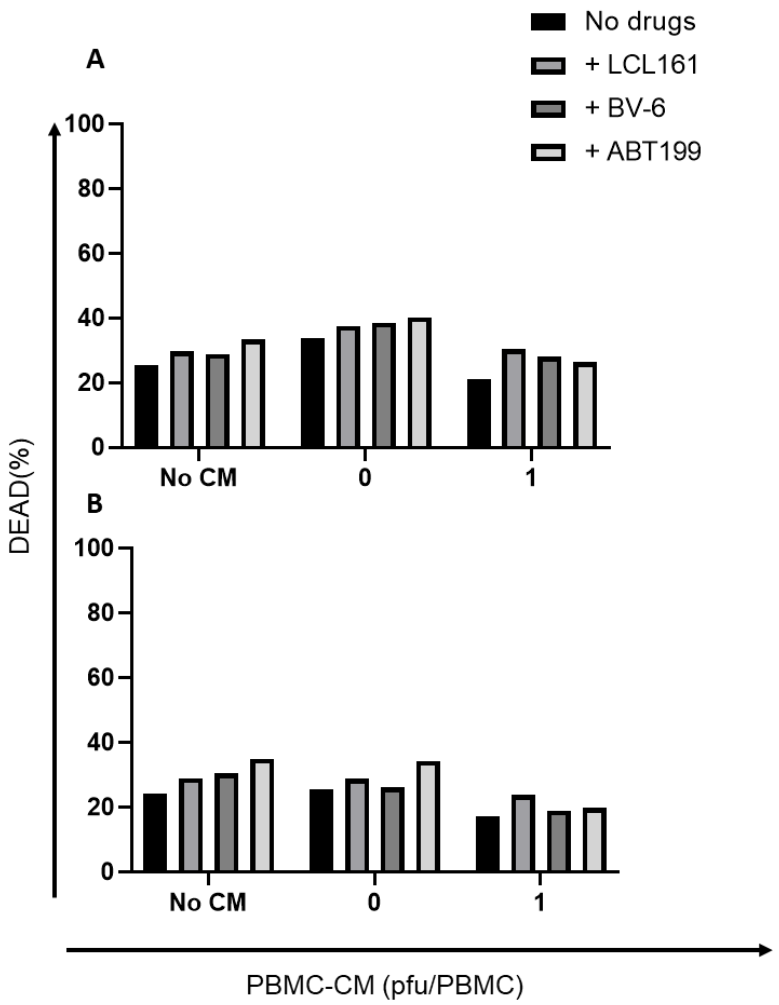

AML101

Figure 8-13: Primary AML cell death induced by Smac or BH3 mimetics in combination with UV-irradiated PBMC-CM ± reovirus treatment. AML-PBMC were treated with 1 µM LCL161, 0.1 µM BV-6 or 0.001 µM ABT-199 in the presence or absence of UV-inactivated HD-PBMC-CM (A)or AML-generated PBMC-CM (B) (± reovirus treatment) for 48 hrs, and cell death was assessed using LIVE/DEAD flow cytometry. The mean percentage of dead cells after treatment with drugs and PBMC-CM (± reovirus treatment) is shown for representative non-responding (AML-101) to the drugs**.**

8.1 Additional information

AML19 trial is a phase III study ends 31/7/2023 and aims to:

1- To compare four induction chemotherapy schedules (namely DA + Mylotarg (3mg/m2) or DA + Mylotarg (3mg/m2 x2, maximum 5mg per day) versus FLAG-Ida + Mylotarg (3mg/m2) or FLAG-Ida + Mylotarg (3mg/m2 x2, maximum 5mg per day) in patients who are not known at entry to have adverse cytogenetics.

2- For patients receiving FLAG-Ida to compare one or two courses of HDAC consolidation versus no further treatment.

3- Patients with FLT3 mutations may enter the AML19 pilot trial.

4- To assess the value of Ganetespib in patients who lack a FLT3 mutation and are not high risk.

5- In high risk patients, and those known to have adverse cytogenetics at entry, to compare novel treatment, CPX-351 vs FLAG-Ida.

6- In high risk patients who have received 2 courses of FLAG-Ida induction, to evaluate in a non-randomised fashion the combination of Fludarabine + CPX-351.

7- In high risk patients, to evaluate, the value of allogeneic stem cell transplantation.